THE DESIGN AND CONTROL OF ANAEROBIC PONDS

WITH SPECIFIC REFERENCE TO WESTERN TREATMENT PLANT

Warren Paul
Dip. App. Sc., Grad. Dip. App. Sc.

A thesis submitted in fulfilment of the requirements
for the degree of Doctor of Philosophy

School of Communications and Informatics
Faculty of Engineering and Science
Victoria University of Technology
Footscray, Melbourne

August 1998

To my wife, Julia, for putting up with the seemingly never-ending story that was this thesis.

Acknowledgments

My thanks to the following people and organisations

- David Hutchison, Terry Scott and Tony Crapper for their support.
- My colleagues and "sounding boards" at Melbourne Water, Brad McLean and Trevor Gulovsen.
- George Alifraco for rowing across an anaerobic *poo* pond with me, at three in the morning, in the name of science.
- Operations staff at Western Treatment Plant for collecting samples of raw sewage.
- Melbourne Water Corporation for sponsoring this research.
- Dr Keith McLean of CSIRO for his advice during the development of methanogenic activity tests and anaerobic culture techniques.
- Water ECOscience for performing all chemical analyses of water samples.
- Lim Ong of Probe Analytical for the electron microscopy and X-ray analyses.
- Mohammed Mohideen and Sue Pepper, at the Centre for Bioprocessing and Food Technology (Victoria University, Werribee campus), for performing the anaerobic cultural counts in 1997 and 1998, after my own laboratory at WTP was closed down in the name of progress.
- My supervisors, Assoc. Prof. Neil Barnett and Assoc. Prof. John Casey, for their advice and for allowing me the freedom to pursue many different avenues in the course of this research.

Abstract

This thesis reports results of a study of the control and improvement of the covered 115E Anaerobic Reactor at Western Treatment Plant. The 115E Reactor treats 60 ML of sewage per day and produces 8000 m^3/d of methane which is harvested for power production. The objectives of this research were to identify ways to enhance treatment efficiency and reduce variability in effluent composition from anaerobic ponds. In particular, the research examined the potential benefits of improved trade waste management and process control.

Because WTP receives a high proportion of trade wastes, the effects of various inhibitory and stimulatory chemicals were studied, using a methanogenic activity test, with a view to increasing the yield of methane in the longer term. These studies showed that sulphate ion is potentially causing 30% inhibition of methanogenesis at concentrations found in raw sewage. Calcium ion, on the other hand, was found to be deficient.

Treatment efficiency could potentially be improved by identifying the components of the raw sewage that could be inhibitory or stimulatory to the treatment process and then altering the composition of the sewage, in the longer term, through changes in regulations dealing with trade wastes. If successful, this would have a two-fold effect on the operating cost of the Western Treatment Plant. Firstly, an improvement in anaerobic treatment efficiency would reduce the power cost associated with aeration in the next stage of the

process. Secondly, improvements in treatment efficiency are concomitant with an increase in methane produced and, therefore, power produced in the on-site power plant that uses methane as fuel. In brief, the operating cost of the Plant would be lowered in the short term by reducing the cost of imported power. In the future, when covers and power plants are installed on two other lagoons at WTP, an increase in treatment efficiency would increase revenue from electricity exports, and this would further offset the operating cost of the Plant.

With regard to reducing variability in effluent composition, both process regulation and process monitoring techniques were explored as mechanisms for controlling the anaerobic digestion process.

A feedforward-feedback control equation was developed which connected the (only) controllable variable, flowrate, to the effluent COD concentration, raw sewage COD concentration and pond temperature. Using the control equation, it was demonstrated that there would be insufficient capacity to divert flows elsewhere within the Plant given the magnitude of the flow control actions required to keep the pond effluent COD at a fixed target value. Process monitoring techniques, accepting the daily, weekly and annual seasonality in the process as normal variability and attempting to identify and eliminate special causes of variation in order to constrain the variability in effluent composition, were therefore considered more appropriate to anaerobic ponds at WTP. This research examined both multivariate and univariate charting techniques for process monitoring of anaerobic ponds.

Although monitoring the anaerobic digestion process typically involves measurement of several related variables including pH, alkalinity, electrode potential and the concentrations of volatile fatty acids, volatile solids, hydrogen, methane and carbon dioxide, the multivariate control charts involving serially correlated data are complicated, difficult to develop and difficult to use. A study of the dynamics of some of these variables showed that measuring the effluent COD or methane flowrate would provide as much information as the suite of other process indicators recommended for anaerobic digestion control. Monitoring only one variable greatly simplified the development of control charts for anaerobic ponds. However, even univariate charts can involve complex time series techniques when the data exhibit serial correlation, and further work is needed to develop simple procedures that are both statistically valid and suitable for routine use by operators of wastewater treatment plants.

While not the original intention of this research, certain findings were made in the course of these studies that could also be used improve the design of anaerobic ponds. A study of the distribution of methanogens within the 115E Reactor, in order to locate the most appropriate sampling point, revealed a distinct peak in anaerobic activity midway along the reactor. This was postulated to correspond to the settlement of suspended and flocculated organic matter. Further studies showed that the zone of peak activity moved toward the outlet of the pond as sludge and scum accumulated and, as demonstrated at WTP, this has serious implications for treatment capacity and gas production if

"washout" occurs. These observations led to the development of a simple model that provides an alternative design approach for anaerobic ponds.

Contents

Acronyms and Abbreviations

ACF	autocorrelation function
ARIMA	autoregressive integrated moving average
ARL	average run length
ATP	adenosine triphosphate
BOD_5	5-day biochemical oxygen demand
CFU	colony forming unit
COD	chemical oxygen demand
cpd	cycles per day
CSTR	continuously stirred tank reactor
Cusum	cumulative sum
DMCC	direct microscopic clump count
EDXA	energy-dispersive X-ray analysis
EP	electrode potential (or redox potential)
ESCOD	115E reactor effluent SCOD
ETP	electron transport phosphorylation
fw	flow weighted
GPR	ground penetrating radar
HRT	hydraulic residence time
ICHART	individual observations chart
MA	moving average
MMSE	minimum mean square error
MPC	measurement process control
MRCHART	moving-range chart
MS	mineral salt
MSE	mean square error
NAD	nicotinamide adenine dinucleotide
NADP	nicotinamide adenine dinucleotide phosphate
NTA	nitrilotriacetic acid
OHPA	obligate hydrogen-producing acetogens
ORP	oxidation-reduction potential
PACF	partial autocorrelation function
PID	proportional-integral-derivative
PTEMP	115E reactor water temperature
QC	quality control
RCOD	raw sewage COD concentration
RFLOW	raw sewage flowrate
SCOD	soluble COD
SEM	scanning electron microscopy
SHE	standard hydrogen electrode
SLP	substrate level phosphorylation

sp.	species
SPC	statistical process control
SRB	sulphate reducing bacteria
SS	suspended solids
SSE	sum of squared errors
TOC	total organic carbon
UASB	upflow anaerobic sludge blanket (reactor)
VFA	volatile fatty acid
VS	volatile solids
VSS	volatile suspended solids
WWTP	wastewater treatment plant

1. Introduction and Summary

Western Treatment Plant (WTP), situated 35 km to the west of Melbourne (Australia) and covering an area of about 10,500 ha, uses a combination of lagoons (all year), land filtration (summer) and grass filtration (winter) to treat approximately 500 ML of sewage per day, which is equivalent to about 55% of the sewage generated in the metropolitan area. It is one of the largest lagoon and land sewage treatment works in the world and services 1.6 million people and 90% of industry from the central, western and northern suburbs of Melbourne. Presently, about 70% of sewage at WTP is processed via lagoons, where anaerobic ponds are the first stage of treatment. Anaerobic ponds are the subject of this research and this chapter presents the context of the research and a summary of the methodology and findings.

Waste stabilisation ponds, or sewage lagoons, are low technology, natural systems for wastewater treatment. They make an attractive alternative to energy-intensive activated sludge plants, particularly for rural areas and developing countries where the land requirements and effluent standards are not prohibitive. They produce a reasonable effluent quality for a fraction of the capital and operating cost. A major drawback to open treatment systems like lagoons, however, is the odour they emit to the atmosphere. For Western Treatment Plant, higher community expectations and the encroachment of residential areas have made it necessary to take steps to reduce odorous emissions.

An extensive two year survey of odours at Western Treatment Plant revealed anaerobic ponds to be one of the main contributors to odour generated by the Plant[1]. To reduce odorous emissions, a three-phase strategy was implemented in new or "advanced" lagoon designs. Firstly, the size (area) of anaerobic ponds was optimised. Most of the BOD_5 reduction in anaerobic ponds occurs within a hydraulic residence time of 1.5 days, even though anaerobiosis continues for up to 3 weeks. Therefore, anaerobic treatment could be compartmentalised in less than 10% of the area it formerly occupied. Secondly, the "anaerobic reactor" was covered with a high-density polyethylene liner to trap odorous gases. Another advantage to covering the anaerobic reactor is the ability to generate electricity from the methane in the biogas. The approximate composition of the biogas is given in Table 1. Thirdly, surface aerators were installed in the first pond following the anaerobic reactor. The aerators create an aerated-facultative environment which encourages aerobic activity and oxidises reduced fermentation products like dissolved sulphide and volatile fatty acids coming from the anaerobic reactor.

Table 1 Approximate composition of biogas.

Methane	80% (v/v)
Carbon dioxide	10% (v/v)
Nitrogen	5% (v/v)
Water	4.5% (v/v)
Hydrogen sulphide	0.5% (v/v)

An aerial photograph of the 115E lagoon, showing the covered anaerobic reactor, aerated-facultative pond, and later ponds, is given in Figure 1-1. A fibre-reinforced plastic barrier separates the anaerobic reactor and aerated pond, shown diagrammatically in Figure 1-2.

The increased capital and operating costs of the new lagoons are partly offset by the shorter hydraulic residence times required and the generation of electricity for powering surface aerators. Presently, only one of the three advanced lagoons, the 115E Lagoon, has a covered anaerobic reactor. The 115E Anaerobic Reactor, with an organic loading of 300 g $BOD_5/m^3.d$, produces about 8,000 m^3/d of gas. The gas is used to generate about 1.2 MW of electrical power for 12 hours each day, which is equivalent to $365K or 30% of the total cost of aeration for the three advanced lagoons.

The operating costs of the Plant are sensitive to the performance of covered anaerobic reactors. A 10 % increase in methane yield from anaerobic reactors at WTP would increase by 10% the energy produced by the 115E Lagoon power plant, but reduce by almost 26% the aeration requirement in the three advanced lagoons. This would have the effect of decreasing the present imported energy cost of the Plant by 40%, or $350K per year. With the two new covers installed there will be sufficient power generated, equivalent to about $1.2M, to meet the needs of the Plant and improvements in treatment efficiency could increase revenue through electricity exports that would further offset the operating cost of the Plant.

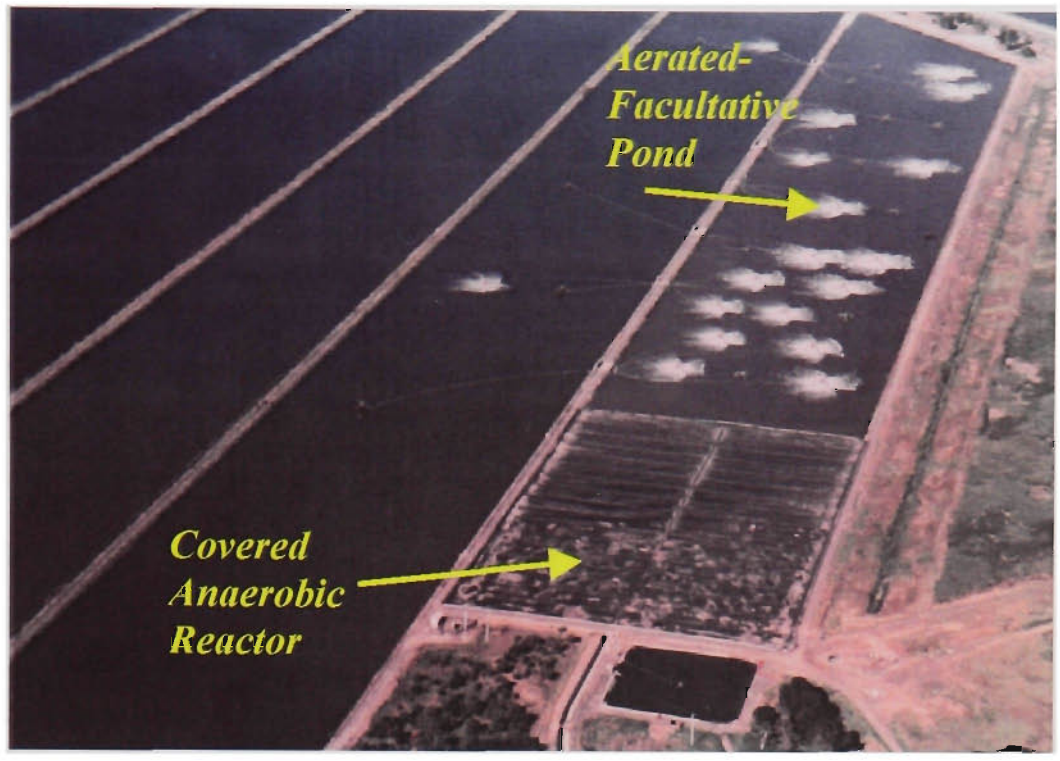

Figure 1-1 An aerial photograph of the 115E lagoon (a 10-pond lagoon) showing the covered anaerobic reactor and the aerated-facultative pond.

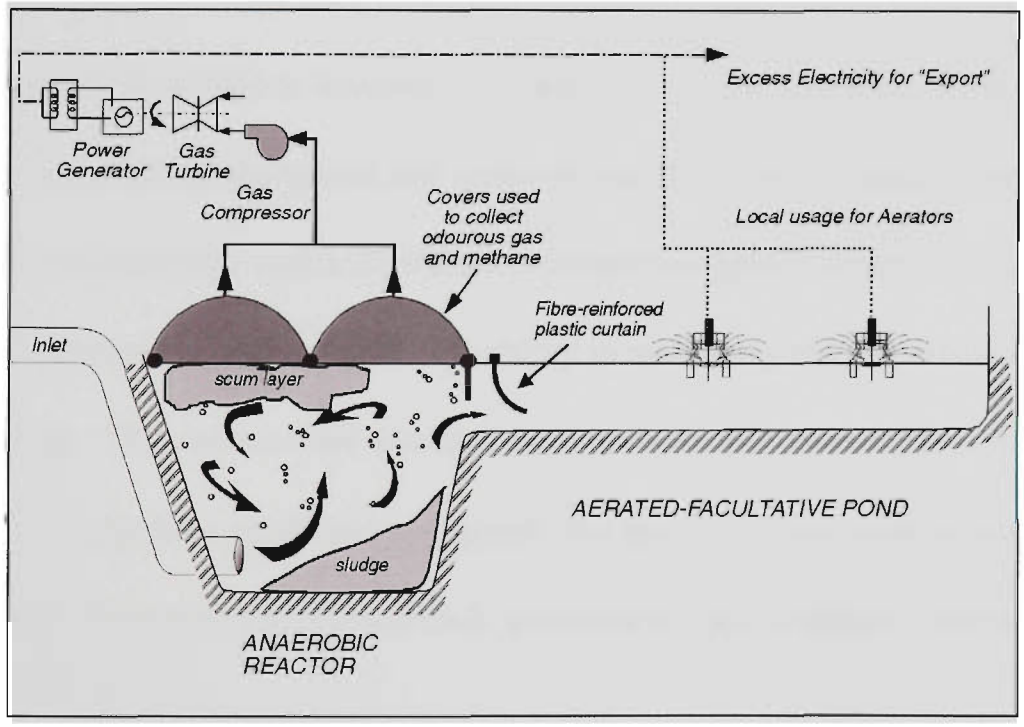

Figure 1-2 Conceptual diagram of the first pond which consists of a covered anaerobic reactor and an aerated-facultative pond. Note that the first pond in the 115E lagoon has a uniform depth of 3 m. In more recent lagoons (25W and 55E) the anaerobic reactors are 6-8 m deep and the aerated-facultative pond is 3 m deep.

Covered anaerobic ponds are becoming increasingly popular because they have a number of distinct benefits. Anaerobic ponds have lower energy needs, lesser sludge production, and are more efficient in terms of land requirements than aerated ponds. Covered anaerobic ponds in particular have minimal odour, retain heat, reduce greenhouse gas emissions, and provide fuel for power generation. Anaerobic digestion processes, however, are generally considered more difficult to control than other types of processes and, therefore, highly variable in terms of effluent composition.

The original intent of this research was to improve the performance of anaerobic ponds through better trade waste management and process control. However, certain findings were made that should also improve their design. The research generally aimed to develop an appreciation of the anaerobic pond process by describing the spatial and temporal variability in the process control variables, including the spatial distribution of methanogenic bacteria, and to study the factors thought to influence the variability in methane yield and effluent composition. This information was then used to develop a process control strategy for anaerobic ponds and to suggest changes to existing trade waste regulations. A summary of the research methodology and findings is presented below.

Initially a review of the literature is presented, covering the microbiology and control of anaerobic digesters, and the application of statistical process control and process regulation methods to wastewater treatment plants in general (**Chapter 2**). Anaerobic digestion once had a reputation for being difficult to

control, though, recent advances in the biochemistry of anaerobes and microbial ecology of anaerobic environments, especially in relation to methanogens and the role they play in the regulation of pH and redox potential, have seen the process gain favour. Better understanding of the process' mechanisms has led to the identification of more meaningful and responsive process indicators and improved control schemes, particularly for "high rate" digesters. Statistical process control methods have been explored in the context of wastewater treatment plants (WWTP's), though, the focus has mainly been on activated sludge systems.

Relatively little attention has been specifically given in the literature to the control of anaerobic ponds and, therefore, prior to studying the control of anaerobic ponds at WTP, some basic information concerning the spatial and temporal variability of some common process indicators was sought (**Chapter 3**). The subject of the study, the 115E Anaerobic Reactor at WTP, nominally treats 60 ML/d of raw sewage and covers an area of 3 ha. It was the first reactor to be fitted with a gas collection cover at WTP. The variables included in the study were pH, volatile fatty acid concentration, volatile solids concentration, alkalinity, electrode potential and temperature. While there appeared to be a diurnal pattern in most variables, and a systematic pattern along the reactor, by far the largest source of variation was depth. The concentration of biomass and the physico-chemical environment were significantly different in the sludge layer.

Chapter 4 took this investigation one step further and looked at the distribution of methanogens within the sludge layer. Samples of sludge were

taken on longitudinal transects and measurements of methanogenic activity and cultural counts of both methanogens and total anaerobes were carried out. The data indicated a clear peak in anaerobic activity about midway along the reactor and it was surmised that this was associated with the settlement of primary sludge. This appeared to be the most appropriate point to sample for process control purposes.

Chapter 4 also reported on an investigation of the nature and possible causes of scum formation and accumulation within the Reactor. Physical, chemical, and microbiological analyses were performed on samples of the scum, which had a fibrous and greasy texture. Microscopy revealed that the scum was composed largely of toilet tissue fibres and bacterial biomass, though counts of viable methanogens and total anaerobes were much lower than in the sludge layer. Furthermore, electron micrographs and X-ray analyses of inorganic granules within the scum suggested they were similar to the granular anaerobic sludge found in Upflow Anaerobic Sludge Blanket Reactors. Interestingly, the end of the scum layer corresponded to the point where the bacterial density in the sludge layer began to decline. This was believed to indicate that scum forms as a result of gas production within the bacterial floc and granules, which then buoy to the surface, collecting colloidal and suspended matter along the way. Scum 'islands' have been observed to form on open anaerobic ponds at WTP in the past. These islands, however, tended to collapse and reform periodically. It is likely that wind-induced turbulence kept the scum in check in these open ponds. With

the construction of the HDPE cover on the 115E Reactor, the scum was no longer subject to this turbulence, and accumulated as a consequence.

It was postulated at that time, that the continued accumulation of sludge and scum would cause the primary sludge to settle out further along the reactor and eventually the zone of peak anaerobic activity would be washed out of the reactor, into the adjacent aerated pond. This, of course, would have serious consequences in terms of treatment performance, power generation, odour production and final effluent quality. Almost two years later, when an increase in the Reactor's effluent BOD_5 was detected, measurement of the densities of methanogens and total anaerobes within the sludge layer was repeated (**Chapter 8**). It was observed that the zone of peak activity was now at the very end of the reactor. A simple model of the settlement of primary sludge showed how the hydraulic velocity increases with increasing sludge volume and the settlement (or active) zone moves along the Reactor. The model predicted quite well the position of the active zone in 1995 and in 1997. This, together with the observation that the flowrate has relatively little effect on the effluent BOD_5 (see also Chapter 6 and Chapter 7), suggests that hydraulic residence time is not the correct basis for designing anaerobic ponds. Indeed the optimal sludge volume within the 115E Reactor was calculated to be about 2.5 ML, and if this volume was maintained then the Reactor would need only be about half of its present size (or area). This finding means that the cost of civil works and the gas collection cover could be reduced by almost half, resulting in savings of millions of dollars for future anaerobic reactors at WTP.

In **Chapter 5** a literature review of the nutritional and inhibitory factors that affect anaerobic digestion is presented. A number of inorganic ions were identified as potential effectors of methanogenesis at WTP, including sulphate, zinc, cobalt, nickel, iron, calcium, and magnesium ions. These ions were further investigated using a methanogenic activity test and it was found that both sulphate and calcium may be present in concentrations that affect anaerobic treatment. Sulphate is potentially causing a 30% inhibition of methane production while calcium, an essential trace nutrient, appears to be deficient. These two chemical species were incorporated into a regression analysis of the factors affecting methane yield in the 115E Reactor. With regard to improving the yield of methane, the findings of Chapter 5 were also discussed in the context of changes to trade waste regulations.

In **Chapter 6** data are presented on a range of variables believed to affect methane production, including the wastewater flowrate and the properties and composition of the wastewater such as temperature, pH, type and amount of carbon source, calcium and sulphate. Nitrogen and phosphorus were deemed not to be limiting on the basis of information reported in the literature. A regression analysis of the data was performed and most of the variation in the methane flowrate appeared to be explained by temperature. The raw sewage COD concentration and flowrate improved the prediction capability of the model, though, neither sulphate nor calcium produced a discernible effect on the variability of methane flowrate over the range of concentrations experienced in the raw sewage.

Chapter 7 reports the use of process regulation and process monitoring (or statistical process control) techniques for the operation of anaerobic ponds. It is important to recognise that while there is little scope for manipulating the total flowrate of sewage to the WTP, there is scope to control the distribution of flow to the various processes within the Plant. Indeed it happens every day. Given this flexibility, it was believed possible to improve the performance of anaerobic reactors through improved flow distribution.

To establish the worth of a control scheme, and how complex that scheme needs to be, an initial study of the dynamics of the 115E Reactor using frequency domain and time domain analyses was undertaken. The study looked, in particular, at the dynamic relationships between the reactor's effluent soluble COD and the input variables: flowrate, raw sewage COD concentration and reactor water temperature. All factors were found to be important, but temperature and raw sewage COD explained most of the variation. A feedforward-feedback control model was developed and while it appeared technically feasible to control the process by this means, the magnitude of the flow control actions required to keep the effluent SCOD at a fixed target level meant that there would probably be insufficient capacity to divert flows elsewhere within the Plant. This will be particularly true in the future, as it has recently been decided to phase out the direct application of raw sewage to land and grass filtration processes.

Process monitoring methods were, therefore, deemed more appropriate to anaerobic ponds at WTP. The essential difference between the two methods of

control is that process regulation aims to minimise deviations of the process output from a set target value, whereas process monitoring accepts the slow drift about a deterministic weekly and annual cycle as normal process variability. The objective of process monitoring is to signal when a change has occurred and then identify and eliminate the special cause of variation, thereby reducing variability in the process output.

Process monitoring of anaerobic ponds could potentially involve the measurement of several related variables, as recommended in the literature, including pH, VFA and VS concentrations, alkalinity, electrode potential, and the concentrations of hydrogen, carbon dioxide and methane. These variables are reported to be useful as early warning indicators of process failure, or as diagnostic tools in the identification of the cause of an upset. However, their value as diagnostic tools is yet to be proved and, in the context of anaerobic ponds, a study of the dynamics of some of the variables indicated that the process outputs would respond as quickly as (say) hydrogen. This suggests that the effluent SCOD concentration or methane flowrate would provide as much information as a suite of other indicators.

Given the presence of serial correlation and seasonality in the effluent SCOD and methane flowrate, time series modelling of the data was required for the construction of statistically valid control charts. The residuals of the time series models satisfied the assumptions of data independence and normality, which underpin the classical control charting procedures. The resulting control charts suggested that the process was in a state of statistical control throughout

the three month study. While this procedure was not particularly complex, various simpler methods have been proposed in the literature which may be more acceptable to operators of wastewater treatment plants. To date, the simplest method relies on time series plots of the original variables, perhaps with some form of smoothing to clarify trends and shifts in process level, and the keen ability of the human mind to detect patterns.

Process monitoring, as applied to anaerobic ponds or other "natural" systems, is actually a mechanism for risk management where the objective is not to adjust the process to keep it on target, but, to identify and eliminate the causes of excessive variability. In a broad sense, the potential hazards to anaerobic ponds include organic, hydraulic, temperature, pH and toxic shock loads. Excessive sludge accumulation would need to be added to this list. In most cases, the risks can be minimised by management of discharges to the sewerage system. Trade waste regulation, for example, is a form of risk management. Statistical process control charts are a tool for detecting, identifying and quantifying the risks to the process and, in this capacity, can play an important role in the operation of anaerobic ponds.

For Western Treatment Plant, this research provides a range of opportunities for improving the design and performance of anaerobic ponds and, while specific to WTP, many of the findings are applicable to anaerobic ponds world wide.

2. Literature Review

2.1 INTRODUCTION

Historically, anaerobic digestion processes had the reputation of being unstable and difficult to control[2,3]. This perception has undergone considerable change in recent times, as understanding of the controlling mechanisms has improved[4,5,6]. Today, anaerobic digestion is an increasingly popular method for the treatment of biodegradable organic wastes. It is an efficient process resulting in comparatively little sludge production (compared to aerobic treatment processes) and it generates methane which can be used to produce electrical energy. Monitoring the anaerobic digestion process, however, still involves the measurement of several related variables and the subsequent interpretation of the multivariate data can be challenging. Scope exists for better methods of data analysis that will enable the performance of working digesters to be refined. Statistical process control (SPC) and process regulation are two techniques available for the control and improvement of many different processes, including wastewater treatment processes. To date, though, "high rate" anaerobic digesters and activated sludge processes (an aerobic process) have received considerably more attention than anaerobic ponds (see Section 2.4).

Advances in the understanding of anaerobic digestion have come through fundamental studies of the ecology of anaerobic habitats, the biochemistry of anaerobes, and experimentation with dynamic-mechanistic mathematical models

(see Sections 2.2 and 2.3). In brief, the bioconversion of complex organic matter to methane involves the balanced interaction of four broad groups of bacteria: acidogens, acetogens, H_2-utilising methanogens, and acetoclastic methanogens. The stability of the process depends on the capacity of the bacteria to self-regulate the pH and redox potential of their environment.

The *acidogenic group* first hydrolyse, and then metabolise, complex organic matter (carbohydrates, proteins and lipids) to short chain fatty acids (mainly acetic acid, propionic acid and butyric acid), hydrogen (H_2) and carbon dioxide (CO_2). Acetic acid is primarily formed because it results in the largest energy yield for the growth of the acidogenic bacteria. Propionic and butyric acids are formed in response to accumulations of H_2 during times of stress (e.g. organic shock loads).

The *acetogenic bacteria* produce acetate from either propionic acid, butyric acid or H_2/CO_2. The obligate hydrogen producing acetogens (OHPA), a relatively small but vital group of bacteria, are the propionate and butyrate degraders of the system, and they help to stabilise the pH of the environment by preventing the accumulation of short chain fatty acids. The homoacetogenic bacteria produce acetate from mainly H_2/CO_2 and their role seems to be in lowering the H_2 partial pressure in the system.

Hydrogenotrophic methane bacteria metabolise H_2/CO_2 to methane, and the *acetoclastic methane bacteria* ferment acetate to methane and carbon dioxide. The methane bacteria are the primary bioregulators of the process. The H_2-utilising methanogens regulate the redox potential by removing H_2 from the

system, and the acetoclastic methanogens regulate the pH by removing acetic acid.

Studies aimed at improving the operation of working digesters have focused on the development of more meaningful process indicators (see Section 2.3). The ideal process indicator is thought to be one that is representative of the activities of the various bacterial groups involved in the anaerobic fermentation process, and it should preferably be measurable on-line. A number of promising methods have been proposed in the literature, including immunology and microcalorimetry, but further work is needed to verify their applicability. The trace gases H_2 and CO seem to show the most potential as early-warning indicators, although, most researchers agree that they should be interpreted in conjunction with a number of complimentary variables like pH, volatile fatty acids concentration, alkalinity, CH_4 and CO_2 concentrations, and gas production rate. The analysis and the interpretation of the multivariate data are problems that need to be more thoroughly addressed.

The technique of statistical process control has the potential to extract the information necessary for the control and improvement of the anaerobic digestion process. Control charts are the linchpin of SPC and various methods have been proposed for the construction of statistically valid control charts for wastewater treatment processes (see Section 2.4). Some of the methods, however, are quite intricate and, in most cases, probably unsuitable for routine use by plant operators. In recent literature there has been a considerable emphasis on

simplifying techniques, or simple techniques, for the operation of wastewater treatment plants.

This chapter outlines, and critically reviews, developments in the microbiology and control of the anaerobic digestion process, and the application of SPC and process regulation in the wastewater treatment industry.

2.2 THE MICROBIOLOGY OF ANAEROBIC DIGESTERS

The conversion of complex organic matter to methane in anaerobic digesters depends upon the coordinated actions of a metabolically diverse group of microorganisms. Fundamentally, the anaerobic digestion process consists of four stages: hydrolysis, acidogenesis, acetogenesis and methanogenesis. These stages are depicted in Figure 2-1 and some common reactions that occur in the course of anaerobic digestion are shown in Figure 2-2.

Hydrolysis and acidogenesis are carried out by acidogenic bacteria. These bacteria first hydrolyse carbohydrates, proteins and lipids to monosaccharides, amino acids, glycerol and long-chain fatty acids. The simple sugars, amino acids and glycerol are then further catabolised to volatile fatty acids (mainly formic, acetic, propionic and butyric acids), lactate, ethanol, molecular hydrogen and carbon dioxide. Obligately hydrogen-producing acetogens (OHPA) catabolise

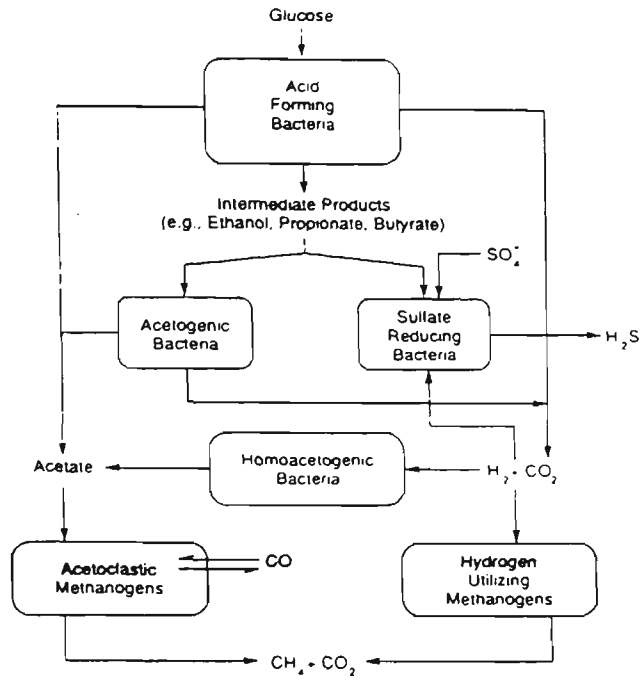

Figure 2-1 Microbial ecology of the anaerobic digestion process (Switzenbaum and Giraldo-Gomez et. al.[7]).

Hydrolysis

$$(C_6H_{10}O_5)_n + nH_2O \rightarrow nC_6H_{12}O_6$$

Acidogenesis

$$C_6H_{12}O_6 + 2H_2O \rightarrow 2CH_3COOH \text{ (acetic)} + 2CO_2 + 4H_2$$

$$C_6H_{12}O_6 \rightarrow CH_3CH_2CH_2COOH \text{ (butyric)} + 2CO_2 + 2H_2$$

$$C_6H_{12}O_6 + 2H_2 \rightarrow 2CH_3CH_2COOH \text{ (propionic)} + 2H_2O$$

Acetogenesis

$$CH_3CH_2COOH + 2H_2O \rightarrow CH_3COOH + CO_2 + 3H_2$$

$$CH_3CH_2CH_2COOH + 2H_2O \rightarrow 2CH_3COOH + 2H_2$$

$$2CO_2 + 4H_2 \rightarrow CH_3COOH + 2H_2O$$

Methanogenesis

$$CH_3COOH \rightarrow CH_4 + CO_2$$

$$CO_2 + 4H_2 \rightarrow CH_4 + 2H_2O$$

Figure 2-2 Common reactions occurring in anaerobic digestion.

certain fatty acids (e.g. propionate, butyrate, lactate) and neutral end products (e.g. ethanol) to acetate and hydrogen. Homoacetogenic bacteria catabolise unicarbon compounds (H_2/CO_2 and HCOOH) or hydrolyse multicarbon compounds (e.g. simple sugars, lactic acid, and pyruvate) to acetic acid. Finally, methanogenic bacteria catabolise acetate and single carbon compounds like H_2/CO_2, formic acid and methanol, to methane. Present understanding of the anaerobic digestion process is the culmination of more than 200 years of research, although the last 50 years have been the most progressive.

Knowledge of the fundamental mechanisms involved in the bioconversion of complex organic substrates to methane in anaerobic environments has come from studies of the growth, nutrition and metabolism of anaerobic bacteria and a quantitative description of the microbial ecology of anaerobic habitats. In 1776 the Italian physicist Alessandro Volta discovered that "combustible air" was formed in the sediments of streams, bogs and lakes where organic matter was being vigorously decomposed[8]. In the mid-1800s, Louis Pasteur established the concept of anaerobiosis as a result of his work on butyric fermentation[9]. A microbial basis for the formation of methane was eventually established through discoveries by Béchamp, Popoff, Tappeneiner, Hoppe-Seyler, Söhngen and Omelianski[8]. Much of what is known today about the anaerobic digestion process, though, has stemmed from the pioneering work on anaerobic culture techniques by R. E. Hungate almost 50 years ago.

An analysis of any microbial habitat requires knowledge of the number and types of microorganisms present. Hungate was the principal founder of

techniques for the culture and isolation of strict anaerobes. In his review of the bacteriology of anaerobic digesters, Hobson[10] pointed out that Hungate's early work with rumen flora led to advances in our knowledge of the microbial ecology of anaerobic sewage digesters. Earlier studies of anaerobic habitats suggested, erroneously, that facultative bacteria predominate in anaerobic digesters, and are the principal decomposers of organic matter in these habitats. High numbers of facultative bacteria exist in untreated sewage and therefore in anaerobic sewage digesters. Their main role, however, is now believed to be in maintenance of the low redox potentials in which the anaerobic bacteria flourish. A study of anaerobic digesters by Mah and Susman[11] showed that viable counts of bacteria grown on a nutrient agar medium and incubated aerobically were in the order of 10^5 or 10^6 per mL, whereas counts on anaerobic media were as high as 10^9 per mL.

The Hungate roll-tube method for cultivating strict anaerobes relies on the exclusion of all traces of oxygen from the medium during preparation, inoculation and incubation. The media originally used by Hungate for culturing rumen bacteria are essentially designed to simulate the rumen habitat. The media contained a solution of bicarbonate and phosphate for buffering, carbohydrate as substrate, reducing agent and ORP indicator for maintaining low redox potentials, and 10-20% rumen fluid as a source of nitrogen and growth factors. Roll-tubes were gassed with oxygen-free CO_2 (or 80% H_2-20% CO_2 for growing methanogens). The Hungate roll-tube method enabled counts of bacteria to be made and, by utilising different substrates, it was possible to enumerate the

various trophic groups in rumen and digester habitats. Hungate used these techniques to enumerate and develop cultures of anaerobic asporogenous cellulolytic bacteria which enabled an assessment for the first time of their importance in cellulose decomposition. Earlier workers, using impure cultures derived by enrichment culture techniques, had suggested, incorrectly, that cellulose could be fermented directly to methane by cellulolytic bacteria.

Bacteria that decompose complex organic matter to volatile fatty acids, carbon dioxide and methane, have been counted and isolated using the Hungate technique. Studies involving the isolates have revealed microbial associations and physical, chemical and biochemical factors that influence the anaerobic digestion process.

Perhaps one of the most notable discoveries made with the Hungate technique was the resolution of *Methanobacterium omelianski* by Bryant and Wolin et. al.[12]. The significance of substrate coupling became apparent when it was discovered that *M. omelianski* was actually a mutualistic association of two species and molecular hydrogen was their metabolic link. The two species were the 'S' organism, an obligate H_2-producing acetogen (OHPA), and *Methanobacterium* strain MoH, a H_2-catabolising methanogen. As Wolfe[13] explains, Bryant and Wolin et. al. demonstrated that the S organism oxidises ethanol to acetate and H_2 and is, in fact, inhibited by the H_2 produced. In an ethanol-carbonate medium, the S organism requires *Methanobacterium* strain MoH to use the H_2 which accumulates. Reddy and Bryant et. al.[14] showed that the S organism could grow axenically when metabolising pyruvate, but needed an

efficient H_2-using methanogen to facilitate its proton-reductive metabolism of ethanol. By removing H_2 from the system, the methanogen makes the metabolism of ethanol thermodynamically favourable for the OHPA. This form of substrate coupling is now known as interspecies hydrogen transfer.

Numerous other examples of associations have since been documented. In the presence of sulphate, sulphate-reducing bacteria (SRB) catabolise acetate and H_2 and produce H_2S. In the absence of sulphate these bacteria are OHPAs and metabolise ethanol or lactate in a mutualistic coculture with a methanogen[15]. *Clostridium thermocellum* forms stable associations with methanogenic and non-methanogenic species[16]. *C. thermohydrosulphuricum* utilises pentoses, which *C. thermocellum* cannot, and a commensalistic coculture of the two accounts for greater metabolism of total plant sugars than monocultures. In coculture with *Methanobacterium thermoautotrophicum* increased rates of cellulolysis and growth are due to interspecies hydrogen transfer. Many other associations have been described by Archer and Kirsop[17] and Zeikus[16].

Various modifications have since been made to the Hungate technique but the principal of preparing and sterilising media in the complete absence of oxygen remains. The serum-bottle technique[18] is easier to use and it reduces the risk of contamination during the transfer of media and cultures. In the serum-bottle method, media are prepared and transferred to serum bottles prior to sterilisation, and transfers are made with disposable hypodermic syringes and needles. Anaerobic chambers[19] have enabled the use of spread plates, replica plating, antibiotic sensitivity testing, and other standard bacteriological

techniques. The VPI technique[20] combines the simplicity of the Hungate and serum-bottle techniques and is very useful for the rapid inoculation of different media with one culture.

Many of the techniques that have been used to elucidate the ecology of, and the processes occurring within, an anaerobic digester have been described by Hobson and Summers[21]. These techniques include chemical analysis, microscopic observation, and the batch or continuous culture of pure or mixed populations. The chemical analysis of the inputs and outputs of a digester can indicate the main reactions occurring and may enable suggestions for improving the process, but an explanation is only possible when the microorganisms and their metabolism are considered. Microscopic observation can reveal large shifts in the proportions of morphological forms with variations in conditions (such as type and amount of input, pH, accumulation of certain metabolites) but the utility of microscopy is limited by pleomorphism, the difficulty in detecting small changes in mixed populations and the fact that it tells nothing about the reactions occurring. Batch culture in specialised media and colony counting allows an assessment of the predominant bacteria, and isolation of species enables classification of the microorganisms according to reactions, morphology or other criteria. Selective media can be used to enumerate species with particular biochemical properties and the relative concentrations of species or trophic groups can be investigated with respect to changing conditions or time. However, only bacteria capable of growing in a particular medium will be isolated or counted. Direct counts have the advantage that they do not rely on

growth in artificial media, but they tell nothing about the metabolic status of the bacteria being counted. Batch cultures can also be used to investigate growth rates, cell yields and substrate utilisation rates, but during growth in batch culture the bacteria are subject to varying conditions of substrate concentration, pH, end product concentration and bacteria concentration. These may all affect bacterial metabolism and the proportions of end products may be different from that occurring in the natural habitat. Continuous cultures in chemostats more closely approximate natural conditions. Studies of pure cultures can suggest how interactions of microorganisms may occur in heterogeneous systems. Many aspects of interactions, however, can only be determined using mixed cultures.

Activity tests can be used to assess the relative sizes of the various trophic groups in anaerobic digesters[22]. The usual method of batch culture and counting can suffer from suboptimal culture conditions, incomplete dispersion of bacteria that naturally occur in conglomerates (flocs, pellets or granules), and the fact that not all metabolically active cells are culturable (e.g. the obligate hydrogen-producing acetogens). In the activity test, a simple mineral salt medium containing a specific substrate is inoculated with anaerobic sludge and the rate of methane production is measured by gas chromatography. Comparing the activity of the sludge to a pure culture can indicate the size of the population. Activity testing can be a useful alternative to viable counting for studying the ecology of digesters.

Isotopic labelling has been used to determine the relative contributions of acetate and H_2-CO_2 to methane production in anaerobic digesters[23]. Using

labelled CO_2, and assuming that all methane not produced from labelled CO_2 was formed from acetic acid, Jeris and McCarty[24] deduced that acetate is the precursor of 70% of the methane produced during anaerobic digestion. Smith and Mah[25] used an isotopic dilution procedure to determine the contribution of acetate to methane formation in anaerobic sludge. Using a large pool of acetic acid (4.7μmol/mL) which is taken to be constant over the course of the experiment, and a small concentration of labelled acetic acid, it can be inferred that the rate of dilution of the isotope is due to the formation of new acetic acid molecules. Assuming that each mole of acetate produces one mole of methane, and comparing the rate of formation of acetic acid (0.024 μmol/mL/min) to the rate of methane production (0.033 μmol/mL/min), Smith and Mah established that acetic acid accounted for 73% of the methane formed.

Wolfe[13] studied the biochemistry of methane formation using labelled substrates. Wolfe used a modified Warburg flask to determine which substrates are active in the formation of methane by cell-free extracts. The Warburg-flask method was also used to study inhibitors of methane formation and the role of adenosine triphosphate (ATP) and coenzyme M.

The energy within cells is carried by ATP and the production of ATP is coupled to intracellular energy-yielding processes. Substrates are not completely oxidised by anaerobic metabolism and so less moles of ATP are produced per mole of substrate, compared to aerobic metabolic processes, and compounds like ethanol, butyric acid and methanol are excreted.

Fermentation is an energy yielding process in which ATP is generated by substrate level phosphorylation (SLP). The electron donor is an organic compound and the terminal electron acceptor is an organic intermediate metabolite. Many of the catabolic pathways are branched and the branches have different thermodynamic efficiencies and yields of ATP. The organism optimises its metabolism to suit the prevailing conditions of pH and temperature, for example, and as a consequence different proportions of end-products can result. SLP is used almost exclusively by many anaerobes for the production of energy. Phosphophenyl pyruvate, acetyl phosphate and butyrl phosphate are among the few energy rich compounds that serve as intermediates in SLP reactions.

Carbohydrates are fermented via the Embden-Meyerhof-Parnas and butyric pathways to mainly acetate, propionate, butyrate, hydrogen, lactate, formate, ethanol and carbon dioxide. Amino acids, which derive from proteins, can be fermented by *Clostridium* sp. via the Strickland reaction[9]. In the Strickland reaction pairs of amino acids are fermented, one serves as the electron donor and the other acts as the terminal electron acceptor. Many butyric acid producing clostridia also ferment single amino acids via pyruvate and some clostridia ferment carbohydrates by pathways other than the butyric pathway. Neutral fat is hydrolysed to glycerol and long chain fatty acids. Glycerol is fermented along with carbohydrates whilst the long chain fatty acids are not catabolised by acidogenic bacteria.

Some acidogenic bacteria that utilise the same substrates as one another actually have very different metabolisms at the enzyme level[16].

Thermoanaerobium brockii and *Clostridium thermocellum* both ferment glucose and cellobiose to H_2, CO_2, acetic acid, lactic acid and ethanol, but the end-product ratios are quite different. The difference is related to the specific activities and regulatory properties of their enzymes. For example, the ethanol/H_2 ratio is about twenty times higher for *T. brockii*. *T. brockii* exhibited reversible nicotinamide adenine dinucleotide (NAD) and nicotinamide adenine dinucleotide phosphate (NADP) linked ethanol dehydrogenases, whereas *C. thermocellum* had irreversible NAD linked ethanol dehydrogenase. Unlike *C. thermocellum*, growth of *T. brockii* is inhibited by high H_2 partial pressures and, in the presence of an efficient H_2 sink, such as a methanogen, growth occurs solely on ethanol. *T. brockii* will either produce or consume ethanol depending on environmental conditions.

Anaerobic respiration is an energy yielding process that utilises an electron transport chain, located in the cytoplasmic membrane, in which oxygen is not the terminal electron acceptor. Electron transport phosphorylation (ETP) depends on the potential difference between redox couples to drive the production of ATP. The energy yield in anaerobic ETP is much lower than in oxidative phosphorylation and accordingly, growth yields and rates are low compared to aerobic bacteria.

Methanogens derive energy from ETP. Some of the electron transport proteins detected in methanogens include flavoproteins and cytochromes. The structure and function of coenzyme M and coenzyme F_{420} are understood but,

generally, the electron transport pathway in methanogens is not yet fully characterised[16].

The electron carriers are membrane bound, most are oxygen sensitive, and they operate at extremely low redox potentials. Almost all species of methanogenic bacteria utilise hydrogen and carbon dioxide as substrates, and some species can also utilise acetate. Of the substrates used by methanogens, acetate actually provides the smallest energy yield. Owing to the microbial ecology of anaerobic digesters, and the balance that is achieved between the various trophic groups, acetate is the more abundant substrate and, therefore, the precursor of most of the methane produced.

Despite the fact that digesters have not been fully characterised in terms of ecology and metabolism, a reasonable description of the anaerobic digestion process has been built from knowledge of the growth, nutrition and metabolism of selected species from each of the four main trophic groups. Fundamental to this description is the way in which the various groups of bacteria can effectively self regulate their environment by interacting to control pH and redox potential (i.e. H_2). A departure from neutral pH (i.e. ± 0.4 pH units) can inhibit methanogens, and high H_2 partial pressures ($>10^{-4}$ atm) have been reported to inhibit acidogenesis[3], acetogenesis from propionate and butyrate, and even acetoclastic methanogenesis[17]. Further to their role in controlling the pH and redox potential, methanogens may also play a role in nutrient regulation. It is thought that methanogens actually excrete vitamins and amino acids that are used

by representatives of all trophic groups[16]. Methanogenic bacteria are now believed to be the main bioregulators of the anaerobic digestion process.

2.3 MATHEMATICAL MODELING AND CONTROL OF THE ANAEROBIC DIGESTION PROCESS

The information derived from fundamental ecological and biochemical studies of the anaerobic digestion process, reviewed in Section 2.2, has been funnelled into the process control domain through the development of mechanistic mathematical models and the identification of meaningful process indicators. Most models of the anaerobic digestion process are expressed as deterministic-mechanistic differential equations which are solved numerically and used to examine hypotheses, study system dynamics and evaluate process control schemes. One advantage of this kind of simulation is the reduced cost of experimentation, but, the real value of mechanistic models lies in the insight they provide into the workings of the process. Many of the mechanistic models proposed for anaerobic digestion have not, however, been calibrated or verified experimentally, and have not been applied to the operation of a working anaerobic digester. For the operators of wastewater treatment plants (WWTP), deterministic models are "theoretical" and have little application in the "real world".

Wastewater treatment processes are significantly affected by stochastic disturbances. These disturbances include the highly variable nature of influent

quantity and composition, and environmental factors, like temperature. To bridge the gap between "theoretical" and "real world" models, some researchers are working on a stochastic-mechanistic model of the anaerobic digestion process. The modelling approach adopted by these researchers is examined later in this section. The fundamental difference between a deterministic process and a stochastic one, is that the former follows a predetermined pattern (e.g. a linear or quadratic equation), whereas a stochastic process evolves in time according to the laws of probability.

In addition to the modeling approach, other process control efforts have focused on the development of better process indicators. Effective control of the anaerobic digestion process, especially high-rate systems, is contingent upon reducing the time delay between the onset of an upset and its detection. For clarity, the terms "response variables", "state variables" and "process indicators" are interchangeable.

Early models of the anaerobic digestion process were based on a two-stage process (the acidogenic stage and the methanogenic stage) and considered four trophic groups of bacteria, including acidogens, hydrogen-producing acetogens, acetoclastic methanogenic bacteria and hydrogenotrophic methanogenic bacteria[26]. Acidogenic bacteria were responsible for the acidogenic phase, while the methanogenic phase involved a syntrophic consortium of hydrogen-producing acetogens and methanogenic bacteria.

The dynamic models were developed from material balances for a continuously stirred tank reactor (CSTR), and rate equations were based around

Monod kinetics[26]. The acidogenic and methanogenic phases were separated in a chemostat, by controlling the dilution rate, in order to evaluate the biological kinetic and cell-yield coefficients for each phase. For example, a model for the rate of change of bacterial biomass, X, in a CSTR can be written as:

$$\begin{array}{lcccccc} \textit{Mass rate of change in } X & = & \textit{change due to inflow} & + & \textit{change due to growth} & - & \textit{change due to outflow} \\ \dfrac{dX}{dt} & = & 0 & + & \mu X & - & \dfrac{Q}{V}X \\ \dfrac{dX}{dt} & = & \mu X & - & \dfrac{Q}{V}X & & \end{array}$$

where μ = specific growth rate

Q = flowrate

V = volume of the CSTR.

Similar mass-balance equations can be written for initial and intermediate substrate concentrations. The dependence of the specific growth rate on substrate concentration is described by the Monod equation:

$$\mu = \frac{\mu_{\max} S}{K_s + S}$$

where μ_{max} = maximum specific growth rate

K_s = Monod coefficient (or half-saturation constant)

S = substrate concentration.

The dynamic models are based on these fundamental equations, and can include terms that take into account various biological mechanisms like the inhibition of methanogenesis by un-ionised fatty acids[26]:

$$\mu = \frac{\mu_{\max}}{1 + K_s/[HS] + [HS]/K_{I,a}}$$

where $[HS]$ = concentration of un-ionised fatty acids

$K_{I,a}$ = inhibition coefficient of un-ionised fatty acid.

The concentration of total fatty acid depends on the balance between the acidogenic and methanogenic phases. The concentration of un-ionised fatty acid depends on the total fatty acid concentration and the pH. The pH in the digester (or CSTR) is affected by the alkalinity and by the CO_2 concentration in the gas phase, and these in turn are affected by the flowrate, initial substrate concentration and growth rates of the bacteria. These relationships, and others, are expressed mathematically as differential equations and chemical equilibria. Together, these equations describe the phenomena in the anaerobic digestion process.

The formulated models and estimated coefficients provide the means to clarify process characteristics and develop reactor design criteria. The comparison of model parameters for the acidogenic and methanogenic stages highlights some important differences. The growth yield coefficient for acidogens (0.16 - 0.40) is higher than that for methanogenic bacteria (0.02 - 0.12). This indicates that acidogenic bacteria predominate in anaerobic digesters. In fact, this substantiates earlier studies of the ecology of anaerobic digesters. The maximum specific activity of acidogenic bacteria on glucose or starch is greater than the maximum methanogenic activity, which indicates that methanogenesis is rate-limiting when these substrates are used as feedstock. The acidogenic activity on cellulose or sewage sludge, however, is comparable to that for the methanogenic phase, suggesting that hydrolysis might be rate-limiting in

this case. Furthermore, acidogenic bacteria need much shorter retention times (0.03 - 0.6 days) than methanogenic bacteria or hydrogen-producing acetogens (0.9 - 13 days).

Various models have been developed to investigate the effect of temperature, the relationship between pH and VFA toxicity, heavy metal toxicity and the antagonistic or synergistic relationships between certain metals, and the inhibitory effect of long-chain fatty acids[26]. Of particular interest, though, is the application of dynamic models to the control of the anaerobic digestion process.

Graef and Andrews[27,28] found that methane production rate, substrate concentration, CO_2 concentration in dry gas, and pH, were useful indicators of process upsets. They also experimented with a feedback control scheme that was based on the pH of the reactor contents, and evaluated four control actions including gas scrubbing and recycling (to remove CO_2 and raise the pH), base addition, cell recycling, and flow regulation. Collins and Gilliland[29] experimented with feedforward control and found that predictive flow control was an effective means of controlling the pH.

With the discovery of substrate-coupling came new models of the anaerobic digestion process. Mosey[3] presented a dynamic model that took into account the rates of substrate utilisation and cell growth of four trophic groups of bacteria involved in the fermentation of glucose to methane and carbon dioxide. This model included the new regulatory function of interspecies hydrogen transfer. The basic premise of the model is that hydrogen-utilising methane bacteria regulate the metabolism of acidogenic and acetogenic bacteria by

controlling the redox potential of the process (i.e. by consuming H_2 gas), and acetotrophic methane bacteria control the pH by removing acetic acid.

Mathematical expressions for the regulation of metabolism by hydrogen were derived from the known redox potential of the NAD/NADH (the oxidised and reduced forms of the carrier molecule nicotinamide adenine dinucleotide) couple. Thermodynamics shows that acidogenic bacteria derive the biggest energy yield from the conversion of glucose to acetate. However, in response to H_2 accumulation during surge loads, acidogens re-direct their metabolism to butyric and propionic acid formation (see Figure 2-2, p. 2-5). This has the dual effect of reducing the H_2 and total acid output.

The acetogenic bacteria are assumed to be obligate propionate utilisers and obligate butyrate utilisers. High H_2 concentrations can inhibit propionate degradation (50% inhibition at 670 ppm in this model) and it has been reported that the accumulation of propionic acid could be the cause of the condition known as a "stuck" digester.

Hydrogen-utilising methane bacteria control the redox potential of the system by removing H_2. As the proportion of NADH to NAD increases, due to an increase in the H_2 concentration, the rate of acid formation slows and both butyric acid and propionic acid accumulate.

Acetoclastic methane bacteria, not generally affected by high H_2 partial pressures according to Mosey, normally control the pH of the system by removing acetic acid. Their inability to metabolise propionate can contribute to propionic acid overload.

One drawback with the models presented by Hanaki and Noike et. al.[26] and Mosey[3] is that that the models have not been calibrated or verified. Smith and McCarty[30], on the other hand, developed a dynamic energetic-kinetic model, based on expected biological transformations, and compared the experimental results with the model's predictions in order to detect and identify limitations in the understanding of anaerobic fermentation mechanisms.

The model used by Smith and McCarty[30] simulated methane production, organic substrate and product concentrations, hydrogen partial pressure, and bacteria concentrations in an anaerobic CSTR which was fed a mixture of ethanol and propionate. The differences between the observed and predicted effect of a quantitative shock-loading highlighted the significance of the formation of reduced intermediates following a sudden increase in substrate concentration. In both the simulated and actual experiments, methane production followed a cyclic pattern after shock-loading. Metabolism of the excess ethanol resulted in an increase in hydrogen and acetate concentrations. The increase in hydrogen partial pressure caused propionate metabolism to stop. Methane production increased initially from hydrogen, and then later from acetate. When the hydrogen level dropped, propionate degradation resumed with a consequent rise in methane production from the hydrogen and acetate that was produced.

The actual pattern in methane production differed from the model in that it was more erratic and apparently affected by the formation of reduced intermediates (including n-butyrate, n-valerate, n-caproate, n-heptanoate and n-propanol) that were not considered in the model. Smith and McCarty[30] theorised

that the production of reduced products buffered the shock-loading by consuming excess electrons and preventing an excessive accumulation of organic acid. Despite the buffering effect, though, only 30% of the additional substrate was converted to methane.

Smith and McCarty[30] also noted that whilst the rate of methane formation can serve as an indicator of process performance, it is affected by the activities of both the methanogens and the numerous other bacterial groups involved in the bioconversion of complex organic wastes. That is, it is not specific to the methane formers.

It is interesting that none of the models proposed in the literature have considered the role of the homoacetogenic bacteria. Zeikus[16] believes that the homoacetogens play a part in the regulation of the redox potential by consuming hydrogen and by fermenting multicarbon compounds without producing hydrogen. Their ability to lower the hydrogen partial pressure seemingly outweighs their ability to compete with methanogens for H_2/CO_2.

Jones and MacGregor et. al.[31,32] have experimented with a dynamic model that can be used for on-line estimation and forecasting in an actual process control system. Aware of the limitations of deterministic models of biological treatment processes, these authors attempted a stochastic-mechanistic model of the anaerobic digestion process that takes into account unmeasured stochastic disturbances and the complex mechanisms that do not appear in mechanistic models. The basic postulate in their modelling approach is that certain variables, like the concentration of acetoclastic methane bacteria, are a more direct measure

of process performance than conventional response variables like pH. However, counts of bacteria are difficult and time consuming, and are therefore not useful in a process control sense. To overcome this problem, Jones and MacGregor et. al. developed a Kalman filter state estimation algorithm that combines data from on-line sensors with a mechanistic model in order to track process states that are not directly measured.

The components of the Kalman filter model are:

- Measured inputs: feedrate and feed concentrations (soluble organics, propionic acid, butyric acid, acetic acid and non-biodegradable compounds).
- Deterministic states: effluent concentrations of biodegradable soluble organics, propionic acid, butyric acid, acetic acid, and non-biodegradable compounds. The deterministic states are modelled as a function of the input variables and the bacteria concentrations, growth rates and yields.
- Stochastic states: bacteria concentrations (acid formers, propionate-degrading acetogens, acetoclastic methanogens).
- Measured states: the deterministic states plus an additional measured output, methane gas flowrate.
- Unmeasured states: the stochastic states.

Essentially, all measurements on process outputs (i.e. the measured states) are expressed as a function of the input variables and state variables (deterministic and stochastic) at previous points in time. The Kalman filter uses the prediction errors (i.e. the difference between the observed and the predicted outputs) to update the state estimates, thereby tracking the bacteria concentrations. Note that

making control decisions is not an explicit purpose of the Kalman filter model in this case, although the unmeasured states can provide the feedback signals necessary for process adjustments. A schematic of the extended Kalman filter algorithm is shown as Figure 2-3.

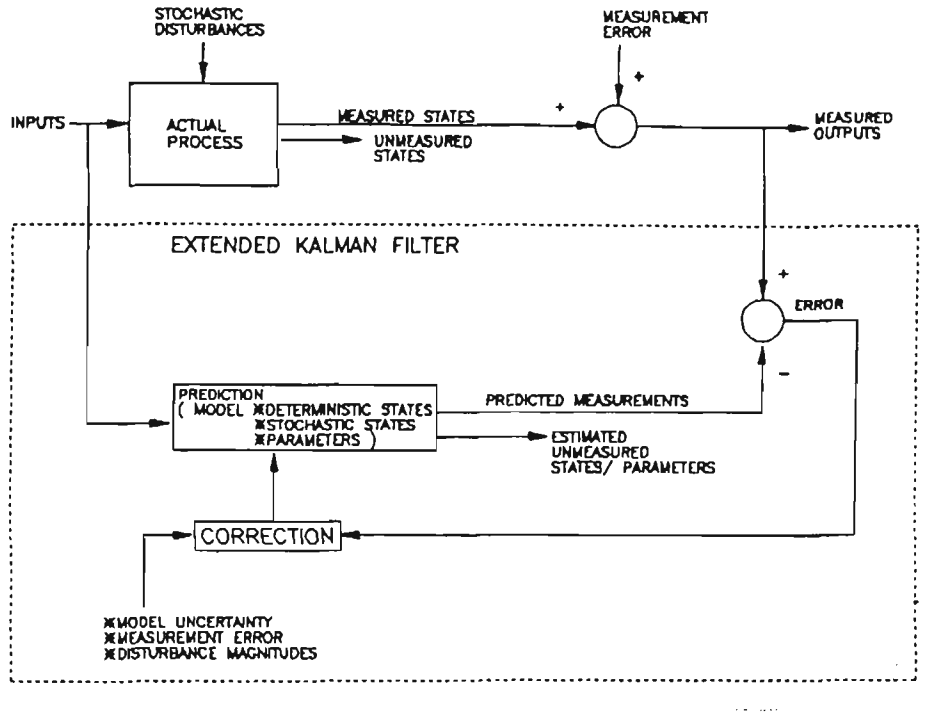

Figure 2-3 Schematic representation of the extended Kalman filter (Jones and MacGregor et. al.[32])

Whilst promising, Jones and MacGregor et. al. acknowledge that the model needs further development, particularly in the area of bacterial mass balances. In addition, they note that verifying such a model is problematic due to the difficulty in measuring concentrations of bacterial groups, and they suggest that a method for the on-line measurement of the activities of bacterial groups is required. It seems, however, that if such a method existed then there would probably be no need for the model.

Improved control of the anaerobic digestion process can be achieved by reducing the time between the occurrence of an upset and the detection of that upset[7]. In addition to the modelling approach to process control, considerable work has been done to develop more meaningful and more responsive process indicators.

Switzenbaum and Giraldo-Gomez et. al.[7] claim that the classical response variables, like pH and gas production rate, are useful for detecting and correcting gradual process changes, but cannot adequately protect against process failure in modern high-rate digesters. The ideal indicator, according to these authors, should be easy to measure, it should be indicative of the metabolic state of the bacteria, and it should be measurable on-line. These are the criteria that they have used in their review of the various techniques that have been developed or used to monitor the anaerobic digestion process.

Switzenbaum and Giraldo-Gomez et. al. have grouped the many available indicators into three categories - solid phase, liquid phase and gas phase- and discussed each in turn (Figure 2-4).

The solid-phase indicators generally aim to warn of process upsets through the measurement of viable cells and their current metabolic status. Based on the review presented by these authors, microcalorimetry and the immunology of methanogens are two techniques that show promise. Both of theses techniques are suitable for on-line measurement but further development is required.

Liquid-phase indicators including pH, volatile fatty acids (VFAs), and alkalinity, are the most commonly monitored variables. They are not, however,

particularly useful as early warning indicators because changes are generally signalled some time after an imbalance has developed.

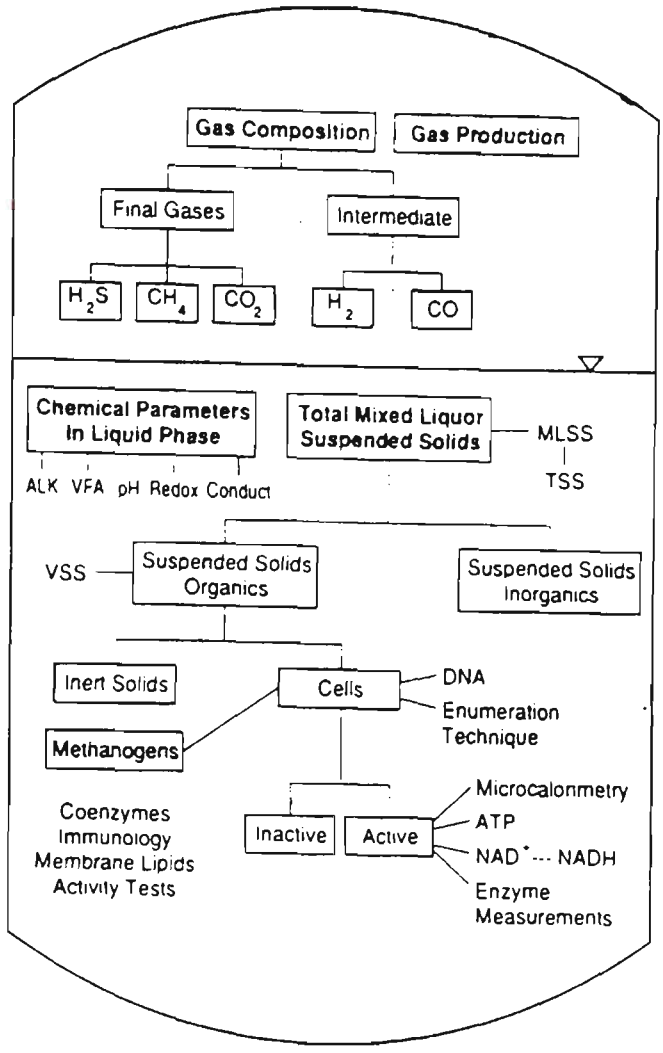

Figure 2-4 Process indicators of the anaerobic digestion process (Switzenbaum and Giraldo-Gomez et. al[7])

Similarly, in the gas phase, methane and carbon dioxide are useful process indicators, but they are sluggish in their response to changes. Trace gases, H_2 and CO, on the other hand, provide useful information on the metabolic status of the digester, have relatively short response times, and are easily measured on-line.

Switzenbaum and Giraldo-Gomez et. al. believe that H_2 and CO are two of the better indicators available. However, due to the incomplete knowledge of

digester ecology, these variables should be interpreted in conjunction with more conventional indicators like pH, the concentration of VFAs, alkalinity, and levels of CH_4 and CO_2. They proposed that more work be done to develop simple tests that characterise the metabolic activities of the various bacterial groups. These tests should quickly detect changes in the metabolism of the population affected and thus permit timely corrective action to be taken.

Fitzgerald[33] studied the critical response variables, in a pilot scale fluidised-bed anaerobic reactor, to determine which variables are most suitable for rapid monitoring and control. The reactor was fed a semi-defined medium containing yeast extract. The variables studied were pH, electrode potential (or redox potential), and concentrations of acetic and propionic acids, CH_4, CO_2 and H_2. The response of these variables was measured after perturbing the system (either by deliberately increasing the feed strength or as a result of equipment failure).

The changes in the concentrations of CH_4 and CO_2 were detected before changes in gas volume production. Moreover, CO_2 reacted more quickly than CH_4. Acetic acid responded more quickly than propionic acid. The H_2 concentration had the quickest reaction. When the organic loading rate was increased, H_2 levels responded almost immediately, followed by acetic acid and propionic acid. CO_2 and CH_4 seemed to show small changes in level (not discussed by Fitzgerald).

Fitzgerald employed a daily sampling program, but suggested that earlier detection of process upsets would have been possible if continuous analysers or

more frequent sampling was used. Fitzgerald summarised the response times of various indicators, as found by other researchers. Typical response times for the variables considered were H_2<10 min, VFA<2 hr, CH_4 and CO_2<1 hr.

Like Fitzgerald, Mathiot and Escoffier et. al.[34] had studied the response times of a number of variables in a pilot scale fluidised bed reactor. This reactor was fed wastewater from a wine distillery. The variables included VFA (acetic and propionic acid), pH, temperature, effluent TOC, CH_4, CO_2 and H_2 levels, and overall gas production rate. When the influent concentration was increased the concentrations of H_2, CH_4, VFA, and effluent TOC increased, whilst the gaseous CO_2 concentration decreased. A change in influent flowrate produced a similar pattern in the response variables. When the temperature was decreased, the pH dropped and the effluent TOC remained stable. A change in the VFA concentration was not observed but others have reported that it can increase[35]. The CH_4 concentration increased and the CO_2 concentration decreased, perhaps due to the dissolution of CO_2. A change in substrate resulted in an increase in the H_2 concentration, but all other variables remained stable.

Generally, all of the variables studied reacted quite rapidly - usually less than 1 hour after shockloading - and most can be measured on-line. For the rapid detection of upsets, Mathiot and Escoffier et. al.[34] suggest monitoring a number of complimentary variables. They say that gaseous H_2 is a useful indicator but it should be interpreted in conjunction with CH_4, CO_2 and gas production rate.

There are a number of patterns emerging from past research on the process control of anaerobic digesters. Firstly, wholly deterministic models of the

anaerobic digestion process are not particularly suitable for controlling an actual digester. This is because the actual behaviour of biological wastewater treatment processes is affected by unmeasured stochastic disturbances and, due to the incomplete understanding of the process, there are some complex mechanisms that are not accounted for in these models. Secondly, there is no universal process indicator for the anaerobic digestion process. Process control is apparently best effected through the use of a number of complimentary variables like pH, VFA, alkalinity, VS (volatile solids), CH_4, CO_2, H_2, and gas production rate. Lastly, it is possible that the multivariate pattern in these variables may be used to determine the nature of process upsets.

2.4 STATISTICAL PROCESS CONTROL AND PROCESS REGULATION APPLIED TO WASTEWATER TREATMENT PLANTS

Simply stated, statistical process control (SPC) is a statistical tool for the control and improvement of any process. The control chart, the linchpin of SPC, is a graphical device that tracks process performance over time. Control charts clarify the process data by distinguishing between randomness and process upsets. SPC originated in the discrete-parts manufacturing industries but has evolved to find application in continuous-flow processes, including wastewater treatment plants. Normal distributions, data independence and homoscedasticity are the standard assumed properties of data generated in the parts industries. These properties underpin the classical use of process control charts. Wastewater

treatment plant data usually exhibit quite different statistical properties and, as a result, new techniques for constructing control charts were investigated. Various methods have since been proposed for the design of statistically valid control charts that apply to wastewater treatment plant operation. In the course of evolution, however, the control chart has become a much more complex 'animal'. In recent literature, there is a considerable focus on simplifying procedures, or simple procedures, for quality control. The purpose of this new direction is to ensure that control charts remain understandable to process operators.

The classical control charts include the Shewhart chart, the cusum (cumulative sum) chart, the moving average chart and the exponentially weighted moving average (EWMA) chart. In essence, these charts are constructed by estimating the natural variability in a process (i.e. a process characteristic like BOD_5) and then expressing this variability as control limits on a time-series chart. All future observations are plotted on the chart and referenced against these control limits. Control limits are typically set at plus and minus three times the standard deviation. By doing so, the probability of an observation falling outside these limits purely by chance is very small (0.003). This probability is known as the level of significance and is given the symbol α. An example of a Shewhart control chart is shown in Figure 2-5.

The natural variability in a process arises from a "common" cause system which might include sampling error, measurement error, and fluctuations in the composition of raw sewage. If an observation falls outside the control limits, it is

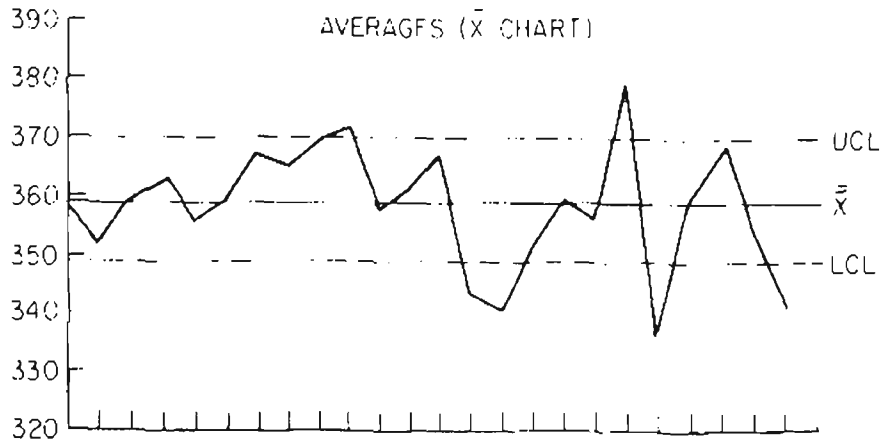

Figure 2-5 An example of a Shewhart chart, or $\overline{X}$ chart (Juran and Gryna[36], Ch. 28).

likely that an "assignable" cause of variation exists. An assignable cause of variation might be an illegal discharge to the sewer or a mechanical fault.

In classical SPC theory, the objective is to identify and eliminate the assignable causes of variation, thereby maintaining the process on target and containing process variability. The same objective applies to WWTP's when the assignable cause of variation is fixable in the short term. Examples might include mechanical faults, power interruptions, bio-fouling of process sensors, the gradual wear of pump impellers, or the build-up of scale in pipes. In some cases, the elimination of assignable causes requires careful regulation and monitoring of industrial discharges, and strategic planning. These are long-range tasks. However, if a process upset is attributable to a shockload or a gradual change in sewage composition, the short term objective is to compensate for (rather than eliminate) the assignable cause of variation - before it translates into a breach of licence conditions. The long term objective is to identify the cause of the upset,

measure its effect on the process (i.e. small, reasonable or disastrous) and determine its frequency of occurrence. This will enable an objective assessment of the risks before choosing an appropriate action.

All of the standard control charting methods assume that the underlying process conforms to the model:

$$\overline{X}_t = \mu + a_t \qquad \textbf{Equation 2-1}$$

where $\overline{X}_t$ = observations of the process characteristic (an observation can be the average of a subgroup of size n_g, or an individual observation)

t = 1,2,3,...,n

n = number of observations in the data series

μ = mean of X (assumed fixed)

a_t = random disturbances which are assumed to be independent and identically distributed with zero mean and variance σ_a^2.

The various control charting methods differ in the way they weight previous observations[37]. If V_t denotes the performance indicator then the various charts are based on:

Shewhart chart $V_t = \bar{x}_t$

CUSUM chart $V_t = \sum_{i=1}^{t} (\bar{x}_i - T)$

where T = target value (often equal to μ)

Moving Average (MA) chart

$$V_t = \frac{1}{k} \sum_{i=t-(k-1)}^{t} \bar{x}_i$$

where k = subgroup size

Exponentially Weighted Moving Average (EWMA) chart

$$V_t = (1-\lambda) \sum_{i=0}^{\infty} \lambda^i . \bar{x}_{t-i}$$

$$\Rightarrow \quad V_t = (1-\lambda)\bar{x}_t + \lambda V_{t-1}$$

where $0 < \lambda$ (the weight factor) < 1

The Shewhart chart places a weight of one on the current observation and zero weight on all previous observations. The cusum gives equal weight to all observations. The moving average (MA) gives equal weight to the k most recent observations and zero weight to all others. The EWMA gives the most weight to the current observation and progressively less weight to previous ones. Depending on the weighting factor λ, an EWMA chart can approximate any of the other classical control charts.

The weight placed on the current and past observations is one factor that determines the ability of a chart to detect certain shifts in mean level. The Shewhart chart is good for detecting large changes in the mean of a process characteristic. The cusum chart is particularly suited to detecting small steady changes in level. The MA and EWMA charts lie somewhere in between the Shewhart and cusum charts. On a more quantitative level, the charts can be compared in terms of their in-control and out-of-control average run lengths. These measures of chart performance will be explained in more detail later in this section.

Most wastewater treatment processes are characterised by more than one variable. For example, effluent quality is often described by the levels of suspended solids, nitrogen compounds and phosphorus compounds, the pH, and the biochemical oxygen demand. The state of an anaerobic reactor is often measured in terms of the pH, the VFA level, alkalinity, concentrations of H_2, CH_4, and CO_2, and gas production rate. In addition to the classical univariate control charts already briefly discussed, multivariate procedures exist for the control of two or more variables simultaneously[37].

With any control chart procedure there is a risk associated with each control decision. Deciding that a process is out-of-control when it is actually in control is called the Type I error (α). Deciding that a process is in-control when it is actually out of control is the Type II error (β). When several variables need to be considered, multivariate procedures can provide a single answer with a prescribed Type I error size and can be more sensitive to out-of-control states than their univariate counterparts. When several variables are monitored it is common to plot them on separate control charts, though, this can lead to problems with both Type I and Type II errors. The following example of an effluent that is characterised by its BOD_5 and SS concentrations is adapted from Berthouex[37]. Assuming the two variables are uncorrelated and each is plotted separately on a chart with Type I error risk of 0.003, the effective Type I error size when considering both variables is $1-(.997)^2 = 0.006$. The consequence is that more false alarms can be expected. Now, suppose that an effluent sample is found to have BOD_5 and SS (suspended solids) levels that both fall between +2

and +3 standard deviations of their respective means. The probability that an observation will lie outside $\bar{x}+2\sigma$, due to chance alone, is approximately 0.0228. Therefore, if the BOD_5 and SS were considered separately, the process would be deemed in a state of statistical control. However, the probability that both variables will exceed their long term averages by two standard deviations, purely by chance, is (0.0228)(0.0228)=0.00052. That is, given that the joint probability of this occurrence is less than 0.003 (the prescribed Type I error size, α), the process should actually be judged out-of-control. The problem becomes even more complicated when the variables are correlated.

Perhaps the most common of the multivariate techniques is Hotelling's T^2 chart. Like Student's t, Hotelling's T^2 is a measure of statistical distance, and it can be calculated directly from the original variables using:

$$T^2 = (\boldsymbol{x} - \bar{\boldsymbol{x}})' \boldsymbol{S}^{-1} (\boldsymbol{x} - \bar{\boldsymbol{x}})$$

where $\boldsymbol{x}$ and $\bar{\boldsymbol{x}}$ are vectors of the original variables and their means, respectively, and $\boldsymbol{S}$ is the variance-covariance matrix[38]. The T^2 statistic provides an overall measurement of the conformance of an observation vector to its mean or established standard. Hotelling's T^2 can also be calculated from the principal components of the original variables:

$$T^2 = \boldsymbol{y}\boldsymbol{y}'$$

where $\boldsymbol{y}$ is a vector of the standardised principal components. In fact, an alternative to a Hotelling's T^2 chart, is to chart each of the sample principal components separately. This approach has the advantage that it may better

indicate which variable(s) are out of control (depending on the component loadings) whilst retaining a sensitivity comparable to the Hotelling's T^2 chart.

A problem with univariate and multivariate charting procedures alike, is that a reasonable amount of 'in-control' data needs to be gathered before the control chart parameters can be determined. For anaerobic digestion, in particular, this means that the process will be without a formal control procedure during its most vulnerable stage, start-up. Tang[39] has investigated a multivariate control procedure which can be used during start-up of the process, or start-up of the charting procedure, without requiring prior estimates of the process parameters. The procedure uses a probability integral transformation of a (Hotelling) T^2-type statistic to produce sequences of independent or approximately independent standard normal variables.

As mentioned earlier, control limits have traditionally been set at plus and minus three times the standard deviation (sigma) of the process variable. With the 3 sigma control limits, the probability that an observation will fall outside the limits, due to chance alone, is 3 in 1000. Shewhart originally chose to use 3 sigma limits quite arbitrarily. These days, however, the 3 sigma limits are a quasi-standard.

Berthouex and Hunter[40] have discussed the economic design of a Shewhart chart, in the context of a WWTP, which provides an economic rationale for choosing the width of control limits. This approach to control chart design incorporates the control chart parameters and sampling frequency into an economic model. An economically reasonable control chart is found by

minimising the cost function with respect to the width of the control limits, the sampling frequency and the number of samples taken at each sampling time.

Whilst there are some errors in the paper by Berthouex and Hunter[40], it still provides an excellent introduction to the economic design of control charts and choice of sampling frequency. Essentially, the average daily cost of the control program, C, is the average cost per day when the plant is operating satisfactorily (in control), A, plus the average daily cost of being out of control, R, that is, $C=A+R$. The in-control cost includes the cost of sampling and testing, and the cost of analysing the data:

$$A = \frac{b + c}{S}$$

where b = average daily sampling cost

c = average daily cost of testing and data analysis

S = time between samples.

The average daily cost of being out of control is:

$$R = a_f T + \xi W + \gamma C_p$$

where a_f = average number of false alarms per day

T = average cost of searching for an assignable cause when none exists

ξ = average number of out-of-control times per day

W = average cost of searching for an assignable cause when one exists (usually $W=T$)

γ = fraction of time the process is out of control; and

C_p = daily penalty cost for being out of control.

In the paper by Berthouex and Hunter[40], T was wrongly defined as the total daily cost of searching for an assignable cause when none exists. Actually, T is the average cost of searching for an assignable cause when none exists, and the daily cost is $a_f T$, where a_f is the average number of false alarms per day. Assuming that the time between the occurrence of assignable causes is exponentially distributed with mean $1/\lambda$, the average daily cost of the control program can then be shown to be:

$$C = \frac{b+c}{S} + \frac{\alpha T}{t_c \lambda S} + \frac{W}{t_c} + \frac{t_r C_p}{t_c}$$

where α = Type I error probability, or level of significance

t_c = average length of one control cycle

λ = average frequency of upsets

t_r = average length of time the system is out of control in one control cycle.

In the equation given by Berthouex and Hunter[40], the last two terms on the right-hand side were not divided by t_c. This is the cost model that is used to estimate the economic sampling interval and the control chart parameters. It should be noted that the model is based on a number of simplifying assumptions which have not been discussed here.

The economic basis for control chart design acknowledges that there must be a balance between the cost of a monitoring program and the protection afforded by that program. The three basic costs, considered by Berthouex and

Hunter, are the cost of sampling and testing, the cost of investigating out-of-control signals, and the cost of producing substandard effluent. The protection aspect of a monitoring and control program is essentially related to the consequences of producing substandard effluent and the time it takes to detect an upset.

For a Shewhart chart, the in-control average run length (ARL), which measures the efficiency of the control scheme, is equal to $1/\alpha$. The in-control ARL is the number of samples taken before it is wrongly decided that the process has changed. The out-of-control ARL, which measures the delay and amount of substandard material produced before action is taken, is equal to $1/(1-\beta)$, where α and β are the Type I and Type II error sizes. The out-of-control ARL is the expected number of samples taken before an action signal is generated.

The control chart parameters are related to α and β, which in turn are related to the cost of investigating action signals and the cost of producing substandard material. Similarly, the frequency of sampling is related to the cost of investigating action signals, the cost of producing substandard material, and also the cost of sampling and testing. These form the basis for the cost model that enables the economic design of a control chart and monitoring program.

Fairall[41] provided one of the first published works that dealt with the application of control charts to WWTP operation. In this case study, Fairall retrospectively examined the utility of an individual observations chart (i.e. a Shewhart chart with a subgroup size of one) and moving range chart to influent-

effluent monitoring of an aerated lagoon. In particular, his focus was on the daily observations of the COD load to the receiving stream and the discussion centred on the process' capability to meet discharge standards.

The control chart used by Fairall was based on the model given as Equation 2-1, p.2-33. The assumptions that the data are serially independent, normally distributed, and have constant variance, underpin the model and the chart. However, other workers who have examined the stochastic characteristics of WWTP data have found that serial correlation, seasonality, nonnormal data distributions and nonconstant variance are the norm[42,37]. If present, these properties can have an adverse impact, to varying degrees, on the performance of the classical control charts. To overcome these problems, adjustments are usually made to the data in order to satisfy the necessary assumptions.

According to Berthouex[37], a nonnormal distribution and nonconstant variance are not major problems. A simple transformation of the data (usually a log transformation) can usually overcome these problems. Small departures from normality and homoscedasticity will not have an appreciable effect on chart performance.

More serious issues are serial correlation and seasonality, to which control charts are not robust. For example, positive serial correlation can significantly increase the frequency of false alarms. Negative serial correlation will seriously attenuate the sensitivity of the control chart.

One approach to these complications is to correct the estimated variance to account for serial correlation and seasonality. This approach, however, is only

applicable if the data series is stationary in level. Furthermore, it means sacrificing some of the discriminatory power of control chart tests because runs tests will be meaningless. Vasilopoulos and Stamboulis[43] actually give auxiliary quality control factors, for a second order autoregressive process, that can be used to correct the sample variance and which eliminate the need for model estimation.

A method that extracts more information from the data is to first define the underlying stochastic process with a time-series model and then apply an appropriate control chart to the model's residuals[44,37] - where a residual, or one-step-ahead forecast error, equals the observed value minus the predicted value. If the model is adequate then the residuals will be independent and approximately normally distributed. A departure from the model will show up as a large residual or a systematic pattern in the residuals.

Wastewater treatment processes are dynamic-stochastic processes and, as such, are best described by dynamic-stochastic models. A general class of models known as ARIMA (autoregressive integrated moving average) models, can be used to describe almost any stochastic process[45]. This includes stationary processes which have a fixed mean level, nonstationary processes which are characterised by a drifting mean level, and seasonal processes.

In the ARIMA framework, the current observation can be modelled as a finite linear function of past observations and a random shock a_t (the autoregressive component). Alternatively, it is modelled as a finite linear function of the current and past random shocks (the moving average component). The integration term is included when the process is nonstationary in level. To

achieve parsimony (i.e. a model with as few parameters as possible) it may be necessary to include both autoregressive and moving average terms. The MA component describes the die-off in the dependence between successive observations. The AR component accounts for the "extra" carryover between successive observations. The weights exerted by past observations govern the way that a process evolves in time. These weights are described by the transfer function, and it is the transfer function that determines the form of a model and the magnitudes of the model's parameters. The general formula for the ARIMA models is:

$$\phi(B)\nabla^d z_t = \theta(B)a_t$$

where z_t = deviation from the mean of the time series at time t, i.e. x_t-μ

x_t = original (or transformed) observation at time t

∇^d = backward difference operator of order d

and $\nabla^d z_t = z_t - z_{t-d} = (1-B^d)z_t$

B = backward shift operator e.g. $B^d z_t = z_{t-d}$

$\phi(B)$ = autoregressive operator of order p

$=1-\phi_1 B-\phi_2 B^2-\ldots-\phi_p B^p$

$\theta(B)$ = moving average operator of order q

$=1-\theta_1 B^1-\theta_2 B^2-\ldots-\theta_q B^q$

a_t = random noise (shock or residual) which is independent and identically distributed with zero mean and variance σ_a^2.

An ARIMA process of order (p,d,q) can be abbreviated to ARIMA(p,d,q). Likewise, a seasonal ARIMA process is abbreviated to ARIMA(p,d,q)$(P,D,Q)_s$, where s is the seasonal period and (P,D,Q) is the order of the seasonal autoregressive, difference, and moving average terms. The fitted model is arrived at after a process of model identification, parameter estimation and diagnostic checking.

As Berthouex[37] points out, it is important to recognise that the model's residuals do not necessarily have to be random because the aim is not to build the "best" model for forecasting purposes, but to build a "sensible" model that will form the basis for control. That is, the objective is to make the process conform to the model that the operator has defined as desirable performance.

Building a sensible model means that the traditional diagnostic tests need to be supplemented with practical knowledge of the process and the problem. It may be that the operator wishes to impose a fixed mean level on the process, in which case a stationary model like an AR(1) might be appropriate. Alternatively, if the process is naturally a seasonal one, then the operator might incorporate a deterministic drift into the model. For example, consider the natural logarithm of the effluent BOD_5 in Figure 2-6, which has had the seasonal component modelled as a deterministic function. The residuals of the deterministic model are then described as an ARIMA process. The resulting Shewhart chart, applied to the residuals of the combined ARIMA-deterministic model, is shown as Figure 2-7.

If, however, the process is truly a nonstationary one, then it may be better to opt for feedback control rather than to try to make the process conform to a

stationary model by way of a control chart. Feedback control will be discussed later in this section.

Berthouex[37] notes that most treatment plants are probably not equipped to undertake the rather complex task of identifying time series models. To simplify matters, he has proposed a "family of models" which have been tested on a large number of WWTP processes. He suggests that control charting with respect to a model should only be undertaken if one of the models fits. The problems of estimation and diagnostic checking still remain, however, and Berthouex says that it should be possible to automate these steps with an expert system.

The family of models suggested by Berthouex consists of:

Model A

$$(1-\phi B)\nabla^7 x_t = b_1 \sin\left(2\pi t/365\right) + b_2 \cos\left(2\pi t/365\right) + (1-\theta B)(1-\theta_7 B^7)a_t$$

Model B

$$(1-\phi B)\nabla^7 x_t = (1-\theta B)(1-\theta_7 B^7)a_t$$

Model C

$$\nabla x_t = (1-\theta B)a_t$$

Model D

$$x_t = \mu + b_1 \sin\left(2\pi t/365\right) + b_2 \cos\left(2\pi t/365\right) + (1-\theta B)a_t$$

Model E

$$x_t = \mu + a_t$$

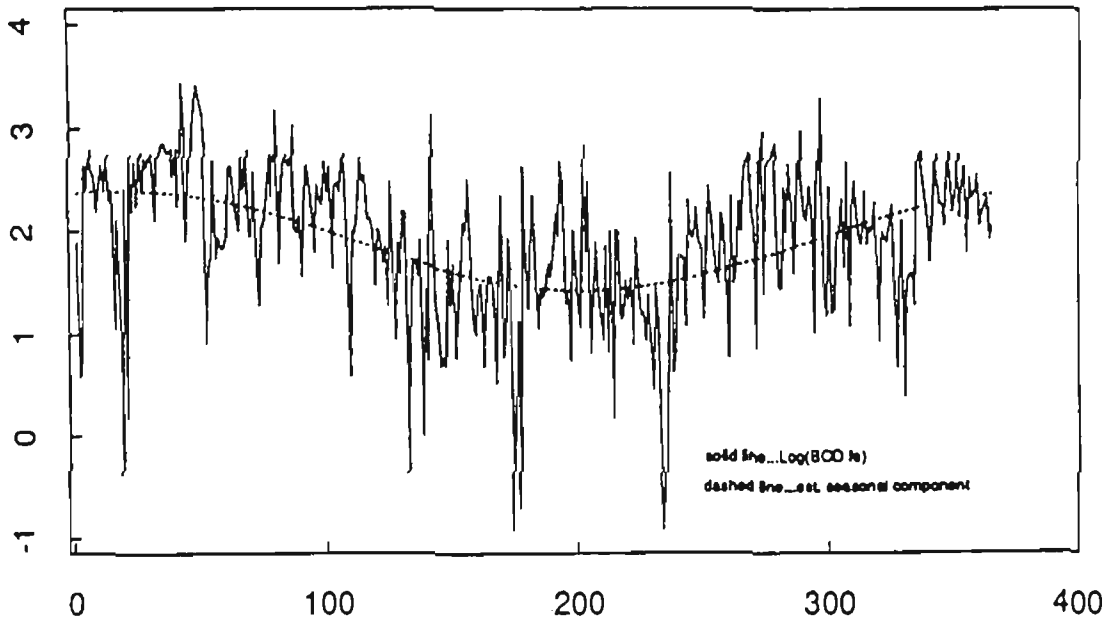

Figure 2-6 Time series plot of the natural logarithm of the effluent BOD_5, with the seasonal deterministic model overlayed (Berthouex[37]).

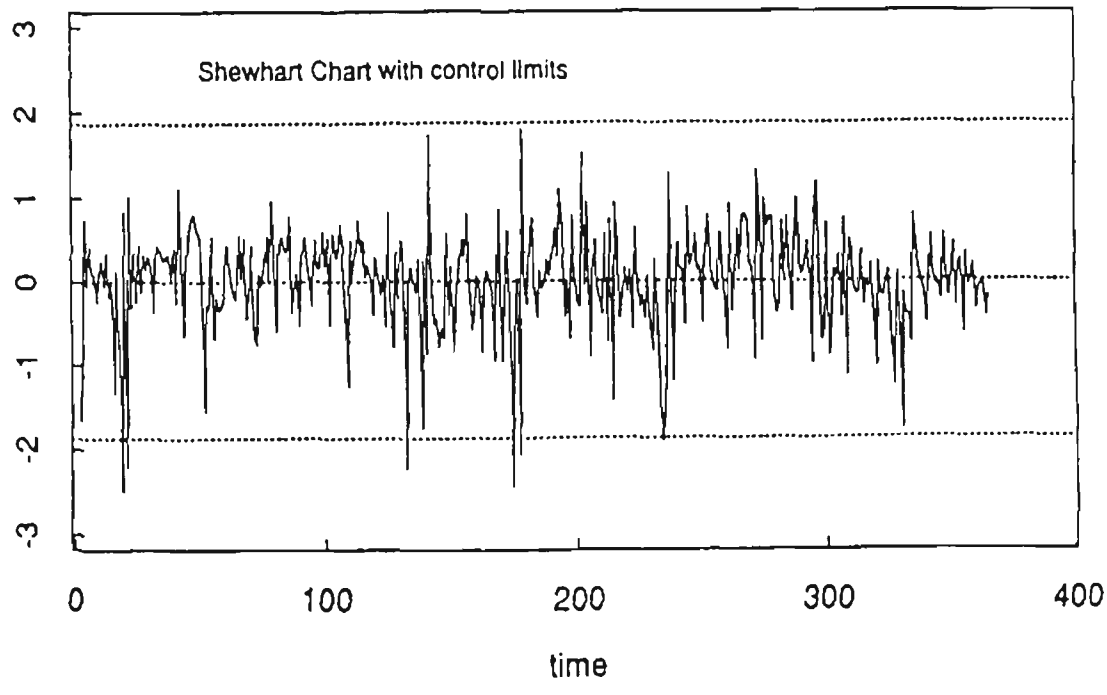

Figure 2-7 Shewhart chart of the residuals from the combined ARIMA-deterministic model of the natural log of the effluent BOD_5 (Berthouex[37]).

The x_t in these equations are the original observations or a log transformation of them, and the μ is a fixed mean level.

Models A, B and C represent nonstationary processes, that is, processes that do not have a fixed level. Models A and B are nonstationary in the seasonal pattern (i.e. the weekly cycle). This indicates that the mean level tends to shift from week to week. Model C is nonstationary at short lags, and so the mean level tends to change more frequently.

Model A is characterised by a stochastic weekly cycle overlaying a deterministic annual cycle. The remaining autocorrelation structure has been accounted for by first-order autoregressive and moving average components. Model B is similar to A, but without the annual cycle. Model C has no seasonal components, but has the advantage of only one parameter to estimate and it is capable of tracking many processes.

Models D and E are stationary models. They represent a process that fluctuates about a fixed level. In model D the fluctuations follow a deterministic annual cycle with some dependence between successive values. In model E, the pattern is entirely random.

Berthouex claims that a disadvantage of nonstationary models, the IMA(1,1) in particular, is that they adapt too easily to new levels. This behaviour can result in residuals that seem good when plotted on a control chart, even though the actual level of the process has shifted.

Berthouex also states that a process is not necessarily in control just because it gives "acceptable" performance as defined by the operator. The

IMA(1,1) model, however, might actually provide a good compromise between statistical control and "acceptable" performance. Forcing a fixed level on an IMA(1,1) process is the business of PID (proportional-integral-derivative) controllers. In certain situations, though, the treatment plant might not have the flexibility or capacity for the precise regulation of inputs.

For example, at Melbourne Water's Eastern Treatment Plant, the effluent from anaerobic digesters is discharged to open drying beds. If the VFA level is high (approximately 2000 mg/L) an odour problem can result. The VFA concentration in the digesters follows an IMA(1,1) process[46]. By control charting with respect to an IMA(1,1) model, the operator can track the VFA level and make adjustments when the risk of an odour event becomes too great.

Furthermore, it is possible to detect trends in IMA(1,1) processes with the aid of runs tests or tracking signals[47] applied to the model's residuals. Step changes in level, however, would be difficult to detect.

When control charting with respect to an IMA(1,1) model, Montgomery and Mastrangelo[47] recommend using an EWMA centre-line chart when it is desirable to visualise the dynamics of the process as well as display information concerning the state of statistical control. With the EWMA centre-line chart, the original observations are plotted along with the one-step ahead forecast (i.e. the EWMA) and control limits. The EWMA is given by:

$$Z_t = \lambda X_t + (1-\lambda) Z_{t-1}$$

where Z is the EWMA, X_t is the current observation and $0<\lambda\leq 1$. The control limits are set at:

$$UCL_{t+1} = Z_t + t_{\alpha/2}\sigma_a$$
$$LCL_{t+1} = Z_t - t_{\alpha/2}\sigma_a$$

The problem with the EWMA centre-line chart, though, is the difficulty in detecting systematic patterns in the residuals. If the ability to perform runs tests is desired, it is also necessary to chart the residuals. An example of an EWMA centre-line chart is shown as Figure 2-8.

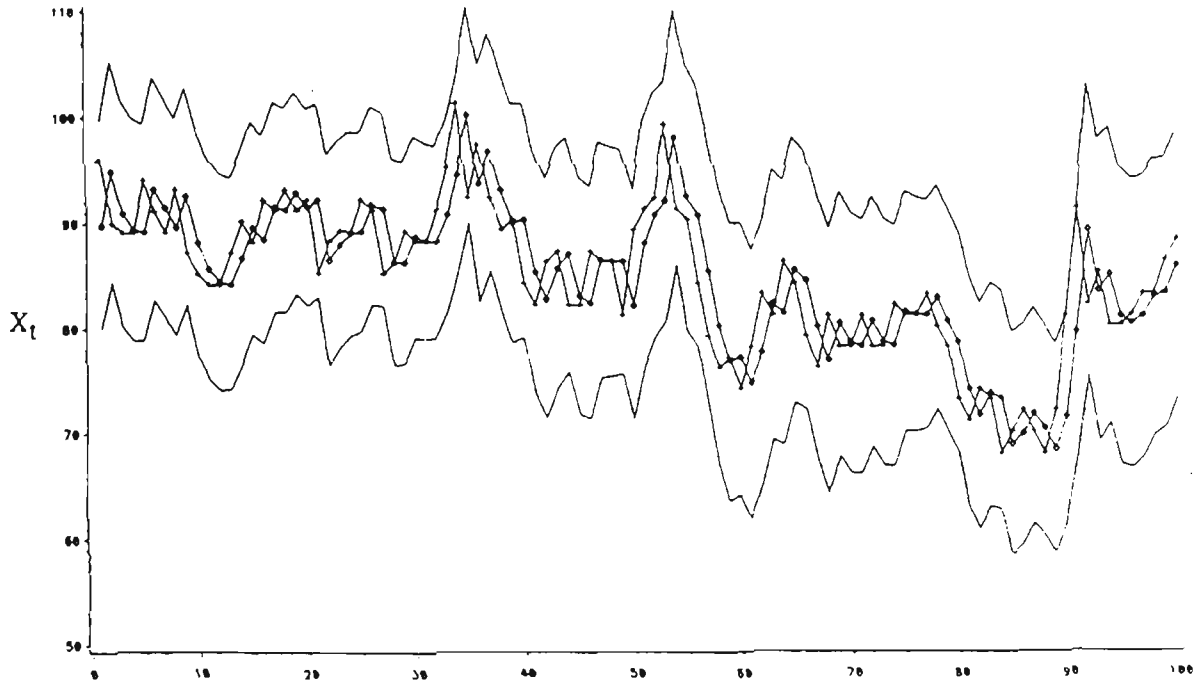

Figure 2-8 An example of an EWMA centre-line chart (Montgomery and Mastrangelo[47]).

Montgomery and Mastrangelo, like Berthouex, say that the time series approach can be awkward and time consuming, especially when several variables need to be monitored. They propose using the EWMA statistic as the basis of an approximate procedure for handling autocorrelated data.

The EWMA, with an appropriate value of λ, will provide a good one-step-ahead prediction in cases where the process observations are positively correlated Mastrangelo suggest selecting the value of λ that minimises the sums of squares of the one-step-ahead prediction errors. An EWMA centre-line chart or a residuals chart can then be used, as discussed above. In their paper, they give examples where the EWMA statistic has been applied to AR(1) and AR(2) processes.

Another difficulty with the time series approach to control charting, as noted by Berthouex[37], is in recognising when a model is no longer appropriate for the process it represents. Bagshaw and Johnson[48] describe a technique for detecting changes in a time series model. Procedures for detecting a change in the mean or the variance of the forecast errors will indicate when a model is no longer adequate. The procedure presented by Bagshaw and Johnson, however, can indicate the precise nature of the change.

In general, when a model has a change in a parameter, the resulting residuals e_t will follow an ARMA model:

$$\phi(B)e_t = \theta(B)a_t$$

Bagshaw and Johnson's procedure is based on likelihood ratio statistics which consist of cumulative sums:

$$T_n(\beta_1, \beta_2) = \sum_{t=1}^{n}(e_{1t}^2 - e_{2t}^2)$$

where T_n = log likelihood ratio statistic

β_1 = vector of parameters $(\phi_1,...,\phi_p,\theta_1,...,\theta_q,\sigma_a^2,p,d,q)$ for the

existing model

β_2 = vector of parameters for the new model

e_{1t} = one-step-ahead forecast error at time t using $\beta=\beta_1$

e_{2t} = one-step-ahead forecast error at time t using $\beta=\beta_2$

The distributional properties of $T_n(\beta_1,\beta_2)$ can be estimated using a Wiener approximation and critical values can be defined.

It would seem, however, that recognising when a model is no longer appropriate is not so much a difficulty as it is a practical problem. If a chart indicates that the process has changed, and the cause can be identified, it is then a matter of deciding whether this cause can and should be eliminated, or whether it is going to remain a permanent feature of the process. If it is to remain, then the model should be changed to accommodate the new characteristics of the process. The residuals (or more precisely the autocorrelations of the residuals) obtained with the old model can be used to suggest how the model should be modified[45].

Another problem facing the development of control strategies is that treatment plants typically suffer a great deal of inertia. In many cases, if a process output indicates an upset there is usually little that can be done to correct the problem in time, that is, before a breach of licence occurs. This fact is recognised in some discharge standards, as noted by Berthouex et. al.[44]. For example, the long term (30 day) BOD_5 average must not exceed 30 mg/L, but the short term (7 day) average must not exceed 45 mg/L. This suggests that process regulation may be more appropriate in some situations.

There are some basic differences between statistical process control and process regulation methodologies. SPC uses statistical hypothesis testing to determine whether there has been a change in the process. If there is evidence of an assignable cause of variation, the objective is to identify it and eliminate it. Process regulation applies a form of statistical estimation to gauge the current level of a disturbance, which is then compensated for by process adjustment[49]. Process regulation has particular application in situations where certain causes of variation, like the properties of natural feedstocks (or sewage), are "uncontrollable" and must be compensated for. Furthermore, the essence of process regulation is the development of a dynamic model of the process, which takes into account the inertia of the process, so that disturbances can be estimated and compensated for ahead of time.

As a hypothetical example (adapted from Box and Kramer[49]), consider controlling the BOD_5 output of an anaerobic reactor. The aim is to control the BOD_5 at some target value T by adjusting the flowrate (or residence time), but due to the stochastic nature of the sewage composition, the output BOD_5 is affected by a disturbance Z_t which can cause the BOD_5 to wander away from the target value (Figure 2-9).

The appropriate PID control equation (i.e. the one that gives the minimum mean square error at the output) can be derived from the transfer function and noise model that describes the dynamic relationship between output BOD_5 and the flowrate (Q).

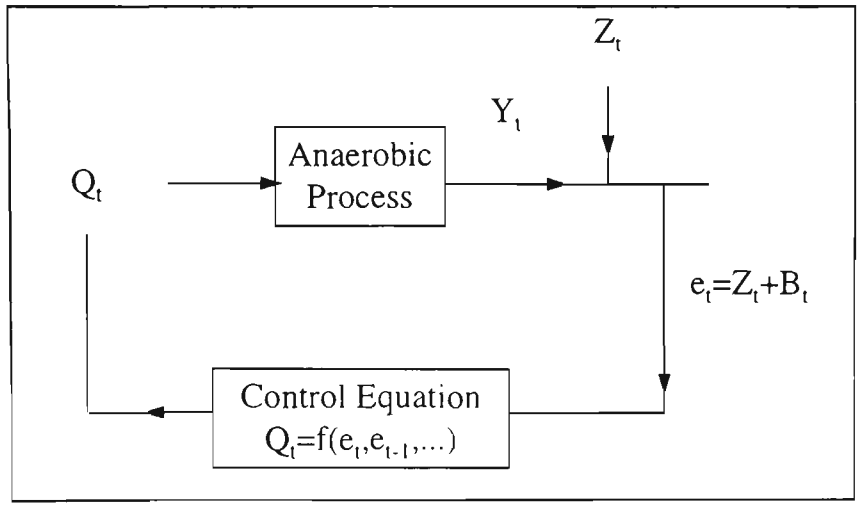

Figure 2-9 A schematic of a feedback control scheme (adapted from Box and Kramer[49]).

The error e_t at the output can be considered to be the sum of the attempted BOD_5 compensation B_t and the noise Z_t:

$$e_t = Z_t + B_t$$

The aim is to estimate the disturbance ahead of time and then apply appropriate compensation to minimise the error at the output. The control equation allows the new flowrate setting, needed to overcome the disturbance, to be calculated from the current and previous e_t's:

$$Q_t = K_D \nabla e_t + K_P + K_I \sum_{i=1}^{t} e_i$$

where K_P, K_I and K_D are the coefficients of the proportional, integral and derivative terms, respectively. The required adjustment can be determined by a computer or by a chart and put into effect by transducers or manually.

By characterising WWTP inputs and outputs with ARIMA models and determining an adequate transfer function for the system, the added value of an elaborate process control scheme can be assessed[40]. One practical difficulty in

the operation of WWTP's is that many important factors may not be known much less measured. This, of course, impacts the value of any process control scheme.

As a prelude to developing control strategies for sewage treatment plants, Berthouex and Hunter et. al.[50] set out to describe the dynamic and stochastic nature of inputs to and outputs from, and the basic mechanisms of, an activated sludge plant.

Applying various regression techniques (simple regression, lagged regression and autoregression) in a stepwise fashion, Berthouex and Hunter et. al.[50] developed a model that related the output BOD_5 to the input BOD_5, detention time and suspended solids.

$$(1-\phi B)(1-\Phi B^7)BOL_t = \alpha_1(B)BIL_t + \beta^*\nabla DT_t + \gamma^*\nabla SSL_{t-1} + N_t$$

$$\Rightarrow \quad (1-0.566B)(1-0.311B^7)BOL_t = (0.466+0.166B)BIL_t - 24.16\nabla DT_t + 0.243\nabla SSL_{t-1} + N_t$$

where BOL_t = natural log of the output BOD_5 at time t

BIL_t = natural log of the input BOD_5 at time t

DT_t = detention time at time t

SSL_{t-1} = natural log of the mixed liquor suspended solids at time t-1

N_t = noise at time t

B = backshift operator

∇ = backward difference operator

Some interesting features that were gleaned from this modelling exercise were:

- There was no advantage in using a BOD_5-removal efficiency measure, in place of (simply) BOD_{out}, as the dependent variable.

- Temperature is not a factor in the model. Berthouex suggests that the slow change in temperature was perhaps compensated in some way.
- Most of the variation in BOD_{out} was explained by previous values of the BOD_{out}.
- The BOD_{out} exhibited a weekly cycle.
- In the range of *DT's* encountered, the change in *DT* seemed to have more influence on BOD_{out} than the actual magnitude of the *DT*.
- The effect of the mixed liquor *SS* was lagged by one day, and the change in *SS* was more important than the magnitude of the *SS*.

It is interesting that Berthouex and Hunter et. al. have not used the well established methods of Box and Jenkins[45] for identifying and fitting transfer functions - including the use of diagnostic tests. Perhaps, they believed their approach, whilst approximate, was more attainable by WWTP operators.

Berthouex and Hunter et. al. have indicated that planned experiments would be needed to assess the usefulness of the model for control purposes. However, the model would first need to be expressed in the form of a control equation where *DT* is the controllable variable. Consider, for example, a feedforward control scheme. If *DT* was held at a constant value, then the total error in the output BOD_5, or $\ln(BOD_5)$, would be:

$$\varepsilon_t = N'_t + \frac{\alpha_1(B)BIL_t}{(1-\phi B)(1-\Phi B^7)} + \frac{\gamma^* \nabla SSL_{t-1}}{(1-\phi B)(1-\Phi B^7)}$$

where the total effect of the disturbance is:

$$\frac{\alpha_1(B)BIL_t}{(1-\phi B)(1-\Phi B^7)} + \frac{\gamma^* \nabla SSL_{t-1}}{(1-\phi B)(1-\Phi B^7)}$$

and the total effect of compensation is:

$$\frac{\beta^* \nabla DT_t}{(1-\phi B)(1-\Phi B^7)}$$

The control equation can therefore be written as:

$$\beta^* \nabla DT_t = \alpha_1(B)BIL_t + \gamma^* \nabla SSL_{t-1}$$

If more was known about the noise term N_t, a combined feedforward-feedback control equation could be postulated.

An alternative feedforward control scheme for an activated sludge plant has been proposed by Berthouex and Lai et. al.[51]. In their paper, Berthouex and Lai et. al. discuss the merits and applications of discriminant upset analysis and feedforward control schemes, in general.

In the activated sludge process, upsets can occur as a result of shock loads or sudden equipment failure. Such events cannot be anticipated. Most problems, however, result from conditions that should be detectable in advance[52].

As mentioned earlier, feedforward and/or feedback control can be used to keep a process on target. Feedback control always lags the process, however, and if the lag is great enough then feedforward control is recommended. Feedforward control anticipates deviations from the target quality and makes adjustments before the potential upset becomes real. In a treatment plant setting, feedforward control is desirable when: 1), tests take a long time to perform (e.g. 5

days in the case of BOD_5), or; 2), when an upset, once detected, cannot be quickly rectified.

If the key variables that determine product quality are known, then they can be incorporated into a model to predict the outcome. Treatment plants are dynamic systems, and many factors often affect effluent quality. Traditional methods of feedforward control for multivariable dynamic systems are quite sophisticated. Not so discriminant upset analysis, which has been used for the early detection of upsets in an activated sludge process.

As the name suggests, discriminant upset analysis uses a discriminant function to classify multivariate process data as either "in control" or "out of control", ahead of time. The discriminant function, which is essentially a set of linear or nonlinear equations, is derived from a set of historical data which includes periods of stable process behaviour, as well as periods when the process was out of control.

The use of discriminant upset analysis, as opposed to the more elaborate transfer function approach, is characteristic of the move to develop simple techniques for controlling WWTP processes, and continuous processes in general. The difficulties associated with control charting WWTP processes have already been discussed, and while simplified procedures have been proposed, the statistical properties of WWTP data can still require complex control methodologies.

Recognising the ability of the human mind to detect patterns, Berthouex and Hunter[53,44] suggest that simple time series plots of raw data, transformed

data, or simple statistics like moving averages and cumulative sums, can often provide adequate information for process control. A plot of log transformed data can often highlight spikes in data records. Moving averages can smooth out random variations and help to clarify trends. EWMA's are often appropriate to environmental data because organisms tend to "remember" yesterdays water quality more so than the water quality of two or three days ago. Cusum plots, without the V-mask, are useful for detecting small shifts in level.

In addition, reference distributions can often provide a simple means of analysing process data[54]. A reference distribution is constructed by first identifying periods of stable operation from time series plots. A histogram is then drawn from data representing "stable" performance, and critical levels (usually 1% or 5% levels) are determined by counting in from the high and/or low end of the ordered data. Whilst not suitable for nonstationary processes, reference distributions are a statistically valid way of handling data that exhibit serial correlation, seasonality and nonnormal characteristics.

Ward and Loftis et. al.[55] have noted that the analysis of treatment plant data often stops at calculating means and medians, noting maximums and counting licence breaches. This is a symptom of, what they have called, the "data-rich but information-poor syndrome". As demonstrated, however, there is a plethora of techniques available for extracting more information from treatment plant data. With continued development and implementation, these techniques have the potential to accelerate the understanding of treatment processes and improve treatment plant performance.

2.5 CONCLUSION

There appears to be a considerable body of literature on the microbiology and control of high-rate anaerobic digesters, and anaerobic habitats in general. Little attention, however, has been given specifically to the microbial ecology and process control of anaerobic ponds. Both process regulation and process monitoring techniques appear suitable for the control of anaerobic ponds, though work is needed to identify and quantify the main causes of variation in methane yield and effluent COD from anaerobic ponds at WTP. The following chapters explore the microbial ecology and control of anaerobic ponds at WTP with the objective to improve their performance in terms of yield of methane and variability in effluent composition.

3. Spatial and Temporal Variability of Some Common Process Control Variables in the 115E Anaerobic Reactor (over a single loading period)

3.1 INTRODUCTION

Unlike the conventional CSTR anaerobic digester, and most "high-rate" reactors, the contents of the 115E reactor are not well mixed. This characteristic of anaerobic ponds can complicate the sampling method to be used in a process control program.

The 115E reactor is loaded on an intermittent basis, and the loading rate and duration depends basically on the total loading rate to the Plant, the performance and capacity of the various treatment units, and the water requirements of land filtration pastures. For more than 2 hours each day the linear flowrate in the reactor is quite low (less than 1 m/h), and while some mixing does occur as a result of gas production, the bacterial biomass and the influent suspended matter tend to settle to the bottom or accumulate as a scum at the surface. Furthermore, sewage ponds typically exhibit a dispersed-flow hydraulic pattern (i.e., they are not necessarily completely-mixed systems[56,57]) and it is likely that bacterial densities, nutrients, metabolites and environmental variables like pH, electrode potential (EP) and temperature will vary systematically throughout the reactor.

In order to develop a sampling protocol, it was first necessary to investigate the spatial and temporal variability of the reactor's contents over a loading period. This chapter focuses on the variability in some of the common process-control variables, including pH, temperature, EP, and the concentrations of VFA, alkalinity, volatile solids and total solids.

3.2 MATERIALS AND METHODS

3.2.1 Description of Sampling Sites

When this study of the 115E anaerobic reactor was undertaken, the FRP curtain was in place but the HDPE cover had not been constructed. The 115E reactor is 3 m deep, 150 m wide and about 240 m long. Samples were taken at two depths (0.75 m and 2.25 m) in a grid consisting of 7 rows and 3 columns (Figure 3-1). The actual coordinates of each sampling site, taking the north corner as the origin, are given in Appendix A. Each sample was meant to represent an equal volume of the reactor. The last row of sample sites was intended to represent conditions near the outlet (i.e. at the FRP curtain).

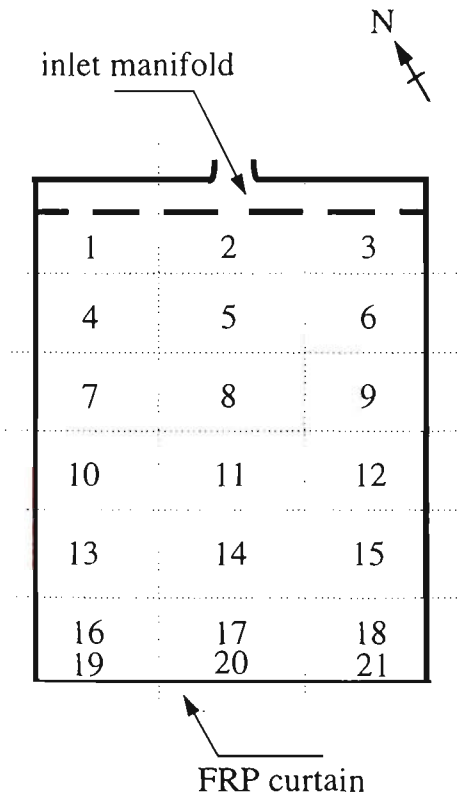

Figure 3-1 A plan of the sampling sites.

Samples were taken on three occasions over the course of a single loading period (refer to Figure 3-2). The first were taken just after loading began (3/3/92 6:00 PM), the second set was taken toward the end of the loading period (4/3/92 3:00 AM), and the last set was taken after the flow to the reactor had ceased (4/3/92 10:00 AM). A grab sample of the influent was also taken on the first two sampling occasions. The cumulative volume of sewage, the air temperature, wind speed and wind direction at each sampling time are given in the following table. The relatively low wind speed suggests that wind-induced mixing would have been minimal and that the conditions on the day should reasonably simulate a covered pond.

Date & time	Cumulative sewage volume (ML)	Air temperature (°C)	Wind speed (km/h)	Wind direction (° from N)
3/3/92 6:00 PM	20	24.7	10.8	117.5
4/3/92 3:00 AM	55	20.1	4.3	218.7
4/3/92 10:00 AM	70	24.8	8.3	77.6

Samples were taken from a dinghy. The rows and columns of sampling sites were marked with pegs on the banks of the pond. A rope was strung across the pond and attached to a vehicle at either end. Manoeuvring between sampling sites was accomplished by pulling the dinghy along the rope or towing the rope and dinghy along the pond with the vehicles.

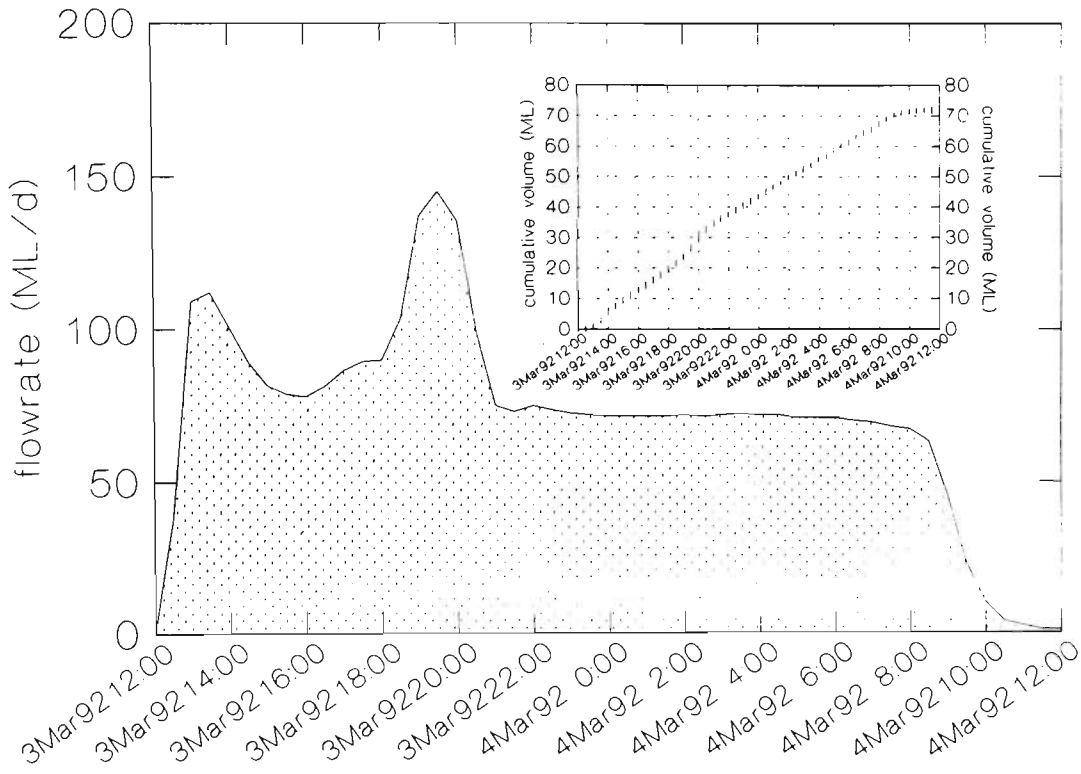

Figure 3-2 The flowrate and cumulative volume of raw sewage on the day of sampling.

Samples were taken with a depth sampler that essentially consisted of a stoppered narrow-mouthed 1 litre glass bottle at the end of a metal rod. A lever attached to the rod allowed the stopper to be withdrawn and replaced into the neck of the bottle at the required depths.

The temperature of samples was measured immediately. The samples were then transferred to 1 litre narrow-mouthed polyethylene bottles, labelled and stored in a cooler. Samples were transported to the laboratory at the end of each run. Upon receipt at the laboratory, the pH and EP were measured and then the samples were stored in a refrigerator at 4°C prior to conducting further analyses over the next two days. On each sampling run, between 2 and 3 hours elapsed

between taking the first sample and storing all samples in the laboratory refrigerator. On the first two sampling occasions, only every second row of sites was sampled due to time limitations.

3.2.2 Analytical Methods

pH was measured with a Hanna Instruments pH probe (model HI 1332) and an Orion 940 Expandable Ionanalyzer pH meter.

Electrode potential (EP) was measured with a platinum indicator electrode, a saturated calomel reference electrode and a Metrohm E 588 pH-mV meter. The half-cell potential of the reference electrode is +244 mV at 25°C. The EP values given in Figure 3-6 and Appendix A can be approximately scaled to the Standard Hydrogen Electrode by adding +244 mV.

Temperature was measured with a hand-held digital thermometer (Anritsu Meter Co. Ltd., model HLC-80P).

Total volatile fatty acids (VFA) was measured colorimetrically, using a Shimadzu UV-240 UV-Visible Spectrophotometer, according to *Analysis of Raw, Potable and Waste Waters* (HMSO: London, 1972). The results are expressed as mg/L acetic acid.

Total solids (TS), volatile solids (VS), alkalinity and **BOD_5** were analysed according to *Standard Methods for the Examination of Water and Wastewater* (APHA: USA, 18th ed., 1992). TS and VS were measured gravimetrically according to Methods 2540B (Total Solids Dried at 103-105°C)

and 2540E (Fixed and Volatile Solids at 500°C) . Alkalinity was measured according to Method 2320B (Titration Method) using an Orion 960 Autochemistry System. BOD_5 was measured by Method 5210B (5-Day BOD Test).

3.3 RESULTS AND DISCUSSION

Data on all variables, sampling sites and times are given in Appendix A.

3.3.1 Total Solids and Volatile Solids

TS and VS are measures of biomass concentration and Figure 3-3 (p. 3-9) indicates that the biomass is considerably more dense (about 30 times) in the lower part of the reactor. TS and VS appear strongly positively correlated and, at 2.25 m, both tend to show an upward trend along the reactor. Influent sewage flowing through the subsurface inlets probably tends to scour the suspended matter from the front of the reactor. There was no apparent change in the spatial pattern over time and there was no apparent systematic pattern in concentrations across the reactor.

At 0.75 m depth, the spatial pattern does appear to change over the loading cycle. At the beginning, the TS and VS concentrations are higher at the front of the reactor. Over the next two sampling occasions, this pattern tends to flatten out and the levels decrease. This is indicative of the scouring that occurs at the front of the reactor during loading, and the settlement of suspended matter when conditions are still.

3.3.2 Volatile Fatty Acids and Alkalinity

At 2.25 m depth, Figure 3-4 (p. 3-10) illustrates that there may be a transient increase in the concentration of VFA midway along the reactor at 4/3/92 3:00 AM. This is likely a response of the biomass to a fresh supply of organic nutrients. The VFA concentration was higher and more variable at 2.25 m than at 0.75 m. The alkalinity was much higher at 2.25 m. There was no apparent change in alkalinity over the loading cycle but, like TS and VS, the alkalinity tends to show an upward trend along the reactor.

At 0.75 m depth, the spatial pattern in VFA does appear to change over time. At the beginning of the loading period (3./3/92 6:00 PM), the VFA concentration appears to be raised at the front of the reactor (Figure 3-4). This, however, is not necessarily indicative of the biomass responding to the organic load. It is more likely due to the higher concentration of VFA in the feed. When loading had ceased (4/3/92 10:00 AM) there was a slight upward trend in the VFA concentration along the reactor.

3.3.3 pH and VFA/Alkalinity Ratio

The VFA/alkalinity ratio was lower at 2.25 m (about 0.1 at 2.25 m and 0.2 at 0.75 m). This is a result of the higher alkalinity at 2.25 m. Generally, however, the pattern in the VFA/alkalinity ratio (Figure 3-5, p. 3-11) was similar

to the pattern in VFA concentration described earlier. There was no notable pattern in pH.

3.3.4 Temperature and EP

Figure 3-6 (p. 3-12) indicates that there was generally a downward trend in temperature along the reactor (about 0.5°C lower at the outlet). At 0.75 m, the median pond temperature was lowest at 3:00 AM, presumably due to heat losses and gains across the air-water interface.

The median pond EP was apparently lower (by about 30 mV) on the first sampling occasion. This could be due to a higher concentration of highly reduced metabolites (like fatty acids, alcohols, ammonia, hydrogen sulphide, and dissolved molecular hydrogen and methane) from the breakdown of organic matter in the previous loading cycle. In addition, the EP was generally about 10 mV lower at the 2.25 m depth.

3.4 CONCLUSION

The levels of all variables, except pH, differed between the two sampling depths. In particular, the biomass (as measured by the total and volatile solids) was considerably more concentrated at 2.25 m depth. This would suggest that the process control program should focus on changes occurring in the lower part of the reactor, because bacterial biomass is the 'real' object of the control effort.

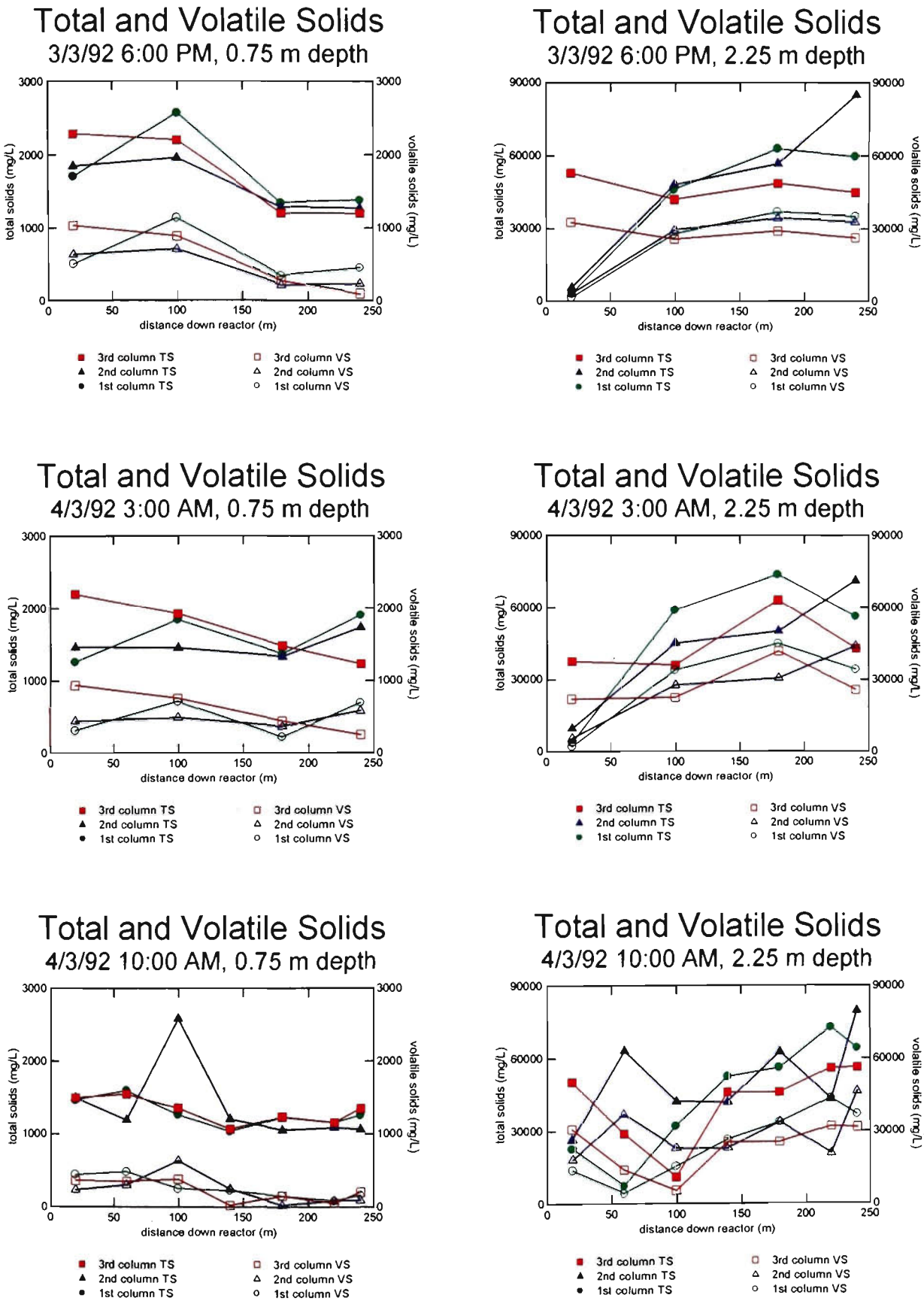

Figure 3-3 Spatial and temporal variability in total and volatile solids.

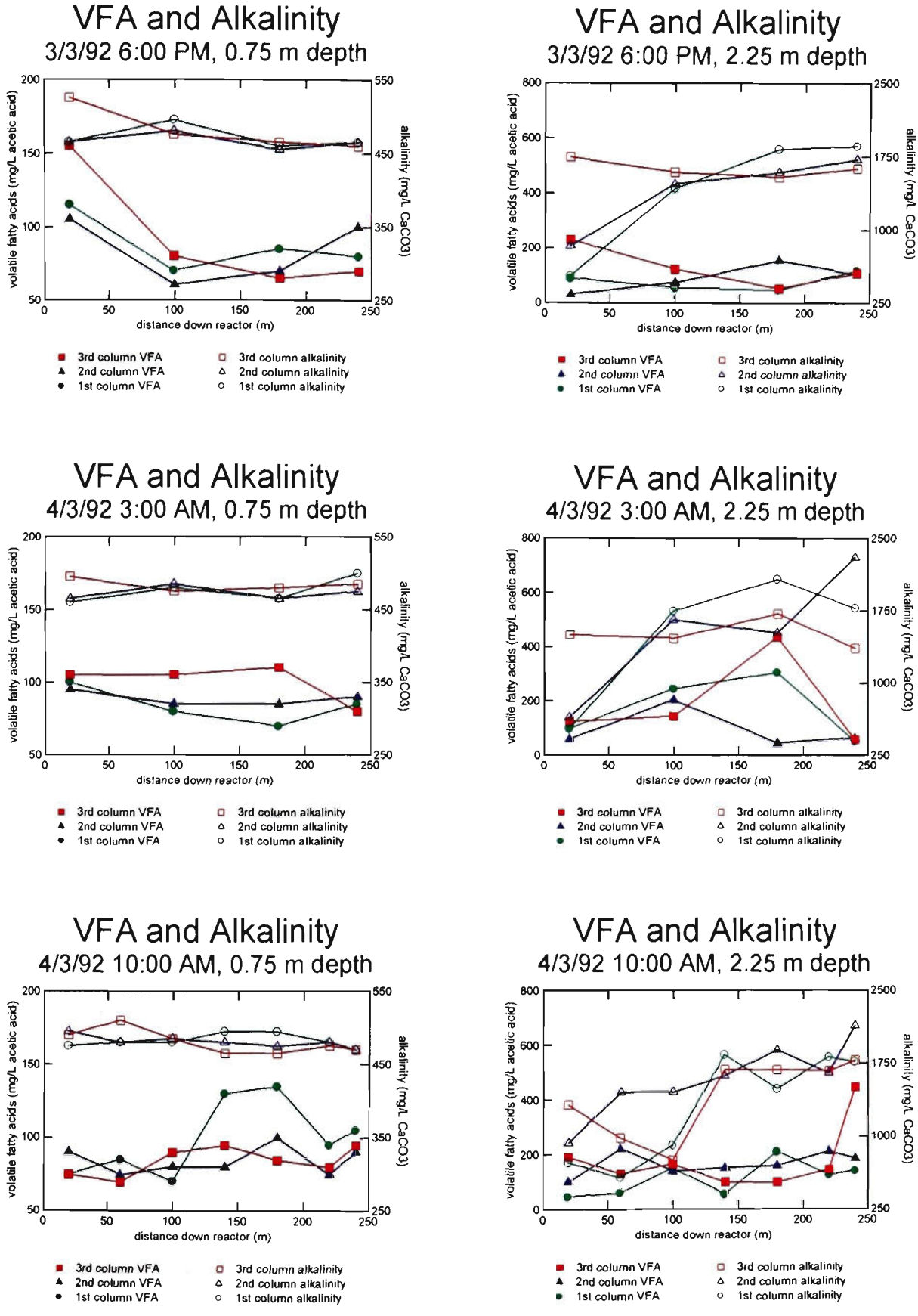

Figure 3-4 Spatial and temporal variability in VFA and alkalinity.

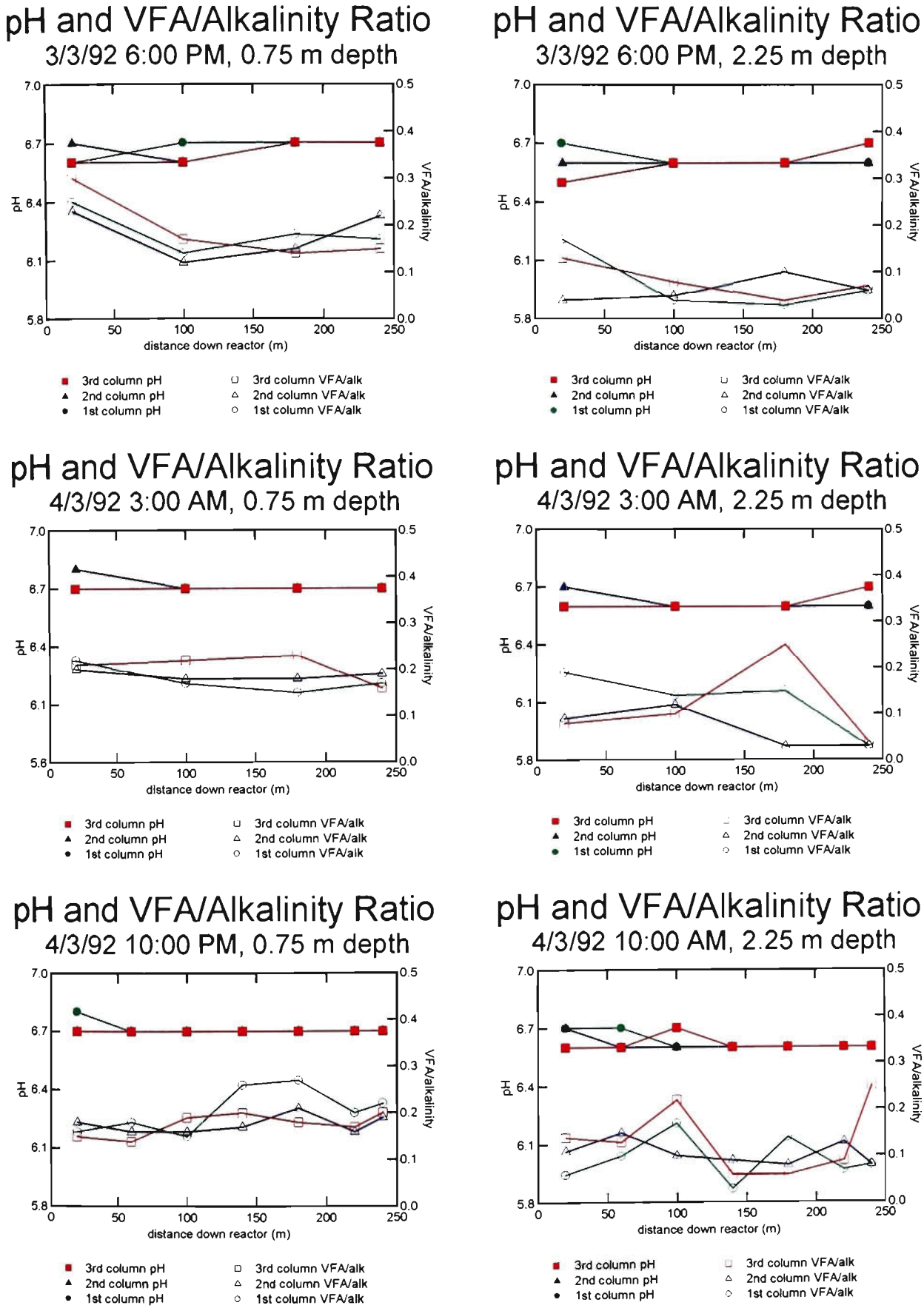

Figure 3-5 Spatial and temporal variability in pH and VFA/alkalinity ratio.

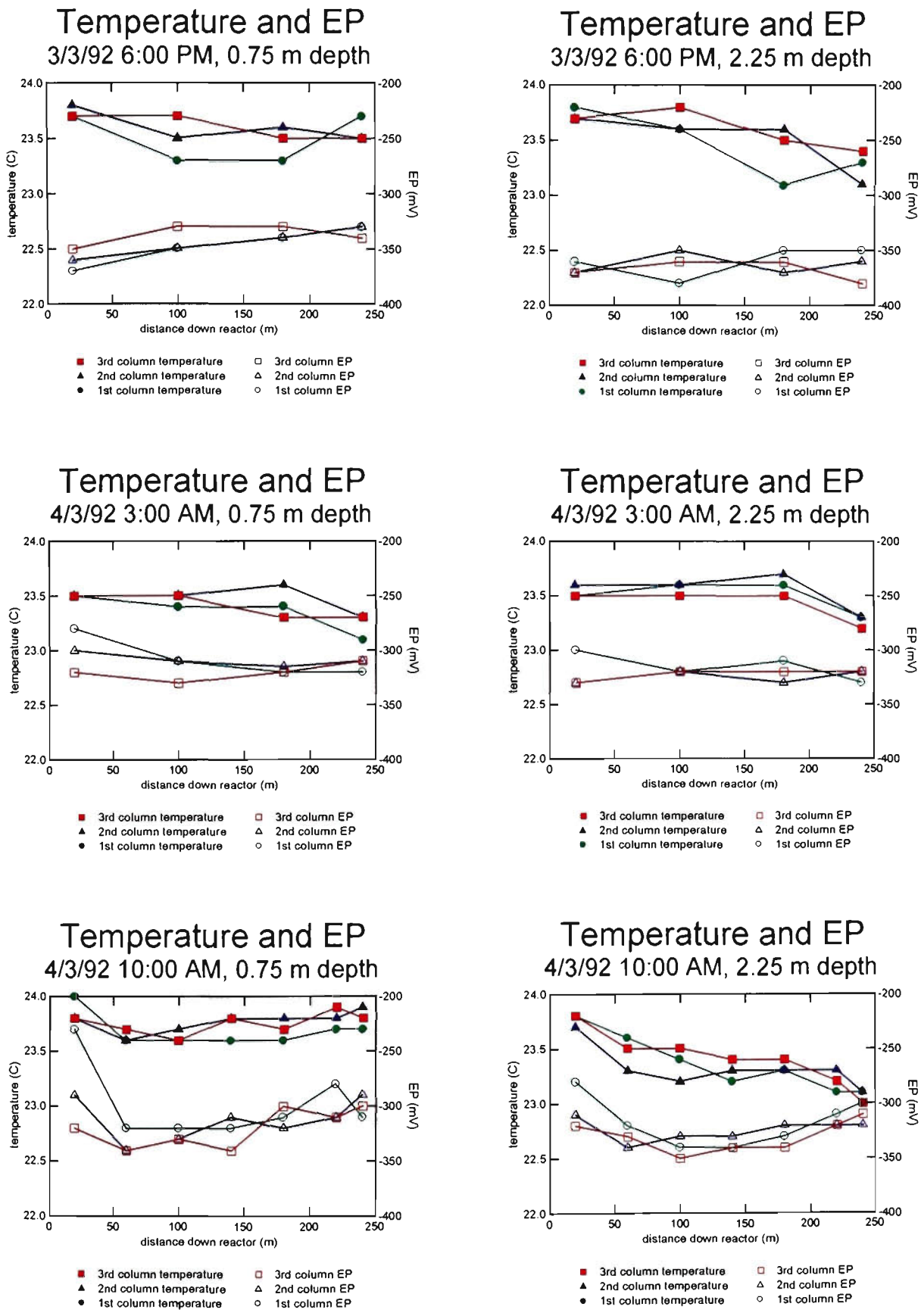

Figure 3-6 Spatial and temporal variability in temperature and EP.

At 2.25 m, all variables (except pH) appeared to exhibit systematic patterns along the reactor and/or over time. None of the variables studied showed a systematic pattern across the reactor. These observations suggest that samples taken for process control purposes should be taken from within the sludge layer at the bottom of the reactor and, to minimise noise due to systematic patterns in spatial and temporal variability, the samples should be taken at the same location (or at least at the same distance along the reactor) and at the same time of day. The data, however, give no clear indication of whether samples should be taken, for example, at the start, middle, or end of the reactor.

Intuitively, to control the treatment process, samples should be taken from the most active part of the reactor. Bacterial activity, however, is not necessarily proportional to the total or volatile solids concentration. The observed pattern in the VFA concentration is weak evidence that the bacteria were more active in the region of 100-200 m down the reactor, but this is confounded by the fact that volatile fatty acids are intermediary metabolites and are being both produced and consumed at roughly similar rates. Measuring the volume of methane generated at various locations along the reactor would be particularly informative. In fact, Safley and Westerman[58] measured the total biogas and methane generation rate on a number of anaerobic lagoons in the USA. Whilst they noted that the gas production rate varied considerably over the surface of the lagoons, it is not clear whether the patterns were random or systematic. In an experiment similar to that performed by Safley and Westerman, methane production rates from the 115E

anaerobic reactor had been estimated previously, but because the method was awkward and time-consuming, only one site was sampled.

A more direct way to measure the activity is to quantify the size and distribution of the methanogenic population. The next chapter describes a survey of the distribution of methanogens and total anaerobes in the 115E anaerobic reactor using a methanogenic activity test, and a variation of the Hungate roll-tube method for cultural counts, to estimate the size of the bacterial populations.

4. Survey of the Distribution of Methanogens and Total Anaerobes in the 115E Anaerobic Reactor

4.1 INTRODUCTION

Knowledge of the spatial variability in bacterial activity within the 115E anaerobic reactor should help to pinpoint the most appropriate location to sample for process control purposes. This chapter presents the findings of a survey of the distribution of methanogens and total anaerobes within the sludge layer at the bottom of the reactor. Bacterial densities were estimated using a methanogenic activity test and a variation of the Hungate roll-tube method for cultural counts of total anaerobes and methanogens.

4.2 MATERIALS AND METHODS

4.2.1 Description of Sampling Sites and Methods

This study was carried out after the floating HDPE cover had been installed on the 115E anaerobic reactor. The cover was constructed with a grid of sampling ports (100 mm I.D. PVC pipe with screw cap), arranged in a similar fashion to the sampling sites described in Chapter 3. The grid consists of 6 rows and 3 columns of sampling ports. The first 5 rows of sampling ports were approximately arranged to represent an equal volume of the reactor. The last row of sampling ports was meant to represent conditions near the outlet of the reactor.

The middle column of sampling ports was offset from centre to avoid the longitudinal stormwater channel on the cover.

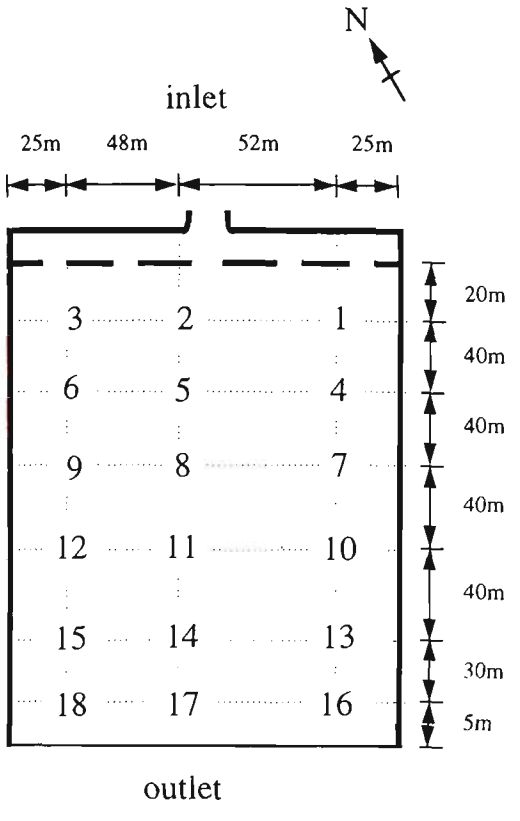

Figure 4-1 Location of sampling ports on the 115E anaerobic reactor.

Care needed to be taken when removing the caps from the sampling ports because the small pocket of gas in the port contains approximately 2000 ppm H_2S. A full-face mask respirator (Protector Safety model RFF90) equipped with the appropriate canister (RC224) was always worn and samples were always taken from the upwind side of the port. In addition, a strip of moistened lead acetate paper was worn to signal the presence of H_2S.

Sludge samples were taken at a depth of approximately 2.5 m using a 2.5 m length of 40 mm I.D. PVC pipe. A steel rod ran through the centre of the pipe, with a rubber bung affixed at one end. The pipe allowed samples of sludge to be taken from beneath the scum layer which was up to 2 m thick in some places. The pipe was inserted through the sample port (and the scum if necessary) to a depth of 2.5 m and then the bung was pushed out of the end of the pipe. When the pipe was completely full, the bung was replaced and the pipe withdrawn from the sampling port. The sample was then poured from the pipe

into a narrow-mouthed 1 litre polyethylene bottle. The bottle, which had been previously purged with anaerobic-grade carbon dioxide (BOC Gases), was filled completely to ensure the maintenance of anaerobiosis during transport to the laboratory.

Samples of the scum were also taken. These samples were collected by taking a core of the scum with a length of 75 mm I.D. PVC pipe. A small amount of scum (about 50 g) was scooped from the bottom of the core and then transferred to 50 mL glass jars. The jars were purged in the field, during sample transfer, using tedlar bags that had been filled with anaerobic-grade carbon dioxide.

Once in the laboratory, liquid samples were mixed, by gently inverting the bottle, and then an aliquot was transferred by pipette into serum vials containing an anaerobic salts solution. The sample bottle and serum vials were continuously gassed with anaerobic-grade carbon dioxide during the procedure. Scum samples were homogenised with a spatula, whilst being gassed, and then transferred to serum vials. The vials were then sealed with butyl rubber septa and aluminium crimp seals.

4.2.2 Anaerobic Methods

The serum bottle modification of the Hungate technique was used for preparing, dispensing, autoclaving and inoculating media, and for culture transfers[59,18,60,13,19]. The VPI Anaerobic Culture System[20] (distributed by Bellco

Glass Inc.) was used for activity tests and cultural counts. Gases used for cultural counts were deoxygenated using an Activon oxygen trap (catalogue no. RDOT3) and indicating oxygen trap (catalogue no. RDIOT).

4.2.3 Medium for Activity Tests

The activity test method used in this study is essentially that of Dolfing and Bloemen[22]. The mineral salt (MS) medium contains:

1) NH_4Cl	0.5 g/L
2) K_2HPO_4	0.3 g/L
3) KH_2PO_4	0.4 g/L
4) $NaHCO_3$	10 g/L
5) Cysteine hydrochloride	0.25 g/L
6) $Na_2S.9H_2O$	0.25 g/L
7) Resazurin	1 mL of a 0.1%w/v solution.

1 L of the medium was prepared by first weighing out and then dissolving ingredients 1-4 in deionised water. The solution was then deoxygenated by boiling (for about 2 minutes) and chilling whilst gassing with anaerobic-grade CO_2. 20 mL of a solution containing cysteine-HCl and sodium sulphide (1.25%w/v each and stored under N_2) was then added. CO_2 was bubbled through the solution till the pH was about 7.0 and then 50 mL aliquots were dispensed into 125 mL serum vials (actual vol. 160 mL). The vials were sealed with slotted butyl rubber septa and aluminium crimp seals, and autoclaved at 121°C for 15

minutes. After sterilisation, the vials were allowed to equilibrate at room temperature. The pH at this stage was shown in earlier experiments to be 6.9±0.1.

The various methanogenic activity tests proposed in the literature have employed different initial concentrations of the substrate acetate. Speece[61] states that methanogens should be operating at 90% of their maximum capacity at acetate concentrations of $10 \times K_s$. K_s values ranging between 20-400 mg/L (0.33-6.66 mM) have been reported in the literature[61,62]. Speece used an acetate concentration of 125 mM and states that this concentration is not inhibitory to methanogens. Soto and Méndez et. al.[62] proposed that 33 mM acetate be used. Dolfing and Bloemen[22] used between 20-50 mM.

Similarly, the various methods proposed differ in their use of trace nutrients (i.e. trace elements and vitamins). Sotto and Méndez et. al.[62] propose that no sort of nutrients be added in order that growth of the biomass be limited and the measuring period lengthened. Dolfing and Bloemen[22] argue that trace nutrients are not required because it is a short term test and no significant growth should occur.

The medium used by Dolfing and Bloemen did not contain the redox indicator resazurin, or the reductants cysteine hydrochloride and sodium sulphide. It was found, however, that when resazurin was added to the medium of Dolfing and Bloemen, it remained pink even after sterilisation. This suggested that redox potential of the medium was above -42 mV[59] and could be inhibitory to methanogens.

4.2.4 Activity Test Procedure

Anaerobic activity tests have been used in a variety of ways to study the anaerobic digestion process, including:

- Monitoring reactor performance[7,63].
- Selecting a seed sludge prior to start-up of an anaerobic digester[63].
- Estimating the population size of the different trophic groups involved in methane formation[22].
- Determining the biodegradability of a waste[64].
- Determining the kinetic parameters of the different steps involved in the anaerobic digestion process[62].

The basis of all methanogenic activity tests is to first dilute out all substrates in the sample of biomass being tested, to negligible levels, by inoculating a serum vial containing a relatively large volume of mineral salt medium. The medium is then supplemented with a specific substrate (acetate or H_2/CO_2) so that only the trophic group that uses that substrate will be active. The vial is then incubated and the concentration of methane in the headspace of the vial is followed over time. The measured activity is specific to the test substrate and the test conditions. In this study, the aim was to make relative measurements of the size of the acetoclastic methanogenic population in the 115E anaerobic reactor. As mentioned in Section 2.2, the acetoclastic methanogens are responsible for about 70% of the methane produced in anaerobic digesters.

In order for the activity to be expressed by a single parameter, it is necessary that the substrate concentration be much greater than the estimated values for the half-saturation coefficient (K_s)[62]. This ensures that the activity is independent of substrate concentration (i.e. the reaction is zero order). Furthermore, it is important that negligible growth of the biomass occurs in the course of the test. This ensures that there are minimal changes in the medium and negligible accumulation of toxic metabolites during the test. Under these conditions, the plot of methane produced versus time should be linear, and the activity can be calculated from the slope of the line.

The vials containing MS medium were weighed prior to inoculation. The vials were then opened, whilst gassing with anaerobic-grade CO_2, and inoculated with an aliquot of sludge. The sludge was stirred and gassed with CO_2 continuously whilst being distributed. The vials were sealed again, and weighed. The sludge sample was analysed for volatile suspended solids and volatile solids. Note that the volatile solids measurement was used in the calculation of activity (see Section 4.3.1.1). Finally, each vial was supplemented with 1 mL of a stock solution of sodium acetate trihydrate (22.9 g/100 mL, stored under N_2), to give a final concentration of approximately 30 mM acetate. The final pH and EP were shown in initial experiments to be about 6.9±0.1 and -160 mV (SHE), respectively. The pH and EP were measured again at the end of each test to check if any significant changes occurred in the course of the test.

The vials were incubated at 20°C for a period of about 2 days. Samples of the headspace were taken periodically with a 1 mL SGE gas-tight syringe. The

syringe was first flushed with 0.5 mL of sample, before taking a sample of 0.5 mL for analysis. Methane in the headspace of the vial was determined by gas chromatography. The number of mole of methane in the headspace was calculated from:

$$n_{CH4,headspace} = \left(n_{CH4,sample,t} \times \frac{V_{headspace}}{V_{sample}} \right) + \left(2 \times n_{CH4,sample,t-1} \right)$$

where $n_{CH4,sample}$ = number of mole of methane in the sample

$$= \frac{R_{sample}}{R_{std}} \times n_{CH4,std} \ \mu mol$$

$$= \frac{R_{sample}}{R_{std}} \times 16.49 \ \mu mol$$

t=sampling time=1,2,3,4,5.

R_{sample}=detector response of sample

R_{std}=detector response of standard

$n_{CH4,std}$ = number of mole of methane in the standard

$$= \frac{c_{CH4,std} \times V_{std}}{V_m} \ \mu mol$$

$$= \frac{0.793 \times 500}{24.04} \ \mu mol$$

$$= 16.49 \ \mu mol$$

$c_{CH4,std}$=concentration of methane in the standard=0.793 µL/µL

V_{std}=volume of standard=500 µL

V_m=molar volume of an ideal gas at 20°C and 1 atm=24.04 L/mol

$V_{headspace}$=volume of serum vial (160 mL) less the volume of the liquid contents.

V_{sample}=volume of headspace taken for gas analysis.

The second term on the *R.H.S.* of this equation is included to correct for the amount of methane removed in the previous sampling of the headspace, including the 0.5 mL used to flush the syringe.

Methanogenic activity is then calculated from:

$$\text{methanogenic activity } (\mu\text{mol } CH_4 \text{ / day / g VS}) = \frac{\text{methane production rate } (\mu\text{mol } CH_4 \text{ / day})}{\text{volatile solids (g)}}$$

Error estimates for the activity measurements are propagated from the standard error of the methane production rate (obtained from regression analyses), as this is the largest error component in the calculation.

4.2.5 Media for Cultural Counts

Balch no. 1 medium[8], with 10% digester fluid added, was used for culturing anaerobes. The same medium, supplemented with antibiotics, was used to enumerate methanogens[65]. The recipe for the dilution solution is taken from Holdeman and Cato et. al.[20]. The methods for preparing the medium are adapted from Miller and Wolin[18], Latham and Wolin[60] and Holdeman and Cato et. al.[20].

Salts Solution for Anaerobic Dilution Blanks

$CaCl_2$ (anhydrous)..... 0.2 g (or 0.26 g $CaCl_2.2H_2O$)

$MgSO_4$ (anhydrous) ..... 0.2 g (or 0.48 g $MgSO_4.7H_2O$)

K_2HPO_4 ..... 1.0 g

KH_2PO_4 ..... 1.0 g

$NaHCO_3$ ..... 10.0 g

NaCl ..... 2.0 g

Mix $CaCl_2$ and $MgSO_4$ in 300 mL distilled water until dissolved. Add 500 mL water and, while swirling, slowly add remaining salts. Continue swirling until all these salts are dissolved. Add 200 mL distilled water, mix and store at 4°C.

Dilution Blanks

gelatin ..... 0.2 g

distilled water ..... 48.0 mL

salts solution ..... 50.0 mL

resazurin solution ..... 0.1 mL

Boil and cool whilst gassing with CO_2. Add 2 mL cysteine HCl-sodium sulphide solution and then tube (usually 9.0 or 9.9 mL per tube). This medium is usually still slightly pink when tubed.

Media Solutions

Mineral Solution 1:

K_2HPO_4 ..... 0.6% (w/v) in distilled water

Mineral Solution 2:

NaCl ..... 1.2% (w/v)

$(NH_4)_2SO_4$ ..... 1.2% (w/v)

KH_2PO_4 ..... 0.6% (w/v)

$CaCl_2.2H_2O$ ..... 0.16% (w/v)

$MgSO_4.7H_2O$ ..... 0.25% (w/v)

All dissolved in distilled water.

Trace Minerals:

nitrilotriacetic acid ..... 0.15% (w/v)

$MgSO_4.7H_2O$ ..... 0.3% (w/v)

$MnSO_4.2H_2O$ ..... 0.05% (w/v)

NaCl ..... 0.1% (w/v)

$FeSO_4.7H_2O$ ..... 0.01% (w/v)

$CoSO_4$ (or $CoCl_2$)..... 0.01% (w/v)

$CaCl_2.2H_2O$ ..... 0.01% (w/v)

$ZnSO_4$..... 0.01% (w/v)

$CuSO_4.5H_2O$ ..... 0.001% (w/v)

$AlK(SO_4)_2$ ..... 0.001% (w/v)

H_3BO_3 ..... 0.001% (w/v)

$Na_2MoO_4.2H_2O$..... 0.001% (w/v)

Dissolve the nitrilotriacetic acid with NaOH to pH 6.5; then proceed to add minerals. Adjust final pH to 7.0 with 10M NaOH.

Trace Vitamins:

BME vitamins stock solution..... 1:200 dilution with distilled water

Store at 0°C. Note: BME vitamins from SIGMA (catalogue no. B6891).

Resazurin Solution:

resazurin..... 0.1% w/v in distilled water.

Store in the dark because light inactivates resazurin.

Sodium Carbonate Solution:

Na_2CO_3 ..... 8.0% (w/v)

Boiled, chilled and equilibrated with CO_2 (prepare and store in a serum bottle).

Cysteine HCL - Sodium Sulphide Solution:

cysteine HCl ..... 1.25% (w/v)

$Na_2S.9H_2O$ ..... 1.25% (w/v)

Boil and then chill water whilst gassing with N_2. Add cysteine, adjust pH to 10.0 with 10M NaOH, and then add sodium sulphide. Store under N_2 in a 500 mL serum bottle.

Antibiotic Solution:

cephalothin ..... 340 ppm

clindamycin ..... 80 ppm

Prepare anaerobically and store under N_2 in a sealed serum vial.

Ferrous Sulphate Solution:

$FeSO_4.7H_2O$ ..... 1.0% (w/v) in 1.0% (v/v) HCl

Digester Fluid:

Transfer an approximately 500 mL sample of digester fluid to a 500 mL serum bottle, gas the headspace with N_2, then seal the bottle and autoclave at 121°C for 15 minutes. After cooling, filter through Whatman no.1 filter paper, adjust the pH of the filtrate to 7.0 then store under nitrogen in refrigerator.

Medium

Prepare 100 mL of medium as follows:

trypticase peptone (BBL)	0.2 g
yeast extract	0.2 g
sodium formate	0.25 g
sodium acetate	0.25 g
mineral solution 1	5 mL
mineral solution 2	5 mL
ferrous sulphate solution	0.1 mL
trace minerals	1.0 mL
resazurin solution	0.1 mL
digester fluid	10 mL

Ingredients, except sodium carbonate and cysteine HCl-sodium sulphide solutions (and agar), are dissolved in water, the pH adjusted to 6.8 with 1M NaOH and the volume made up to 93 mL. The medium is boiled and chilled, whilst being gassed continuously with CO_2.

sodium carbonate solution	5.0 mL
cysteine HCl-sodium sulphide solution	2.0 mL

After 5 minutes, 5 mL of the sodium carbonate solution is added to the mixture. After a further 5 minutes of gassing, the cysteine HCl-sodium sulphide solution is added and the medium is distributed to gassed serum bottles. The resazurin is usually reduced within 5 minutes after addition of reducing agent.

The serum bottles are sealed, capped and crimped, and autoclaved at 121°C for 15 minutes.

When agar is added to the medium (at 1.5% w/v), the agar is melted by heating the solution in a round bottom flask on a heating mantle and then cooling to 50°C in a water bath, whilst gassing with anaerobic-grade CO_2. The sodium carbonate solution and reducing agent are then added as described above. The agar medium is distributed to Hungate roll-tubes (4.5 mL per tube) which are then sealed with butyl rubber septa and screw caps. The tubes are then autoclaved at 121°C for 15 minutes.

Just prior to inoculation, the tubes are autoclaved to melt the agar and then equilibrated in a water bath at 50°C. Vitamins and antibiotics are injected into the agar tubes via a 0.2 µm sterile syringe filter. The medium is mixed by gently inverting the tubes.

trace vitamins ..... 2% (v/v)

antibiotic solution..... 2% (v/v)

After inoculation, the agar tubes are rolled in a Hungate tube spinner till the agar has solidified.

Quantities Of Anaerobic Dilution Solution And Medium To Prepare

For total anaerobe and methanogen counts, 9 dilution blanks and 12 agar tubes (6 with antibiotics) are needed for each sample. Therefore, the following quantities are needed per sample:

12×4.5 mL = 54 mL Modified Balch No.1

9×9.0 mL = 81 mL anaerobic dilution solution.

1 L each of medium and dilution solution will be sufficient for at least 10 samples.

4.2.6 Enumeration Methods

The enumeration methods are based on the methods of Holdeman and Cato et. al.[20] and Miller and Wolin[65]. Approximately one gram (wet weight) of sludge or scum was inoculated into 9 mL of sterile pre-reduced dilution solution in a 15 mL serum tube with a few glass beads (about 2 mm in diameter). The bottle was opened aseptically and gassed with anaerobic-grade CO_2 while the sample was added. The bottle was resealed with a butyl rubber stopper and aluminium crimp seal. The 10^{-1} dilution was vortexed for 2 minutes, and then serial 10-fold dilutions were prepared.

For total anaerobic counts, a syringe was used to transfer 1 mL of the appropriate dilutions to replicate roll tubes of melted and cooled modified Balch no.1 medium, under 1 atm CO_2. To enumerate methanogens, duplicate dilutions were added to roll tubes containing modified Balch no.1 medium with cephalothin (6.7 µg/mL) and clindamycin (1.7 µg/mL) under 1 atm of 3% H_2-97% CO_2. The antibiotics were prepared anaerobically under N_2 and transferred to the roll tubes just prior to inoculation with a sterile 1 mL syringe equipped with a sterile 0.2 µm syringe filter and 26 gauge needle. Tubes were incubated at 37°C and counted after 7 days. On two occasions, additional tubes were prepared

and incubated at 20°C, which is roughly the in-situ temperature of the anaerobic reactor, and counted after 21 days. There was no statistically discernible difference between the two incubation temperatures (see Section 4.3.3.1). Blank tubes were also prepared with each sample to check that no contamination occured during the procedure.

4.2.7 Direct Microscopic Clump Counts (DMCC)

Direct microscopic clump counts are based on the method of Holdeman and Cato et. al.[20]. DMCC's are useful for checking cultural counts and for describing the dominant morphological forms. The method is as follows:

1. With a calibrated loop, smear 5 µL of an appropriate dilution (from the cultural counts) evenly in a 1 cm square marked on a slide (with a diamond tip or solvent-resistant pen). Smear a duplicate square. Air dry and heat fix.
2. Gram stain.
3. Count six edge fields and four centre fields. Count at least 10 fields or 100 organisms, whichever is greater. Count chains, pairs, etc., as '1'. Calculate the average number of organisms per field.
4. Calculate: Uncorrected DMCC

   $= (\text{av. organisms / field}) \times (\text{fields / cm}^2) \times (\text{dilution}) \times (1 / \text{sample size})$ per mL

5. Calculate: Correction Factor

$$= \frac{(\text{grams sample used}) \times (10\ \text{mL})}{9\ \text{mL} + \text{grams sample used}}$$

= grams sample per 10 mL of first dilution

6. Calculate: Corrected DMCC=Uncorrected DMCC×10/Correction Factor

7. If the volatile solids concentration of the sample was measured, then the corrected DMCC can be divided by the VS concentration (%w/w) and expressed as 'per gram VS'.

4.2.8 Analytical Methods

Methane was analysed by gas chromatography. A Varian 3400 GC, equipped with a thermal conductivity detector and 12′×1/8″ stainless steel column packed with Haysep-Q. The column temperature was 30°C and the carrier gas was argon (15 $mL.min^{-1}$). 0.5 mL samples of the headspace in the vials were taken for analysis using a 1 mL SGE gas-tight syringe fitted with a gas-tight valve and 23G needle. Syringes were cleaned with acetone, dried and flushed with 0.5 mL of sample before taking a sample for analysis.

Volatile solids were determined gravimetrically according to Method APHA 2540C from *Standard Methods for the Examination of Water and Wastewater* (APHA: USA, 18th ed., 1992).

Volatile suspended solids were determined gravimetrically by centrifuging a sample of sludge, decanting the centrate, washing the pellet and centrifuging again. The pellet was then transferred to a porcelain crucible, dried

at 105°C for about 2 hr, weighed and then ignited at 800°C. The loss on ignition is equivalent to the volatile suspended solids.

Individual **volatile fatty acids** were measured by gas chromatography according to *HMSO Methods for the Examination of Waters and Associated Materials 1979 (Determination of volatile acids in sewage sludge).*

pH was measured with a Metrohm glass electrode and Metrohm pH Meter E588.

Electrode potential (or redox potential) was measured with a Metrohm ORP combination electrode. The probe uses a Ag/AgCl/c(KCl)=3M reference electrode. The half-cell potential of the reference electrode is +208 mV at 25°C. The measured EP values given in this chapter can be approximately scaled to the Standard Hydrogen Electrode by adding +208 mV.

Electron micrographs and elemental scans were obtained by coating sludge particles with carbon and analysing with a Jeol JSM 6400 Scanning Electron Microscope (SEM) and a Tracor Northern, Series II, Energy Dispersive X-ray Analyser (EDXA).

4.3 RESULTS AND DISCUSSION

4.3.1 Activity Test Method Development

4.3.1.1 Repeatability of biomass subsampling

Dolfing and Bloemen distributed a sample of sludge to the vials and measured the biomass in each vial at the completion of the activity test. If the biomass subsampling error is small, however, an easier procedure is to measure the volatile solids concentration in the original sample (on a w/w basis) and weigh the vials before and after inoculation. The biomass, expressed as volatile solids, can then be determined by multiplying the mass of wet sludge by the volatile solids concentration.

Table 4-1 Biomass measurements.

Replicate	VS % w/w	VSS % w/w
1	3.64	3.57
2	3.68	3.50
3	3.68	3.56

Triplicate measurements of volatile solids and volatile suspended solids were made on a sample of sludge collected from sampling port 12 (Table 4-1). The mean VS and VSS concentrations are 3.67 % w/w and 3.54 % w/w, respectively. The percent relative standard deviations of the VS and VSS concentrations are 0.6% and 1.1%. The combined biomass measurement and subsampling error is small relative to the error in the measurement of the methane production rate (approx. 5-10%). It is not necessary, therefore, to measure the biomass in individual vials at the end of the test.

Furthermore, VSS is typically used as a measure of the biomass concentration, but VS is easier to measure, and if the concentration of soluble organic matter is relatively low, then VS is an acceptable surrogate measure of biomass. A two-sample t-test (using separate variance estimates) shows that the difference between VS and VSS is statistically significant at the p=0.014 level. However, the mean difference between VS and VSS is quite small (0.124 %w/w, or 3.3%) and VS was therefore used to measure biomass concentration.

4.3.1.2 Inoculum size and the period of the activity test measurement

Soto and Méndez et. al.[62] explain that activity can be expressed by:

$$Ac = (1/X_0)(-dS/dt)$$
$$= (Ac_m/X_0)S\left[X_0 + Y_{xs}(S_0 - S)\right]/(K_s + S)$$

where Ac = activity ($gCOD \cdot g^{-1}VSS \cdot d^{-1}$)

Ac_m = maximum specific activity ($gCOD \cdot g^{-1}VSS \cdot d^{-1}$)

X_0 = initial microbial concentration ($gVSS \cdot L^{-1}$)

S = limiting substrate concentration ($gCOD \cdot L^{-1}$)

Y_{xs} = yield (ratio of microbial growth rate and substrate removal rate)

S_0 = initial substrate concentration ($gCOD \cdot L^{-1}$)

K_S = the half-saturation constant ($gCOD \cdot L^{-1}$).

In order that the activity be represented by a single parameter, they show that the kinetic behaviour of the test should approximate a zero order model, and to do this the size of the inoculum must satisfy the conditions:

$$X_0/Y_{XS} >> (S_0 - S) \text{ and } S >> K_S$$

Under these conditions, the required inoculum size can be calculated from:

$$X_0 = S_0 Y_{XS}$$

Using the example given by Soto and Méndez et. al.[62], an estimate of Y_{XS} for *Methanosarcina* sp. is 0.04 gVSS·g^{-1}COD, and if the initial substrate concentration is fixed at 2.0 g·L^{-1} (33 mM) acetic acid, which is approximately equal to 2 gCOD·L^{-1}, then the minimum inoculum size will be 0.08 gVSS·L^{-1}. Given, however, that only about 1-10% of the biomass in anaerobic digesters will be able to produce methane from acetate, Soto and Méndez et. al.[62] recommend an inoculum size of 0.8-8.0 gVSS·L^{-1}.

To further narrow down the size of inoculum to use, and to define the period of measurement to be employed, a series of activity tests were performed using inoculum sizes in the range of 0.1 to 4.0 gVS·L^{-1}. The source of the inoculum was sludge taken from the bottom of the 115E anaerobic reactor at sampling port no.15. The VS concentration of the sludge was 2.10 %(w/w).

Five measurements of the methane concentration in the headspace were made for each vial, over a period of approximately two days. The results of the experiment are given in Table 4-2, including estimates of the correlation between methane production and time.

Table 4-2 Relationship between methane production rate, methanogenic activity and inoculum size.

Inoculum (g wet weight/ vial)	Inoculum (g VS/L)	Methane Production Rate (µmol CH_4/day)	Pearson correlation coefficient	Methanogenic activity (µmol CH_4/day/g VS)	Error (µmol CH_4/day/g VS)
0.3498	0.131	0.065	0.962	8.85	1.5
0.7861	0.295	0.172	0.763	10.4	5.1
1.8001	0.675	0.540	0.985	14.3	1.4
4.9026	1.839	3.446	0.996	33.5	1.8
7.3618	2.761	7.146	0.995	46.2	2.6
10.0748	3.779	9.736	0.996	46.0	1.5

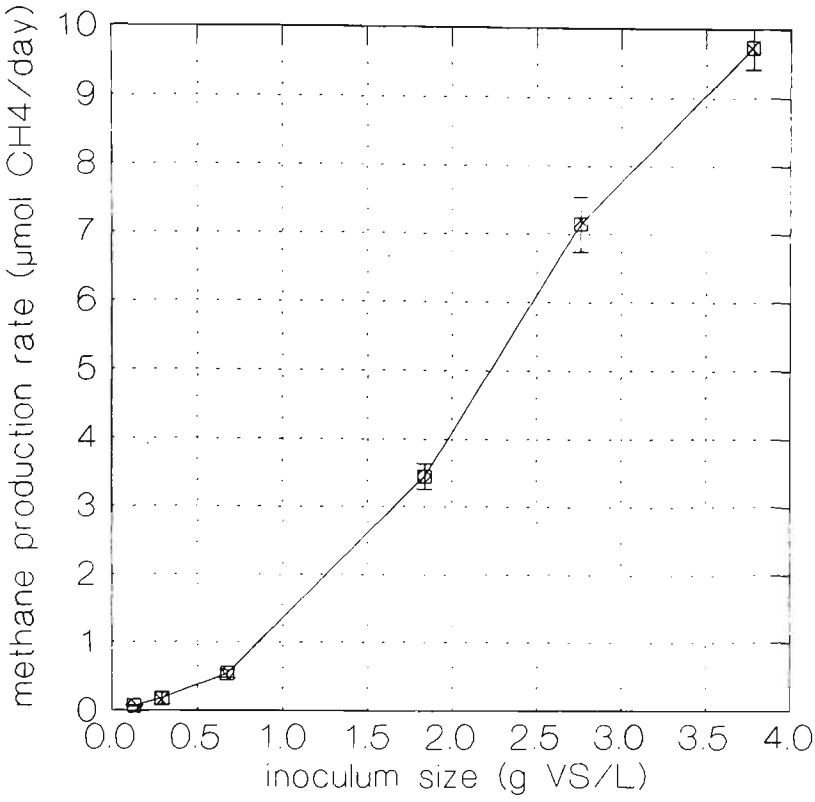

Figure 4-2 Relationship between methane production rate and inoculum size.

Firstly, it is noted that methane production varied linearly with time, which indicates that adaptation, significant growth of the biomass or substrate depletion did not occur within the two day period of measurement. This is a necessary prerequisite for the activity test.

Secondly, it can be seen in Figure 4-2 that the rate of methane production seemed to increase exponentially up to an inoculum size of about 2.8 $gVS \cdot L^{-1}$. As a result, the methanogenic activity (Table 4-2) was not constant below 2.8 $gVS \cdot L^{-1}$, it was dependant on inoculum size. This indicates that the minimum inoculum size to employ is approximately 2.8 $gVS \cdot L^{-1}$.

It should be noted that the volatile solids concentration, in the sample of sludge used in this experiment, was unusually low. The VS concentration is typically about 3 %(w/w) which, for an inoculum size of 2.8 $gVS \cdot L^{-1}$, translates to about 5 g of wet sludge per 50 mL of MS medium.

4.3.1.3 Background activity from residual substrates in the biomass

As explained in Section 4.2.4, the basis of all methanogenic activity tests is to first dilute out all substrates in the sample of biomass being tested, to negligible levels, by inoculating a serum vial containing a relatively large volume of mineral salt medium. If this is done, then there should be no need for 'controls' (or blanks) because there will be negligible background activity and the test should be specific to the substrate being tested. Sørensen and Ahring[63] argue that while this approach may be suitable to granular sludge, which is relatively easy to separate from the liquid phase and suspend in an artificial medium, it may not be appropriate when the inoculum consist of a slurry of active cells and dissolved and suspended organic nutrients. Because the cells cannot be conveniently separated from other components of the mixed liquor, activity tests on these biomasses typically show non-specific methane production. To correct for the background activity, Sørensen and Ahring[63] recommend doing a 'control' (or blank) with each batch of biomass. The paper by Sørensen and Ahring[63] was discovered only after performing all of the activity tests for Chapter 4 and 5, and as a consequence it was thought necessary to check both theoretically and

experimentally (see Section 4.3.1.4) the assumptions and conclusions made in these two chapters.

With particular reference to the specific methanogenic activity from acetate, an appreciable background concentration of volatile fatty acids can result in a significant increase in the acetate pool, which in turn will affect the rate of methanogenesis. When looking for patterns in acetoclastic activity along the 115E anaerobic reactor, differences in the background concentrations of volatile fatty acids could complicate the interpretation of the activity test data.

Similarly, if there is an appreciable background concentration of hydrogen, then there will also be an appreciable hydrogenotrophic activity. This, too, can complicate the interpretation of the data.

An analysis of sludge from the 115E reactor (sampling port 12) for C2-C4 volatile fatty acids gave the following results:

acetic acid	100 mg/L (1.66 mM)
propionic acid	8 mg/L (0.11 mM)
i-butyric acid	1 mg/L (0.01 mM)
n-butyric acid	3 mg/L (0.03 mM)

Given that there is about a 5/56 dilution of the biomass in the test, the background concentration of acetate (0.15 mM), whilst possibly sufficient to produce a detectable control activity given reported K_s values ranging between 0.21 and 15.9 mM[66], would not significantly alter the size of the acetate pool (30 mM). Similarly, while propionate and butyrate are degraded via acetate, it is unlikely that the background levels of propionic and butyric acids would lead to a

significant change in the acetate pool. For example, it has been reported that mesophilic sludge has a K_s for propionate of 0.04-0.19 mM[66], but the background propionate concentration in the test is approximately 0.01 mM. That is, the propionate degraders should not be operating at an appreciable rate.

Hydrogen is usually produced during activity tests. The K_s of some *Methanobacterium* sp. for H_2 is between 0.011-0.015 atm (110-150 μL/L)[67], and for mesophilic sludge a $K_{s,H2}$ of 0.105 atm (1050 μL/L)[67] has been recorded. The hydrogen concentration in the headspace of the vials, however, is usually less than 10 μL/L and it is unlikely that there would be an appreciable hydrogenotrophic methanogenic activity.

Furthermore, it should be noted that Sørensen and Ahring[63] experimented with biomass from a thermophillic digester treating household solid waste, which had much higher background concentrations of acetate, propionate, and butyrate than the biomass from the 115E Reactor. It should also be noted that when these authors employed dilution factors of 20:1, there was negligible background activity compared to vials supplemented with 30 mM acetate. The concentrations of acetate, propionate and butyrate in the biomass being tested by Sørensen and Ahring[63] were 5.7 mM, 0.6 mM and 0.0 mM, respectively. At a 1:20 dilution, the background concentrations of acetate, propionate and butyrate would have been 0.28 mM, 0.03 mM and 0.0 mM. In the tests performed on biomass from the 115E Reactor, the background concentrations of acetate, propionate and butyrate would typically have been about 0.15 mM, 0.01 mM and 0.004 mM. On the basis of the results from Sørensen and Ahring[63], it would seem reasonable to assume

that the background concentrations of volatile fatty acids would have been negligible, and controls unnecessary, in the experiments on biomass from the 115E Reactor.

These data suggest that the activity test method employed in this research was suitable for relative measurement of acetoclastic methanogenic populations. There is, therefore, no reason to believe that controls would have altered the conclusions made in Chapter 4 and 5. In any case, experiments were conducted to further verify this, and these are discussed in the next section (Section 4.3.1.4)

4.3.1.4 Toxicity of unionised acetic acid

Whilst investigating the level of background activity from residual nutrients in the biomass, it was found that the activity in vials supplemented with 30 mM acetate was considerably lower than the control vials. It is possible that this was due to inhibition by unionised acetic acid. Concentrations of volatile fatty acid greater than 10 mg/L (as acetate) have been reported to inhibit methanogenic activity[68].

Initially, when investigating the level of background activity, triplicate measurements of activity were made with and without the acetate supplement. The sludge used in the experiment was taken from sampling port 8.

To one set of triplicate vials, 1 mL of a stock solution of 1680 mM acetate was added to give a final acetate concentration of 30 mM. To another set of triplicate vials, 1 mL of degassed deionised water was added. The mean and

standard error of the activity in the acetate-supplemented vials was 56±3 μmol CH_4/day/g VS. For the control vials, the mean and standard error of the activity was 103±3 μmol CH_4/day/g VS. Clearly, the activity in the supplemented vials was about 50% of that in the control vials.

To verify this finding, another experiment was performed using a range of acetate concentrations. The sludge on this occasion was taken from sampling port 12. The concentrations of C2-C4 volatile fatty acids in the sludge were:

acetic acid	31 mg/L
propionic acids	<1 mg/L
i-butyric acid	<1 mg/L
n-butyric acid	<1 mg/L

Six acetate stock solutions were prepared with 0, 4.30, 8.30, 12.58, 16.45, and 21.10 g/50 mL of sodium acetate trihydrate. 1 mL of the stock solutions was added to six vials to give 0, 11.3, 21.8, 33.0, 43.2, and 55.4 mM acetate. The background acetate concentration in the sludge made a minor contribution (0.05 mM) to the total acetate concentration in each vial.

The methanogenic activity was observed to decrease exponentially with increasing acetate concentration (Figure 4-3). The concentration of unionised acetic acid was calculated from Equation 4-1 and is shown in Figure 4-3. The final pH and EP were measured and found to be similar in all vials (Table 4-3).

$$pH = pK_a + \log\frac{[Ac^-]}{[HAc]} \qquad \textbf{Equation 4-1}$$

$$\Rightarrow \quad = pK_a + \log\frac{[TAc]-[HAc]}{[HAc]}$$

$$\Rightarrow [HAc] = \frac{[TAc]}{1+10^{(pH-pK_a)}}$$

where pK_a=4.75 @ 25°C

[Ac^-]=ionised acetic acid concentration (mM)

[HAc]=unionised acetic acid concentration (mM)

[TAc]=total acetate concentration (mM)=[Ac^-]+[HAc]

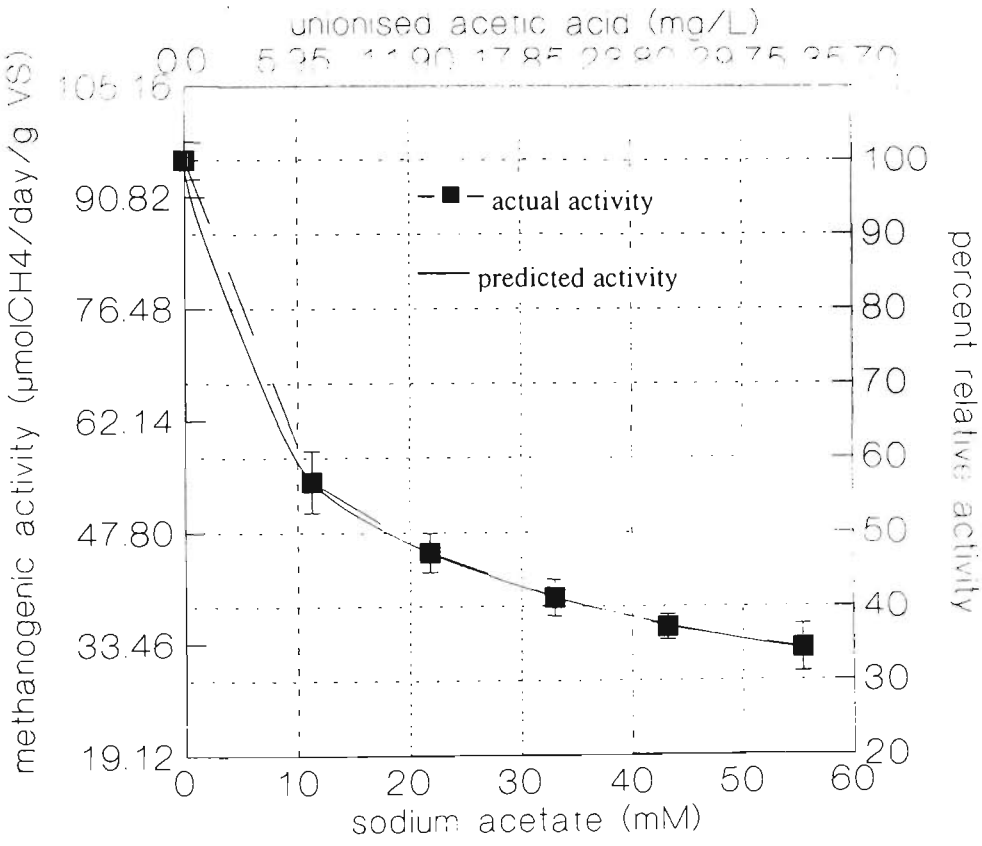

Figure 4-3 Methanogenic activity versus total and unionised acetic acid.

Table 4-3 Final pH and EP in vials.

Vial	pH	EP (mV)*
1	6.75	-330
2	6.75	-325
3	6.75	-330
4	6.75	-340
5	6.75	-340
6	6.75	-340

*relative to Ag/AgCl/c(KCl)=3M reference electrode.

Clearly, there appears to be considerable inhibition of methanogenic activity, even at concentrations less than 10 mg/L unionised acetic acid. The "dose-response" curve was modelled using Equation 4-2[69].

$$A = 100 \times \left[1 + \left(\frac{c}{K} \right)^{a} \right]^{-1} \qquad \textbf{Equation 4-2}$$

where A = percent relative activity

c = concentration of unionised acetic acid in mg/L

K = "half-kill" dose, mg/L (i.e. value of c for which A=50%)

= 10.7 mg/L

a = sensitivity exponent = 0.584

The model was fitted to the data by the method of nonlinear regression using the Gauss-Newton algorithm to estimate the parameters K and a. From the model, it

is deduced that acetoclastic methanogenic activity is inhibited by 50% at 10.7 mg/l unionised acetic acid.

The implication of this finding is that careful consideration needs to be given to the pH of the medium and acetate concentration used for activity tests. Both the concentration of acetate and pH affect methanogenic activity and there is an interaction between them. If correction for background activity is required, then inhibition from unionised acetic acid needs to be minimised. At 30 mM acetate, pH levels of 7.6, 8.0 and 10.5 will give unionised acetic acid concentrations of 2.5 mg/L, 1.0 mg/L and 0.1 mg/L, respectively. From Equation 4-2, these concentrations of unionised acetic acid correspond to 30%, 20% and 6% inhibition. Note, however, that methanogenic activity drops sharply on either side of the optimum pH[22]. At pH 8.0, Dolfing and Bloemen[22] observed an inhibition of about 50%.

All activity tests reported in Chapter 4 and 5 were carried out at pH 6.9±0.1 and total acetate concentration of 30 mM. At this pH, the maximum activity would probably have occurred at around 2 mM total acetic acid. If the optimum conditions were used then the relative error in the activity measurements would have been substantially reduced. However, at this acetate concentration, the measured activity would be influenced by the background concentration of acetic acid and the method may not be specific to acetoclastic methanogens, nor provide an accurate representation of spatial patterns in methanogenic density. Substrate toxicity poses the trilemma: 1) the acetate concentration must be increased to ensure the measured activity is independent of

substrate concentration; 2), if the acetate concentration is increased the bacteria will be growing under suboptimal conditions, and; 3), adjusting the pH to counter the substrate inhibition would only lead to significant pH inhibition.

Substrate toxicity and its relationship to pH does not appear to have been addressed in the literature on methanogenic activity tests[22,60,62,63,64,67], though it certainly needs to be considered in the quest for a standard method. Essentially, in the design of an acetoclastic methanogenic activity test, it is desirable to have an acetate pool large enough that it can be considered constant throughout the course of the experiment, and adequate dilution to minimise the effect of background volatile fatty acids. If the concentrations of volatile fatty acids in the biomass cannot be sufficiently diluted out, then it would be necessary to perform controls (or blanks) to correct for the background activity. However, in the presence of substrate toxicity, controls make no sense at all. The question, then, is how can the effect of residual substrates on the measured activity be experimentally quantified and accounted for? One way would be to deliberately test the sensitivity of the method to small changes in the supplemented acetate concentration (using acetate or other volatile fatty acids). This has, in fact, essentially been done in the experiment described above. Using Equation 4-1 and Equation 4-2, it can be shown that at pH 6.9 a change of 0.15 mM in the supplemented acetate concentration (i.e. a change from 30 mM to 30.15 mM) would change the measured activity by only 0.15% (coincidentally).

With regard to the work carried out in Chapter 4 and Chapter 5, this suggests that: 1), controls would have made no sense in the context of the activity

test method employed; 2) background activity was likely to have been negligible, and; 3), conditions for bacterial growth would have been less than optimal. The fact that growth conditions may have been suboptimal is unlikely to have had any bearing on the conclusions made in Chapter 4 and 5. In any case, the spatial pattern in methanogenic density was actually verified by cultural counts of methanogens in Section 4.3.4. Further research is clearly needed to define a standard protocol for methanogenic activity measurements.

4.3.1.5 Repeatability of Activity Measurements

To demonstrate the repeatability of the activity test, six replicates were performed using sludge from sampling port 12 (VS=3.25 %w/w). The results are presented in Figure 4-4. The mean and standard deviation of the activity measurements were 29 and 2 µmol CH_4/day/g VS, respectively. The relative standard deviation was 6.6%.

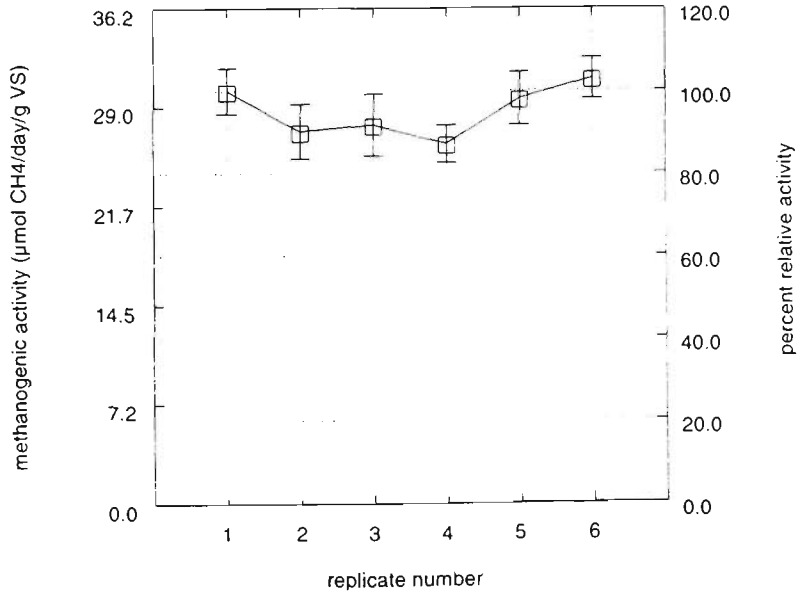

Figure 4-4 Repeatability of activity test.

4.3.2 Methanogenic Activity along the 115E Anaerobic Reactor

To survey the distribution of methanogens in the 115E anaerobic reactor, sludge samples were taken at 2.5 m depth from each row of sampling ports along the reactor. Two sampling runs were done on different days (1/5/95 and 15/5/95). On each day, a sample was taken from each row of sampling ports. On the second run, a sample of the scum was also taken, from 1 m into the scum blanket, at sampling port 3. Not all sampling ports were accessible, either due to the collection of storm water in the vicinity of the port, or because the HDPE cover was distended from gas pressure making it too dangerous to open the sampling port. The fact that samples were taken from different columns was believed to have little effect in a study of longitudinal variability, because as shown in Chapter 3 there was no apparent systematic pattern in the common process control variables across (i.e. between columns) the reactor.

The results are presented in Figure 4-5 and Figure 4-6. The inoculum concentrations used are given in Table 4-4. Some of the variability in activity could be explained by suboptimal inoculum concentrations, although, generally the activity appears to peak at about the third or fourth row of sampling ports. This corresponds to 100-140 m along the reactor, or, in terms of the theoretical hydraulic residence time, 0.45 to 0.65 days. After the peak, the activity declines quite sharply.

These results indicate that sludge methanogenic activity is not uniform. The pattern in methanogenic activity is possibly explained by the availability of

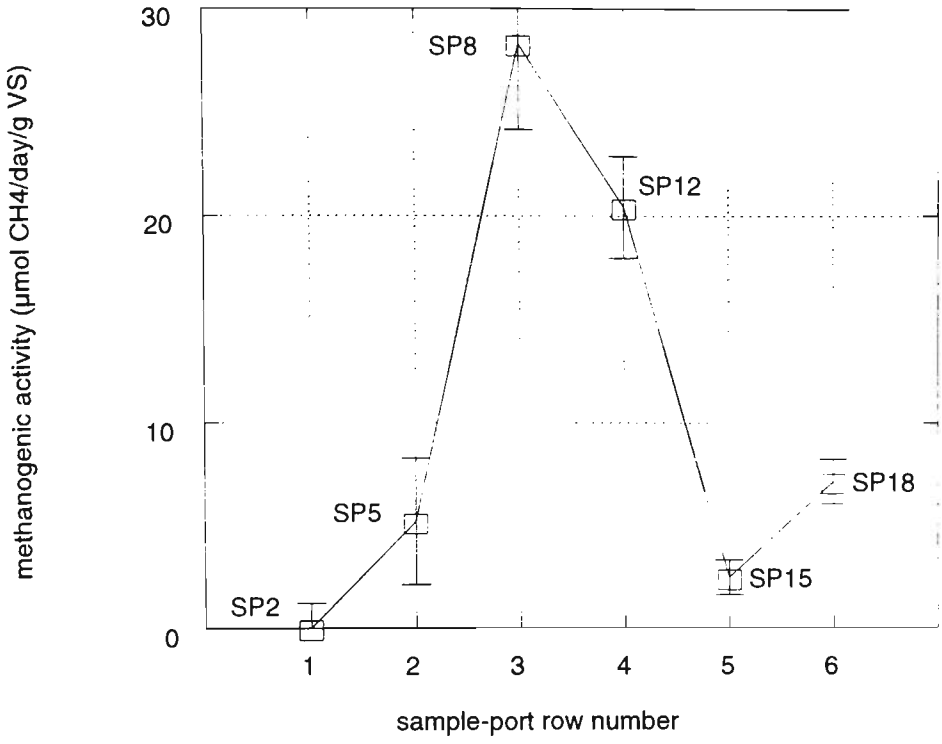

Figure 4-5 Acetoclastic methanogenic activity along the 115E reactor (1/5/95). Sample port numbers are shown adjacent to each data point.

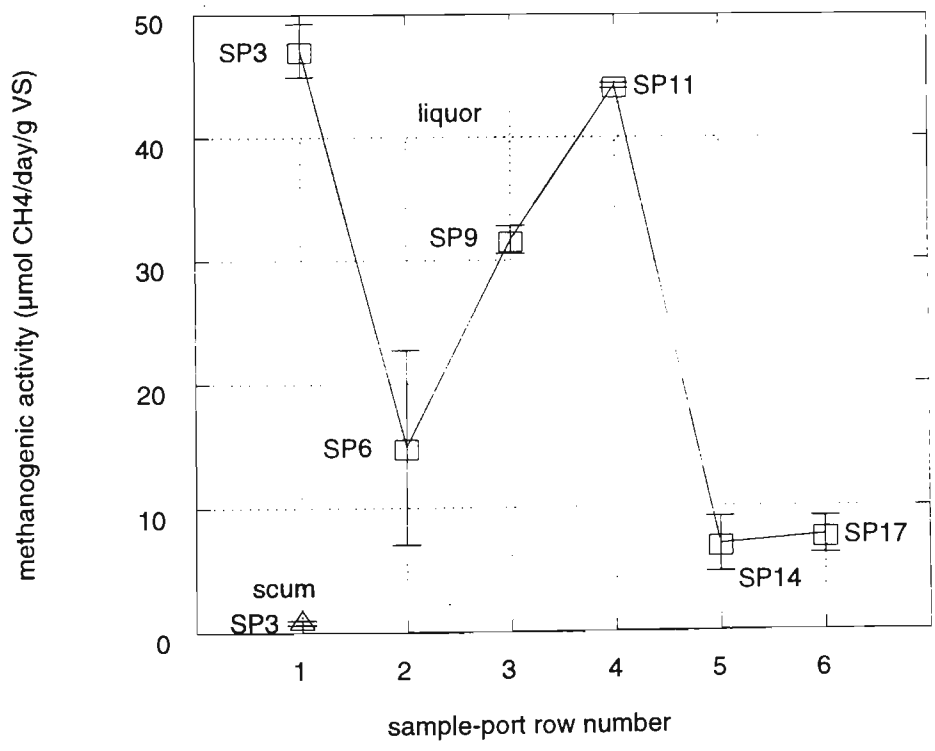

Figure 4-6 Acetoclastic methanogenic activity along the 115E reactor (15/5/95). Sample port numbers are shown adjacent to each data point.

Table 4-4 Inoculum concentrations.

Sample-port row no.	Inoculum concentration (g VS/L)	
	1/5/95	15/5/95
1	0.357	3.518 (liquor) 7.143 (scum)
2	0.464	0.393
3	1.321	3.018
4	1.661	2.714
5	3.357	3.286
6	4.018	4.696

substrate, or, more precisely, the rate at which substrate is produced. Enumeration of total anaerobes and methanogens actually verified and helped to explain the observed pattern in acetoclastic methanogenic activity.

4.3.3 Development of Enumeration Methods for Total Anaerobes and Methanogens

4.3.3.1 Choice of incubation temperature

The in-situ temperature of the 115E anaerobic reactor varies between 15-25°C and it would seem reasonable therefore to incubate tubes at 20°C. However, tubes incubated at 20°C take 3-4 weeks for all colonies to become

Table 4-5 Colony counts at incubation temperatures 20°C and 37°C

Date	Type	Colony counts (CFU/g VS)	
		20°C	37°C
26/6/95	Methanogen	2.5×10^{8}	7.6×10^{8}
26/6/95	Methanogen	3.6×10^{8}	5.2×10^{8}
26/6/95	Total Anaerobe	9.0×10^{9}	8.3×10^{9}
26/6/95	Total Anaerobe	8.3×10^{9}	7.3×10^{9}
3/7/95	Methanogen	1.4×10^{8}	9.4×10^{7}
3/7/95	Methanogen	9.8×10^{7}	7.2×10^{7}
3/7/95	Total Anaerobe	5.0×10^{9}	1.0×10^{10}
3/7/95	Total Anaerobe	5.3×10^{9}	9.8×10^{9}

Table 4-6 ANOVA table for the effect of incubation temperature

Source	Sum of Squares	DF	Mean Square	F-Ratio	Prob.
DATE	0.499	1	0.499	9.845	0.009
TYPE	9.846	1	9.846	194.404	0.000
TEMPERATURE	0.041	1	0.041	0.815	0.386
TEMP* TYPE	0.001	1	0.001	0.025	0.878
ERROR	0.557	11	0.051		

visible, compared to 1 week for tubes incubated at 37°C. Zeikus and Winfrey[70], in their study of sediments from Lake Mendota, found that the number of sediment methanogens remained constant when in-situ (4-24°C) or 30-37°C incubation temperatures were used. To verify that an incubation temperature of 37°C could be used, two samples of sludge from the 115E reactor (sampling port 8) were incubated at 20°C and 37°C.

For both methanogens and total anaerobes, four tubes were plated from the appropriate dilutions of each sample, two of the tubes were incubated at 20°C and two at 37°C. The results are presented in Table 4-5. An analysis of variance performed on the log_{10} transformed counts indicates that the incubation temperature did not have a statistically discernible effect (at the 0.05 level) on the counts of either methanogens or total anaerobes (Table 4-6).

4.3.3.2 Cross-checking counts obtained with the antibiotic medium

To check that the antibiotic resistant bacteria were actually methanogens, methane analyses were done on headspace samples from serial dilution roll tubes that did and did not contain antibiotics. Tubes prepared from three samples of sludge were tested.

Of the antibiotic-supplemented tubes that were tested, all those that had visible colonies also had detectable quantities of methane. One set of replicate tubes that had only one colony, produced approximately 1000 ppm methane after

one month of incubation. At the corresponding dilution, tubes without antibiotics also had detectable quantities of methane. At higher dilutions and with visible colonies, tubes without antibiotics did not have detectable quantities of methane. The detection limit (criterion of detection, α=0.05) for methane is approximately 20 ppm. These results indicate that the antibiotic medium is suitable for cultural counts of methanogens in the sludge from the 115E anaerobic reactor.

4.3.4 Densities of Methanogens and Total Anaerobes in Sludge from the 115E Anaerobic Reactor

To investigate the pattern in the densities of methanogens and total anaerobes along the 115E reactor, a sample of sludge was taken from each row of sampling ports. All samples were taken at 2.5 m depth, except for samples taken from sampling ports 14 and 17 which were taken at 2 m and 1.25 m, respectively, due to the height of the compacted sludge layer at these locations.
One sample was taken per day for each of seven days (between 26/6/95 and 6/7/95), owing to the time involved in processing each sample. The order of sampling from the different rows was determined randomly to avoid problems that might have been caused by systematic patterns over time. The results, which are geometric averages of duplicate tubes, are presented in Figure 4-7.

The pattern in the cultural counts of methanogens and total anaerobes is similar to the pattern obtained with the methanogenic activity tests. The density of total anaerobes, and possibly methanogens, appears to reach a peak about

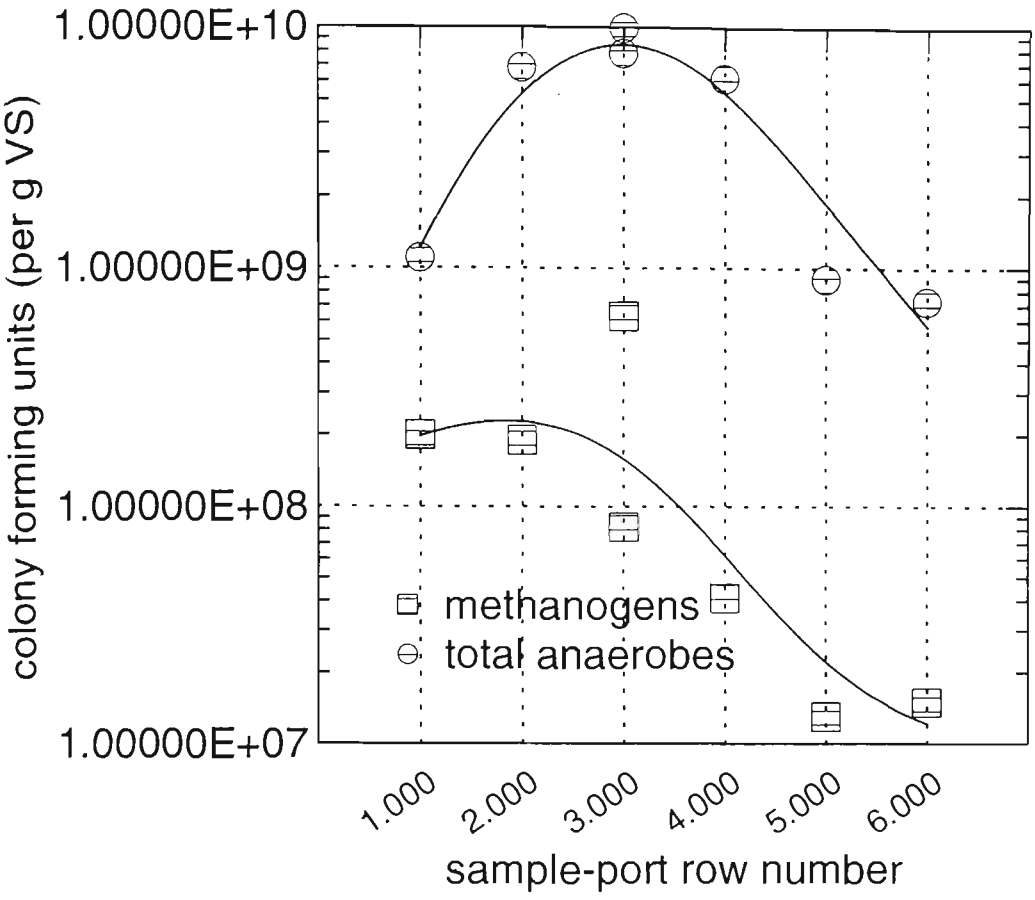

Figure 4-7 Spatial pattern in the densities of methanogens and total anaerobes in the 115E reactor.

midway along the reactor, and then tails off towards the end of the reactor. As alluded to in Section 4.3.2, the decline in the methanogenic population can possibly be attributed to a decrease in the rate of substrate production. The observed, corresponding decline in total anaerobes supports this hypothesis. The densities of methanogens and total anaerobes cannot be compared to other anaerobic ponds because no studies of the microbiology of anaerobic ponds could be found in the literature.

The percentage of methanogens in the sludge flora ranged from 0.6-18.2% by number; the median was 2.1%. There was no apparent systematic pattern in

the percentage of methanogens. Miller and Wolin[65] observed methanogen percentages of 0.001-12.6% in human faeces.

Direct microscopic clump counts (DMCC) ranged between 1.1×10^{11} and 9.4×10^{11} bacteria/g VS. The DMCC's were generally one to two orders of magnitude greater than the cultural counts. This does not necessarily mean that the cultural counts underestimated the numbers of anaerobes. It is quite likely that the sludge in the reactor contains large numbers of dead cells because the solids residence time is in the order of years.

The dominant morphological forms were Gram-positive coccoid and Gram-negative rod-like cells. Zeikus[16] reported that Gram-negative, non-sporing rods that produce hydrogen and volatile fatty acids appear to predominate in sewage sludge, and that Gram-negative facultative rods, Gram-positive cocci, endospore-forming rods and Gram-positive asporogenous rods can be routinely isolated from digesters.

4.3.5 Characterisation of the Scum Matter in the 115E Reactor

Since installing the floating HDPE cover on the 115E anaerobic reactor, in late 1992, a 'scum layer' had developed which occupied almost one quarter of the volume of the reactor in 1995. The scum material had the approximate composition shown in Table 4-7[71].

The scum had a fibrous texture. A sample of the scum was washed and filtered, and some fibres were examined by scanning electron microscopy

Table 4-7 Approximate composition of scum material (note: the balance of the volatile solids is believed to consist of non-cellulose carbohydrates and humic acids, for example).

Moisture	80 %w/w
Total Solids	20 %w/w
NH_3-N	0.25 %w/w
Total Kjeldahl Nitrogen	0.5 %w/w
Fixed Solids (inorganic)	45 %w/w of total solids
Volatile Solids (organic)	55 %w/w of total solids
Crude Fibre (cellulose)	25 %w/w of volatile solids
Oil and Grease	20 %w/w of volatile solids
Protein (6.25 × Kjeldahl nitrogen)	15 %w/w of volatile solids

(SEM)[72]. These fibres appeared to be of plant origin (cellulose) because of their smooth surface; animal hair typically has a rough surface of overlapping keratin plates. The fibres were compared with electron micrographs of household toilet tissue and found to be very similar[72].

A sample of the particulate matter in the scum was similarly examined by SEM, as well as energy-dispersive X-ray analysis (EDXA). The results are shown as Figure 4-8. The particles had porous structures and were composed mainly of silicon, calcium, aluminium, iron, sulphur, phosphorus, sodium, magnesium and potassium. A comparison of the chemical composition and physical structure of the particles to SEM and EDXA of anaerobic granules[4]

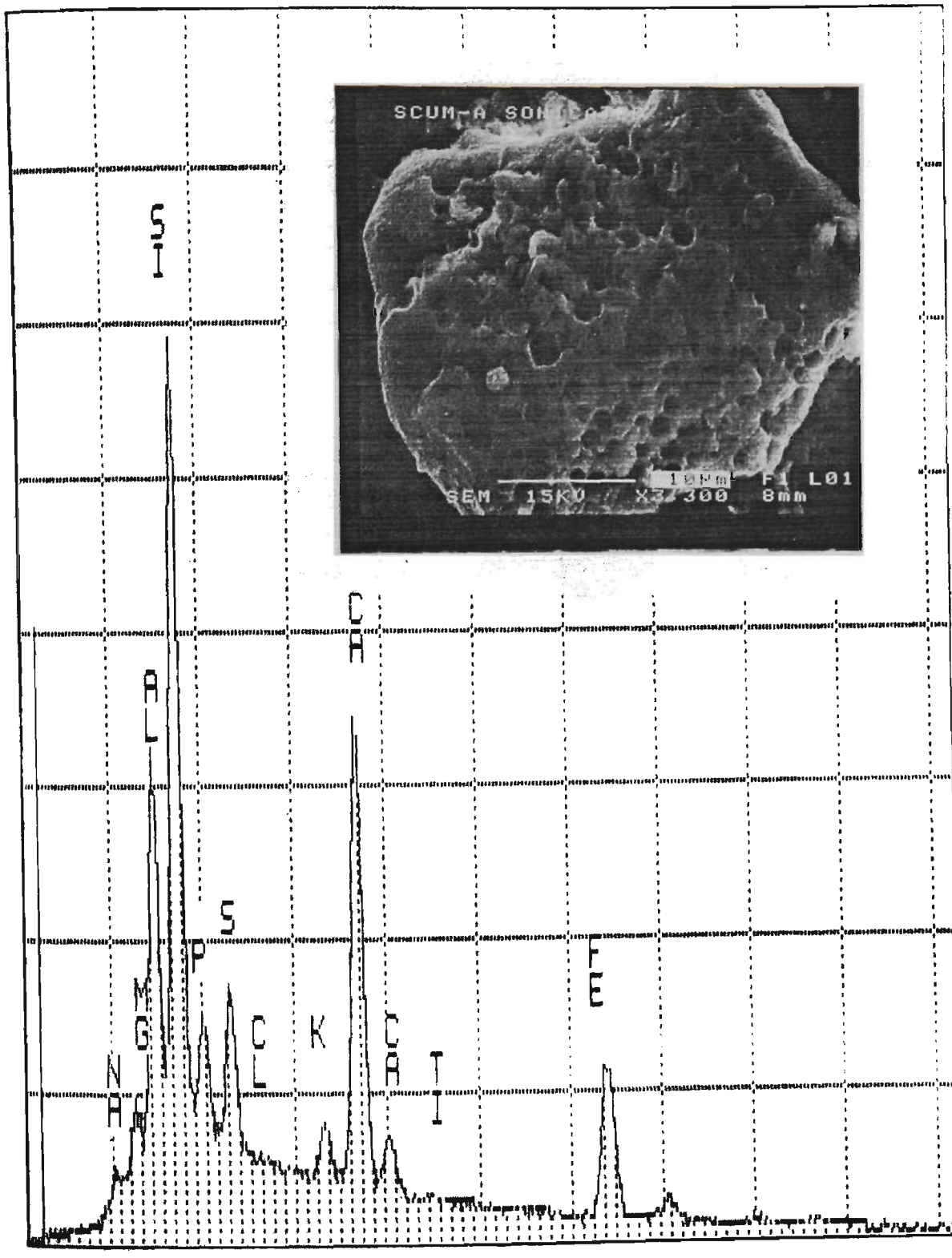

Figure 4-8 SEM and EDXA of a scum particle.

revealed significant similarities. The particles in the scum, however, ranged from 10 to 50 μm, whereas the anaerobic granules found in Upflow Anaerobic Sludge Blanket reactors vary from 0.1 to 8 mm in diameter.

Cultural counts of total anaerobes and methanogens were performed on samples of scum taken from 1.5 m into the scum layer at sampling ports 2 & 5. The percentage of methanogens in the flora of these samples was 0.07 and 0.8 % by number, respectively. The geometric means of the total anaerobes and methanogens were 1×10^{8} CFU/g VS and 3×10^{5} CFU/g VS. The geometric mean of the DMCC was 5×10^{10} bacteria/g VS. Gram negative rod-like and coccoid cells were dominant in these samples.

Further, it was observed in the laboratory that samples of the 'active sludge', taken from the bottom of the 115E reactor at sampling port 8, form a scum layer when allowed to stand under quiescent conditions for 2-6 hours in a beaker. The scum layer that formed, buoyed above the liquid surface and gradually drained of water, forming a firm crust on top. Trapped pockets of gas were observable through the side of the beaker. The scum collapsed with gentle agitation, but reformed. The process of collapsing and reforming the scum layer was repeated a number of times. Eventually, the scum layer did not reappear, presumably due to the exhaustion of nutrients and, hence, the cessation of gas production.

Interestingly, the point at which bacterial densities begin to decline corresponds to the end of the scum layer. It is possible, therefore, that scum formation is the result of gas production within the bacterial floc and granules.

which then buoy to the surface, collecting colloidal and suspended matter along the way. In UASB reactors, sludge granules continuously buoy to the surface, where the solids and gas are separated by a baffle, and then sink again to the bottom[4]. In uncovered anaerobic ponds, the scum which forms is 'controlled' naturally, probably through the action of wind-induced turbulence.

To date, the scum layer has not caused excessive creep in the HDPE cover and there has been no clear indication that the scum has deteriorated process performance. The build-up of scum has, however, altered the contours of the cover and affected the operation of the automatic stormwater collection and pumping system.

4.4 CONCLUSION

From the literature surveyed, it appears that all studies of the microbial ecology of sewage digesters have focused on conventional digesters or high-rate reactors like the Upflow Anaerobic Sludge Blanket reactor. No studies of the microbiology of anaerobic ponds were in evidence. This research has made substantial inroads into describing the ecology of anaerobic ponds.

This study has shown that the densities of methanogens and total anaerobes are not uniform in the sludge of anaerobic ponds. Cultural counts of both methanogens and total anaerobes, on a per volatile solids basis, appear to peak roughly midway along the reactor (0.45 to 0.65 days HRT) and then decline quite sharply thereafter. The decline in bacteria densities is presumably due to

substrate depletion. The peak in the numbers of bacteria numbers possibly corresponds to the point where most of the influent suspended solids settle out. Numbers of methanogens varied from 6×10^{8} CFU/g VS at the middle of the reactor to 2×10^{7} CFU/g VS at the end of the reactor. Total anaerobes varied between 1×10^{10} CFU/g VS and 7×10^{8} CFU/g VS.

The study suggests that sludge sampling, for process control purposes, should be done from the third or fourth row of sampling ports. Incidentally, the information obtained on the microbial ecology of the anaerobic reactor, indicates that anaerobic ponds treating domestic sewage should be designed for a HRT of about 1.25 days. With regard to optimising the size and geometry of anaerobic ponds, other researchers[73,74,75,76] have used input-output analyses to experiment with or compare different sized ponds and most have similarly found that a HRT of 1-2 days is required.

In addition, this research has made important contributions to the methodology used for methanogenic activity tests and anaerobic cultural counts. In particular, consideration of the toxicity of unionised acetic acid was found to be important when choosing the pH and total acetate concentration of the medium used for methanogenic activity tests. For cultural counts, it was found that incubation temperatures at or near the in-situ temperature of the pond did not appear to be necessary. An incubation temperature of 37°C could be used in order to process samples more quickly. Furthermore, the antibiotic medium

proposed by Miller and Wolin[65] appears to be suitable for studying anaerobic pond ecosystems.

5. Using Methanogenic Activity Measurements to Identify Important Trace Nutrients and Inhibitors

5.1 INTRODUCTION

There are many factors that can influence process stability and yield of methane in anaerobic reactors at WTP (Table 5-1). These include the flowrate (or HRT), temperature, and the properties and composition of the wastewater including the pH, EP, type and amount of carbon source, nitrogen, phosphorus and sulphur species, and the concentration of trace metals and toxic or inhibitory substances. These factors can reasonably be investigated by collecting data on the raw sewage and 115E anaerobic reactor in the course of normal operation. However, the cost of testing for all possible trace nutrients and inhibitors, in particular, prohibits such an extensive study.

To reduce the number of possible variables, a review of relevant literature on anaerobic digestion and anaerobic bacteria (especially methanogenic bacteria) was conducted. The information gleaned from the literature was then compared to historical data on the composition of the raw sewage in order to identify the variables that are potentially affecting anaerobic processes at WTP. The "short-listed" variables were then further screened using the same methanogenic activity test that was described in the previous chapter.

Table 5-1 Physical and chemical effectors of bacterial populations in anaerobic digesters (from Zeikus[16]).

Agent	Population response	Influence on methanogenesis
Temperature, e.g., change to 65°C from 35°C	Enrichment of thermophiles	Increase
pH, e.g., change to pH 5 from pH 7	Enrichment of acidophiles	Decrease
Organic substrate composition, e.g., change soluble substrate (glucose) for particulate (ligno-cellulose)	Enrichment of biopolymer decomposers	Decrease
Substrate feed rate, e.g., change from slow to high glucose feed	Enrichment of hydrolytic bacteria	Decrease
Inorganic composition, e.g., addition of excess sulphate	Enrichment of sulphate reducers	Decrease

Activity tests, or anaerobic toxicity assays, usually focus on methanogenic bacteria because methanogenesis is generally considered to be the rate-limiting step in the anaerobic digestion process and, therefore, the source of most process instability problems. Actually, all stages of the anaerobic digestion process, except acidogenesis, have at some time been claimed to be rate-limiting[17]. Hydrolysis, for example, can be rate-limiting when the waste contains a high proportion of insoluble matter like cellulose. Acetogenesis can also be rate-limiting, although the rate of acetogenesis is largely controlled by H_2-utilising methanogens. According to Archer and Kirsop[17], however, most problems with the anaerobic digestion of organic wastes are attributable to an accumulation of acids and so methanogenic bacteria should be the focus of process control efforts.

Acetate is the precursor of approximately 70% of methane produced in municipal-waste digesters and so the ability of the biomass to produce methane from acetate is a good indicator of expected process performance in the presence of various trace nutrients or inhibitors. The methanogenic activity test used, however, is a batch-culture technique and whilst it is useful for evaluating the influence of shock loads it does not, in general, simulate the effects on real systems as well as continuous-culture techniques[21].

This chapter presents the findings of the literature review and activity tests. The important variables identified in this phase of the research were included in a broader study of WTP anaerobic treatment processes presented in the next chapter.

5.2 MATERIALS AND METHODS

5.2.1 Source of Sludge and Sampling Method

Samples of sludge were collected anaerobically from the bottom of the 115E anaerobic reactor (i.e., at approximately 3 m depth) at sampling port 12 (refer to Figure 4-1, p. 4-2). Samples were collected using the depth sampler shown in Figure 5-1. The sampler was purged with anaerobic-grade CO_2 prior to collecting samples. The weighted sample bottle was lowered to the bottom of the reactor and then the rubber bung was pulled out of the neck of the bottle. The sludge sample was transferred to a narrow-mouthed 1 litre polyethylene bottle, which had been previously gassed with anaerobic-grade CO_2. The plastic sample bottle was completely filled with sludge to ensure the maintenance of anaerobiosis during transport to the laboratory, which usually took about ½ hour.

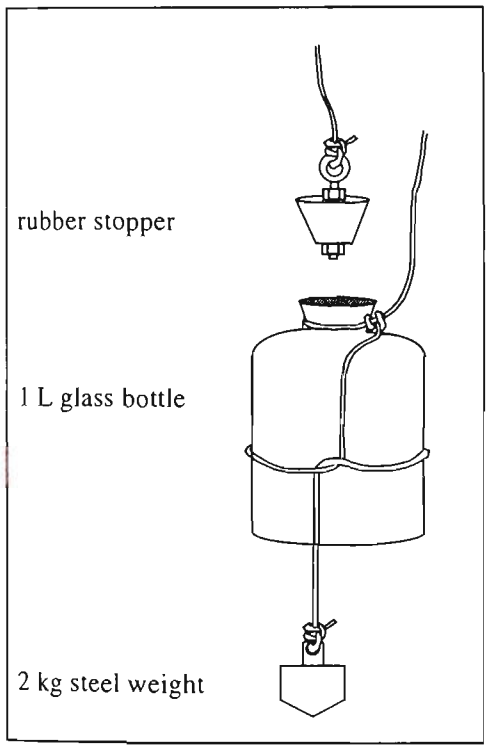

Figure 5-1 Depth sampler.

Once in the laboratory, the sample was mixed by gently inverting the bottle a number of times. A 200 mL portion of the sludge was then transferred to a conical flask whilst gassing continuously with CO_2. The contents of the flask were stirred with a magnetic stirrer while aliquots were withdrawn and transferred to 125 mL serum vials containing 50 mL of pre-reduced MS-medium.

The remainder of the sample was stored in a refrigerator at 4°C pending chemical analyses.

5.2.2 Medium for Activity Tests

The MS medium used for the activity tests is essentially the same as that described in Section 4.2.3. When the effect of metals was being studied, 60 mg/L nitrilotriacetic acid was added to the medium, as chelating agent, to prevent the metal ions from precipitating out of solution as metal sulphides. Nitrilotriacetic acid (NTA) was chosen because it is also used in Balch no. 1 medium (Section 4.2.5) and it presumably does not inhibit enzymatic activity like ethylenediaminetetraacetate (EDTA). The concentration of NTA used was based on the stoichiometric relationship between NTA and the metals under study. For example, Fe^{2+} has a hydration number of six and NTA is a quadridentate chelating agent. The maximum concentration of Fe^{2+} used was 10 mg/L (0.18 mM), which therefore equates to 52 mg/L (0.27 mM) NTA. Ca^{2+} and Mg^{2+} were employed at much higher concentrations, but the sulphide salts of these metals are hydrolysed in water.

5.2.3 Activity Test Procedure

The procedure is described in Section 4.2.4.

5.2.4 Analytical Methods

The methods used for the analysis of **methane**, **volatile solids**, **pH** and **EP** are described in Section 4.2.8.

Soluble sulphate was determined by nonsuppressed ion chromatography. A Waters ion chromatograph equipped with a conductivity detector and IC-Pak A HC anion-exchange column was used. The eluent contained di-sodium octane sulphonate and boric acid. Pretreatment of anaerobic sludge samples (which can contain up to 20 mg/L free sulphide) involved addition of 1 g zinc acetate to 50 g of sludge to precipitate the free sulphide as zinc sulphide, and thus prevent it from being oxidised by air to sulphate. The sample was then centrifuged at 4500 g for 10 minutes. The centrate was decanted, and the pellet washed (with degassed Milli-Q water) and centrifuged again. The combined centrate was made up to known volume with degassed Milli-Q water. The results were expressed on a wet weight basis.

Soluble sulphide was determined by Method APHA 4500-S^{2-}D (Methylene Blue Method) from *Standard Methods for the Examination of Water and Wastewater* (APHA: USA, 18th ed., 1992). Pretreatment involved filtration through a 0.2 µm syringe filter. Results were expressed on a weight per volume basis.

Metals were determined according to Method APHA 3120B (Inductively Coupled Plasma (ICP) Method) from *Standard Methods for the Examination of Water and Wastewater* (APHA: USA, 18th ed., 1992). Pretreatment for total metal determinations was done according to Method APHA 3030D (Preliminary

Digestion for Metals). Pretreatment for soluble metal analyses involved filtration through Whatman GFC filter paper (mean pore size 1.2 μm) followed by digestion according to Method APHA 3030D.

5.3 RESULTS AND DISCUSSION

5.3.1 Trace Nutrients and Inhibitors that Could be Affecting Anaerobic Treatment Processes at WTP

Table 5-2 lists trace nutrients and inhibitors that have been reported in the literature to affect anaerobic bacteria, in particular the methanogenic bacteria, and the anaerobic digestion process. Where available from historical records, the information in this table has been compared to data on the composition of WTP's raw sewage. Most of the data on the raw sewage (Table 5-3) stems from a routine monitoring programme, while the data for some variables has come from one-off studies.

As a result of this exercise, sulphate, zinc, copper, calcium, and magnesium were selected for further investigation using the methanogenic activity test described in Chapter 4. Supplementation of iron, cobalt and nickel ions was also investigated because these metals had been reported to stimulate gas production at concentrations of 10 mg/L[61]. No information on the levels of antibiotics or quaternary ammonium detergents could be found in records at WTP. Antibiotics are used to treat bacterial infections and to a lesser extent,

Table 5-2 *Literature survey of trace nutrients and inhibitors that affect anaerobic bacteria & the anaerobic digestion process.*

VARIABLE	FAVOURABLE RANGE	INHIBITORY RANGE	COMMENTS	REFERENCE
Heavy metals, chlorinated solvents, biocides and pesticides, antibiotics		Yes		Noone, 1990, p. 166[77].
Cu^{2+}, Ni^{2+}, Zn^{2+}		1 mg/L or less	Depends on the pH and the presence of soluble sulphides.	Osborn, 1992, p. 30[78].
Antibiotics: chloramphenicol, lasalocid, monensin, spiramycin, tylosin, virginiamycin, olaquindox, arsanilic acid, metrondiazole, formaldehyde		Yes	Methanogens are resistant to many common antibiotics but are sensitive to agents which affect protein and lipid biosynthesis and those that interfere with membrane function.	Wheatly, 1990, p. 216[79].
Chlorinated solvents: chloroform, carbon tetrachloride		1 mg/L		Wheatly, 1990, p. 216[79].
Common synthetic detergents		> 20 mg/L		Wheatly, 1990, p. 216[79].
Quaternary ammonium detergents		≈ 1 mg/L		Wheatly, 1990, p. 216[79].
Chlorinated solvents and biocides		> 1 to 10 mg/L		Noone, 1990, p. 166[77].
Pesticides: aldrin, lindane, dieldrin			Mixed population can adapt to potential toxins and recalcitrants.	Wheatly, 1990, p. 216[79].
BOD_5:N	700:5			Wheatly, 1990, p. 214[79].
C:N	< 50			Dinges, 1982, p. 54[80].
C:N	10:1 to 100:1			Iza et al., 1991, p. 9[5].

Table 5-2 continued

VARIABLE	FAVOURABLE RANGE	INHIBITORY RANGE	COMMENTS	REFERENCE
NH_4^+		> 1500 mg/L		Dinges, 1982, p. 54[80].
NH_4^+		> 3000 mg/L	Regardless of pH.	Zickefoose and Hayes, 1976, p. 3.23[81].
NH_4^+		1500-3000 mg/L	If pH > 7.4	Zickefoose and Hayes, 1976, p. 3.23[81].
NH_4^+		> 2000 mg/L	@ pH 7.0 to 7.5	Hickey et al., 1991, p. 216[4].
NH_4^+	1 to 10 mM (15 to 150 mg/L NH_3-N)			Archer and Kirsop, 1990, p. 63[17].
NH_4^+		> 6000 mg/L		Dinges, 1982, p. 54[80].
NH_4^+		> 1000 mg/L		Iza et al., 1991, p. 9[5].
BOD_5:P	700:1			Wheatly, 1990, p. 214[79].
C:P	100:1 to 150:1			Archer and Kirsop, 1990, p. 65[17].
C:P	20:1 to 100:1			Iza et al., 1991, p. 9[5].
SO_4^{2-}	0.15 to 0.3 mM (5-10 mg/L SO_4^{2-}-S)		Beneficial to growth of methanogens and fatty-acid degraders.	Thiele and Wu et. al., 1990[82].
SO_4^{2-}		> 0.2 mM (> 6 mg/L SO_4^{2-}-S)	Nearly complete inhibition can occur at 10 mM SO_4^{2-} (≈300 mg/L SO_4^{2-}-S). Carbon and electron flow diverted from methane formation to H_2S production. Sulphate inhibition can be reversed by addition of either H_2 or acetate.	Winfrey and Zeikus, 1977, p. 275-281[15].

Table 5-2 continued

VARIABLE	FAVOURABLE RANGE	INHIBITORY RANGE	COMMENTS	REFERENCE
S^{2-}	1 to 3 mM (30 to 90 mg/L S^{2-})		Optimal for growth of *Ms. Barkeri* (a H_2-CO_2 and acetate utiliser)	Archer and Kirsop, 1990, p. 65[17].
S^{2-}		> 100 mg/L free sulphide	Exact mechanism of inhibition is unknown but it is possible that precipitation or other secondary effects are responsible.	Winfrey and Zeikus, 1977, p. 275-281[15].
S^{2-}		> 0.8 to 1 mM (> 25 to 30 mg/L)	Inhibits acetoclastic methanogenesis @ pH 7.0 to 7.2	Hickey et al., 1991, p. 217[4].
S^{2-}		> 2 to 3 mM (> 60 to 100 mg/L)	Inhibits H_2-CO_2 utilising methanogens	Hickey et al., 1991, p. 217[4].
S^{2-}		> 200 mg/L		Zickefoose and Hayes, 1976, p. 3-23[81].
Ca^{2+}		> 1000 mg/L		Dinges, 1982, p. 54[80].
Ca^{2+}	100 to 200 mg/L	> 2500 mg/L		Zickefoose and Hayes, 1976, p. 3-23[81].
Co^{2+}	10 nM (≈0.5 µg/L)			Wheatly, 1990, p. 214[79].
Fe^{2+}	2 nM (≈0.1 µg/L)			Wheatly, 1990, p. 214[79].
Fe^{2+}, Ni^{2+}	Yes		Can stimulate anaerobic digestion.	Archer and Kirsop, 1990, p. 66[17].
Fe^{2+}, Ni^{2+}, Co^{2+}, Mo^{2+}	Yes		Supplementation may be necessary, particularly during start-up.	Iza et al., 1991, p. 9[5].
K^{+}		> 1000 mg/L		Dinges, 1982, p. 54[80].
K^{+}	200 to 400 mg/L	> 2500 mg/L		Zickefoose and Hayes, 1976, p. 3-23[81].
Mg^{2+}		> 1000 mg/L		Dinges, 1982, p. 54[80].

Table 5-2 continued

VARIABLE	FAVOURABLE RANGE	INHIBITORY RANGE	COMMENTS	REFERENCE
Mg^{2+}	75 to 150 mg/L	> 1000 mg/L		Zickefoose and Hayes, 1976, p. 3-23[81].
Mo^{2+}	10 nM (≈1 µg/L)			Wheatly, 1990, p. 214[79].
Na^{+}		> 5000 to 10000 mg/L		Hickey et al., 1991, p. 216[4].
Na^{+}	100 to 200 mg/L	> 3500 mg/L	If present at toxic concentrations, the effect can be controlled by adding another alkali/alkaline earth metal as an antagonistic element.	Zickefoose and Hayes, 1976, p. 3-23[81].
Na^{+}, K^{+}, Mg^{2+}, Ni^{2+}, Co^{2+}, Mo^{2+}, Se^{2+}, W^{4+}	Yes		Metal ions required for growth of methanogenic bacteria.	Archer and Kirsop, 1990, p. 65[17].
Ni^{2+}	100 nM (≈5 µg/L)			Wheatly, 1990, p. 214[79].
Ni^{2+}, Co^{2+}, Mo^{2+}	Yes		Enhance methanogenic activities.	Hickey et al., 1991, p. 216[4].
Na^{+}		> 1000 mg/L		Dinges, 1982, p. 54[80].
Vitamins, acetate, other volatile acids or amino acids	Yes			Archer and Kirsop, 1990, p. 63[17].
NaCl		Yes	Methanogenic activity of granular sludge was inhibited by 50% at a concentration of about 150 mM (8775 mg/L).	Dolfing and Bloemen, 1985, p. 6[22].

Table 5-3 *Composition of WTP's Raw Sewage* (January 1986 to August 1991). All concentrations are mg/L unless stated otherwise.

VARIABLE	SAMPLING FREQUENCY	NO. OF SAMPLES	MINIMUM	FIRST QUARTILE	MEDIAN	THIRD QUARTILE	MAXIMUM
BOD_5	daily	2030	120	400	500	585	855
COD	weekly	285	28	1000	1141	1280	1822
TOC	weekly	289	62	288	335	385	880
SS	daily	2060	125	379	444	508	1360
VSS	daily	2059	33	312	370	424	1216
TDS	daily	2057	110	860	1020	1155	3469
pH	daily	2055	5.8	6.7	6.8	6.9	10.2
Alkalinity	daily	2050	108	220	245	284	800
NH_3-N	weekly	260	1.7	27.0	29.0	31.0	39.0
NO_2^--N	weekly	294	0.002	0.02	0.030	0.040	0.190
NO_3^--N	weekly	293	0.010	0.100	0.100	0.100	2.60
Organic N	weekly	291	3.2	24.4	28.0	32.0	50.0
TOC:Total N	weekly	289	1.7	9.7	11.8	13.7	280.0
PO_4^{3-}-P	weekly	293	1.1	6.1	7.0	7.9	11.9
Total P	weekly	291	2.9	8.8	11.0	12.3	20.6
TOC:Total P	weekly	287	6	23	32	40	74
Ca	one-off	4	49	50	53	56	56
Co	one-off	4	<0.05				
K	one-off	4	58	58	59	60	80

Table 5-3 continued

VARIABLE	SAMPLING FREQUENCY	NO. OF SAMPLES	MINIMUM	FIRST QUARTILE	MEDIAN	THIRD QUARTILE	MAXIMUM
Mg	one-off	4	25	26	26	26	32
Mo	one-off	1	<0.1				
Na	one-off	4	250	255	256	260	310
Cr	monthly	54	0.0003	0.0020	0.003	0.005	0.005
Cu	monthly	56	0.07	0.18	0.25	0.29	0.59
Fe	monthly	57	1.3	2.0	2.3	2.7	4.6
Hg	monthly	56	<0.001	0.001	0.01	0.002	2.700
Pb	monthly	52	0.010	0.04	0.06	0.09	0.22
SO_4^{2-}	one-off	32	70	89	96	106	164
MBAS	weekly	283	1.2	4.0	4.6	5.2	8.6
chloroform	one-off	1			15 ppb		
dichloro-methane	one-off	1			116 ppb		
trichloro-ethane	one-off	1			270 ppb		
1,4-dichloro-benzene	one-off	1			142 ppb		
1,2-dichloro-benzene	one-off	1			62 ppb		
Aldrin	one-off	1			0.01 ppb		
Dieldrin	one-off	1			0.07 ppb		
Lindane	one-off	1			0.05 ppb		

viruses, yeasts and Rickettsiae. Quaternary ammonium compounds are used in detergents, cosmetics (e.g. deodorants) and disinfectants. These compounds can reasonably be expected to be present in the raw sewage and should be investigated by WTP.

Potassium was also identified in this process as an important variable, but it was not chosen for further study at this stage because the medium used for the methanogenic activity test includes potassium dihydrogen phosphate and potassium hydrogen phosphate in the buffer system. The medium could have been modified, but it was simpler to include potassium in the next phase of the investigation of factors affecting WTP anaerobic treatment processes (Chapter 6).

5.3.2 Effect of Sulphate on Methanogenic Activity

Sulphate has been reported to be beneficial to the growth of methanogens and obligate hydrogen-producing acetogens (OHPA) at concentrations in the range of 5-10 mg/L SO_4^{2-}-S (Table 5-2, p. 5-8). At higher concentrations, however, sulphate can cause inhibition of methanogenesis. Sulphate-reducing bacteria (SRB) like *Desulfovibrio* sp. form a part of the group of bacteria known as OHPA in anaerobic digesters and other anaerobic ecosystems (Section 2.2). SRB metabolise lactate and ethanol, to acetate and hydrogen, in the absence of sulphate. In the presence of sulphate, however, SRB metabolise acetate and hydrogen and, in doing so, compete with methanogenic bacteria. Virtually complete inhibition of methanogenesis can occur at 300 mg/L sulphate[15]. Other

sulphur-containing compounds such as sulphite, thiosulphate and even elemental sulphur may also be metabolised. In addition, sulphide is produced as a product of the dissimilatory reduction of sulphate, and can cause inhibition of acetoclastic methanogenesis at concentrations above 25 mg/L[4]. The exact mechanism of inhibition of methanogenesis by sulphide is not known but it is thought to be related to the precipitation of trace metals[15]. The experiment described in this section aimed to investigate the effect of sulphate on the acetoclastic methanogenic activity of anaerobic sludges from the 115E anaerobic reactor.

Stock solutions of sodium sulphate at various concentrations (0-80 g/L) were prepared anaerobically (using degassed, deionised water) and stored in serum vials under nitrogen. A 1 mL volume of each stock solution was added to six serum vials containing mineral salt medium. The vials were then inoculated with 5 mL of anaerobic sludge (from the bottom of the reactor at SP12) and acetate was added to give a final concentration of about 30 mM acetate and a final volume of 57 mL per vial. The anaerobic sludge had a volatile solids concentration of 3.54 %w/v and a residual sulphate concentration of 6 mg/kg wet weight. The contribution by the inoculum to the sulphate ion concentration in the vials was negligible at approximately 0.5 mg/L. The vials were incubated at 20°C and samples of the headspace were periodically withdrawn for methane analysis over a period of two days. The results of the test are shown diagrammatically in Figure 5-2.

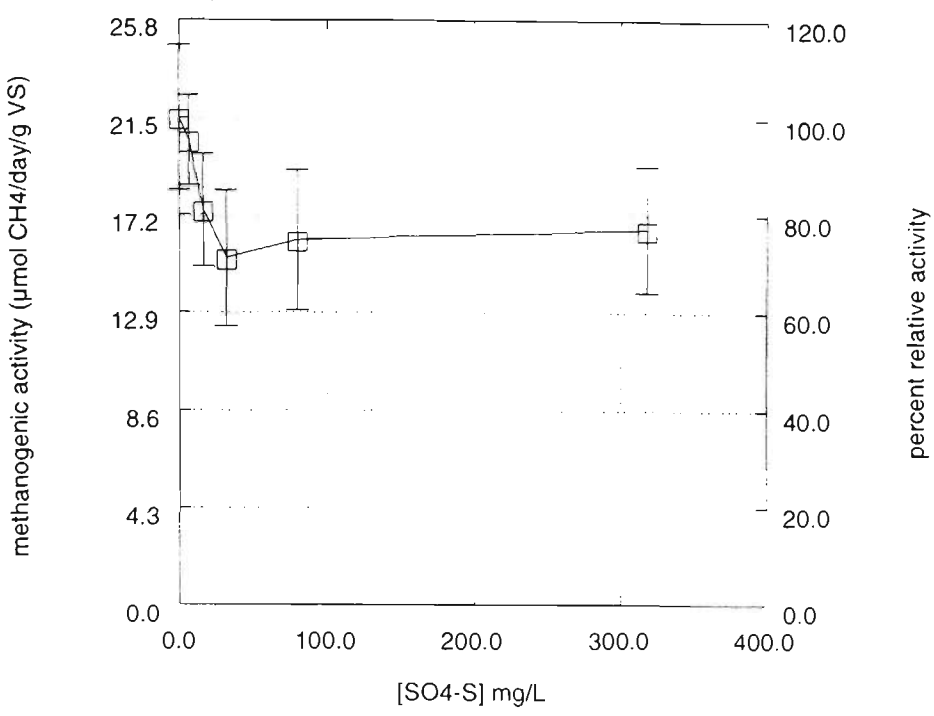

Figure 5-2 Effect of sulphate on acetoclastic methanogenic activity.

It appears that inhibition of methanogenic activity increases with sulphate concentration up to 30 mg/L SO_4^{2-}-S. At 30 mg/L SO_4^{2-}-S there is approximately 30% inhibition of methanogenic activity. Between 30 mg/L and 300 mg/L SO_4^{2-}-S there was no discernible change in the level of inhibition. It is possible that the activity of the SRB increases with sulphate concentration to a maximum at 30 mg/L SO_4^{2-}-S, and the maximum growth rate of the SRB species and the size of the SRB population limits the degree of inhibition. The breakpoint of 30 mg/L corresponds to the sulphate concentration in raw sewage and it may be that this concentration of sulphate has determined the size of the SRB population in the sludge of the 115E reactor.

The concentration of free sulphide was measured in each of the vials at the end of the test. The concentrations of free sulphide, in order of increasing

sulphate concentration, were 29.5, 29.5, 29.5, 29.5, 29.0, and 25.0 mg/L. The fact there was no discernible increase in sulphide suggests that the pattern in methanogenic activity in Figure 5-2 was attributable to inhibition by sulphate.

Both domestic and industrial sources contribute to the sulphate load at WTP, in roughly equal proportions. Infiltration of seawater into the sewerage system is also a source of sulphate ion. Sulphite is used as a preservative in photographic developer solutions and photographic wastewaters usually contain an appreciable amount of sulphate and other oxidised sulphur species. Sulphate is also commonly found in domestic wastewaters because it is used as an inert filler in washing powders. In fact, some powders can contain up to 50% by weight of sodium sulphate[83]. In washing powders, a certain amount of sodium sulphate is required to produce a crisp washing powder, and it can marginally reduce the critical micelle concentration of ionic surfactants. However, its main purpose is apparently to form a free flowing powder and add bulk to the product.

5.3.3 Effect of Zinc and Copper Ions on Methanogenic Activity

Zinc and copper ions are essential trace metals, required for microbial nutrition. At excessive concentrations, however, they are also well known antimicrobial agents. Heavy metals ions, like zinc and copper, can bind to enzymes and inhibit their intended function in living systems. The toxicity of a heavy metal ion is, however, strongly dependent on the speciation of the metal and its partitioning in the anaerobic system[84,85]. Many factors can influence the

bioavailable concentration of a heavy metal ion. In sewage, inorganic and organic materials like chloride, sulphide, ammonium, carbonate, hydroxide, humic acids and carbohydrates, form complexes or precipitates with metal ions[86,87], and the stability of metal complexes and precipitates is pH dependent. In addition, active and dead bacterial cells are capable of binding and accumulating high quantities of heavy metals[88,89]. Zinc ion is reportedly toxic to anaerobic bacteria at concentrations less than 1 mg/L (Table 5-2, p. 5-8) and it has been observed to have a maximum (total) concentration of 1.2 mg/L in raw sewage. The experiment described in the following investigated the effect of zinc on acetoclastic methanogenic activity.

Initially, zinc acetate was added to a series of serum vials containing 50 mL of MS-medium only, to determine whether appreciable losses of soluble zinc occurred due to precipitation as zinc carbonate or zinc sulphide. Stock solutions of zinc (II) acetate were prepared anaerobically and stored under nitrogen. A 0.2 mL aliquot of each stock solution was added to respective vials to give zinc concentrations ranging between 0-10 mg/L. No loss of zinc from solution could be detected (Table 5-4).

The concentrations of total and soluble zinc in the inoculum (taken from sample port 12) were measured at 75 mg/kg wet weight and <1mg/kg wet weight, respectively. The contribution by the inoculum to the total zinc concentration, and possibly the soluble zinc concentration, in the vials would therefore be

Table 5-4 Concentration of soluble Zn in the mineral salt medium.

Concentration of Zn added (mg/L)	Concentration of soluble Zn measured (mg/L)
0	0.04
0.56	0.59
1.08	1.1
2.75	2.8
5.58	5.2
11.2	11

Table 5-5 Total and soluble Zn concentrations in the serum vials.

Total Zn concentration (mg/L)	Initial soluble Zn concentration (mg/L)
6.50	0.15
6.81	0.32
7.31	0.46
8.80	0.92
11.78	1.8
16.68	3.4

appreciable and so two sets of replicate vials were prepared containing MS medium, acetate supplement, inoculum and zinc acetate. One set of vials was used for the activity test and the other was used to estimate the initial concentrations of soluble zinc. Note that the contribution by zinc acetate to the total acetate concentration was negligible. The total (including the inoculum's contribution) and initial soluble zinc concentrations in the vials are given in Table 5-5.

The results of the activity tests are displayed in Figure 5-3. Basically, the graphs of methane production over time were not linear and, in fact, the rate of methane production appeared to increase exponentially. One possible reason for

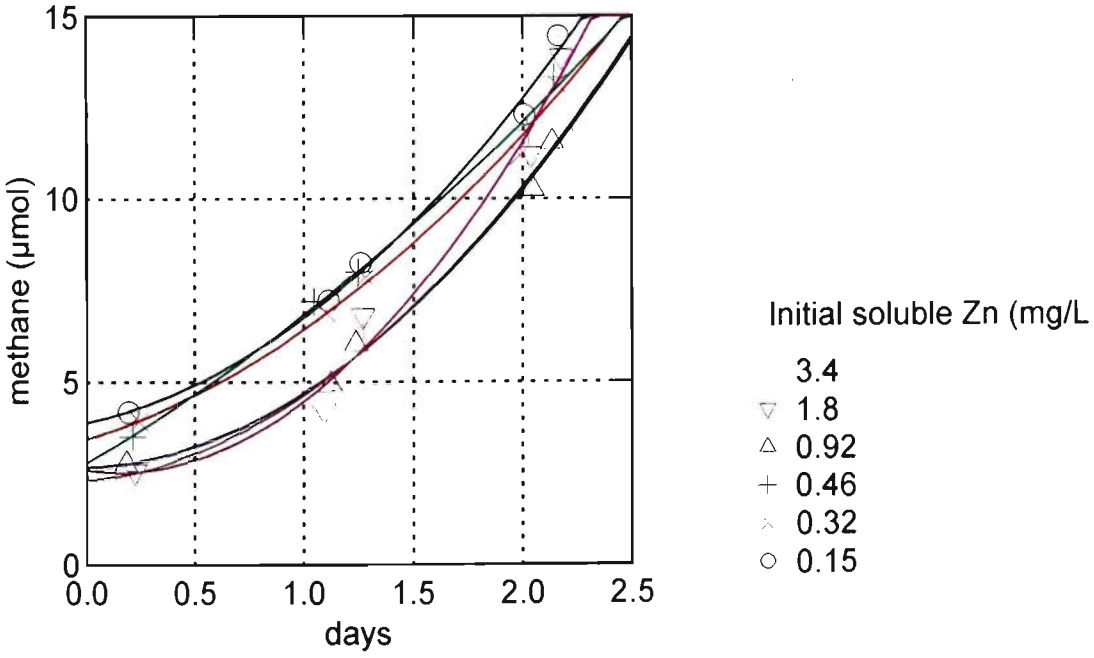

Figure 5-3 Effect of zinc ion on methanogenic activity.

this is that the zinc gradually became less bioavailable. Another set of vials was therefore prepared which contained MS medium, inoculum, acetate supplement and zinc acetate. Each of the vials received 10 mg/L Zn in the form of zinc (II)

and zinc acetate. Each of the vials received 10 mg/L Zn in the form of zinc (II) acetate. The vials were incubated at 20°C. This time, however, the soluble zinc concentration was followed over time by removing a new vial from the incubator at intervals over a two day period, opening the vial and measuring the soluble zinc concentration of its contents. The results are given in Figure 5-4. The rapid exponential decrease in the concentration of soluble zinc would likely explain the exponential increase in methanogenic activity over time.

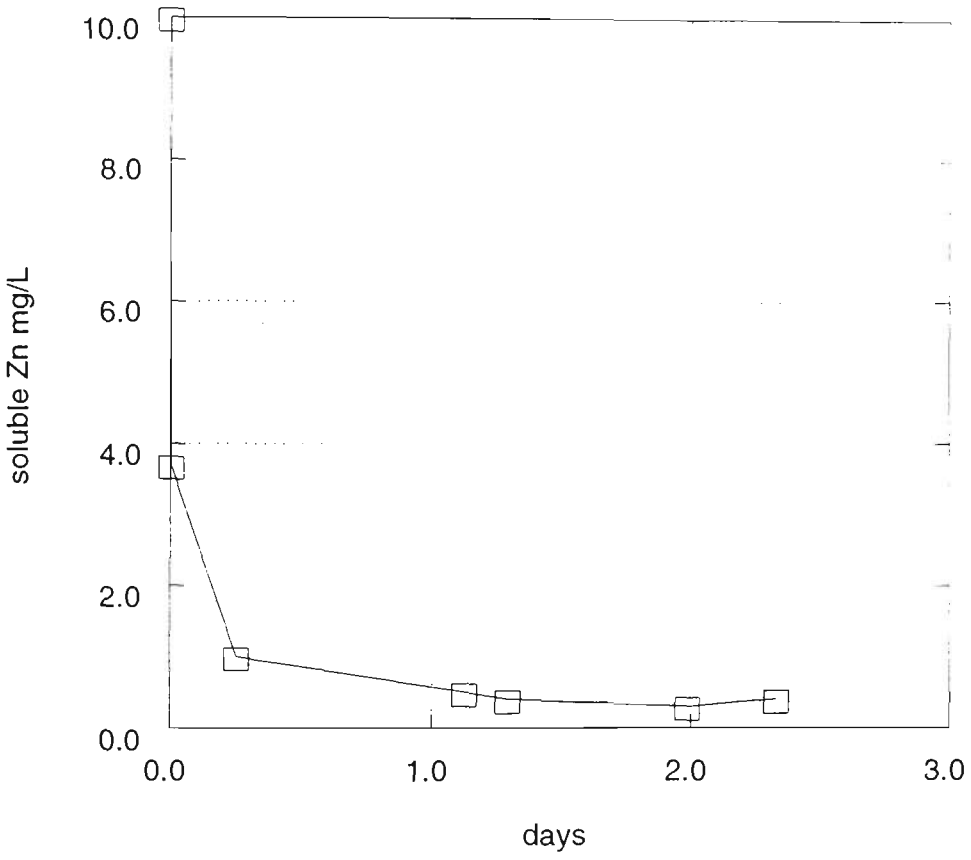

Figure 5-4 Decrease in soluble zinc concentration over time.

The contribution by the inoculum to the sulphide concentration in the serum vials was minor. The MS medium used for the activity tests contains about 25 mg/L free sulphide and the inoculum contains 10-20 mg/L free sulphide.

Given a dilution of 5:56, the contribution by the inoculum to the free sulphide concentration was at most 2 mg/L. This suggests that precipitation of zinc sulphide was not the main removal mechanism of zinc from solution. In fact, adsorption of metals on the biomass and their extracellular polymeric substances has been reported to be the most important phenomena that reduces the concentration of soluble metals in biological wastewater treatment systems[90,91,92]. It has also been reported that microorganisms could release high molecular weight proteins to sequester heavy metal ions as a mechanism of defence against heavy metal ion toxicity[93,94], and this complexation may play a significant role in the removal of predominantly soluble metals from wastewater[95]. Jones and Greenfield[96] state that the order of metal-ion complex stabilities is almost independent of the nature of the ligand and follows the sequence $Fe^{3+}>Pb^{2+}>Cu^{2+}>Ni^{2+}>Co^{3+}>Zn^{2+}>Co^{2+}>Cd^{2+}>Fe^{2+}>Mn^{2+}>Mg^{2+}Ca^{2+}$ $>Sr^{2+}>Ba^{2+}>Na^{+}>K^{+}$. This sequence is similar to the Irving-Williams series reported in Churchill and Walters et. al[89]. Churchill and Walters et. al.[89] observed that affinity of semi-intact bacterial cells for free metal ions tends to follow the same sequence as the metal-ion complex stabilities, and noted that other workers have observed similar patterns with intact cells, extracted bacterial polymers and activated sludge bacteria biosorption. Mueller and Steiner[86] observed that the inhibition of anaerobic digestion by heavy metal ions followed the sequence Ni>Cu>Cd>Cr>Pb and that the metal immobilisation affinity of the sludge followed the reverse sequence.

Given the efficacy of the natural removal and detoxification mechanisms for heavy metal ions in anaerobic treatment systems, it seems unlikely, therefore, that zinc ions would be inhibitory to anaerobic treatment processes at WTP. Similarly, given that biosorbents would probably have a higher affinity for copper than for zinc, it is unlikely that copper ions would be inhibitory.

5.3.4 Effect of Cobalt Ion on Methanogenic Activity

Cobalt ion is a necessary trace element required for the growth of methanogenic bacteria[97]. It is reported to be favourable at 0.05 µg/L (Table 5-2, p. 5-8) and is present in the raw sewage at a total concentration of less than 0.05 mg/L. That is, the analytical method used was not designed to measure cobalt at sub ppb concentrations. In any case, Speece[61] observed that, even in a digester containing 0.4 mg/L of soluble cobalt, the addition of 10 mg/L cobalt stimulated acetoclastic methanogenic activity. Speece hypothesised that there are natural chelators of trace metals in the sludge that could bind the metal so tightly as to limit its bioavailability. This experiment aimed to investigate the effect of cobalt ion at concentrations of up to 10 mg/L on acetoclastic methanogenic activity.

Stock solutions of cobalt (II) chloride hexahydrate were prepared anaerobically and stored under nitrogen in serum vials. Six vials containing 50 mL MS medium were inoculated with 5 mL of anaerobic sludge taken from sample port 12 (volatile solids content 3.38% w/w). To these vials a 0.2 mL aliquot of the cobalt stock solutions was added to give cobalt concentrations of

between 0-10 mg/L. The vials were then supplemented with 1 mL of a sodium acetate stock solution to give a final acetate concentration of 30 mM, and incubated at 20°C. Methane production in the vials was followed over a two day period. The results are displayed in Figure 5-5.

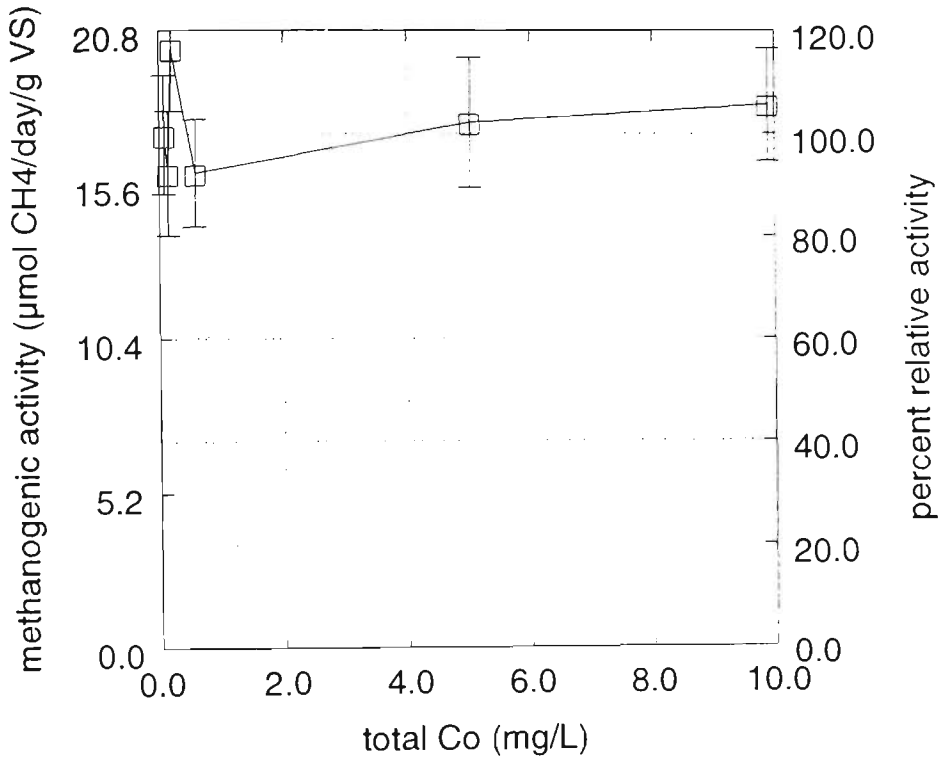

Figure 5-5 Effect of cobalt ion on methanogenic activity.

The total concentration of cobalt in each vial at the start of the test, and the soluble concentrations measured at the end of the test, are given in Table 5-6. The total and soluble concentrations of cobalt in the anaerobic sludge were measured at 0.9 mg/kg wet weight and <0.01 mg/kg wet weight, respectively. The contribution by the inoculum to the cobalt concentration in the test vials was approximately 0.08 mg/L.

Table 5-6 Concentration of cobalt in test vials.

Total Co in each vial (mg/L)	Soluble Co measured at the end of the test (mg/L)
0.08	-0.027
0.14	0.019
0.20	0.059
0.58	0.340
5.02	1.877
9.89	6.386

Despite the fact that most of the cobalt added remained in solution, there was no clear effect of cobalt on acetoclastic methanogenic activity in the range of concentrations tested. That is, cobalt does not appear to be limiting the growth of acetoclastic methanogens.

5.3.5 Effect of Nickel Ion on Methanogenic Activity

Like cobalt, nickel is an essential trace metal for methanogenic bacteria[97] and it has been reported to be required at 5 μg/L (Table 5-2, p. 5-8). Nickel ion is required for the synthesis of methyl-coenzyme M reductase which is an enzyme involved in the formation of methane by acetotrophic methanogens[9]. From monthly grab samples of the raw sewage at WTP, nickel has been observed to have a median (total) concentration of 0.07 mg/L. This suggests that nickel is not

limiting, although Speece[61] has noted that the nickel in anaerobic digesters is not necessarily in a bioavailable form, and found that acetoclastic methanogenesis could be stimulated with the addition of nickel ion at 10 mg/L in digesters that contained 0.1-0.2 mg/L soluble nickel. This experiment investigated the effect on acetoclastic methanogens of supplementing nickel up to a concentration of 10 mg/L.

Aliquots of 0.2 mL of nickel (II) chloride hexahydrate stock solutions (prepared anaerobically and stored under nitrogen) were added to a series of serum vial containing 50 mL MS medium and 5 mL anaerobic sludge (3.40 %w/w volatile solids) to give final nickel concentration ranging from 0-10 mg/L. The vials were then supplemented with sodium acetate to give a final acetate concentration of 30 mM, and incubated at 20°C. The methane content of the headspace in the vials was followed over a period of two days. The results are presented in Figure 5-6.

The total concentration of nickel in each vial at the start of the test, and the final concentrations of soluble nickel that were measured at the end of the test, are given in Table 5-7. The total and soluble concentrations of nickel in the anaerobic sludge were measured at 2.8 mg/kg wet weight and 0.024 mg/kg wet weight, respectively. The contribution by the inoculum to the total nickel concentration in the vials was approximately 0.25 mg/L.

Despite the high proportion of nickel that remained in solution, there was no discernible effect of nickel on acetoclastic methanogenic activity. The

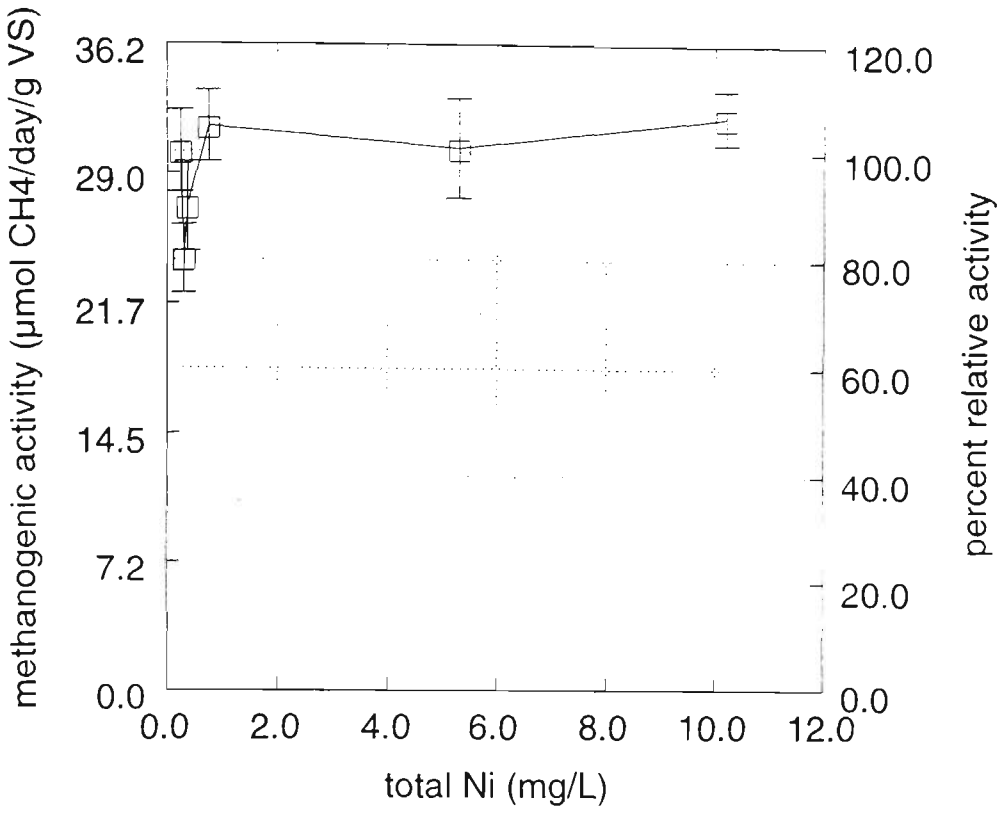

Figure 5-6 Effect of nickel ion on methanogenic activity.

Table 5-7 Concentrations of nickel in test vials.

Total Ni in each vial (mg/L)	Soluble Ni measured at the end of the test (mg/L)
0.25	0.058
0.31	0.079
0.37	0.134
0.76	0.469
5.31	4.024
10.21	7.761

concentration of soluble nickel that was measured in the anaerobic sludge is, in fact, greater than the amount reported to be required by methanogens.

5.3.6 Effect of Iron (II) on Methanogenic Activity

Iron is reported to be required at 0.1 μg/L for growth of methanogens (Table 5-2, p. 5-8) and has been observed to be present in raw sewage at WTP at a median (total) concentration of 2.3 mg/L. As for cobalt and nickel, however, Speece noted that the soluble concentration of a metal is not necessarily representative of the bioavailable concentration, and observed that supplementation of iron (II) at 10 mg/L can stimulate acetoclastic methanogenesis in digesters containing 0.4-12.4 mg/L soluble iron. This experiment investigated the effect of iron (II) supplementation on acetoclastic methanogenic activity.

Stock solutions of iron (II) chloride tetrahydrate were prepared anaerobically and stored under nitrogen in serum vials. Aliquots of 0.2 mL of each stock solution were added to serum vials containing 50 mL MS medium to give final iron concentrations between 0-10 mg/L. The vials were then inoculated with 5 mL of anaerobic sludge from sample port 12 (3.33 %w/w volatile solids) and supplemented with sodium acetate to a final acetate concentration of 30 mM. The vials were incubated at 20°C and methane production was followed over a two day period. The results are displayed in Figure 5-7.

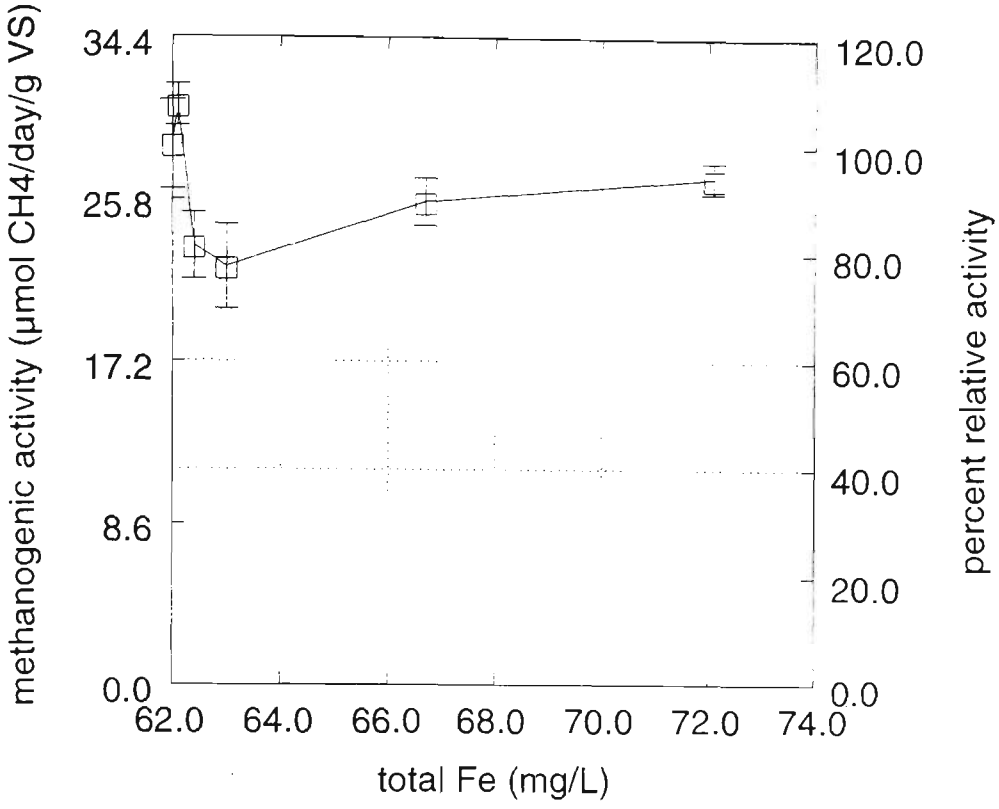

Figure 5-7 Effect of iron (II) on methanogenic activity.

Table 5-8 Concentrations of iron in test vials

Total Fe in each vial (mg/L)	Soluble Fe measured at the end of the test (mg/L)
62.0	1.144
62.1	1.291
62.4	1.523
63.0	1.261
66.7	4.129
72.1	6.490

The total concentration of iron in each serum vial, and the concentrations of soluble iron measured at the end of the test, are given in Table 5-8. The total and soluble concentrations of iron in the anaerobic sludge were measured at 689 mg/kg wet weight and 0.203 mg/kg wet weight, respectively. The contribution by the inoculum to the total iron concentration in the vials was approximately 62 mg/L.

Despite the reasonably high concentrations of soluble iron in the vials, the addition of iron did not seem to stimulate acetoclastic methanogenic activity. In fact, there may have been a decrease in methanogenic activity. Note that, as in the case of nickel, the concentration of soluble iron in the anaerobic sludge is much higher than the concentration required for growth of methanogens.

5.3.7 Effect of Calcium Ion on Methanogenic Activity

Calcium is an essential trace element for growth of methanogens and is reportedly favourable for anaerobic digestion at 100-200 mg/L (Table 5-2, p. 5-8). The concentration of soluble calcium in raw sewage has been estimated at about 50 mg/L. This experiment aimed to investigate the effect of calcium on acetoclastic methanogenic activity at concentrations up to about 200 mg/L.

Aliquots of 0.2 mL of calcium (II) chloride dihydrate stock solutions were added to a series of serum vials containing 50 mL MS medium and 5 mL of anaerobic sludge from sample port 12 on the 115E reactor (3.65 %w/w volatile solids). After supplementation with sodium acetate, to a final acetate

concentration of 30 mM, the vials were incubated at 20°C and the concentration of methane in the headspace of the vials was measured periodically over two days. The results are shown as Figure 5-8.

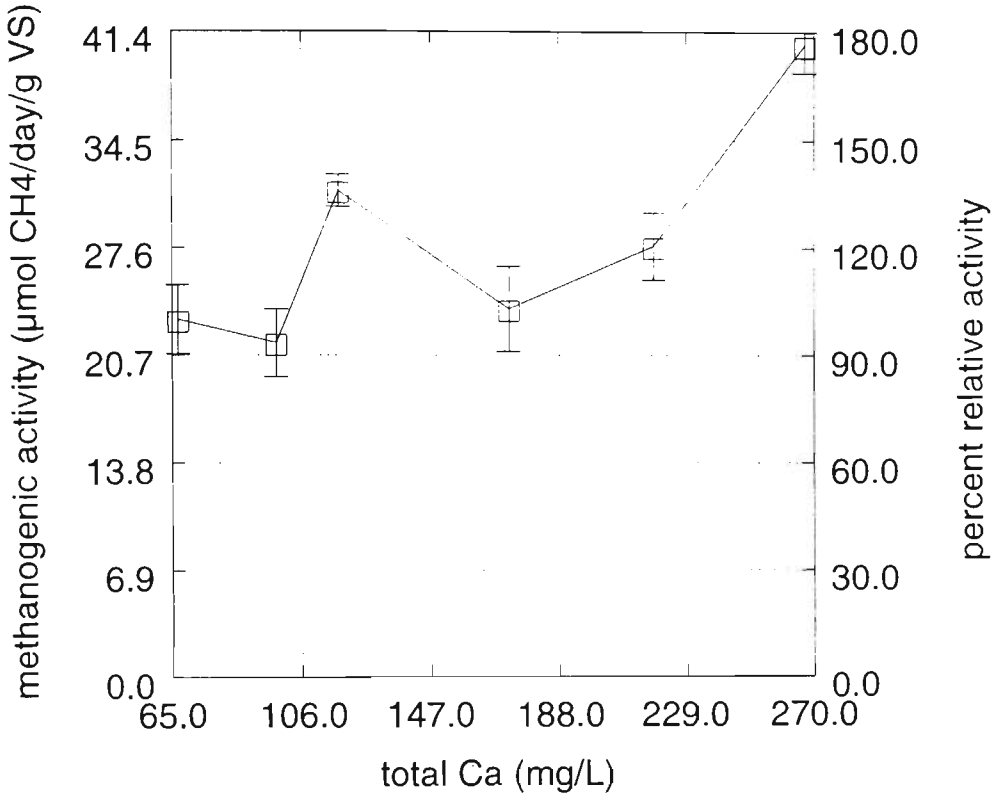

Figure 5-8 Effect of calcium ion on methanogenic activity.

The total and soluble concentrations of calcium in the inoculum were measured as 810 mg/kg wet weight and 61 mg/kg wet weight, respectively. The contribution by the inoculum to the total calcium concentration in the vials was approximately 67 mg/L. The total calcium concentration in the vials at the start of the test, and the concentrations of soluble calcium measured at the end of the test, are given in Table 5-9.

The addition of calcium appeared to stimulate the production of methane. There was approximately an 80% increase in acetoclastic methanogenic activity

Table 5-9 Concentrations of calcium in test vials.

Total Ca in each vial (mg/L)	Soluble Ca measured at the end of the test (mg/L)
66.9	20
97.9	40
117.6	58
172.0	94
218.4	150
267.1	180

when the calcium concentration was increased from about 70 mg/L total calcium (20 mg/L soluble calcium) to 270 mg/L total calcium (or 180 mg/L soluble calcium).

5.3.8 Effect of Magnesium Ion on Methanogenic Activity

Magnesium ion has been reported to be favourable to anaerobic digestion at between 75 and 150 mg/L (Table 5-2, p. 5-8). Magnesium is an essential component of the methyl-coenzyme M reductase system which is involved in the formation of methane in acetoclastic methanogens[9]. The concentration of soluble magnesium in raw sewage is approximately 25 mg/L. The aim of this experiment was to determine the effect of magnesium on methanogenic activity at concentrations up to approximately 150 mg/L.

Aliquots of 0.5 mL of magnesium chloride hexahydrate stock solutions were added to a series of vials containing 50 mL MS medium and 5 mL of anaerobic sludge (3.62 % w/w volatile solids). The vials were then supplemented with sodium acetate to an acetate concentration of 30 mM, and incubated at 20°C. Methane production in the vials was followed over a period of two days. The results are displayed in Figure 5-9.

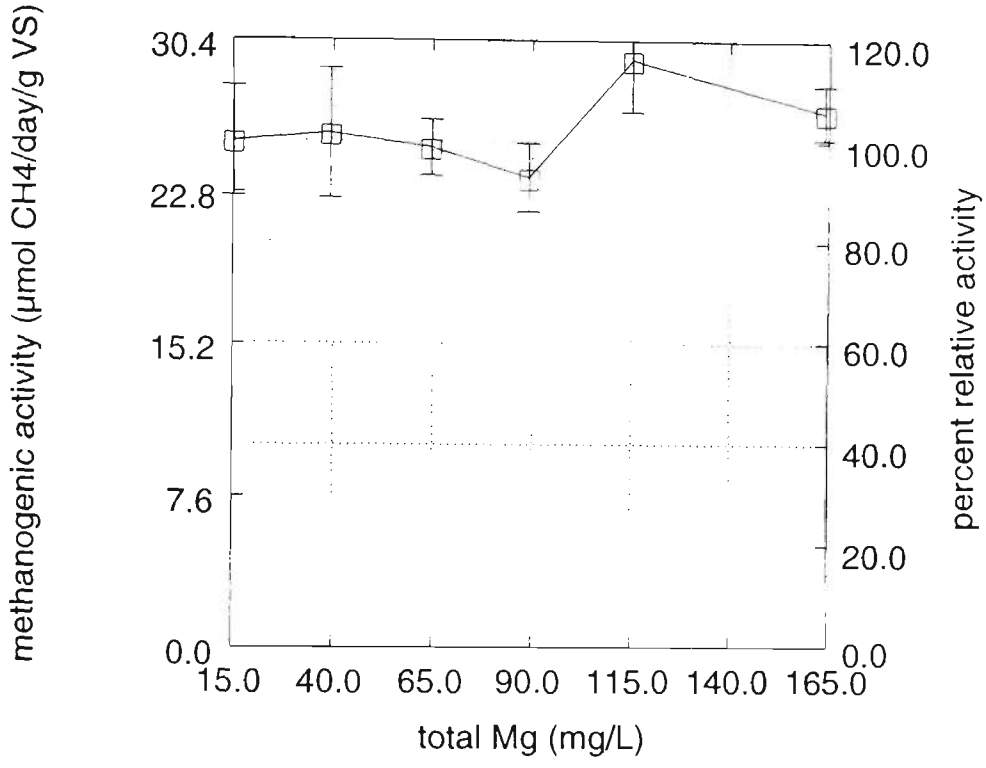

Figure 5-9 Effect of magnesium ion on methanogenic activity.

The total and soluble concentrations of magnesium in the inoculum were 170 mg/kg wet weight and 26 mg/kg wet weight, respectively. The contribution by the inoculum to the total magnesium concentration in each vial was about 15 mg/L. The total magnesium concentration in each vial at the start of the test, and the concentration of soluble magnesium measured at the end of the test, are given in Table 5-10.

Table 5-10 Concentrations of magnesium in test vials.

Total Mg in each vial (mg/L)	Soluble Mg measured at the end of the test (mg/L)
15.2	7
39.3	25
64.6	43
89.1	64
115.3	100
164.1	150

Supplementation of magnesium at concentrations up to 150 mg/L soluble magnesium had no discernible effect on acetoclastic methanogenic activity.

5.3.9 Interactions Between Trace Metal Ions: Cobalt, Iron, Nickel, Calcium and Magnesium

The effect of a metal ion on methanogenic activity can depend on the concentration of other metal ions in solution. The interactions can be synergistic or antagonistic. The antagonism between sodium and calcium has been discussed by Zickfoose and Hayes[81]. This experiment aimed to investigate the effects and interactions of the trace metal ions cobalt, iron, nickel, calcium and magnesium.

A 2^5 fractional factorial experiment was designed with QCStat (a module of the SYSTAT statistical package). In this experimental design, to reduce the

number of tests to be done, the magnesium effect was aliased with the nickel*calcium interaction on the grounds that magnesium alone did not appear to have an effect on methanogenic activity in the range of concentrations studied. Even though the number of trials was halved from 32 to 16, the trials had to be carried out over two weeks using samples of anaerobic sludge taken on two different days. As a result, it was necessary to account for (or "block" out) the "day" effect by confounding it with the cobalt*iron*nickel*calcium interaction. On each occasion, the anaerobic sludge was collected from sampling port 12 and the volatile solids content of the samples were 3.31 %w/w (13/12/94) and 3.34 %w/w (19/12/94). The experimental design and measured activities are given in Table 5-11.

Given that an unreplicated experiment design was used, a Bayesian Posterior Probability plot was made (with QCStat) to assess which effects and interactions are 'active' as opposed to a random deviation from zero (Figure 5-10). The Bayesian Posterior Probability analysis is based on the prior assumptions that about ten percent of the effects will be due to active variables, and the standard deviation of the active variables will be about ten times the standard deviation of inactive variables. These assumptions have been shown to be robust for many sets of real data.

An alternative analysis of the effects was performed using a prior estimate of the error obtained from previous 'repeatability' experiments. A pooled

Table 5-11 Experiment design used to test for interaction effects of trace metal ions on acetoclastic methanogenic activity.

Test No.	Block No.	Cobalt added (mg/L)	Iron added (mg/L)	Nickel added (mg/L)	Calcium added (mg/L)	Magnesium added (mg/L)	Methanogenic activity (μmol CH_4/day/g VS)
1	1	0	0	0	0	149.1	52.069
2	2	9.81	0	0	0	149.1	56.254
3	2	0	10.1	0	0	149.1	56.254
4	1	9.81	10.1	0	0	149.1	63.183
5	2	0	0	9.7	0	0	45.697
6	1	9.81	0	9.7	0	0	54.401
7	1	0	10.1	9.7	0	0	51.470
8	2	9.81	10.1	9.7	0	0	44.199
9	2	0	0	0	198.0	0	52.753
10	1	9.81	0	0	198.0	0	58.429
11	1	0	10.1	0	198.0	0	68.916
12	2	9.81	10.1	0	198.0	0	52.436
13	1	0	0	9.7	198.0	149.1	58.971
14	2	9.81	0	9.7	198.0	149.1	57.134
15	2	0	10.1	9.7	198.0	149.1	57.650
16	1	9.81	10.1	9.7	198.0	149.1	62.536

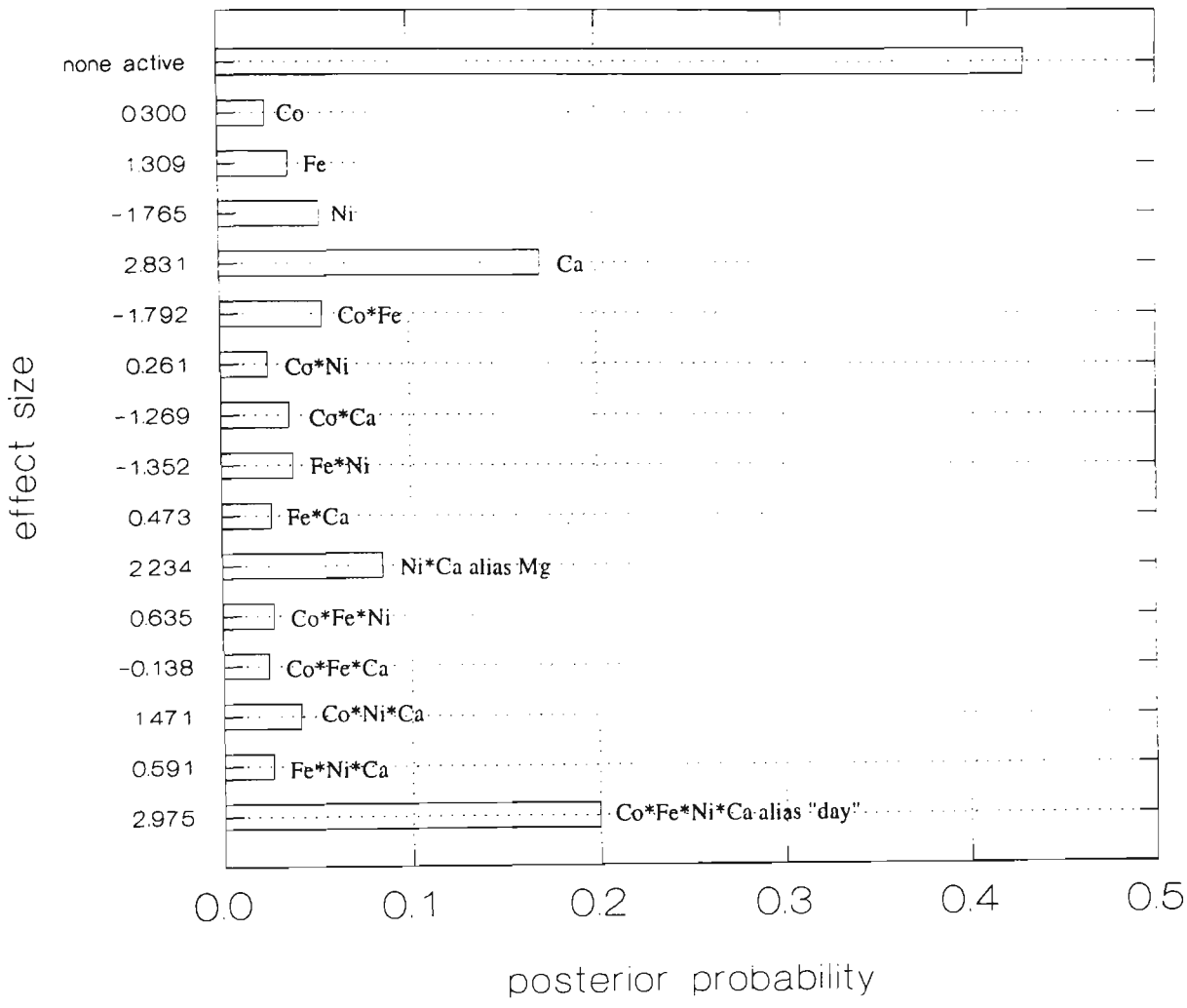

Figure 5-10 Bayesian Posterior Probability plot.

estimate of the relative standard deviation was calculated to be 8.3% with ten degrees of freedom. Using the relative standard deviation made sense because the random error in methane analyses (e.g., due to error in measuring a volume of gas with the syringe) will be proportional to the level of methane and hence to the measured activity. The mean methanogenic activity for all tests in this experiment was 55.722 μmol CH_4/day/g VS and, therefore, the standard deviation estimate was 4.6 μmol CH_4/day/g VS. The results of the analysis of variance are given in Table 5-12.

Table 5-12 ANOVA table for the effect of trace metal ions on methanogenic activity.

Factor	Effect	SS	DF	MS	F	$F^*_{.05}$
Co	0.6	1.44	1	1.44	0.07	4.96
Fe	2.618	27.42	1	27.42	1.30	4.96
Ni	-3.530	49.84	1	49.84	2.36	4.96
Ca	5.662	128.23	1	128.23	6.06	4.96
Co*Fe	-3.584	51.38	1	51.38	2.43	4.96
Co*Ni	0.522	1.09	1	1.09	0.05	4.96
Co*Ca	-2.538	25.77	1	25.77	1.22	4.96
Fe*Ni	-2.704	29.25	1	29.25	1.38	4.96
Fe*Ca	0.946	3.58	1	3.58	0.17	4.96
Ni*Ca alias Mg	4.468	79.85	1	79.85	3.77	4.96
Co*Fe*Ni	1.27	6.45	1	6.45	0.30	4.96
Co*Fe*Ca	-0.276	0.30	1	0.30	0.01	4.96
Co*Ni*Ca	2.942	34.62	1	34.62	1.64	4.96
Fe*Ni*Ca	1.182	5.59	1	5.59	0.26	4.96
Co*Fe*Ni*Ca	5.950	141.61	1	141.61	6.69	4.96
Error		211.6	10	21.16		

Like the Bayesian Posterior Probability analysis, an analysis of variance using a prior estimate of error also suggests that calcium ion has a positive effect on acetoclastic methanogenic activity. The Co*Fe*Ni*Ca interaction also appears to be active, though this is likely due to differences in the inoculum used. The average increase in methanogenic activity due to calcium supplementation is 5.662 μmol CH_4/day/g VS or 10.7%.

5.4 CONCLUSION

From information in the literature on the effects of trace nutrients and inhibitors on methanogenesis, and historical data on the composition of raw sewage at WTP, a number of inorganic ions were identified as potential effectors of methanogenesis in anaerobic reactors, including sulphate, zinc, cobalt, nickel, iron, calcium, and magnesium ions. These ions were further investigated using an acetoclastic methanogenic activity test. Two classes of compounds that were identified in the literature survey as potential inhibitors of anaerobic digestion, but for which there was no information in terms of their levels in raw sewage, were antibiotics and quaternary ammonium compounds. These compounds will need to be investigated further by WTP.

Of the chemical species tested, it appears that sulphate and calcium ion are present in concentrations that could be affecting anaerobic treatment at WTP. It is worth noting, however, that each of cobalt, nickel and iron, appeared to have erratic effects on methanogenic activity at low concentrations.

Sulphate can potentially cause a 30% inhibition of methane production. In the presence of sulphate (sulphur, sulphite or thiosulphate), sulphate-reducing bacteria in anaerobic digesters can out compete methanogens for acetate and hydrogen and thus reduce methane yields. In a batch test like the acetoclastic methanogenic activity test, the concentration of SRB appears to limit the extent of the inhibition, rather than the concentration of sulphate. In continuous culture, however, the SRB population would increase with increasing sulphate concentration, and methanogenesis could be completely inhibited.

As mentioned earlier, domestic sources are a major contributor to the sulphate load in sewage and this is probably due to the high sulphate content of some washing powders. The mean concentration of sulphate in Melbourne's domestic sewage has been reported to be about 15 mg/L SO_4^{2-}-S[98]. Sulphate is not only inhibitory to anaerobic treatment processes, it is also a primary cause of concrete corrosion and odour generation in sewers. There seems, therefore, to be a reasonable case for reducing the sulphate concentration in sewage and this effort would probably need to consider domestic sources.

Calcium ion, on the other hand, is an essential trace nutrient, and seems to be limiting at WTP. In one experiment, increasing soluble calcium by approximately 200 mg/L resulted in a general increase in the methanogenic activity, with a maximum increase of 80% occurring at about 270 mg/L total calcium (180 mg/L soluble calcium). In a second experiment aimed at investigating the effects and interactions of certain trace metal ions (Co^{2+}, Fe^{2+}, Ni^{2+}, Ca^{2+} and Mg^{2+}), calcium was again the only statistically discernible factor.

In this experiment, supplementation with 200 mg/L calcium produced an average increase of 10% in methanogenic activity.

The effect of calcium ion on WTP treatment processes was unknown until now. Melbourne Water, through the independent Trade Waste Advisory Acceptance Committee, is currently trying to reduce the trade waste load of soluble salt (or total dissolved solids), mainly because it limits the reuse potential of effluent. Rather than a blanket limit on total dissolved solids, however, trade waste standards could, for example, reflect the need for calcium ion as opposed to sodium ion. Calcium is not only beneficial to anaerobic treatment processes, it can also reduce the sodium absorption ratio of the wastewater, which can be beneficial to the land and grass filtration treatment processes at WTP.

Another implication of the effect of calcium ion is that the start-up times of new digesters could be reduced if supplementation with calcium chloride was practiced. As a preliminary estimate, this would require the addition of about 400 kg/ML $CaCl_2$. Neither calcium carbonate nor calcium hydroxide are suitable alternatives because of their effect on pH.

As the effects of certain chemicals on treatment processes become better understood, the opportunity arises for longer term improvement of processes, or prevention of problems, through trade waste policy and community education. In the short term, the effects of sulphate and calcium on the performance of the 115E Reactor, relative to other factors like COD and temperature, need to assessed to establish whether they should be included in a feedforward-feedback control scheme. Chapter 6 investigates the effects of a broader range of

variables, including sulphate and calcium, on the performance of the 115E Anaerobic Reactor.

6. Regression Analysis of the Methane Yield from the 115E Anaerobic Reactor

6.1 INTRODUCTION

As mentioned in the previous chapter, process stability and yield of methane[#] in anaerobic reactors at WTP can be influenced by the flowrate of the wastewater (or HRT) and the properties and composition of the wastewater including the temperature, pH, type and amount of carbon source, nitrogen, phosphorus and sulphur species, and the concentration of trace metals and inhibitory substances. The influence of these factors on anaerobic processes at WTP can be investigated through a regression analysis of data collected in the course of normal operation.

The carbon source in a municipal wastewater is composed mainly of proteins, carbohydrates and lipids. In this study, the amount of carbon source was measured in terms of these three components and also by the Chemical Oxygen Demand (COD) which is an aggregate measure of the amount of organic material in the wastewater.

The carbon to nitrogen ratio (C:N) and carbon to phosphorus ratio (C:P) of the raw sewage, as determined from the literature survey given in the previous chapter, are within acceptable ranges for anaerobic digestion and were therefore not included in this study.

[#] Yield is defined as the volume of methane per mass of COD loaded.

Of the many trace metals and inhibitory substances that can affect anaerobic digestion, calcium ion and sulphate ion were determined from methanogenic activity tests (see Chapter 5) to have the most potential to influence anaerobic processes at WTP. Both of these variables were included in this study.

WTP, like most municipal wastewater treatment plants, experiences periodical high flows due to wet weather events, and cyclical variations in temperature, volume of sewage to be treated, and the concentrations of most variables due to seasonal, domestic and industrial cycles. Unlike the methanogenic activity tests conducted in the previous chapter, a regression analysis of data collected in the course of normal operation will highlight the relative effects that the variables have on the yield of methane from WTP's anaerobic reactors. Together, the methanogenic activity tests and regression analysis will help to pinpoint those variables that can influence process stability or which may be useful in a feedforward-feedback control scheme. In this chapter the results of the regression analysis are presented, while the next chapter will investigate the use of various statistical process control and process regulation techniques for the daily operation of anaerobic reactors at WTP.

6.2 MATERIALS AND METHODS

6.2.1 Statistical Analyses

Statistical analyses were performed using Systat[99,100].

6.2.2 Sampling Methods

Note that owing to the reactor's loading cycle, which is shown in Figure 3-2 on p.3-4, the daily averages for on-line measurements (raw sewage flowrate and gas flowrate) were calculated for the interval 12:00 PM to 12:00 PM, and recorded for the latter's date. For example, raw sewage flows between 12:00 PM 1/6/95 and 12:00 PM 2/6/95 were averaged and recorded for 2/6/95. To align measurements made on the raw sewage, samples taken at 11 PM 1/6/95 were recorded for 2/6/95. Measurements made on the anaerobic reactor (including the methane concentration) at 8:30 AM 2/6/95 were recorded with the date 2/6/95

6.2.2.1 Raw sewage

The raw sewage flowrate to the 115E anaerobic reactor is measured continuously with a flume and Bestobell Mobrey ultrasonic level measuring system and, as part of the routine monitoring of treatment processes at WTP, a grab sample is taken of the raw sewage at 11 PM each day from "Head of Road" (Figure 6-1). Note that there is approximately a 2 hour lag between Head of Road and the 115E anaerobic reactor.

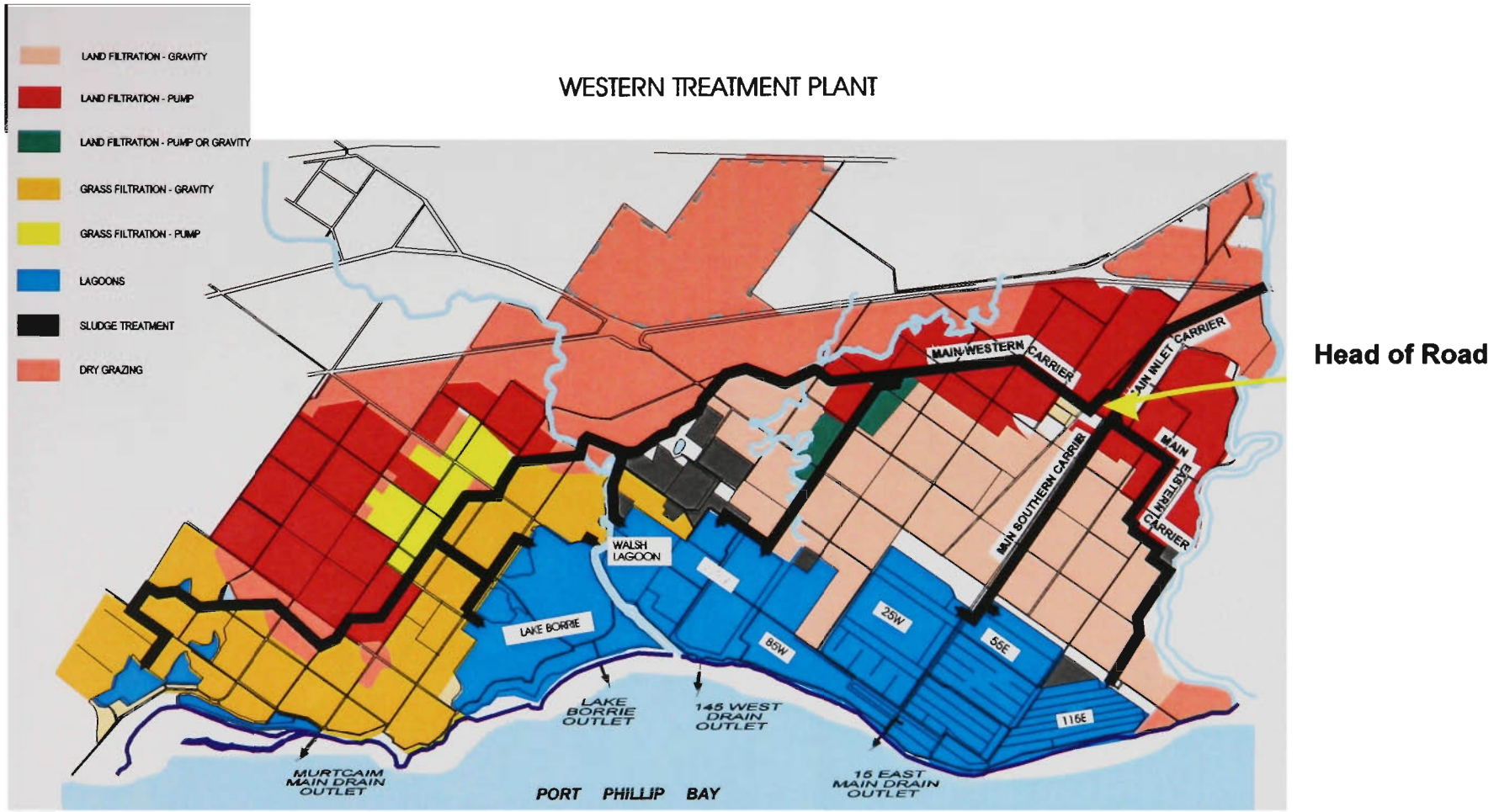

Figure 6-1 Map of the Western Treatment Plant.

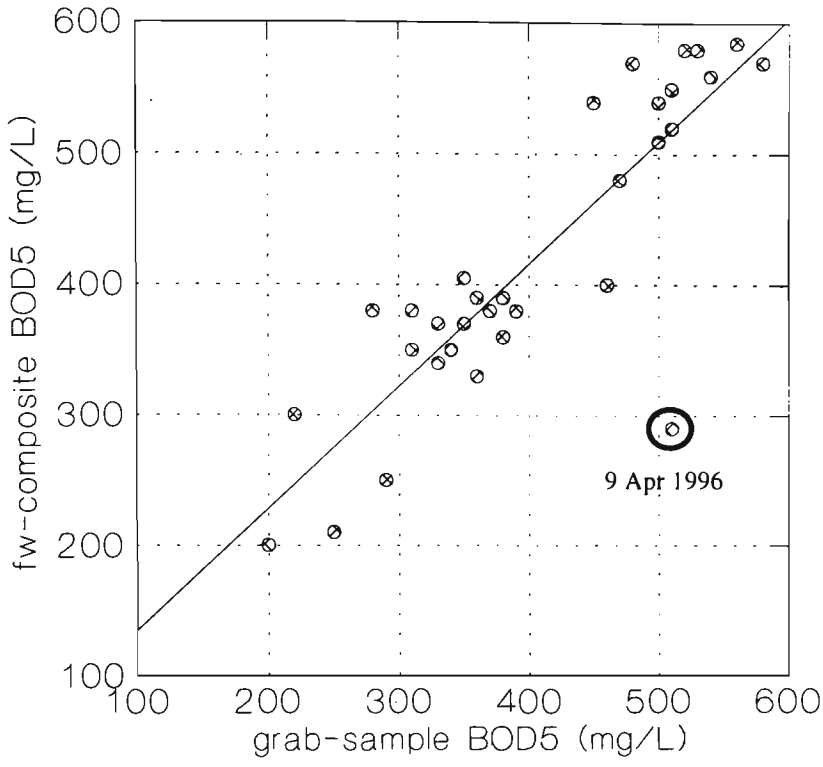

Figure 6-2 Raw sewage fw-composite BOD_5 versus the grab-sample BOD_5

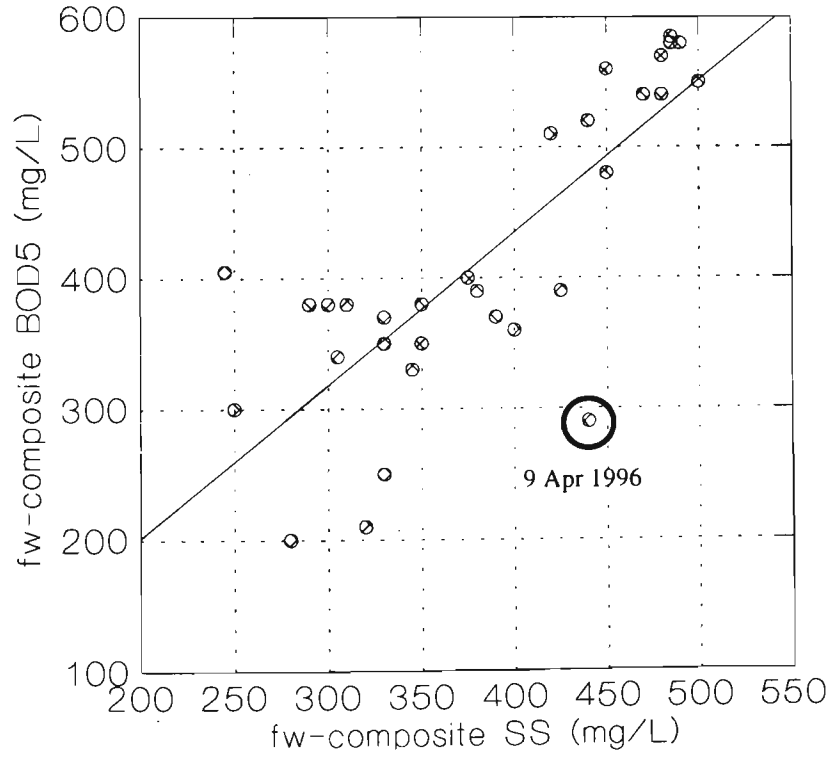

Figure 6-3 Raw sewage fw-composite BOD_5 versus the fw-composite suspended solids

Over the years, the exact reason for sampling at 11 PM has been lost. Some people at WTP believe that the 11 PM grab sample best represents the 24 hr flow-weighted (fw) composite, while others believe it was simply convenient because it coincided with the change of shift.

During a trial of an ISCO autosampler in early 1996, the opportunity was taken to compare the measured BOD_5 (another aggregate measure of organic material) in the 11 PM grab sample and the 24 hr flow-weighted composite sample. Samples of the raw sewage were collected daily between 26/3/96 and 26/4/96. The 24 hr flow-weighted composite sample was prepared by combining hourly samples of the raw sewage stream in proportion to the flowrate at the time of sampling. The results are shown in Figure 6-2. The line of best fit was derived from all data except the point shown circled which is believed to be an outlier. A plot of the 24 hr flow-weighted suspended solids (SS) values against the 24 hr flow-weighted BOD_5 values (Figure 6-3), suggested that the composite BOD_5 value of 290 mg/L (on 9 Apr 1996) was not consistent with the relationship between SS and BOD_5, as set by the balance of the data. The 11 PM grab-sample, therefore, appears to be a satisfactory surrogate for the 24 hr flow-weighted composite sample, in terms of BOD_5.

6.2.2.2 Digester gas from the 115E Anaerobic Reactor

The gas flowrate from the 115E anaerobic reactor is measured continuously with a Sarasota FM700 mass flowmeter. The methane

concentration in the gas is measured on-line with a non-dispersive infrared analyser (Rosemount Analytical Inc. Model 880). Owing to frequent operational problems with the on-line methane analyser, however, it was decided to use methane concentration values determined from grab samples of the gas taken each morning at 8:30 AM. Grab samples of the gas were collected using the liquid displacement method described in Method APHA 511 (Sludge Digester Gas) from *Standard Methods for the Examination of Water and Wastewater* (APHA: USA, 15th ed., 1980) and analysed by gas chromatography. A 250 mL borosilicate gas sampling bulb (Bartelt Instruments Pty. Ltd.) was used.

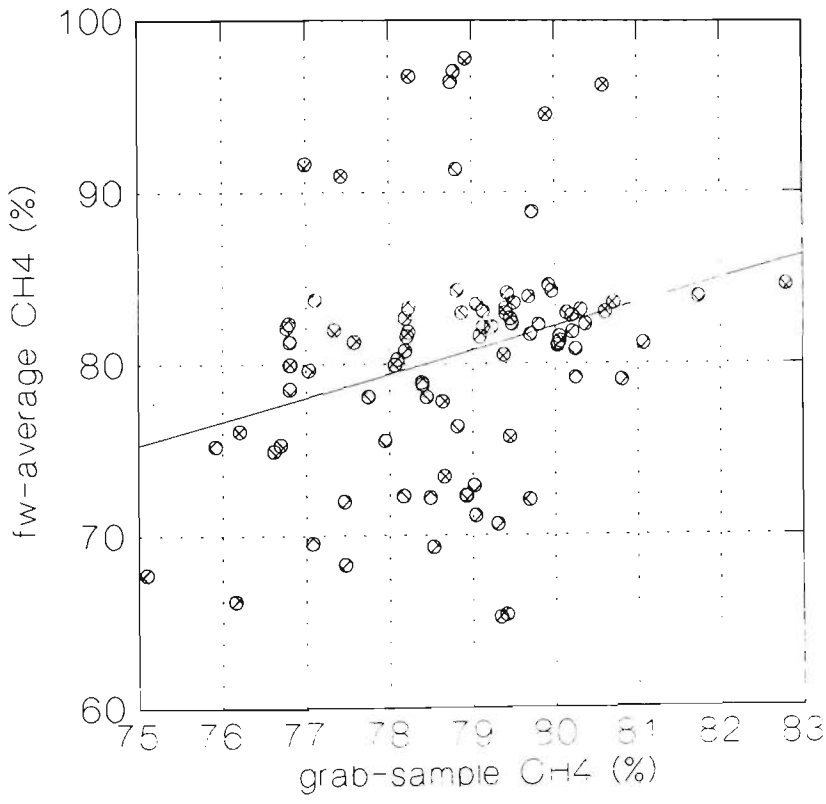

Figure 6-4 Reactor gas fw-average methane concentration versus the grab-sample methane concentration.

A comparison of the 24 hr flow-weighted average methane concentration (using measurements from the on-line analyser) and the grab-sample methane concentration is given in Figure 6-4. The equation for the regression line was $y=-28.2+1.4x$. It should be noted that the on-line analyser was frequently out-of-control during the period of study (which is discussed further in the next paragraph) and this impacts on the coefficients of the regression model. Despite the apparent problems with the operation of the on-line analyser, there seemed to be a reasonable correspondence between the 24 hour flow-weighted average and the grab-sample methane concentration.

A time-series plot of the flow-weighted average methane concentration and grab-sample concentration is given in Figure 6-5. It is clear from this plot that there were large systematic differences between the flow-weighted average and grab-sample measurements on a number of occasions. An examination of the Gas Plant maintenance log book revealed that most of the step-shifts in methane concentration measurements made with the on-line analyser corresponded to calibration events (see Figure 6-5), suggesting that there was a problem with calibration. Another step-shift on 2/8/95 coincided with restarting the Plant after a shutdown period. There was also a period between the 10th and 20th of July where the analyser response appeared to drift, although the cause was not identified. This result highlights the need for measurement control in any process control scheme and this subject is dealt with further in Section 7.3.3.

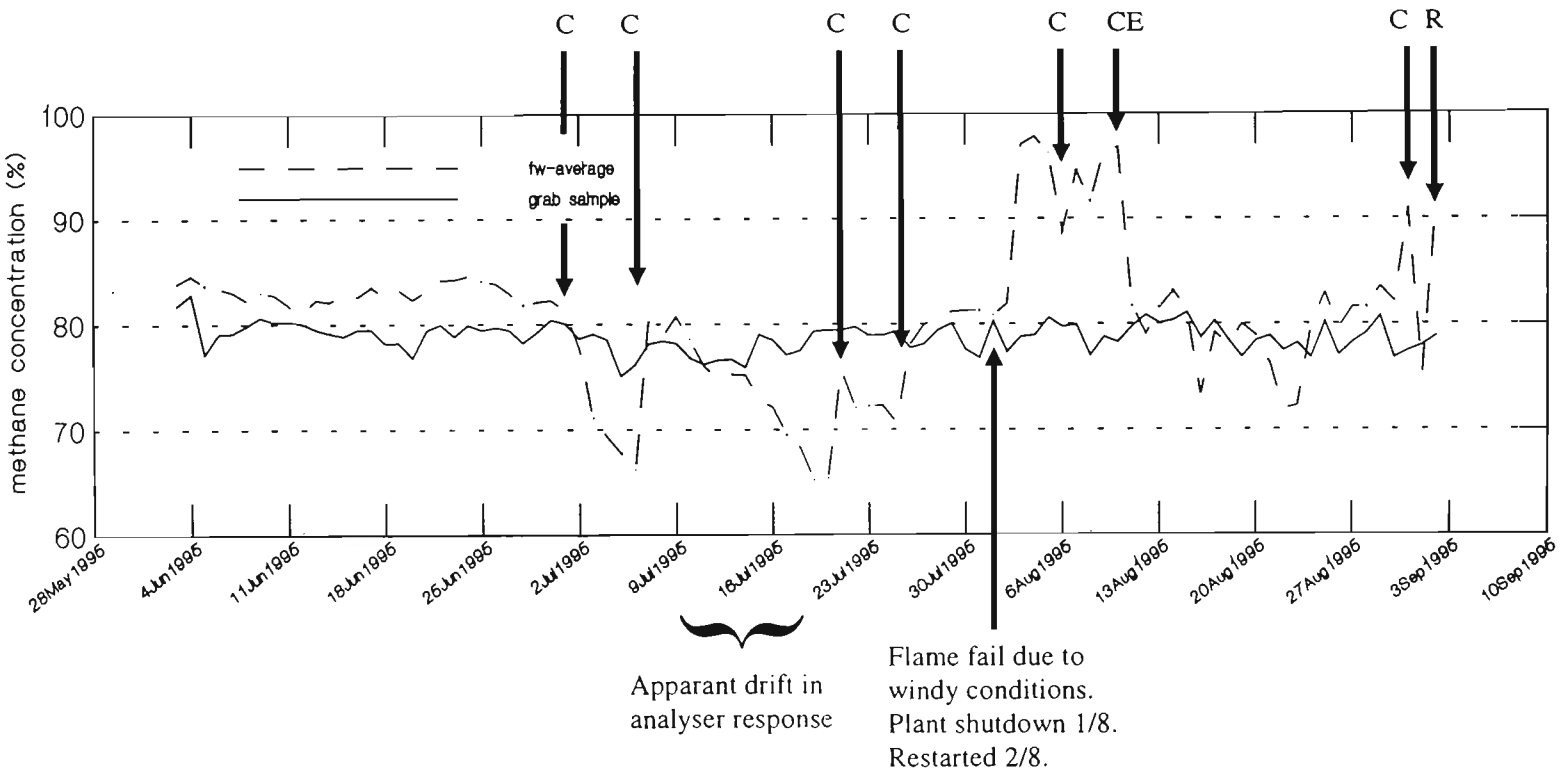

Figure 6-5 Time series plot of the grab-sample methane concentration and 24 hr flow-weighted average methane concentration (C - online analyser calibrated by WTP, CE - online analyser calibrated by Rosemount Instruments, R - online analyser repaired).

6.2.3 Analytical Methods

The **chemical oxygen demand** (COD) was measure according to Method APHA 5220 B (Open Reflux Method) from *Standard Methods for the Examination of Water and Wastewater* (APHA: USA, 18th ed., 1992).

pH was measured with a Hanna Instruments pH probe (model HI 1332) and an Orion 940 Expandable Ionanalyzer pH meter according to Method APHA 4500-H^+ (pH Value) from *Standard Methods for the Examination of Water and Wastewater* (APHA: USA, 18th ed., 1992)

Temperature was measured with a thermocouple and Hanna HI 9023 pH meter.

Total Kjeldahl Nitrogen (TKN) was measured according to Method APHA 4500-N_{org} B (Macro-Kjeldahl Method) from *Standard Methods for the Examination of Water and Wastewater* (APHA: USA, 18th ed., 1992). The ammonia removal step was omitted and organic nitrogen was calculated as the difference between the total Kjeldahl nitrogen and ammonia-nitrogen values.

Ammonia-Nitrogen (NH_3-N) was determined according to Method APHA 4500-NH_3 B (Preliminary Distillation Step) and Method 4500-NH_3 E (Titrimetric Method) from *Standard Methods for the Examination of Water and Wastewater* (APHA: USA, 18th ed., 1992)

Carbohydrate was determined colorimetrically using the Anthrone Test for Carbohydrates described in Ramanathan, M., Gaudy, A. F. Jr. and Cook, E.

E.: Selected Analytical Methods for Research in Water Pollution Control, (Okalahoma State University: USA, 1968).

Oil & Grease was determined according to Method 5520 B (Partition Gravimetric Method) from *Standard Methods for the Examination of Water and Wastewater* (APHA: USA, 18th ed., 1992)

Soluble sulphate was determined by nonsuppressed ion chromatography. A Waters ion chromatograph equipped with a conductivity detector and IC-Pak A HC anion-exchange column was used. The eluent contained di-sodium octane sulphonate and boric acid. Pretreatment of raw sewage samples involved filtration with a 0.2 μm syringe filter.

Soluble calcium was measured according to Method APHA 3120B (Inductively Coupled (ICP) Method) from *Standard Methods for the Examination of Water and Wastewater* (APHA: USA, 18th ed., 1992). Pretreatment involved filtration through Whatman GFC filter paper (mean pore size 1.2 μm) followed by digestion according to Method APHA 3030D.

Methane was analysed by gas chromatography. A Varian 3400 GC, equipped with a Thermal Conductivity Detector and 12′ × 1/8″ stainless steel column packed with Haysep-Q. The column temperature was 30°C and the carrier gas was argon (@ 15 $mL.min^{-1}$). Calibration was carried out using a special gas mixture (purchased from BOC Gases) that contained:

Methane	79.3±0.2 %
Carbon dioxide	10.3±0.2 %

Hydrogen	104±4 ppm
Oxygen	0.998±0.02 %
Nitrogen	9.4% (by difference)

Samples of gas to be analysed were transferred to a 0.5 mL (approx.) gas sampling loop on the GC by displacing the gas in the gas sampling bulb with an acidified gas-displacement liquid (refer to Method APHA 511 from *Standard Methods for the Examination of Water and Wastewater* (APHA: USA, 15th ed., 1980)).

6.3 RESULTS AND DISCUSSION

6.3.1 Preliminary Data Assessment

A preliminary assessment of the data was made to identify important regressors and investigate characteristics of the data such as heterogenous variance, serial correlation and cross correlation, which can influence the approach taken in a regression analysis. Non-uniform variance can bias the regression coefficients. Serial correlation in the dependent variable, if unaccounted for, can invalidate hypothesis tests involving the model's coefficients. Correlations between regressors (i.e., multicollinearity) can seriously inflate the variance of regression coefficients, and adversely affect predictions at points that represent extrapolation outside the range of data.

In this study of the methane yield from the 115E anaerobic reactor, daily measurements were made on the methane flowrate from the reactor, the temperature of the reactor, the raw sewage flowrate to the 115E reactor, and the concentrations of COD, protein, carbohydrate, oil & grease, soluble sulphate ion, soluble calcium ion, and soluble potassium ion in the raw sewage. The protein content of the raw sewage was calculated from 6.25×[Organic Nitrogen]=6.25×([Total Kjeldahl Nitrogen]-[Ammonia Nitrogen])[101]. The data, which are presented in Appendix B, were collected between 26/6/95 and 26/8/95. Time series plots of all variables are shown in Figure 6-6 to Figure 6-17.

All variables appeared, from the time series plots, to have reasonably homogenous variance. Some variables, however, exhibited a degree of serial correlation. Examination of the sample autocorrelation function revealed serial correlation in the methane flowrate, raw sewage flowrate, pH, raw sewage COD and sulphate ion concentrations, and the 115E reactor temperature data. The presence of serial correlation in the dependent variable (methane flowrate) will produce correlated errors in the regression model. The serial correlation can be removed by modelling the autocorrelative structure in the methane flowrate and then using the time-series model to transform both the dependent and independent variables[102].

Only the raw sewage COD concentration (Figure 6-9) exhibited a clear weekly cycle. Note that both the raw sewage COD and raw sewage flowrate to the Plant show weekly cycles due to the weekly pattern in industrial discharges.

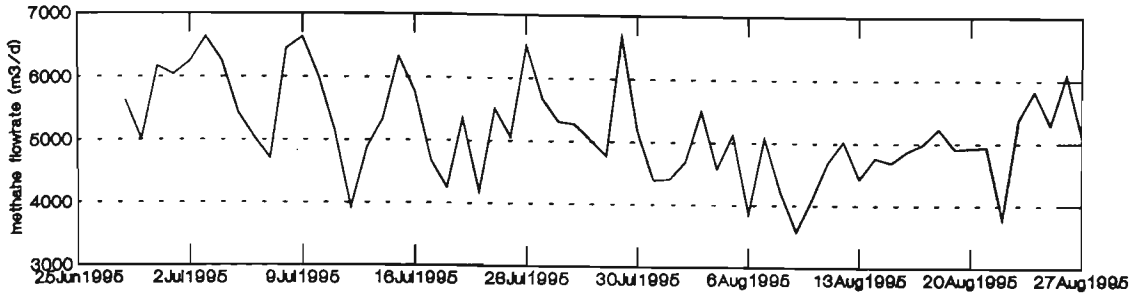

Figure 6-6 115E reactor methane flowrate (m^3/d).

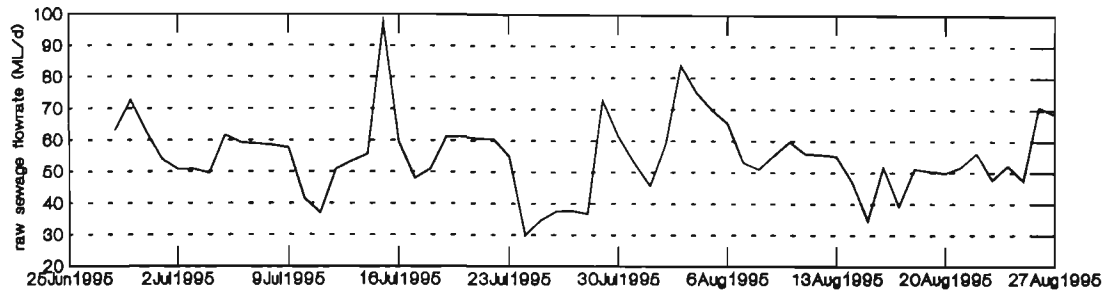

Figure 6-7 Raw sewage flowrate (ML/d).

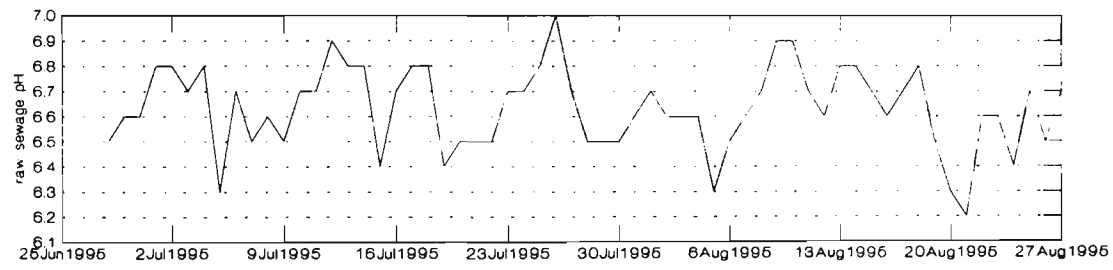

Figure 6-8 Raw sewage pH.

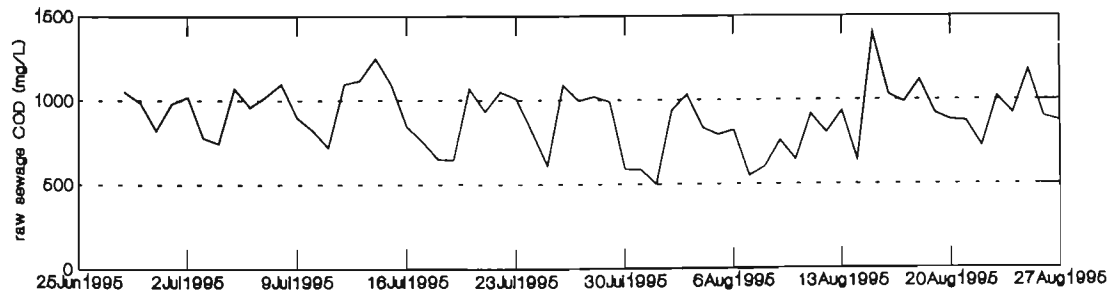

Figure 6-9 Raw sewage COD (mg/L).

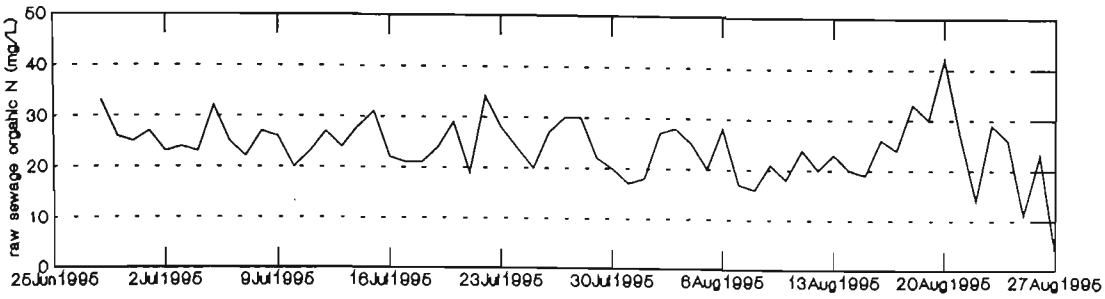

Figure 6-10 Raw sewage organic nitrogen (mg/L).

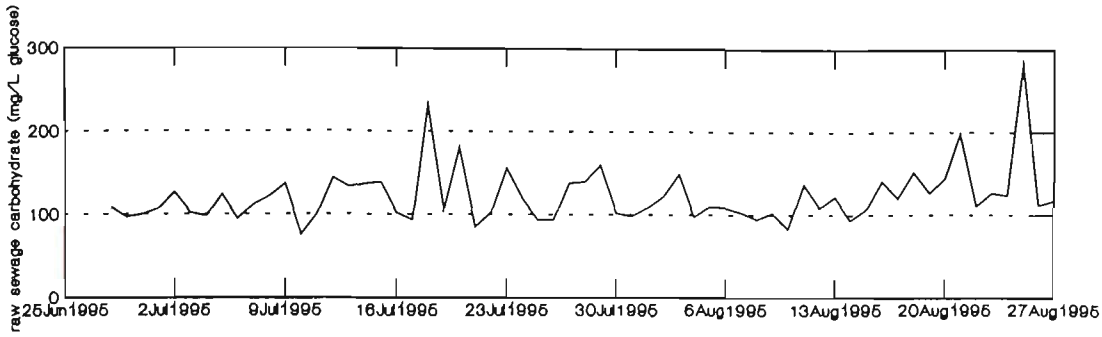

Figure 6-11 Raw sewage carbohydrate (mg/L glucose).

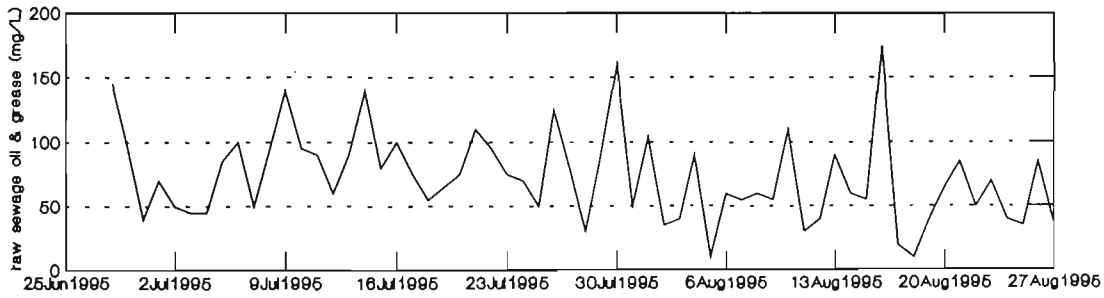

Figure 6-12 Raw sewage oil & grease (mg/L).

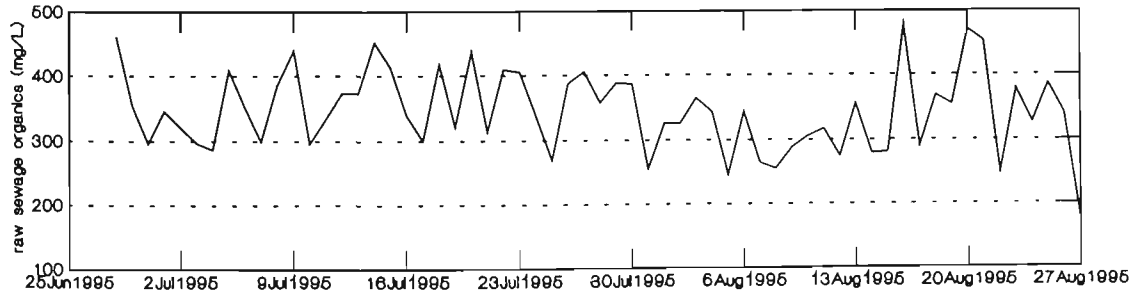

Figure 6-13 Sum of raw sewage protein, carbohydrate and oil & grease.

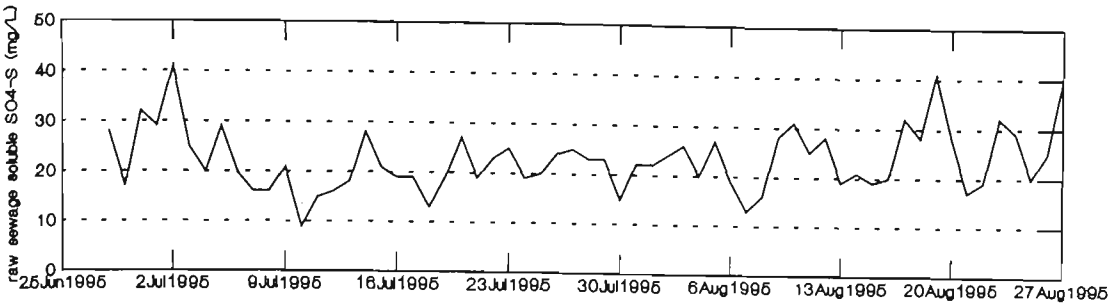

Figure 6-14 Raw sewage soluble sulphate ion (mg/L SO_4^{2-}-S).

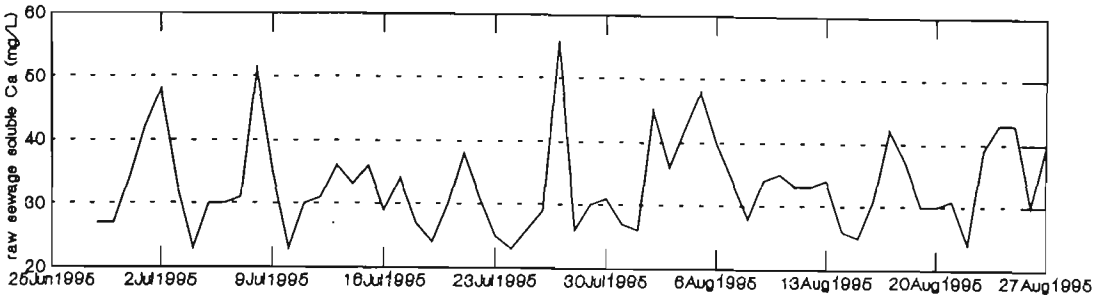

Figure 6-15 Raw sewage soluble calcium ion (mg/L).

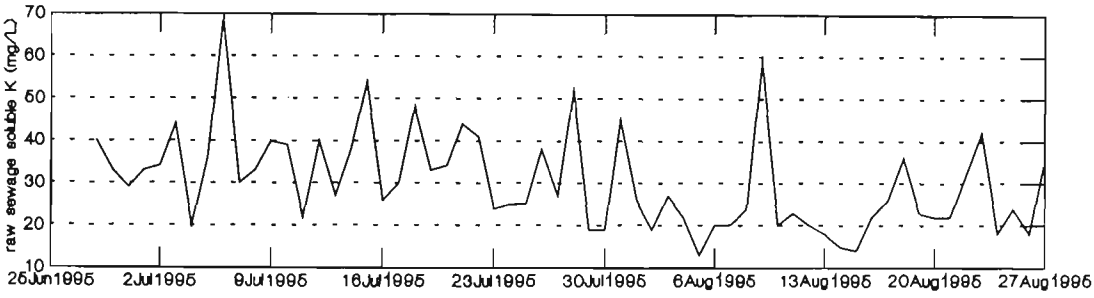

Figure 6-16 Raw sewage soluble potassium ion (mg/L).

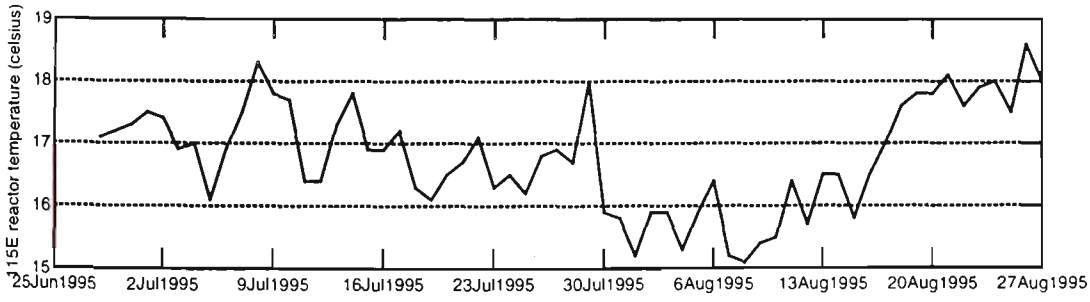

Figure 6-17 115E reactor temperature (°C).

Industry contributes approximately 25% of the raw sewage hydraulic load and 50% of the BOD_5 load to the Plant. There was, however, no evidence of a weekly cycle in the raw sewage flowrate to the 115E reactor (Figure 6-7). This is probably because the incoming raw sewage is distributed to many different sub-processes and, depending on the performance and capacity of these other processes, the 115E Lagoon will not always be subject to a cyclic hydraulic loading rate.

Whilst the autocorrelation plot of the reactor temperature did not signal the presence of seasonality in the data, there did appear to be both a weekly and, possibly, annual cycle. Although the temperature of the raw sewage has not been measured routinely at WTP, and was not measured in the course of this study, the recent installation of a Sewer Sentinel[103] (a device that continuously measures temperature, pH, conductivity and turbidity of sewage) has provided some insight into the pattern exhibited by the raw sewage temperature (Figure 6-18). Figure 6-18 shows that there is both an annual and weekly cycle in the temperature of the raw sewage, and this would likely have significant bearing on the temperature pattern of the anaerobic reactor.

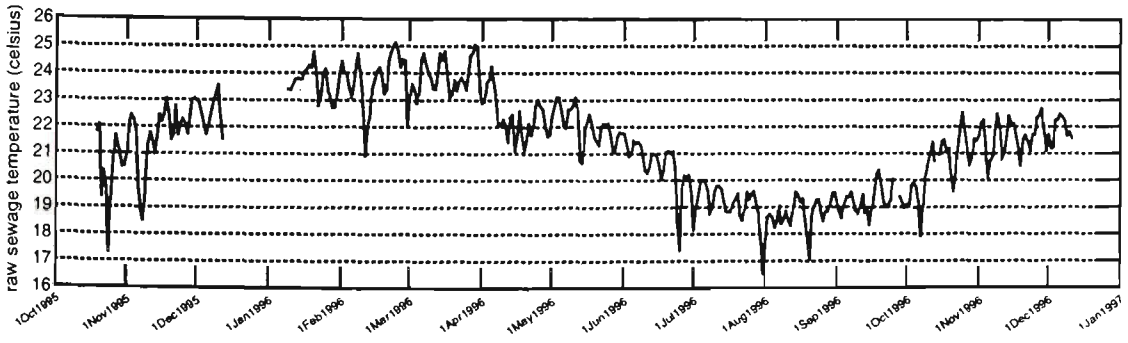

Figure 6-18 Sewer Sentinel measurements of raw sewage temperature.

The weekly cycles in raw sewage temperature and raw sewage COD are in phase, suggesting that the raw sewage temperature is also affected by industry cycles. By removing the annual cycle from the data series in Figure 6-18, by subtracting the 7-day moving average, and plotting a bar chart of the reactor temperature against day of the week, it was clear that the raw sewage temperature tends to peak at the end of the working week, as does the raw sewage COD, temperature of the anaerobic reactor and methane flowrate from the reactor. pH data derived from the Sewer Sentinel also exhibited a weekly cycle, although, it was out of phase by 180°.

An examination of scatterplots and a matrix of correlations (Table 6-1) between independent variables and the dependent variable (methane flowrate) highlighted a number of potentially important regressors and potential problems that could arise due to the presence of multicollinearity among the regressors. The codes used for the variables shown in Table 6-1 are defined in Table 6-3, p. 6-27.

From Table 6-1, it appeared that the reactor temperature and raw sewage COD were the more important determinants of the methane flowrate. The temperature and COD were, however, strongly cross correlated. The impact of this collinearity on the performance of the regression model and on the stability of the regression coefficients was assessed further in Section 6.3.3. Multiple correlations also existed between the reactor temperature, raw sewage COD, calcium ion, sulphate ion, and potassium ion concentrations.

Table 6-1 Matrix of correlations between dependent and independent variables. The cells have been emphasised where correlations are greater than 0.2 (corresponding to a probability of 0.1 for an individual significance test).

	CH4FLOW	RFLOW	RPH	RCOD	RPROT	RCARB	ROG	RORGS	RSO4	RCA	RK	PTEMP
CH4FLOW	1.000											
RFLOW	0.151	1.000										
RPH	-0.172	-0.399	1.000									
RCOD	0.219	0.082	-0.026	1.000								
RPROT	0.181	0.069	-0.308	0.415	1.000							
RCARB	-0.003	0.010	-0.137	0.349	0.083	1.000						
ROG	0.131	0.094	-0.003	0.068	0.156	-0.156	1.000					
RORGS	0.176	0.098	-0.256	0.470	0.715	0.505	0.559	1.000				
RSO4	0.134	0.097	-0.018	0.220	0.149	0.012	-0.281	-0.062	1.000			
RCA	0.108	0.184	-0.041	0.264	0.046	0.150	-0.182	0.008	0.344	1.000		
RK	0.013	0.093	0.121	0.155	0.152	0.003	0.105	0.148	0.021	-0.092	1.000	
PTEMP	0.477	0.027	-0.184	0.429	0.212	0.237	0.047	0.279	0.221	0.159	0.106	1.000

The raw sewage flowrate and pH were also potentially important factors, although, these two variables were also strongly correlated. Flowrate is the more important of the two in the sense that it is a controllable variable and could be used to manipulate methane production in a feedforward control scheme. If necessary, therefore, pH could be omitted from the model.

The raw sewage COD was correlated with other measures of organic concentration (protein and carbohydrate). COD is an aggregate measure of the concentration of organic matter and it would not be used in a regression model in conjunction with other measures of organic matter.

The correlation between the sulphate ion and calcium ion concentrations could be overcome by adding them together, though, it is preferable to estimate their separate effects. The correlation between sulphate and calcium may be the result of sulphate-bearing industrial wastewaters which are treated with slaked lime (calcium hydroxide), leaving residual sulphate and calcium ion concentrations in the treated effluent.

It should be noted that there were missing values in the raw sewage flowrate, gas temperature and gas flowrate series'. The missing values occurred on the 18th, 19th and 20th of August, and were presumably due to a telemetry fault. The missing values were imputed by fitting a second degree polynomial to the series, by least squares, with exponentially decreasing weights[100].

The brief assessment of the data, in the foregoing, revealed the presence of serial correlation and cross correlation. Before proceeding with the regression analysis, serial correlation in the dependent variable had to be accounted for,

through time-series modelling of the methane flowrate and transformation of the dependent and independent variables. The time-series modelling is detailed in Section 6.3.2. The impact of multicollinearity in the regressors was further assessed in the course of the analysis.

6.3.2 Time Series Modelling of Methane Flowrate

The time series plot of the methane flowrate in Figure 6-6 suggests that the methane flowrate is nonstationary and possibly exhibits seasonality with a period of 7 days. The methods of Box and Jenkins[45] were used to identify and fit a time series model to the methane flowrate data. Given the objective of producing an uncorrelated series, the main criterion in choosing an appropriate time-series model was the accuracy of fit rather than accuracy of forecasts.

The sample autocorrelation function (ACF) of the methane flowrate series indicated significant autocorrelation at lags of 1 and 6. At short lags, the sample autocorrelations appeared to tail off rapidly. At seasonal lags, the autocorrelations appeared to die out gradually, and there was possibly a weak trend in the autocorrelation series. The sample partial autocorrelation function (PACF) revealed significant partial autocorrelations at lags 1 and 5. At short lags, the partial autocorrelations cut off at lag 1 and at seasonal lags the partial autocorrelations cut off at lag 5. From this evidence, two possible models are suggested: ARIMA(1,0,0) and ARIMA(1,0,0)$(1,0,0)_7$. A period of 7 was chosen for the seasonal model because there was a clear weekly cycle in the raw sewage

COD concentration and temperature, both of which are likely to affect the pattern in the methane flowrate. Given the weak evidence of nonstationarity in the data series, further models were explored based on the first seasonal differences and first regular differences.

The sample ACF and PACF plots of the first seasonal differences (with period=7) suggested that the differenced series was random and stationary. The appropriate model in this case is ARIMA$(0,0,0)(0,1,0)_7$.

In the sample ACF plot of the first regular differences, owing to the smallness of the autocorrelation at lag 2 relative to adjacent lags, it was unclear as to whether the sample autcorrelation tailed off or cut off at lag 1. In the sample PACF plot, there were significant autocorrelations at lags 1, 5 and 12 and the sample partial autocorrelations appeared to tail off after lag 1. The models suggested by this evidence are ARIMA(0,1,1) and ARIMA(1,1,1).

The five models identified by the ACF and PACF analysis were fitted to the data and compared in terms of model fit and residual diagnostic tests (Table 6-2). The adjusted coefficient of determination (adjusted R^2) and residual mean square error (MSE) were used to assess the fit of the models. The chi-square white noise test (i.e. the Q-criterion referred to by Box and Jenkins[45]) and the chi-square test for normality were used to identify randomness and non-normality in the residuals. Other diagnostic checks, including an autocorrelation check and

Table 6-2 A comparison of the time-series models fitted to the methane flowrate series. The values in brackets are the degrees of freedom and probability value (df; p).

No.	Model	Adj-R^2	Residual MSE	χ^2 white noise test	χ^2 goodness of fit test
1	ARIMA(1,0,0)	0.153	690	23.1 (24; 0.52)	3.3 (3; 0.35)
2	ARIMA(1,0,0)(1,0,0)$_7$	0.156	686	20.8 (23; 0.59)	1.7 (3; 0.63)
3	ARIMA(0,0,0)(0,1,0)$_7$	0.000	815	38.2 (25; 0.04)	7.6 (3; 0.06)
4	ARIMA(0,1,1)	0.100	714	45.3 (24; 0.01)	5.7 (3; 0.13)
5	ARIMA(1,1,1)	0.142	699	27.9 (23; 0.22)	1.5 (3; 0.67)

cumulative periodogram check, were also performed on the residuals from each model.

The residuals from all models, except model 3, seemed random. Model 3 appeared to be underspecified because the residuals exhibited serial correlation. Models 1 and 2 resulted in the best fit. However, the seasonal autoregressive term in model 2 was not statistically significant. Model 1, therefore, was selected for the next stage of the regression analysis.

The fitted ARIMA(1,0,0), or AR(1), model is given as Equation 6-1.

$$a_{y,t} = y_t - 0.41 y_{t-1} \qquad \textbf{Equation 6-1}$$

where $y_t = Y_t - \overline{Y}$

The $a_{y,t}$ are the model's residuals. The uncorrelated residuals became the dependent variable in the regression analysis.

6.3.3 Regression Analysis of Methane Flowrate

The purpose of the regression analysis was to further investigate the effects of the trace nutrients and inhibitors identified in Chapter 5 and to identify those variables that may be useful in a feedforward control scheme for the anaerobic reactor.

The first step in the regression analysis was to identify appropriate models which would then be evaluated in terms of fit and prediction. To begin with, the correlation analysis in Section 6.3.1 suggested that the raw sewage temperature, COD concentration, and flowrate, would be potentially useful predictors of the methane flowrate. These variables formed the basis of all models to be explored in the analysis. In addition to these variables, it was of interest to investigate: 1), substituting the concentrations of protein, carbohydrate and oil & grease (or the sum of all three) for COD, and ; 2), investigating the effects of pH and the concentrations of calcium, sulphate and potassium ions. Given that the initial reactor concentration of a variable is essentially determined by the raw sewage flowrate, the concentration of the variable in the raw sewage, and the volume of the reactor, all concentration variables were entered into the model with flowrate.

Alternatively, the variables were entered into the model as mass loadings by multiplying the raw sewage concentration by the raw sewage flowrate.

The next step was to transform all variables using the AR(1) model given in Equation 6-1. For example the variable x_1 was transformed to:

$$a_{x_1,t} = x_{1,t} - 0.41x_{1,t-1}$$
$$\text{where } x_1 = X_1 - \overline{X}_1$$

The a_t's were generated using the methods described for model estimation in Box and Jenkins[45].

The correlation matrix of the transformed variables was essentially the same as the correlation matrix of the original variables. It was also observed, however, that there were significant cross correlations between some of the regressors (raw sewage COD and reactor temperature) and the transformed methane flowrate. The potential of lagged regressors was explored in the regression analysis.

The various models were then evaluated in terms of fit and prediction. The adjusted R^2 and standard error of the estimate(s) were used to evaluate the fit of a model. Data-splitting was used to assess the prediction capabilities of each of the models. Meyers[102] recommends that the fitting sample be based on $n \geq 2p+20$, where n is the size of the fitting sample and p is the number of regressors, and that the fitting sample and validation sample have roughly equal numbers of observations. Given that as many as 8 regressors could be used in a model, it was decided to base the fitting sample on the first 36 observations. The remaining 25 observations were used to assess prediction capabilities.

A total of 62 models was assessed. The model fit and prediction statistics are given for each model in Table 6-4. The codes used for the variables are defined in Table 6-3.

Various patterns emerged in the early stages of the model building process (i.e. in models with three or less regressors). The importance of raw sewage flowrate, reactor temperature and raw sewage COD concentration became apparent and adding the lagged variables (RCODL1 and PTEMPL1) substantially improved the adjusted R^2. There was no clear advantage in using mass load variables in place of concentration variables. Generally, the concentration variables resulted in a smaller standard error estimate, but larger prediction sum of squares. There was little difference between the regressors RCODLD and RORGSLD, and the sum of the organics (RORGSLD) performed better than its components (RPROTLD, RCARBLD and ROGLD). Of the variables RSO4, RCA, RCASO4, RK, and RPH, only RSO4 added value to the model by improving the model fit, although, the prediction sum of squares also increased.

A number of models were selected for a more detailed evaluation. Given that the main objective was to learn which regressors were important and which were not, the models were selected mainly on the basis of the adjusted R^2 and the standard error of the estimate. The prediction capabilities (which can be affected by multicollinearity) of the models were considered, but were of secondary

Table 6-3 Definition of codes used for the variables in this study.

CH4FLOW	Methane flowrate from the 115E reactor (m^3/d).
RFLOW	Raw sewage flowrate to the 115E reactor (ML/d).
RPH	Raw sewage pH (pH units).
RCOD	Raw sewage COD concentration (mg/L).
RCODL1	Lag 1 raw sewage COD concentration (mg/L).
RCODLD	Raw sewage COD load (t/d).
RPROT	Raw sewage protein concentration (mg/L).
RPROTLD	Raw sewage protein load (t/d).
RCARB	Raw sewage carbohydrate concentration (mg/L).
RCARBLD	Raw sewage carbohydrate load (t/d).
ROG	Raw sewage oil & grease concentration (mg/L).
ROGLD	Raw sewage oil & grease load (t/d).
RORGS	Raw sewage organics concentration i.e. the sum of raw sewage protein, carbohydrate and oil & grease (mg/L).
RORGSLD	Raw sewage organic load (t/d).
RSO4	Raw sewage soluble sulphate ion concentration (mg/L SO_4-S).
RSO4LD	Raw sewage sulphate ion load (t/d SO_4-S)
RCA	Raw sewage soluble calcium ion concentration (mg/L).
RCALD	Raw sewage calcium load (t/d).
RK	Raw sewage soluble potassium ion concentration (mg/L).
RKLD	Raw sewage potassium load (t/d).
PTEMP	115E reactor (also known as the 115E pot) temperature (°C).
PTEMPL1	Lag 1 reactor temperature (°C).

Table 6-4 *Evaluation of model fit and prediction capabilities.*

Model no.	Number of variables in model	Adjusted R^2	s	$\sum_{j=37}^{61}(y_j - \hat{y}_j)^2$	Variables in model
1	1	0.025	715	1.07	RCODLD
2	1	0.027	714	1.06	RORGSLD
3	1	0.077	695	1.18	RFLOW
4	1	0.153	666	1.10	PTEMP
5	2	0.003	723	1.01	RCODLD, RPH
6	2	0.007	721	1.06	RCODLD, RKLD
7	2	0.046	707	1.19	RCODLD, RCALD
8	2	0.049	706	1.18	RFLOW, RPH
9	2	0.057	703	1.26	RFLOW, RCOD
10	2	0.058	702	1.17	RFLOW, RCA
11	2	0.060	701	1.31	RCODLD, RSO4LD
12	2	0.073	697	1.24	RFLOW, RSO4
13	2	0.071	697	1.20	RFLOW, RCASO4
14	2	0.098	696	1.09	RCODLD, RCODLDL1
15	2	0.091	690	1.40	RCODLD, RCASO4LD
16	2	0.094	689	1.24	RFLOW, RK
17	2	0.130	675	1.10	PTEMP, RKLD
18	2	0.136	673	1.07	RCODLD, PTEMP
19	2	0.175	657	1.09	PTEMP, RCALD
20	2	0.188	652	1.12	PTEMP, RPH
21	2	0.203	646	1.16	PTEMP, RCASO4LD
22	2	0.207	645	1.27	PTEMP, RSO4LD
23	2	0.201	645	1.12	RFLOW, PTEMP
24	2	0.234	641	1.31	PTEMP, PTEMPL1
25	3	0.000	725	1.17	RPROTLD, RCARBLD, ROGLD
26	3	0.193	658	1.30	RFLOW, RCOD, RCODL1
27	3	0.176	656	1.12	RFLOW, PTEMP, RCA
28	3	0.181	655	1.13	RFLOW, PTEMP, RCASO4
29	3	0.187	652	1.24	PTEMP, RCALD, RSO4LD
30	3	0.190	651	1.10	RFLOW, PTEMP, RPH
31	3	0.193	650	1.20	RFLOW, PTEMP, RSO4
32	3	0.217	649	1.26	RCODLD, PTEMP, PTEMPL1
33	3	0.214	642	1.16	RFLOW, PTEMP, RK

Table 6-4 continued

Model no.	Number of variables in model	Adjusted R^2	s	$\sum_{j=37}^{61}(y_j - \hat{y}_j)^2$	Variables in model
34	3	0.264	629	1.26	RFLOW, PTEMP, PTEMPL1
35	3	0.269	619	1.59	RFLOW, RCOD, PTEMP
36	4	0.250	629	1.59	RFLOW, RCOD, PTEMP, RCA
37	4	0.258	623	1.58	RFLOW, RCOD, PTEMP, RPH
38	4	0.265	620	1.57	RFLOW, RCOD, PTEMP, RK
39	4	0.280	614	1.80	RFLOW, RCOD, PTEMP, RCASO4
40	4	0.302	613	1.58	RFLOW, RCOD, PTEMP, PTEMPL1
41	4	0.304	611	1.54	RFLOW, RCOD, RCODL1, PTEMP
42	4	0.320	597	2.21	RFLOW, RCOD, PTEMP, RSO4
43	5	0.280	622	1.57	RFLOW, RCOD, PTEMP, PTEMPL1, RCA
44	5	0.281	621	1.57	RFLOW, RCOD, PTEMP, PTEMPL1, RPH
45	5	0.297	614	1.54	RFLOW, RCOD, PTEMP, PTEMPL1, RK
46	5	0.303	612	1.49	RFLOW, RCOD, RCODL1, PTEMP, PTEMPL1
47	5	0.308	610	1.73	RFLOW, RCOD, PTEMP, PTEMPL1, RCASO4
48	5	0.352	590	2.19	RFLOW, RCOD, PTEMP, PTEMPL1, RSO4
49	6	0.285	620	1.72	RFLOW, RCOD, PTEMP, PTEMPL1, RCASO4, RPH
50	6	0.294	616	1.67	RFLOW, RCOD, PTEMP, PTEMPL1, RCASO4, RK
51	6	0.330	600	2.21	RFLOW, RCOD, PTEMP, PTEMPL1, RCA, RSO4
52	6	0.329	600	2.18	RFLOW, RCOD, PTEMP, PTEMPL1, RSO4, RPH
53	6	0.341	595	2.11	RFLOW, RCOD, PTEMP, PTEMPL1, RSO4, RK
54	6	0.363	585	2.14	RFLOW, RCOD, RCODL1, PTEMP, PTEMPL1, RSO4
55	7	0.270	626	1.66	RFLOW, RCOD, PTEMP, PTEMPL1, RCASO4, RK, RPH
56	7	0.305	611	2.20	RFLOW, RCOD, PTEMP, PTEMPL1, RCA, RSO4, RPH
57	7	0.317	606	2.10	RFLOW, RCOD, PTEMP, PTEMPL1, RSO4, RK, RPH
58	7	0.318	605	2.13	RFLOW, RCOD, PTEMP, PTEMPL1, RCA, RSO4, RK
59	7	0.344	593	2.19	RFLOW, RCOD, RCODL1, PTEMP, PTEMPL1, RCA, RSO4
60	8	0.292	617	2.13	RFLOW, RCOD, PTEMP, PTEMPL1, RCA, RSO4, RK, RPH
61	8	0.345	593	2.12	RFLOW, RCOD, RCODL1, PTEMP, PTEMPL1, RCA, RSO4, RK
62	9	0.319	605	2.13	RFLOW, RCOD, RCODL1, PTEMP, PTEMPL1, RCA, RSO4, RK, RPH

importance. A plot was made of the standard error of estimate versus the prediction sum of squares for the models in Table 6-4, and the plot symbols were sized according the adjusted R^2 (Figure 6-19). The graph shows that the models fall into four main groups. Group A consists of the one- and two-variable models which did not include the reactor temperature. Group B includes the two- and three-variable models that had PTEMP and/or PTEMPL1, or RCOD and RCODL1. The three- to seven-variable models in Group C included both RCOD and PTEMP, with or without their lagged counterparts. Group D models included RSO4 in combination with RCOD and PTEMP. Four models were selected from the lower left corners of each of Groups C and D for further evaluation. The model's numbers were 40, 41, 45, 46, 48, 53, 54 and 61.

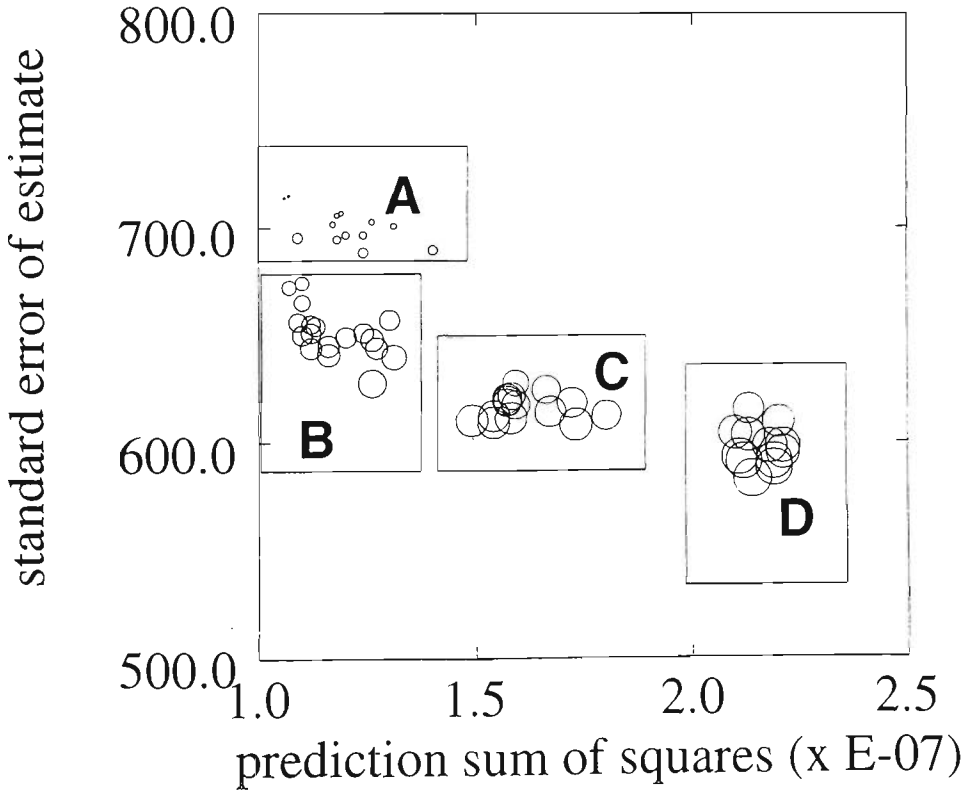

Figure 6-19 A plot of the error variance and prediction sum of squares for each of the models in **Table 6-4**. The plot symbols have been sized according to the adjusted R^2.

The eight models were re-fitted to the entire data set (Table 6-5) and a number of diagnostics[99,102,] were used to examine each of the models in greater detail. The models were diagnosed for the presence and effects of multicollinearity using condition numbers and variance inflation factors . Note that the condition numbers are the square of the condition indices given in Systat's output, and the variance inflation factors are the inverse of the tolerances. The residuals were diagnosed for possible violation of assumptions. The sample autocorrelation function and Fourier decomposition were used to detect serial correlation in the residuals. A plot of the Studentised residual versus the predicted value for the transformed methane flowrate was used to signal

Table 6-5 Adjusted R^2 and standard error of estimate (s) for the "short listed" regression models.

Model No.	Variables in model	Adjusted R^2	s
40	RFLOW, RCOD, PTEMP, PTEMPL1	0.154	638
41	RFLOW, RCOD, RCODL1, PTEMP	0.178	623
45	RFLOW, RCOD, PTEMP, PTEMPL1, RK	0.166	634
46	RFLOW, RCOD, RCODL1, PTEMP, PTEMPL1	0.183	627
48	RFLOW, RCOD, PTEMP, PTEMPL1, RSO4	0.141	643
53	RFLOW, RCOD, PTEMP, PTEMPL1, RSO4, RK	0.153	639
54	RFLOW, RCOD, RCODL1, PTEMP, PTEMPL1, RSO4	0.171	632
61	RFLOW, RCOD, RCODL1, PTEMP, PTEMPL1, RCA, RSO4, RK	0.167	633

possible outliers and trends or heterogenous variance in the residuals. Normality of the residuals was investigated using a normal probability plot. Erroneous observations, i.e. observations having a large residual or leverage, were identified using Cook's D and then the impact of these observations on the regression coefficients was investigated using partial regression plots.

As expected from the correlation matrix in Table 6-1, multicollinearity was detected in the set of regressors for each of the eight models considered. As a rule of thumb, Myers[102] states that a variance inflation factor greater than 10, or a condition number greater than 1000, indicates that one or more coefficients is considerably affected by multicollinearity and consideration should be given to variable deletion or an alternative to least squares estimation. Of the eight models considered, the largest variance inflation factor was 1.4 and the maximum condition number was 4.4. The diagnostics, therefore, suggest that the impact of the multicollinearity is not serious. However, the coefficients on RCA, RSO4 and RK were opposite in sign to what was expected, and this could be the result of multicollinearity. It was thought that calcium and potassium would have positive coefficients, and sulphate would have a negative coefficient, according to the trials performed in Chapter 5 and the literature evidence cited in Table 5-2, p. 5-8.

The residuals from each model appear random and normally distributed, with constant variance. There were, therefore, no serious departures from the assumptions that underpin the least-squares model. Although, it should be noted that whilst the sample autocorrelation function indicated that the residuals were

random, the Fourier analysis suggested that a degree of seasonality (with a period of about 7 days) was still present.

Based on the goodness of fit of the models (Table 6-5), and the diagnostics so far presented, models 41 and 46 performed almost equally as well. Model 41, however, has one less regressor and a slightly smaller standard error of estimate. Model 41, therefore, appears to be the better model for predicting methane production in the 115E reactor.

While no outliers were detected (at the 99.5% confidence level) in the residuals of the final eight models, there were a number of high leverage observations that were common to all of the models. In particular, the raw sewage flowrate to the 115E reactor was high on July 14 and the reactor temperature was high on 28 July. Although, both of these observations seemed to reinforce the trend set by the balance of the data (as determined from partial regression plots). On August 14, however, there was a high raw sewage COD value which did not appear to correspond with a peak in the methane flowrate. From a scatter plot of COD versus the sum of the protein, carbohydrate and oil & grease (i.e. the "organics"), it was evident that the high COD observation did not conform to the pattern in the data. Rather than omitting this observation, though, model 41 was refitted using the COD value predicted from the least-squares regression of COD on the sum of the organics (i.e., the COD value of 1400 mg/L was replaced with 810 mg/L). Replacing the high COD value had considerable impact on the COD and lagged COD coefficients and the adjusted R^2 was increased to 0.209 from 0.178.

In all of the evaluated models, the COD coefficient (i.e. the lag 0 coefficient) was approximately zero and not statistically significant. The lag 0 COD regressor was therefore deleted and Model 41 was refitted to the data. The new model expressed in terms of the original variables is given as Equation 6-2.

$$Y_t - 0.4Y_{t-1} = -256.9 + 7.4X_{1,t} - 3.0X_{1,t-1} + 1.4X_{2,t-1} - 0.6X_{2,t-2} + 256.1X_{3,t} - 104.7X_{3,t-1}$$

Equation 6-2

where Y = methane flowrate (m^3 / d)

X_1 = raw sewage flowrate (ML / d)

X_2 = raw sewage COD (mg / L)

X_3 = reactor temperature (°C)

t = time (days)

The adjusted R^2 for the new model (numbered 41b) was increased from 0.209 to 0.220 and the standard error of the estimate was reduced from 617 to 613. The R^2 for the re-expressed model, which takes into account the variation explained by the autoregression of the methane flowrate, was 0.53. The Studentised residuals for Model 41b are plotted in Figure 6-20 and the observed and estimated values for methane production are given in Figure 6-21.

There are two notable features about the residuals in Figure 6-20. Firstly, there seemed to be a weekly cycle in methane production for the first 2-3 weeks which the model does not capture very well. It appears that the process changed, in some way, after the first three weeks of study. This could be related to the set

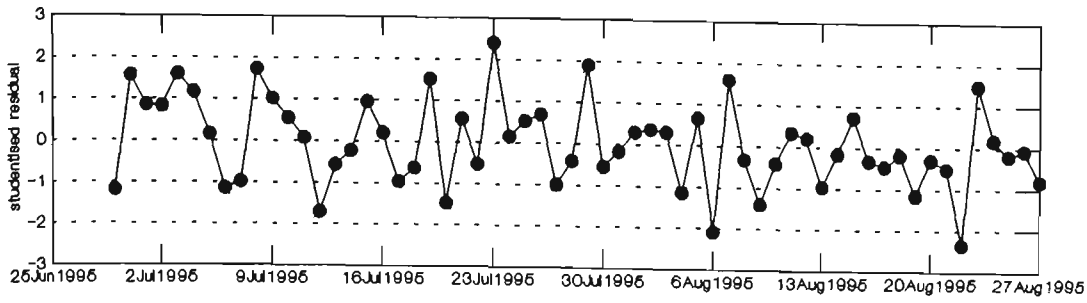

Figure 6-20 Time sequence of the Studentised residuals for Model 41b.

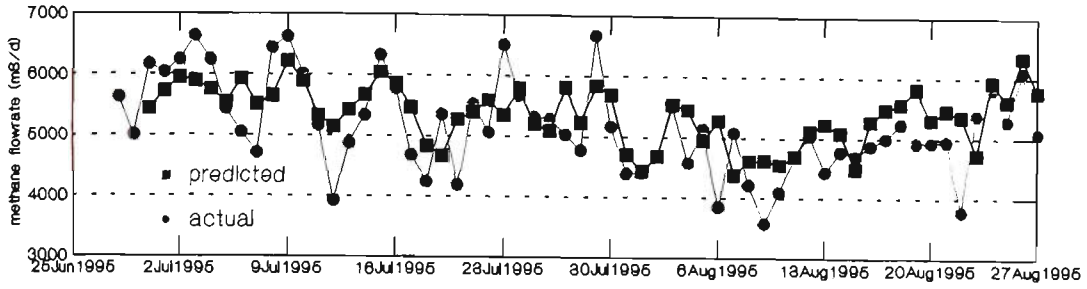

Figure 6-21 Observed and estimated values for methane production from the 115E Anaerobic Reactor.

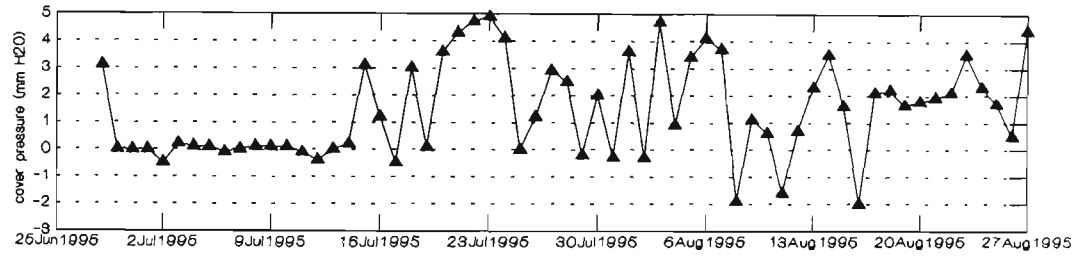

Figure 6-22 Gas pressure under the cover of the anaerobic reactor.

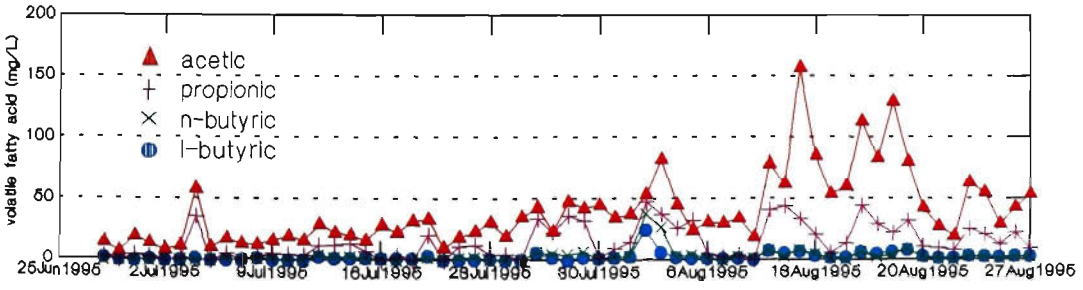

Figure 6-23 The concentrations of C2-C4 fatty acids in the 115E Anaerobic Reactor.

points on the cover pressure which control when the blowers extract gas from beneath the cover. For the first three weeks the cover pressure was kept within a tight band around 0 mm H_2O (Figure 6-22). Later, the cover pressure fluctuated considerably more. The temporary storage of gas under the cover could have attenuated the weekly cycle in gas production.

The other distinctive feature in the residuals is that there appeared to have been downward shift in the level of the residuals in early August which persisted till late August, i.e., the model tended to overestimate methane production during this period . This was possibly related to the increase in fatty acids during this time (Figure 6-23) which in turn appeared to coincide with a trough in the temperature of the reactor (Figure 6-17) and an increase in the raw sewage flowrate to the reactor (Figure 6-7). The raw sewage flowrate was increased on July 28 in an attempt to control nitrification in the later ponds of the lagoon. The accumulation of fatty acids during this period apparently signalled the imbalance in the microbial populations which led to lower than expected methane yields. If process regulation was to be used to control the methane production rate, feedback control would likely need to be included in order to reduce the remaining disturbance not accounted for by the other variables.

6.4 CONCLUSION

An empirical model was developed in order to identify the variables which affect methane production in the 115E anaerobic reactor and to establish whether

a feedforward-feedback control scheme could be applicable to the control of the 115E reactor.

The important variables found in this study to influence methane production were the raw sewage flowrate (or hydraulic residence time), the COD concentration and the temperature of the reactor. The raw sewage temperature, which influences the reactor temperature, has an annual cycle and can vary by 6° over a year. The raw sewage COD and temperature also show weekly seasonality which is probably a function of industrial waste discharges to the sewerage system.

The model was dynamic in the sense that it included lagged terms for both the dependent and independent variables and, interestingly, it seemed that there was a lag of one day before the COD concentration began to exert its effect on methane production. This could be due to the reasonably high proportion of suspended organic matter in the raw sewage and the slower dynamics of hydrolysis. The percentage ratio of particulate COD to total COD is approximately 60% in the raw sewage. A more intensive investigation of the daily pattern in volatile fatty acid concentrations (e.g., by taking hourly samples), as a function of COD loading, might shed more light on the dynamics of methane production.

It was interesting to note that methane yields were lower than expected (i.e. methane production was overestimated by the model) when there was an accumulation of volatile fatty acids (mainly acetic and propionic). This

exemplifies the fact that acetic acid and propionic acid are useful indicators of optimal reactor performance.

Other variables in the study included the raw sewage pH, and the concentrations of protein, carbohydrate, oil & grease, calcium ion, sulphate ion and potassium ion. Measuring protein, carbohydrate and oil & grease offered no advantage, over the aggregate measure of COD, in terms of predicting methane production rates. Neither the pH or concentrations of inorganic ions appeared to influence methane production. Whilst calcium ion and sulphate ion were found to effect methanogenesis in Chapter 5, no effect could be discerned over the range of concentrations observed in the raw sewage.

The fact that there is a relationship between methane production and the raw sewage flowrate, COD concentration and reactor temperature suggests that methane production could be controlled at some target value by manipulating the hydraulic loading rate to compensate for disturbances caused by the raw sewage COD concentration and reactor temperature. A study of the residuals from the model, however, revealed that other disturbances may be at work and so a combined feedforward/feedback control scheme may be necessary to keep methane production on target.

In practice it may be more sensible to control the reactor's effluent COD concentration rather than the methane production rate. The methane captured under the cover can be temporarily stored, and later used to generate electricity on site, when Powercorp's electricity charges are at their peak. There is no need, therefore, to supply the generators with a constant feedrate of methane (though,

there is a need to control the composition of the gas fed to the generators). In fact, under this scenario, it would not be possible to measure the daily methane production rate. The purpose to controlling the reactor's performance is to ensure that conditions are optimal for methane production (and, therefore, COD removal) and to reduce the variability in the COD concentration of the reactor's effluent, which undergoes further treatment in an aerated pond. A reduction in the variability of the reactor's effluent composition should (though, it is still to be established) translate into a more even aeration intensity in the next pond and a more consistent performance of the lagoon overall. Various strategies for controlling reactor performance, including process regulation and statistical process control, will be explored in more detail in the next chapter.

7. Control of Anaerobic Ponds

7.1 INTRODUCTION

Process monitoring and *process regulation* (to use the terminology of George Box[104]), discussed in Section 2.4, are two techniques available to the process engineer or operator for the control of wastewater treatment plants (WWTPs). Process monitoring is applicable when it is feasible to maintain a process in a state of statistical control without continual adjustment. A state of statistical control implies stable random variation about the target value, which could be a fixed mean level or seasonal pattern, due to numerous "common" causes whose identities are unknown. Process regulation, on the other hand, is applicable when the causes of variation are "uncontrollable", like the composition of raw sewage or the weather (temperature), and the process tends to wander from target if continual adjustments are not made.

Process monitoring, also known as statistical process control (SPC) uses control charts to maintain a process in a state of statistical control. Process monitoring involves the detection of process upsets using control charts, and the subsequent search for and elimination of the "assignable" (or special) cause(s) of variation. In a WWTP setting, identification and elimination of assignable causes will reduce variability in effluent composition and, moreover, will lead to a greater understanding that will ensure better management of the process or process inputs in the future.

Process regulation compensates for the effects of uncontrollable variables by estimating the disturbance ahead of time and adjusting the process (e.g. hydraulic residence time) accordingly. Various process regulation methods are available including mechanistic models coupled to an extended Kalman Filter, linear adaptive control and nonlinear adaptive control, which have been discussed by Weiland and Rozzi[105] in the context of anaerobic digestion control.

One of the criticisms of process regulation is that it can conceal the nature of the compensated disturbance, thereby eliminating the opportunity to learn about and improve the process. As Box and Kramer[49] point out, however, this does not have to be the case. A process which must be adjusted to compensate for uncontrollable disturbances may exhibit patterns in the control action or large deviations from target that arise from assignable causes. In a WWTP, for example, the pattern of flow control action may be observed to mirror a certain inhibitory chemical in the raw sewage. If a causative relationship was established then the control system could be changed by reducing the concentration of that chemical (via trade waste regulation), or if this was not feasible, by measuring the chemical and compensating for it by appropriate feedforward control. Similarly, large deviations from target, after feedforward-feedback control, may indicate a fault in the flowmeter, for example.

Box and Kramer[49] noted, however, that deviations from the control model may be blurred and special causes more difficult to detect when the process is improperly tuned, i.e. when the model's parameters are inaccurate. To assist the detection of special causes it may be both possible and desirable, in certain

circumstances, to use both process regulation and SPC. For example, with anaerobic digestion, feedforward-feedback control of the effluent COD could be achieved using a transfer function-noise model with the raw sewage COD, flowrate and temperature as inputs. To check for special causes of variation, control charts could be developed for one or more of the common response variables such as volatile fatty acid concentration or gaseous hydrogen concentration.

In the case where a digester has fast dynamics, such as a heated digester with a short hydraulic residence time, and an imbalance could quickly lead to process failure, it seems desirable to use process regulation. In the case of anaerobic ponds, however, the choice between process monitoring and process regulation is not so clear and depends on whether the operator accepts the existence of a weekly and annual seasonal pattern as normal process variability, or whether there is some reason for needing the process to conform to some other constraint such as a fixed mean level. The objective of this chapter is to explore the feasibility of process regulation and the application of process monitoring to sewage treatment in anaerobic reactors at Western Treatment Plant. The information gleaned from the exercise can answer the questions of how valuable a control system would be, how complex it needs to be, and how urgently it is required. As noted by Berthouex and Hunter et. al.[106], such an analysis might indicate that funds could be more profitably spent on augmenting the treatment plant or upgrading to a newer technology, rather than on process monitoring or installing an elaborate control system. In addition, the use of statistical process

control methods in the laboratory is explored, particularly in relation to instrumental analyses where successive measurements of control standards are affected by intraclass correlation and the usual methods for estimating the variance and setting control limits are deficient. A poorly controlled measurement process can adversely affect any process control scheme (as noted in Section 6.2.2.2).

7.2 MATERIALS AND METHODS

7.2.1 Statistical Analyses

Data analyses were performed using Systat[99,100] and Microsoft Excel version 5.0[107].

7.2.2 Sampling Methods

7.2.2.1 Raw sewage

Refer to Section 6.2.2.1.

7.2.2.2 Digester gas from the 115E Anaerobic Reactor

Refer to Section 6.2.2.2.

7.2.2.3 Sludge from the 115E Anaerobic Reactor

Sludge samples were taken from sampling port 8 on the 115E Anaerobic Reactor, which corresponded to the peak zone of anaerobic activity (see Chapter 4), using the procedure and sludge sampler described in Section 4.2.1.

7.2.2.4 Effluent from the 115E Anaerobic Reactor

Effluent samples were taken at the end of the HDPE cover using the sludge sampler described in Section 4.2.1. Whole column samples were taken from the water's surface to the top of the sludge layer.

7.2.3 Analytical Methods

The **chemical oxygen demand** (COD) was measured according to Method APHA 5220 B (Open Reflux Method) from *Standard Methods for the Examination of Water and Wastewater* (APHA: USA, 18th ed., 1992).

pH was measured with a Hanna Instruments pH probe (model HI 1332) and an Orion 940 Expandable Ionanalyzer pH meter according to Method APHA 4500-H^+ (pH Value) from *Standard Methods for the Examination of Water and Wastewater* (APHA: USA, 18th ed., 1992)

Temperature was measured with a thermocouple and Hanna HI 9023 pH meter.

Electrode potential was measured with a Metrohm ORP combination electrode. The probe uses a Ag/AgCl/c(KCl)=3M reference electrode. The half-

cell potential of the reference electrode is +208 mV at 25°C. The measured EP values given in this chapter can be approximately scaled to the Standard Hydrogen Electrode by adding +208 mV.

Volatile Solids were determined gravimetrically according to Method 2540C from *Standard Methods for the Examination of Water and Wastewater* (APHA: USA, 18th ed., 1992).

Alkalinity was measured according to Method 2320 from *Standard Methods for the Examination of Water and Wastewater* (APHA: USA, 18th ed., 1992).

Total volatile fatty acids was measured by colorimetry according to *HMSO Analysis of Raw, Potable and Waste Waters 1972 (Volatile Acids).*

Individual volatile fatty acids were measured by gas chromatography according to *HMSO Methods for the Examination of Waters and Associated Materials 1979 (Determination of volatile acids in sewage sludge).*

Methane, carbon dioxide and **hydrogen** were analysed by gas chromatography. A Varian 3400 GC, equipped with a Thermal Conductivity Detector and 12′ × 1/8″ stainless steel column packed with Haysep-Q. The column temperature was 30°C and the carrier gas was argon (@ 15 $mL.min^{-1}$). Calibration was carried out using a special gas mixture (purchased from BOC Gases) that contained:

Methane	79.3±0.2 %
Carbon dioxide	10.3±0.2 %

Hydrogen	104±4 ppm
Oxygen	0.998±0.02 %
Nitrogen	9.4% (by difference)

Samples of gas to be analysed were transferred to a 0.5 mL (approx.) gas sampling loop on the GC by displacing the gas in the gas sampling bulb with an acidified gas-displacement liquid (refer to Method APHA 511 from *Standard Methods for the Examination of Water and Wastewater* (APHA: USA, 15th ed., 1980)).

7.3 RESULTS AND DISCUSSION

7.3.1 Process Regulation

Process regulation involves the study of the dynamic relationships between the inputs to a system and the outputs, or quality characteristics. This relationship is known as the transfer function and it can be used to formulate the minimum mean square error (MMSE) control equation. The control equation tells the operator how much to adjust the *controllable* input, given the history of disturbances in the output and the history of inputs to the system, in order to keep the process on target.

In the case of wastewater treatment in the 115E Anaerobic Reactor, the quality characteristic of interest was the effluent soluble COD (ESCOD) concentration and the control variable was the raw sewage flowrate (RFLOW) to the 115E Lagoon. Other inputs to the system known to affect the effluent SCOD

included the raw sewage COD (RCOD) concentration and the water temperature (PTEMP) in the Reactor (see Chapter 6). Neither of these are controllable but they may be used to improve the performance of the control system.

Note that the raw sewage flowrate to the Plant cannot easily be controlled, but the controlled distribution of the flow to lagoons and filtration systems within the Plant is possible. Also notice that SCOD was used instead of COD. This was due to the difficulty in obtaining a representative sample of the suspended matter exiting the Reactor.

The transfer function, describing the system's dynamics, can be identified from the impulse response function and/or the frequency response function for the system. Whilst the impulse response function is estimated relatively easily in the time domain for a single input-single output system, using the method described by Box and Jenkins[45], the solution is not as simple for multiple input-output systems[108]. In this study, frequency domain analysis was used to first estimate the frequency response function of the 115E Reactor. The impulse response function was then obtained by taking the inverse Fourier transform of the frequency response function. Both were then used to identify the transfer function model.

7.3.1.1 Nonlinear transfer functions and linearisation

In practice, most processes are modelled by nonlinear differential equations for which there is no analytical solution. By nonlinear, it is meant that the differential equation contains parameters that are a function of the dependent

variable. When faced with a nonlinear dynamic system the options available include simulation of a theoretical model on a computer and computing the solution numerically, or making assumptions about the range of operating conditions experienced that allow the dynamics of the process to be approximated by a linear model. The linear assumption can be checked if theoretical models are available to examine the relationships between the dependent and independent variables.

Beginning with the relationship between effluent COD and raw sewage flowrate, the steady state mass balance model for a first order reaction and continuously stirred tank reactor is given by:

$$QS_0 = kVS_1 + QS_1 \qquad \textbf{Equation 7-1}$$

where Q=flowrate to reactor≈60 ML/d

S_0=raw sewage COD concentration≈900 mg/L

S_1=effluent COD concentration≈450 mg/L (assuming 50% removal)

V=volume of reactor≈90 ML

k=rate constant for COD removal=5-12 d^{-1} for methanogenesis from acetate[26]

If the equilibrium of the system is disturbed by increasing the mass loading to $(Q+X_1(t))S_0$ then the effluent COD will be changed to $S_1+Y(t)$. Now, the rate of COD consumption, $kV(S_1+Y(t))$, no longer balances the rate of feed and the rate of change of the COD concentration in the reactor is given by:

$$V\frac{dY(t)}{dt} = (Q+X_1(t))S_0 - (Q+X_1(t))(S_1+Y(t)) - kV(S_1+Y(t)) \qquad \textbf{Equation 7-2}$$

Using Equation 7-1 and rearranging Equation 7-2 gives:

$$(kV + Q + VD)Y(t) = X_1(t)(S_0 - S_1 - Y(t))$$

or $$(1 + TD)Y(t) = g_1\left(1 - \frac{Y(t)}{S_0 - S_1}\right)X_1(t)$$ **Equation 7-3**

where $D = d / dt$ $\quad T = \frac{V}{kV + Q}$ and $\quad g_1 = \frac{S_0 - S_1}{kV + Q}$

Equation 7-3 is a nonlinear differential equation because it contains a term $X_1(t)$ multiplied by $Y(t)$, i.e. the gain depends on the level of the output $Y(t)$. If, however, $(S_0\text{-}S_1) >> Y(t)$ then the factor $1\text{-}Y(t)/(S_0\text{-}S_1)$ is approximately unity and the system can be reasonably represented by a linear dynamic model. In the case of the 115E Anaerobic Reactor, the percentage removal of COD is about 50% (from 880 mg/L to 440 mg/L) and the fluctuation in the percentage removal would be about ±10%. The factor $1\text{-}Y(t)/(S_0\text{-}S_1)$ would therefore vary between 0.8 and 1.2. A linear approximation may not perform well in this circumstance.

In the case of the relationship between the effluent COD concentration and the raw sewage COD concentration, if the raw sewage COD mass loading was changed to $Q(S_0+X_2(t))$, the effluent COD concentration would change to $S_1+Y(t)$. Now the rate of consumption of COD would be $kV(S_1+Y(t))$ and the rate of change of the effluent COD would be given by:

$$V\frac{dY(t)}{dt} = Q(S_0 + X_2(t)) - Q(S_1 + Y(t)) - kV(S_1 + Y(t))$$ **Equation 7-4**

which can be rearranged, using Equation 7-1, to give:

$$(1 + TD)Y(t) = g_2 X_2(t)$$ **Equation 7-5**

where $T = \frac{V}{kV + Q}$ and $\quad g_2 = \frac{Q}{kV + Q}$

However, according to the Monod equation (see Section 2.3), the rate constant k is dependent on the COD concentration:

$$k = \frac{(S_1 + Y(t))}{K_s + (S_1 + Y(t))} k_{max} \qquad \textbf{Equation 7-6}$$

If it is assumed that methanogenesis from acetate is the rate determining step, K_s can range between 20-400 mg/L acetate (which is approximately equivalent to 20-400 mg/L COD). Given that the reactor acetate concentration is less than 100 mg/L, it cannot be reasonably stated that $(S_1+Y(t))>>K_s$. Therefore, again, a linear approximation may not be appropriate.

The relationship between effluent COD and temperature stems from the dependence of the rate constant on temperature. If a change in the temperature causes a change in the rate constant from k_{20} to $(k_{20}+k(t))$, and the effluent COD to $(S_1+Y(t))$, then the rate of change in effluent COD will be given by:

$$V\frac{dY(t)}{dt} = QS_0 - Q(S_1 + Y(t)) - (k_{20} + k(t))V(S_1 + Y(t)) \qquad \textbf{Equation 7-7}$$

Using the relationship $k=k_{20}\theta^{(Temp-20)}$ and Equation 7-1, Equation 7-7 can be rearranged to give:

$$(1 + TD)Y(t) = g_3\left(1 + \frac{Y(t)}{S_1}\right)\theta^{(Temp(t)-20)}$$

$$\text{where } T = \frac{V}{k_{20}V + Q} \quad \text{and} \quad g_3 = \frac{-VS_1}{k_{20}V + Q}$$

Equation 7-6 is nonlinear in the parameters and in the variables. In the case of the variables, this theoretical analysis suggests that the temperature should be transformed using $\theta^{(Temp-20)}$, with a value of 1.085 for θ being reported for

domestic sewage. In the case of the parameters, the factor $Y(t)/S_1$ could be as high as 0.2 and a linear approximation may not be suitable in this case.

The preceding theoretical analysis has indicated that the time constant for the system could lie between 0.1-0.2 d and the gains could be 0.4 to 0.9, 0.05 to 0.1 and -3.5 to -8 for the flowrate, raw sewage COD and reactor temperature (or -35 to -80 for $\theta^{(Temp-20)}$), respectively. Therefore, the variability in raw sewage COD could be expected to produce a change of ±15 mg/L in the effluent COD concentration, and the variability in temperature could produce a change of ±6 mg/L. A change in flowrate of 10 ML/d, however, would only change the effluent COD concentration by ±2 mg/L. This suggests that rather large flow manipulations would be required to compensate for disturbances caused by fluctuations in raw sewage COD concentration and reactor temperature.

The implication for the anaerobic reactors at WTP, is that a control equation based on linear dynamics may not be appropriate and, in any case, there may be insufficient capacity within the Plant to allow process regulation of the effluent COD. An empirical analysis of the dynamic behaviour of the 115E Anaerobic Reactor, however, is required to confirm these findings.

7.3.1.2 Orders of the dynamic relationships

Theoretical models and nonequilibrium mass balances can be used to study the order of a dynamic relationship, as well as its linearity. For example, methanogenesis is usually considered to be the rate determining step in the

anaerobic digestion process and the behaviour of the system is well represented by a first order dynamic relationship. However, if other steps in the process proceed at a comparable rate, then the system may display higher order characteristics.

Assuming that hydrolysis of organic polymers and methanogenesis from acetate were of comparable rates then the treatment of the sewage could be represented by a two stage process:

$$A \xrightarrow{k_a} B \xrightarrow{k_b} C$$

where A is the organic polymer, B is acetate and C is methane.

Under steady state conditions, and assuming first order reactions, the rate at which polymer is entering the reactor must balance the rate at which it is leaving:

$$QA_0 = k_a V A_1 + QA_1 \qquad \textbf{Equation 7-8}$$

If the mass loading of organic polymer is changed to $Q(A_0+X_a(t))$ then the effluent concentration changes to $A_1+Y_a(t)$ and the rate of polymer degradation becomes $k_aV(A_1+Y_a(t))$. The rate of change of polymer in the reactor is then given by:

$$V\frac{dY_a(t)}{dt} = Q(A_0 + X_a(t)) - Q(A_1 + Y_a(t)) - k_a V(A_1 + Y_a(t))$$

which, after rearranging and using Equation 7-8, can be written:

$$(1 + T_a D)Y_a(t) = g_a X_a(t) \qquad \textbf{Equation 7-9}$$

where $T_a = \dfrac{V}{k_a V + Q}$ $\qquad$ $g_a = \dfrac{Q}{k_a V + Q}$

Now, with respect to acetate, the steady state relationship is:

$$k_a V A_1 = k_b V B_1 + Q B_1 \qquad \textbf{Equation 7-10}$$

With the concentration of the feed being changed to $A_1+Y_a(t)$, the concentration of acetate becomes $B_1+Y_b(t)$ and the rate of acetate degradation $k_bV(B_1+Y_b(t))$. The rate of change of acetate is therefore given by:

$$V\frac{dY_b(t)}{dt} = k_a V(A_1 + Y_a(t)) - k_b V(B_1 + Y_b(t)) - Q(B_1 + Y_b(t))$$

which can be written:

$$(1 + T_b D)Y_b(t) = g_b Y_a(t) \qquad \textbf{Equation 7-11}$$

where $T_b = \dfrac{V}{k_b V + Q}$ $\qquad g_b = \dfrac{k_a V}{k_b V + Q}$

Substituting Equation 7-9 in Equation 7-11 gives:

$$(1 + \Xi_1 D + \Xi_2 D^2)Y_b(t) = gX_a(t) \qquad \textbf{Equation 7-12}$$

where $\Xi_1 = T_a + T_b$ $\Xi_2 = T_1 T_2$ $g = g_a g_b$

The rate of change of effluent COD will then be the sum of the rates of change of organic polymer and acetate and will display second order behaviour. Notice, from the preceding, that if $k_a >> k_b$ then Equation 7-12 approaches a first order differential equation.

7.3.1.3 Identification and fitting of the transfer function-noise model

Three months worth of daily data were collected on the 115E Reactor in the course of normal operation (Appendix B). Time series plots of the inputs and output from the reactor are given in Figure 7-1 to Figure 7-4. Plots of a variety of supplementary response variables, which will be reported further in the section on

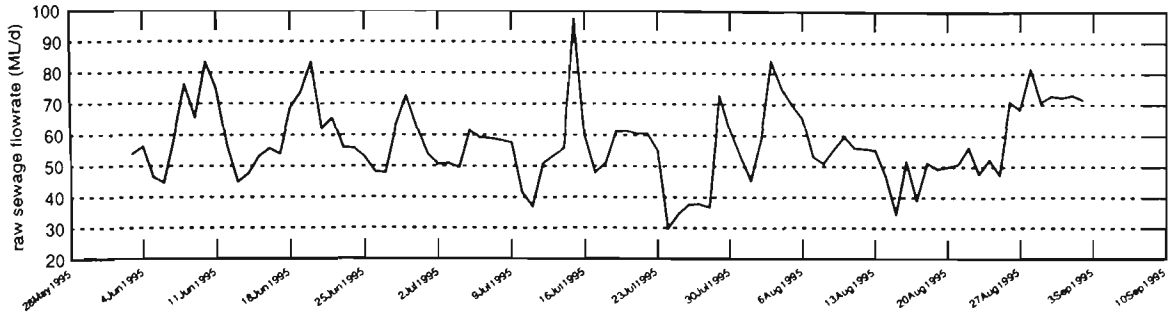

Figure 7-1 Raw sewage flowrate (ML/d)

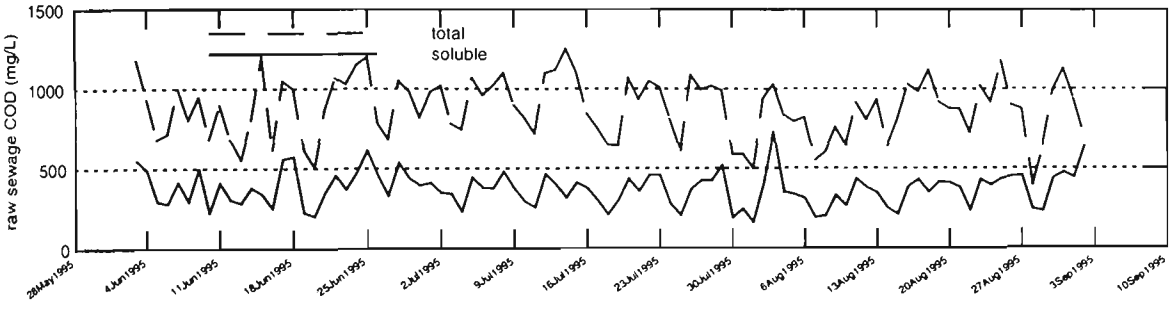

Figure 7-2 Total and soluble raw sewage COD (mg/L)

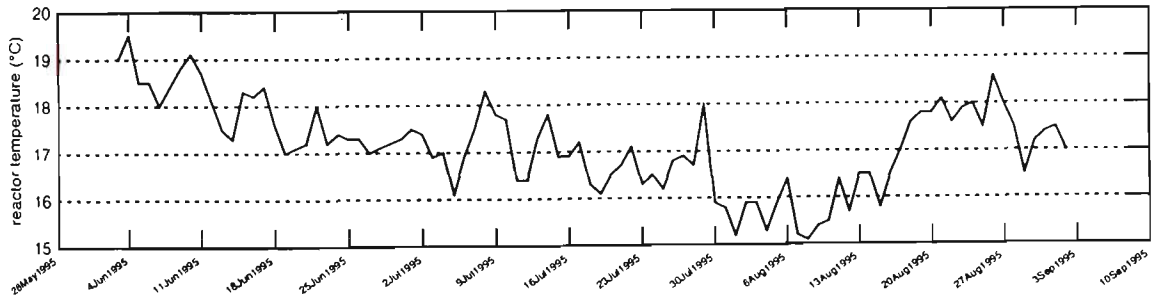

Figure 7-3 115E reactor temperature (°C)

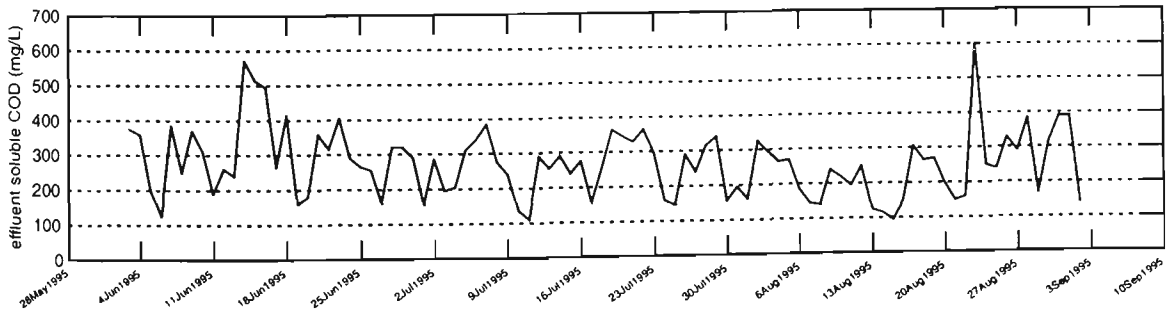

Figure 7-4 Reactor effluent soluble COD (mg/L)

process monitoring (Section 7.3.2), are given on p. 7-52 to 7-54. The time series plots were inspected for trends which could lead to spurious coherencies if not filtered out. The reactor temperature displayed an obvious trend which suggested that the cross spectral analysis should be carried out using the differenced series.

Similarly the sample auto- and cross correlation functions indicated that the reactor temperature was nonstationary and that a first regular difference should be applied to all variables. The differenced auto- and cross correlation functions are used to determine the shift values for alignment and possible truncation points for future spectral calculations.

Alignment is used to minimise the bias that can occur in the estimation of coherency spectra, and to a lesser degree the phase spectra, when there is large delay. Alignment consists of centring the cross correlation function so the largest correlation is at zero lag. The peaks in the cross correlation functions for PTEMP and ESCOD, and RFLOW and RCOD, indicated that shift values of -1 should be applied. However, there is no logical reason why these variables would be related at -1 lag and aligning the series' had little effect on the coherency spectra.

The next step was to choose three possible truncation points for the calculation of smoothed coherency spectra. One of the properties of the sample auto- and cross spectrum is that the variance of the estimates is independent of the sample size. Reducing the variance of the spectral estimator is achieved by an empirical *window closing* technique. Window closing involves splitting the series into a number of smaller series and estimating the sample spectrum for each sub-series. The mean of the spectral estimates for each sub-series is called

the *smoothed spectral estimate* at the frequency f. The resultant spectrum is called the *mean smoothed spectrum.*

The objectives in estimating spectra are *high fidelity* and *high stability.* Fidelity refers to the bias in the mean smoothed spectrum, high fidelity means small bias. High stability means small variance. Dividing the series into too many sub-series may result in high stability but low fidelity. The optimal solution is found empirically in the window closing procedure by first choosing a number of possible truncation points (usually three), which are determined from the sample auto- and cross correlation functions.

The sample auto- and cross correlation functions indicated that the correlations effectively died out after 8 to 46 lags. Four truncation points were therefore chosen corresponding to lags 8, 16, 32 and 50. Jenkins and Watts[108] recommend that the largest truncation point be at least four times the smallest in order to capture the optimal solution. After estimating the mean smoothed auto- and cross spectra using the four truncation points, it was decided that a truncation point of 32 would be used in the final estimation of the spectra. As shown in Figure 7-5, for the RFLOW autospectrum, the spectra tended to converge as the truncation point increased, or as the bandwidth decreased, and there was very little difference after L=32 which suggested that most of the detail in the spectrum had been revealed. Furthermore, the confidence interval at L=32 was small enough (i.e., relative to the peaks in the spectrum) to indicate that the fine detail can be trusted. The smoothed autospectra for RCOD, PTEMP and

The next step was to estimate the squared coherency, squared multiple coherency and partial coherency spectra, the residual spectrum, and gain and phase spectra. The formulae used to estimate these spectra are given in Appendix C.

The squared coherency spectra and the multiple and partial squared coherency spectra are given in Figure 7-9 and Figure 7-10. Coherency is the spectral analog of correlation. These figures show that there is high coherency, particularly in the frequency range 0.1 to 0.35 cpd, between the output, ESCOD, and the inputs RFLOW, RCOD and PTEMP. The three main groups of peaks at about 0.15 cycles per day (cpd), 0.2 cpd and 0.3 cpd are probably associated with

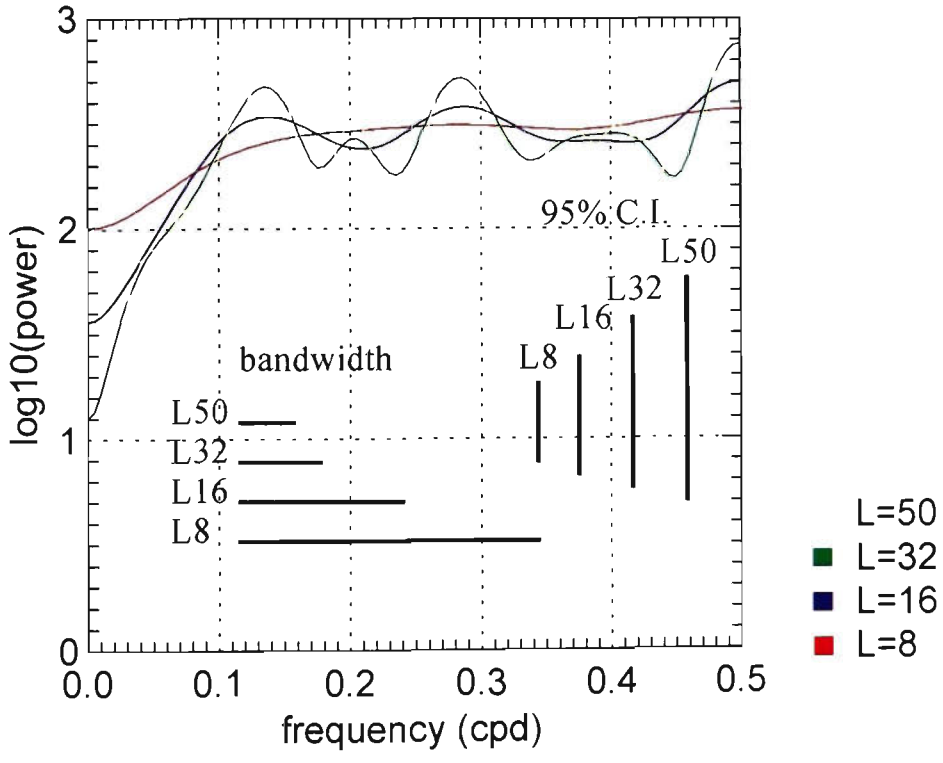

Figure 7-5 Mean smoothed autospectra for RFLOW using a range of truncation points (where cpd = cycles per day).

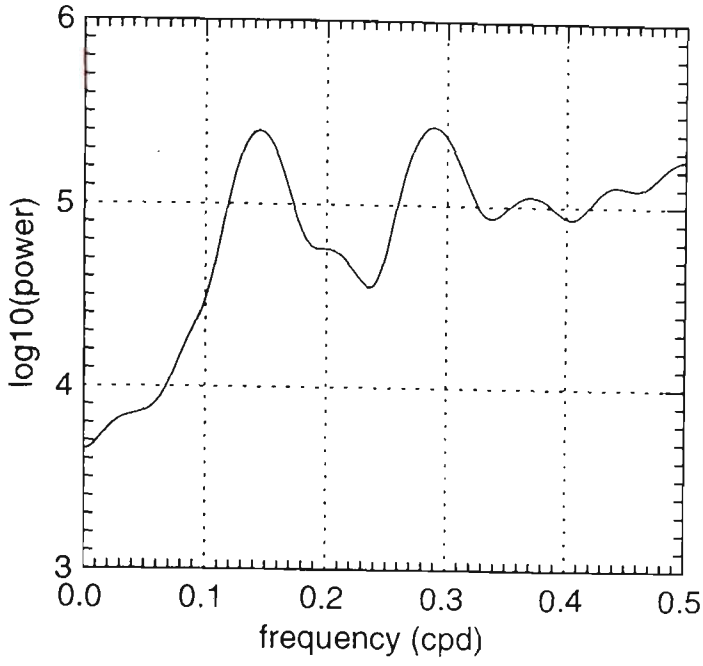

Figure 7-6 Mean smoothed autospectrum for RCOD.

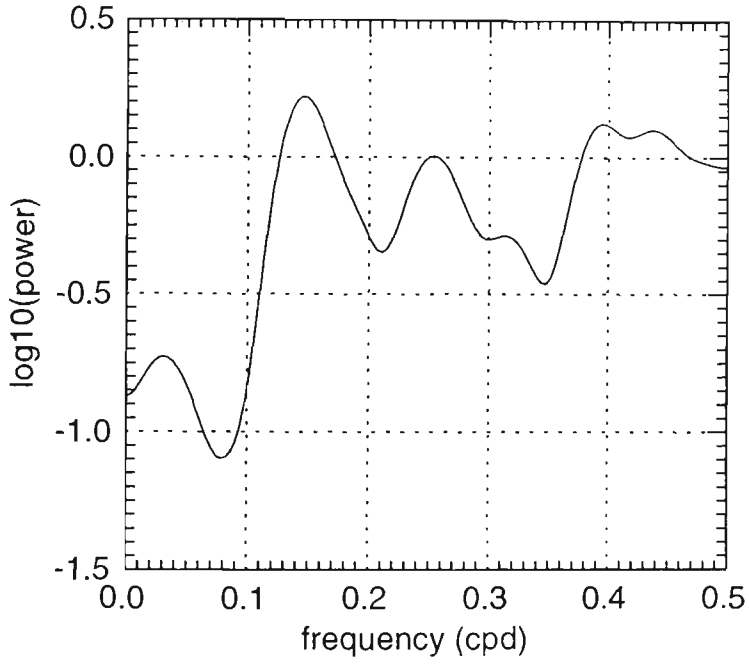

Figure 7-7 Mean smoothed autospectrum for PTEMP.

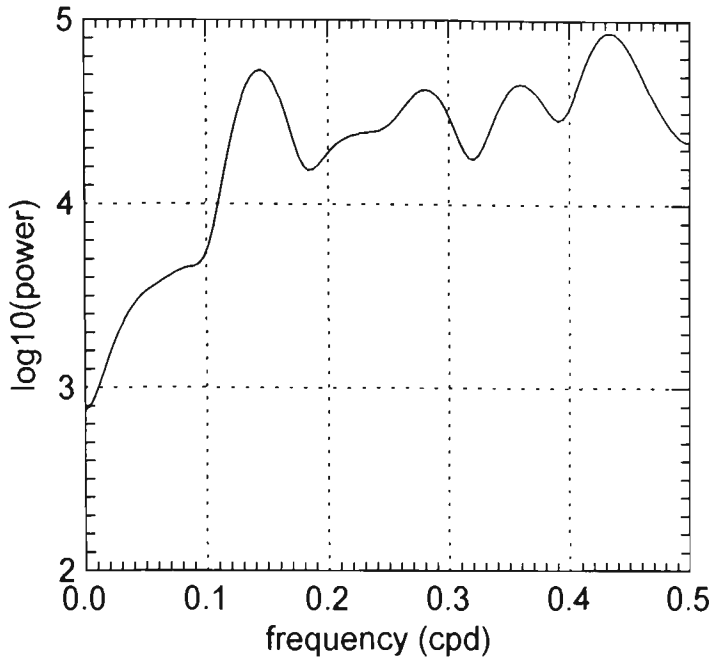

Figure 7-8 Mean smoothed autospectrum for ESCOD.

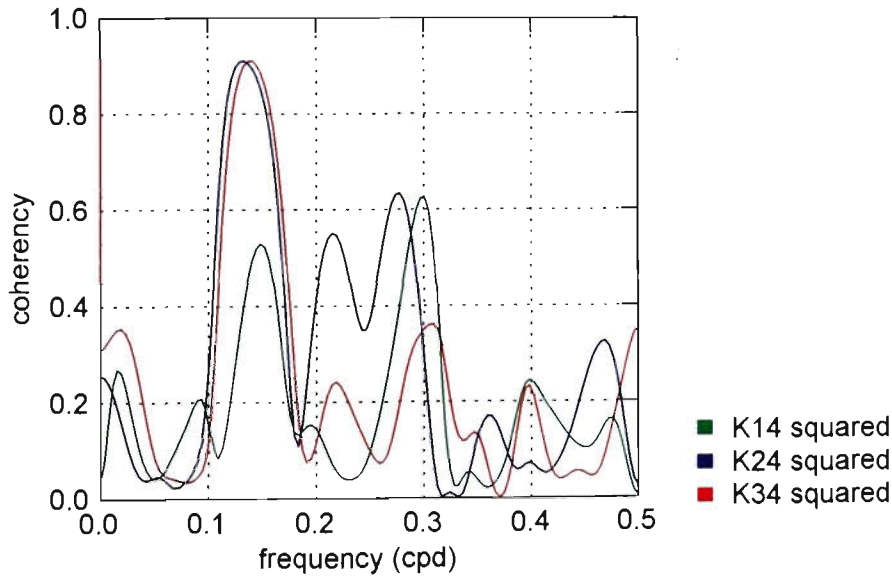

Figure 7-9 Squared coherency spectra where 4=ESCOD, 1=RFLOW, 2=RCOD and 3=PTEMP.

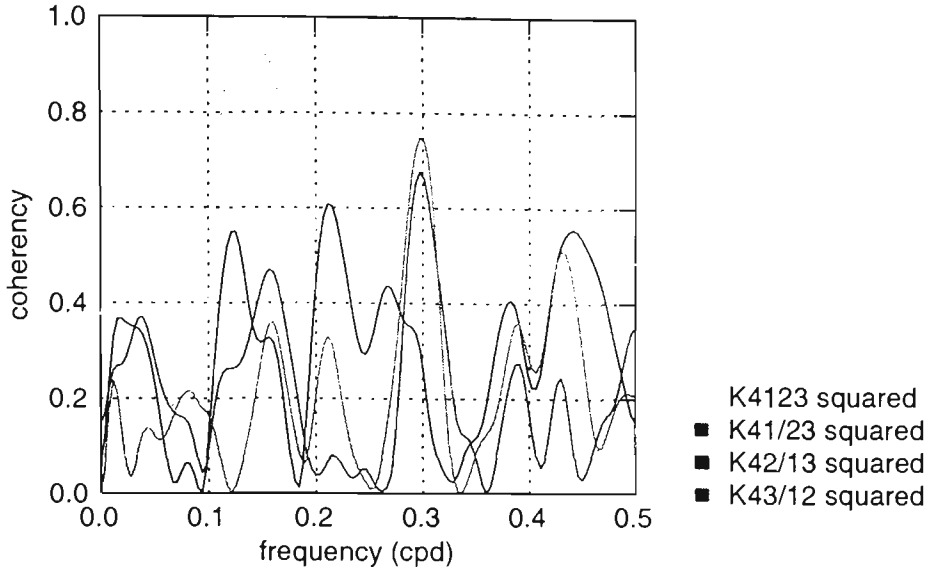

Figure 7-10 Multiple and partial squared coherency spectra where 4=ESCOD, 1=RFLOW, 2=RCOD and 3=PTEMP.

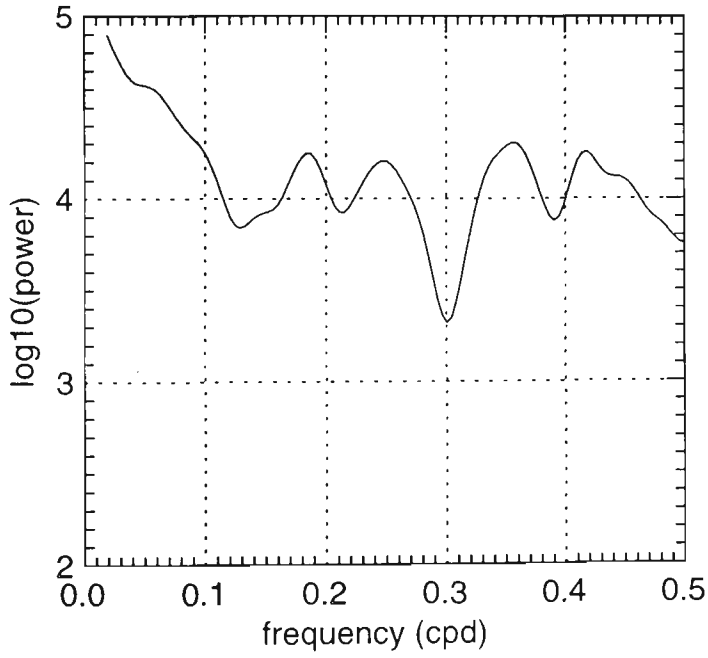

Figure 7-11 Residual or noise spectrum for the anaerobic reactor data.

industry cycles. These three groups of peaks are present in one or more of the autospectra of the inputs and all of the inputs contribute appreciably to the variance in the effluent SCOD. Interestingly, the three groups of peaks appear to represent different industries. The peak at 0.15 cpd in the multiple squared coherency spectrum has contributions from the flow, COD and temperature. The peak at about 0.2 cpd has contributions from flow and COD. The peak at 0.3 cpd has contributions from flow and temperature.

The residual or noise spectrum given as Figure 7-11 is reasonably flat and featureless which suggests that the noise is approximately random. This indicates that the main factors that influence the effluent SCOD have been included in the model. The spectrum in Figure 7-11 represents the original noise that was recovered from the filtered (or differenced) noise by dividing by the square of the gain for the difference filter[108], where the gain of the difference filter is equal to $2|\sin \pi f|$. The autocovariance function for the differenced noise, obtained from an inverse Fourier transform of the filtered noise spectrum, suggests that it follows an ARIMA(1,1,0) or ARIMA(0,1,2) process.

The frequency response functions are depicted by the gain and phase spectra shown as Figure 7-12 to Figure 7-17. The impulse response functions, and corresponding step response functions, were obtained by taking the inverse Fourier transform of the frequency response functions and are given as Figure 7-18 to Figure 7-23. The gain spectra have peaks at high frequencies which may signal the presence of nonlinearities. Alternatively, given that most of the power in the spectra are contained in two or three narrow bands, these peaks may be the

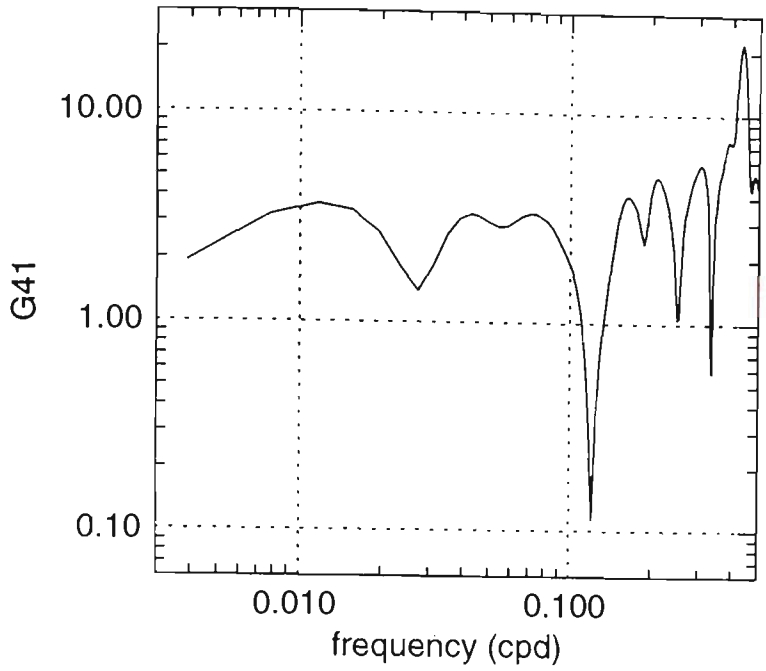

Figure 7-12 Gain spectrum for ESCOD and RFLOW.

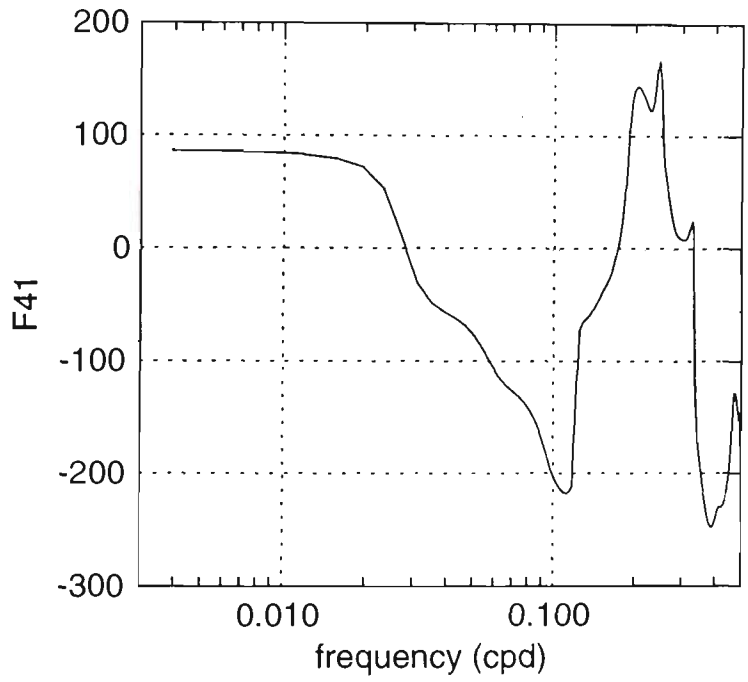

Figure 7-13 Phase spectrum for ESCOD and RFLOW.

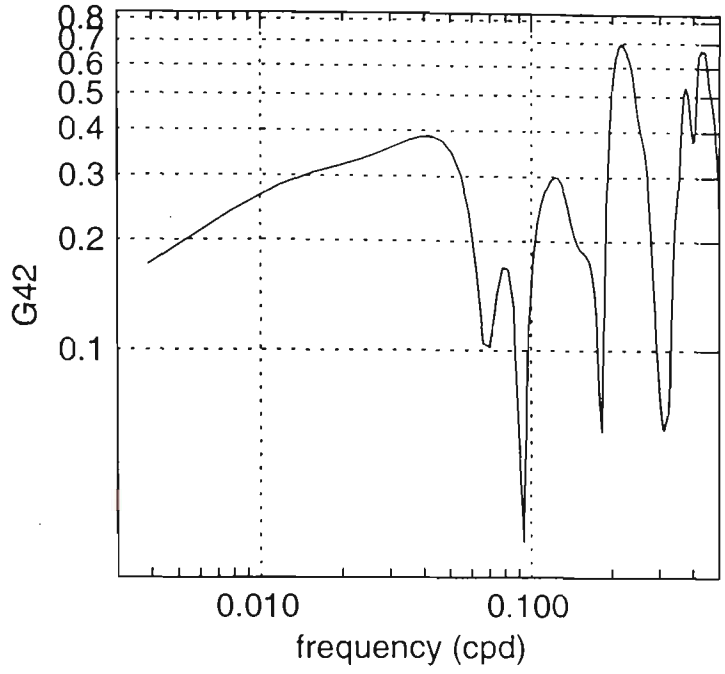

Figure 7-14 Gain spectrum for ESCOD and RCOD.

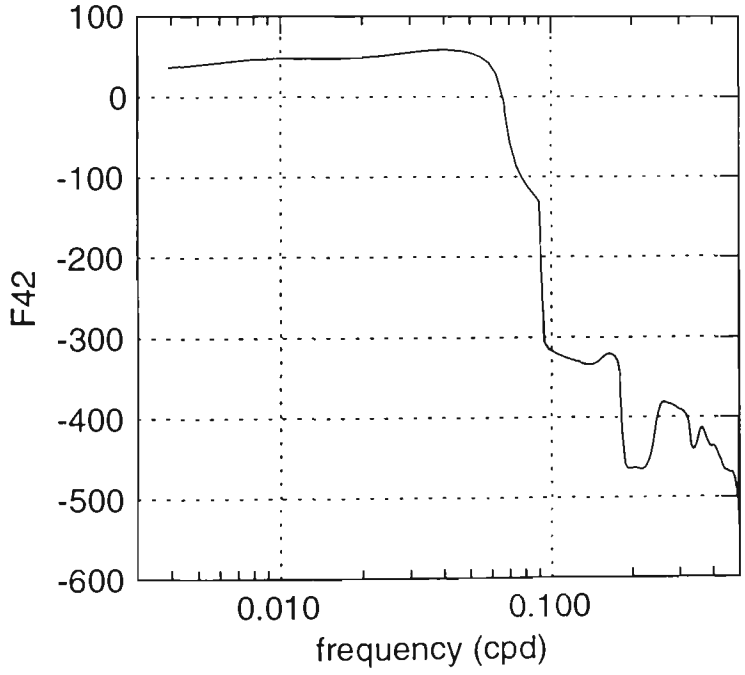

Figure 7-15 Phase spectrum for ESCOD and RCOD.

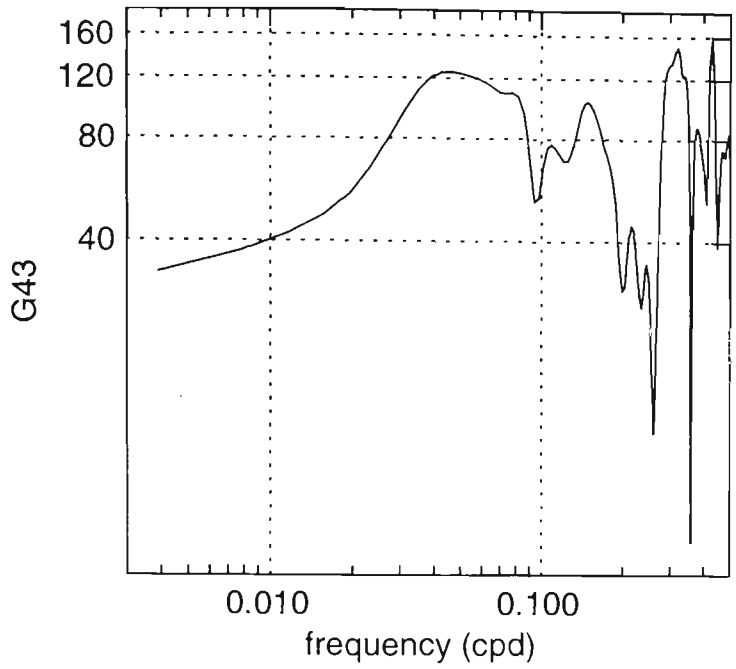

Figure 7-16 Gain spectrum for ESCOD and PTEMP.

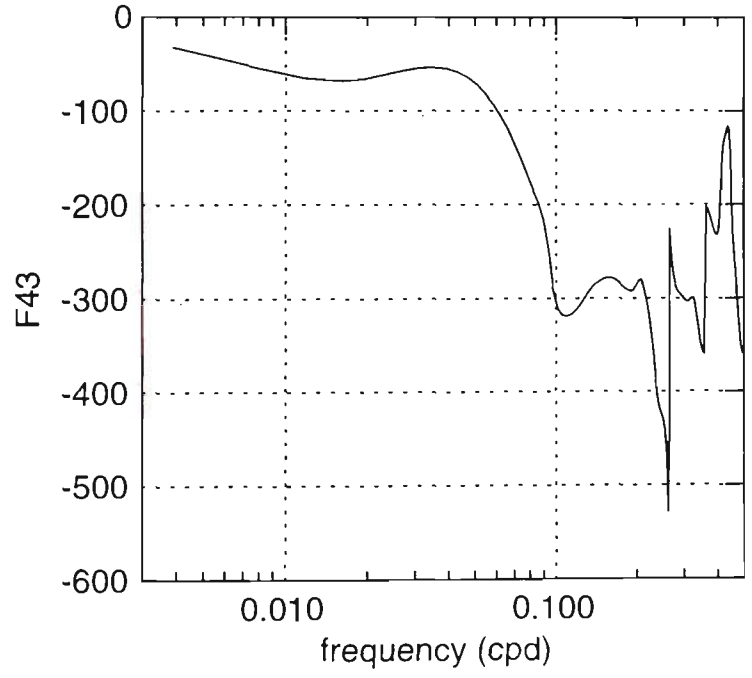

Figure 7-17 Phase spectrum for ESCOD and PTEMP.

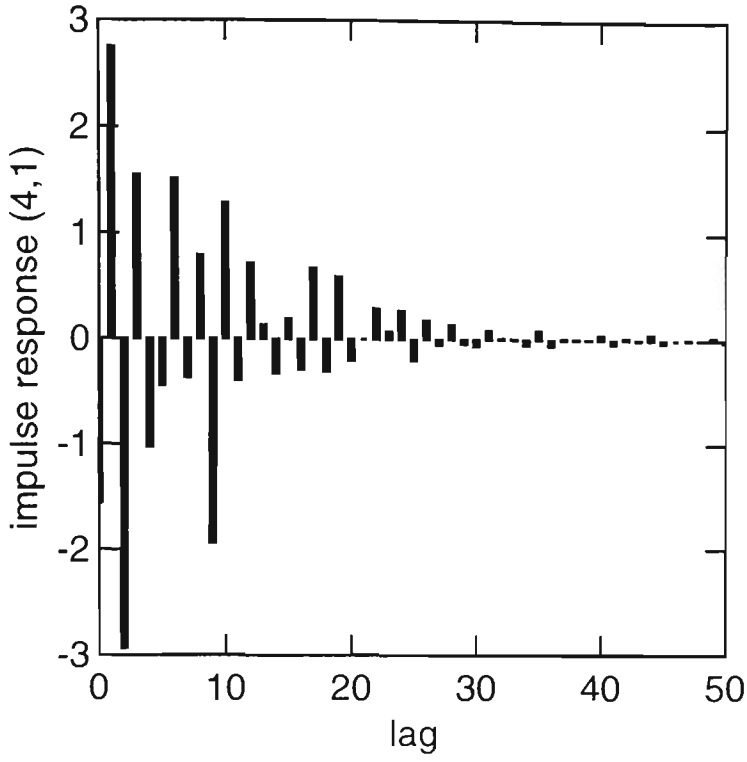

Figure 7-18 Impulse response function for ESCOD and RFLOW.

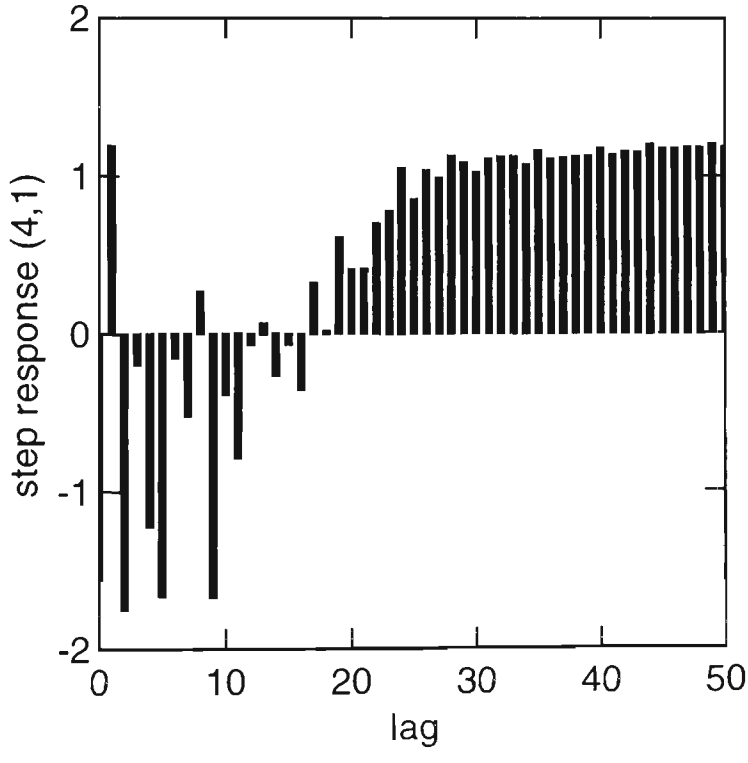

Figure 7-19 Step response function for ESCOD and RFLOW.

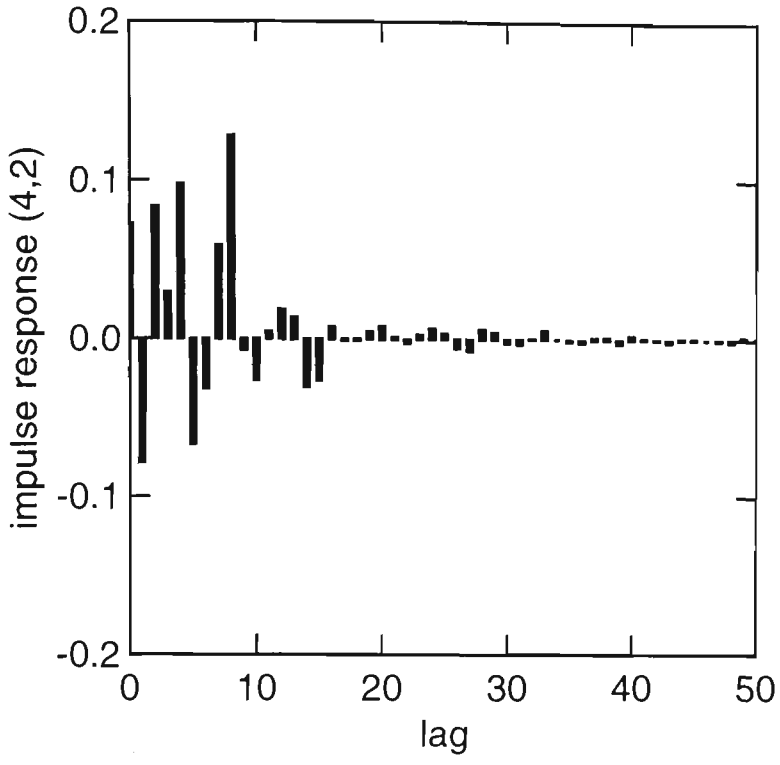

Figure 7-20 Impulse response function for ESCOD and RCOD.

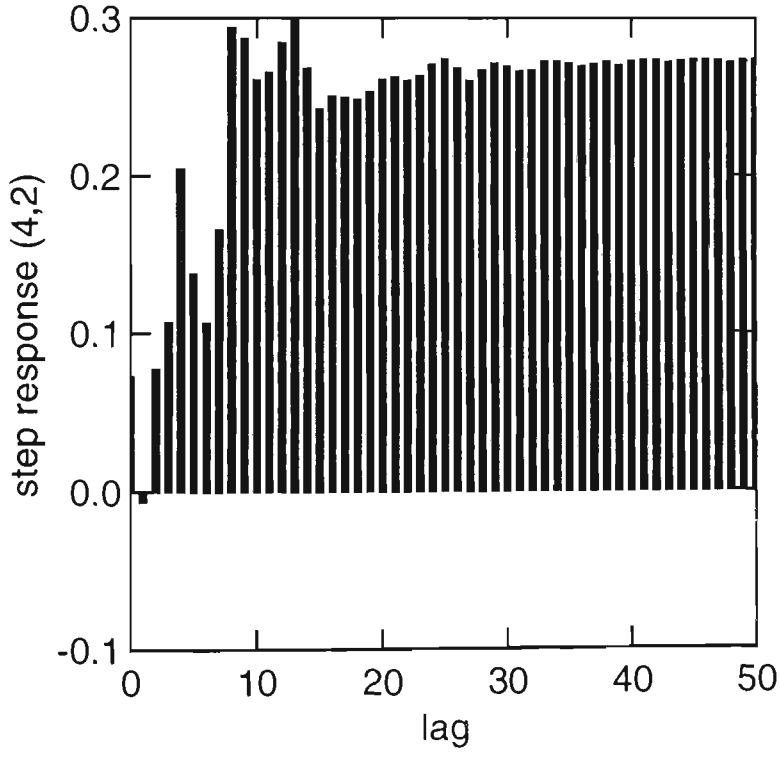

Figure 7-21 Step response function for ESCOD and RCOD.

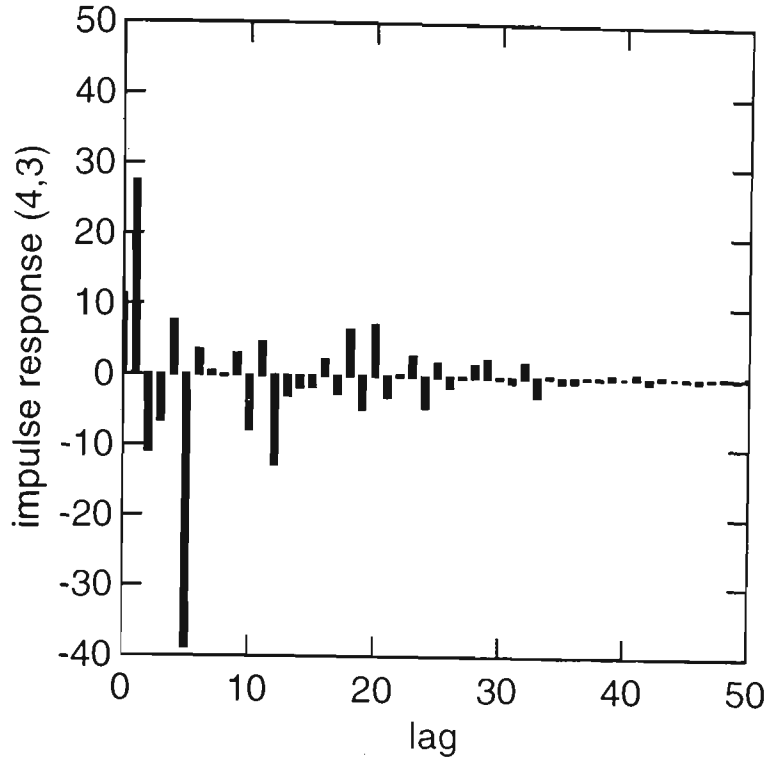

Figure 7-22 Impulse response function for ESCOD and PTEMP.

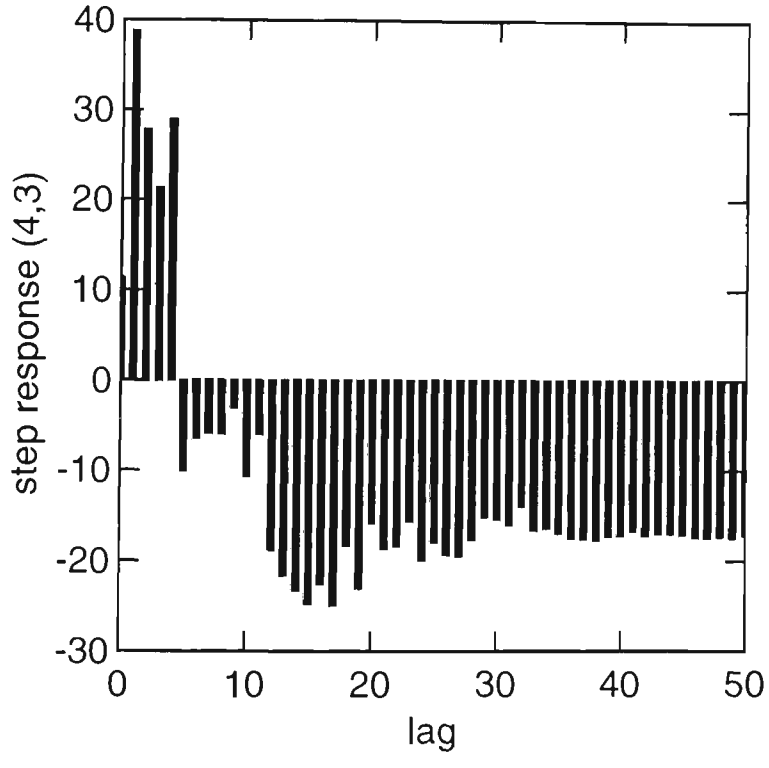

Figure 7-23 Step response function for ESCOD and PTEMP.

result of leakage from the spectral window. Leakage can cause errors in the spectral estimates where there is less power and affect the appearance of the gain and phase spectra and resulting impulse and step response functions. In retrospect, digitally filtering the data to remove power at frequencies outside the 0.1-0.35 cpd band may have helped to clarify the transfer function.

Of immediate interest from the step response functions are the steady state gains, i.e. the increase in effluent SCOD following a unit step increase in the inputs, which are approximately 1, 0.25 and -20 for RFLOW, RCOD and PTEMP, respectively. This suggests, for example, that a flow reduction of 20 ML/d would be required to compensate for a 1°C drop in temperature or an 80mg/L increase in raw sewage COD concentration. This, in turn, suggests that it may not be feasible to compensate for disturbances caused by temperature and raw sewage COD through manipulation of the flowrate. In addition, if it is assumed that the spectral estimates have not been greatly affected by leakage, the impulse and step response functions contain information that may be useful to understanding the mechanisms occurring within the anaerobic reactor. For example, the step response for raw sewage flowrate indicates that an increase in flow would initially cause a decrease in effluent SCOD followed by a sustained increase. The initial decrease may be the effect of turbulence or mixing, which would result in better bacteria-substrate contact. In the case of the water temperature, the step response suggests that an increase in temperature would initially produce an increase in effluent SCOD. This may result from an

increased release of soluble nutrients from the sludge due to an increased rate of bacterial action.

It was initially intended that the impulse and step response functions would be employed, following the procedure described by Box and Jenkins[45], for the preliminary identification of the discrete transfer function model and calculation of initial estimates for the model's parameters. However, this was made difficult, particularly for RFLOW and PTEMP, because of the number of large initial impulse response weights that did not appear to follow a pattern. An attempt was therefore made to identify the frequency response function from the gain and phase spectra and then use the parameter estimates (for gain, delay, time constant, etc.) to calculate starting values for the nonlinear estimation of the discrete model's parameters. The method described by Schwarzenbach and Gill[109] and Jenkins and Watts[108] was used to identify the transfer function in the frequency domain, using the gain and phase spectra (or Bode plots). Initial estimates of the parameters were then obtained by graphically fitting the model's to the gain and phase data. This was achieved by setting up a Microsoft Excel workbook that allowed various model's (e.g. simple gain, delay, single exponential or first order, second order and higher order models) and parameters to be tried out for a good visual fit. The Excel workbook also automatically calculated the impulse and step response functions by performing an inverse Fourier transform on the real and imaginary components of the frequency response function, thus allowing a confirmatory check of the transfer function in the time domain.

Like the impulse and step response functions, the Bode plots were quite complex and so the model fitting and checking process began with simple first (single exponential) or second (two exponentials in series) order models, possibly with one period of delay (i.e. a delay of one day). The identification process focused on the structure of the Bode plots in the vicinity of 0.14 and 0.3 cpd. as this was the region where the inputs generally had greatest power (see Figure 7-5 to Figure 7-7on p. 7-18 to 7-19). Initial estimates of the parameters of the discrete transfer functions were obtained using the known relationships between discrete and continuous models as given by Box and Jenkins[45].

From this graphical estimation process, time constants (T) of 1.1 d for first order models, or 1.1 d and 0.53 d for second order models were chosen. These time constants corresponded to corner frequencies of 0.14 and 0.3 cpd ($f = 1/2\pi T$), respectively. The gains were g_{41}=1.5, g_{42}=0.26 and g_{43}=-30. These parameter estimates were used to calculate the starting values for the nonlinear estimation of the parameters, which was carried out using the method of Box and Jenkins[45] and Microsoft Excel's *Solver* function. The noise model was identified according to the method of Box and Jenkins[45]. The fitted models were assessed in terms of the standard deviation of their residuals, their steady state gains and diagnostic checks on the residuals.

The results for four fitted models are presented in Table 7-1. Note that models with delay did not perform as well as models without delay and were omitted from Table 7-1. Diagnostic checks on each model indicated that the residuals were random, approximately normally distributed and independent of

Table 7-1 Fitted transfer function - noise models.

	Model			
Parameter	**1**	**2**	**3**	**4**
δ_{11}	-0.16	0.02	0.22	-0.71
δ_{12}	–	–	–	0.20
ω_{10}	1.34	1.12	0.88	0.70
ω_{11}	–	–	–	-0.40
δ_{21}	0.13	0.30	0.03	0.92
δ_{22}	–	–	-0.08	-0.47
ω_{20}	0.24	0.18	0.24	0.17
ω_{21}	–	–	-0.03	0.17
δ_{31}	0.654	1.03	0.72	0.64
δ_{32}	–	-0.78	-0.06	-0.99
ω_{30}	-15.14	2.22	-11.24	16.67
ω_{31}	–	21.60	5.62	2.51
ϕ	-0.517	-0.564	-0.49	–
θ	–	–	–	-0.58
b	0	0	0	0
g_{41}	1.16	1.14	1.14	0.69
g_{42}	0.28	0.26	0.26	-0.01
g_{43}	-43.74	-25.97	-49.602	10.47
σ_a	96.1	88.8	94.9	84.2

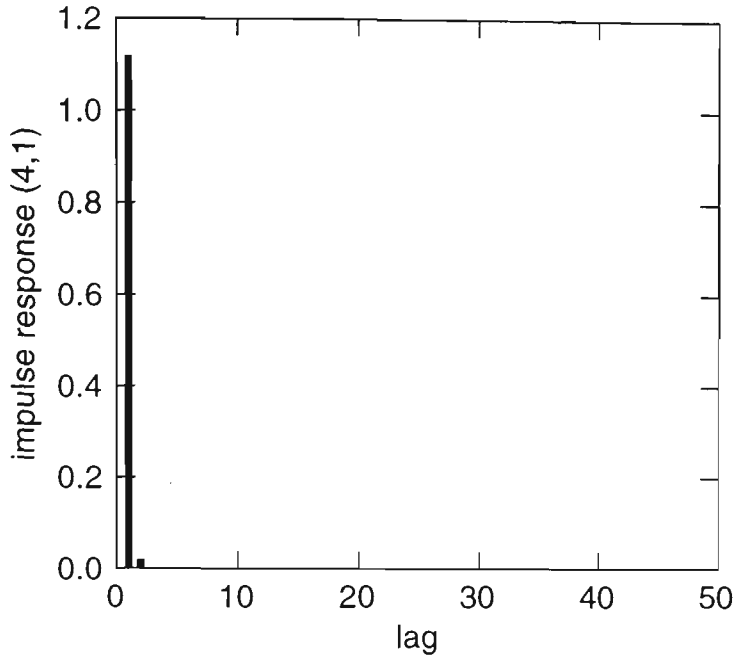

Figure 7-24 Model 2 impulse response function for ESCOD and RFLOW.

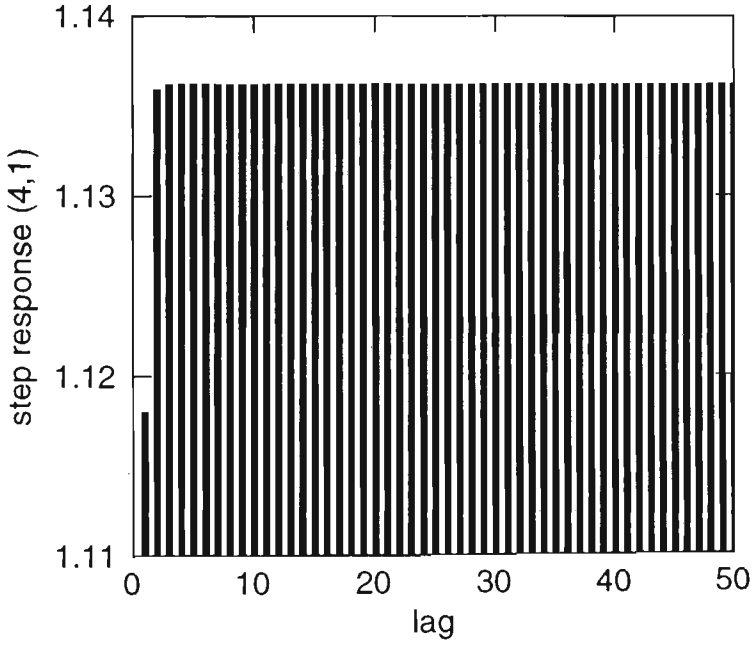

Figure 7-25 Model 2 step response function for ESCOD and RFLOW.

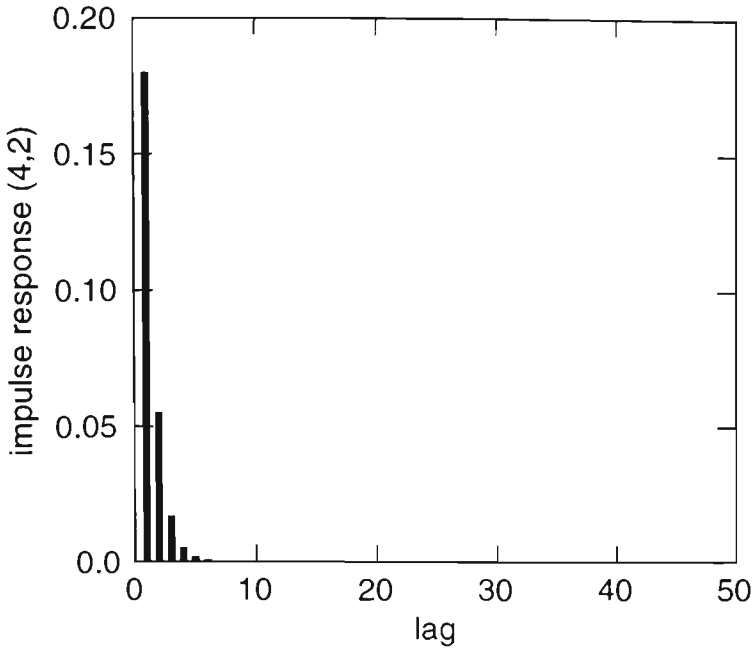

Figure 7-26 Model 2 impulse response function for ESCOD and RCOD.

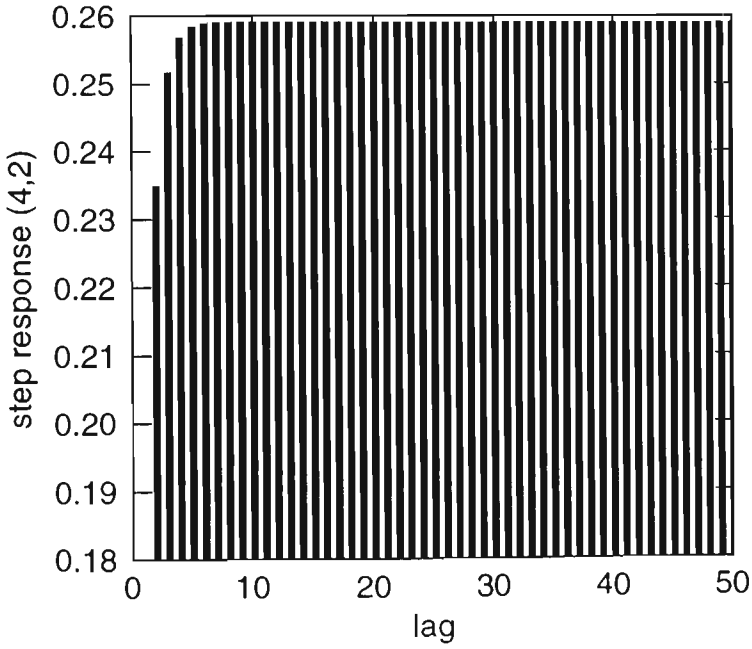

Figure 7-27 Model 2 step response function for ESCOD and RCOD.

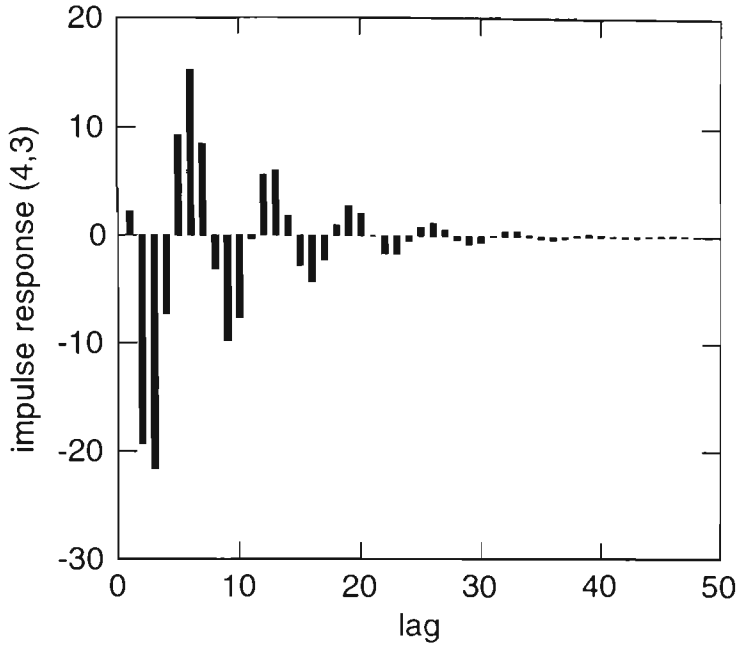

Figure 7-28 Model 2 impulse response function for ESCOD and PTEMP.

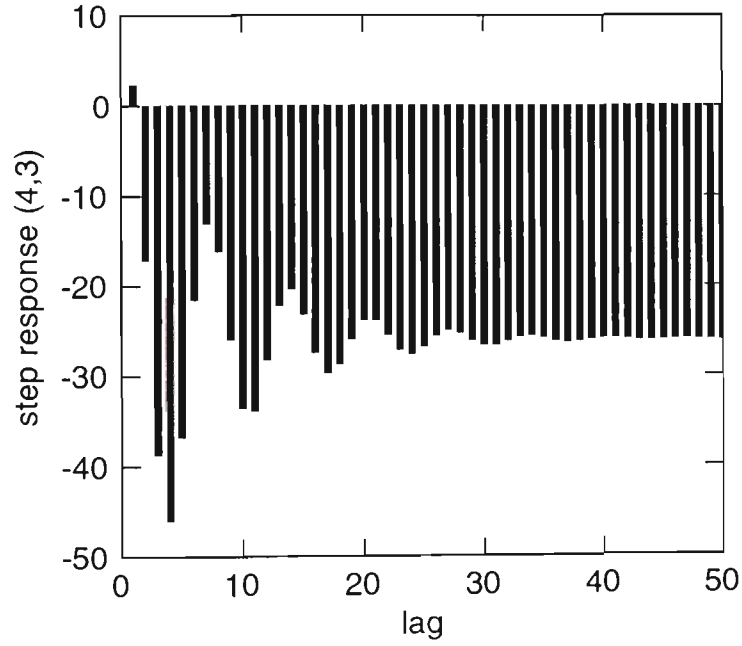

Figure 7-29 Model 2 step response function for ESCOD and PTEMP.

the inputs. Model number 2 was selected for development of the forecast and feedforward-feedback control equations. The impulse and step response functions for model 2 are shown in Figure 7-24 to Figure 7-29, and can be compared to Figure 7-18 to Figure 7-23 on pages 7-26 to 7-28.

The final transfer function-noise model was therefore given by:

$$y_t = \delta_1^{-1}(B)\omega_1(B)x_{1,t} + \delta_2^{-1}(B)\omega_2(B)x_{2,t} + \delta_3^{-1}(B)\omega_3(B)x_{3,t} + n_t \qquad \textbf{Equation 7-13}$$

where Y=effluent SCOD (mg/L)

X_1=raw sewage flowrate (ML/d)

X_2=raw sewage COD concentration (mg/L)

X_3=reactor water temperature (°C)

$y=\nabla Y$

$x_1=\nabla X_1$

$x_2=\nabla X_2$

$x_3=\nabla X_3$

$\delta_1=1-0.02B$

$\omega_1=1.12$

$\delta_2=1-0.30B$

$\omega_2=0.18$

$\delta_3=1-1.03B+0.78B^2$

$n_t=(1+0.56B)^{-1}a_t$

$a_t \sim N(0,7885)$

The model can be rearranged and written as follows:

$$
\begin{aligned}
Y_{t+1} &= 1.79Y_t - 1.14Y_{t-1} - 0.02Y_{t-2} + 0.51Y_{t-3} - 0.14Y_{t-4} + 0.002Y_{t-5} \\
&+ 1.12X_{1,t+1} - 1.98X_{1,t} + 1.24X_{1,t-1} + 0.05X_{1,t-2} - 0.57X_{1,t-3} + 0.15X_{1,t-4} \\
&+ 0.18X_{2,t+1} - 0.27X_{2,t} + 0.12X_{2,t-1} + 0.04X_{2,t-2} - 0.08X_{2,t-3} + 0.001X_{2,t-4} \\
&+ 2.22X_{3,t+1} - 23.28X_{3,t} + 15.42X_{3,t-1} + 9.45X_{3,t-2} - 3.87X_{3,t-3} + 0.06X_{3,t-4} \\
&+ a_{t+1} - 1.35a_t + 1.11a_{t-1} - 0.25a_{t-2} + 0.004a_{t-3}
\end{aligned}
$$

and then, by taking conditional expectations, the one-step-ahead forecast is given by:

$$
\begin{aligned}
\hat{Y}_t &= 1.79Y_t - 1.14Y_{t-1} - 0.02Y_{t-2} + 0.51Y_{t-3} - 0.14Y_{t-4} + 0.002Y_{t-5} \\
&+ 1.12\hat{X}_{1,t+1} - 1.98X_{1,t} + 1.24X_{1,t-1} + 0.05X_{1,t-2} - 0.57X_{1,t-3} + 0.15X_{1,t-4} \\
&+ 0.18\hat{X}_{2,t+1} - 0.27X_{2,t} + 0.12X_{2,t-1} + 0.04X_{2,t-2} - 0.08X_{2,t-3} + 0.001X_{2,t-4} \\
&+ 2.22\hat{X}_{3,t+1} - 23.28X_{3,t} + 15.42X_{3,t-1} + 9.45X_{3,t-2} - 3.87X_{3,t-3} + 0.06X_{3,t-4} \\
&- 1.35a_t + 1.11a_{t-1} - 0.25a_{t-2} + 0.004a_{t-3}
\end{aligned}
$$

Equation 7-14

In Equation 7-14, $\hat{Y}_t$ is the one-step-ahead forecast for the effluent SCOD made at time origin *t*, and $\hat{X}_{1,t-1}$, $\hat{X}_{2,t-1}$ and $\hat{X}_{3,t-1}$ are the one-step-ahead forecasts for raw sewage flowrate, raw sewage COD concentration and reactor water temperature made at time origin *t-1*. The RFLOW, RCOD and PTEMP were represented by the models AR(1), ARIMA(1,0,0)(1,0,0)$_7$ and ARIMA(0,1,1)(1,0,0)$_7$, respectively, and the forecast equations were:

$$\hat{X}_{1,t} = 25.4 + 0.56X_{1,t}$$

$$\hat{X}_{2,t} = 372.5 + 0.20X_{2,t} + 0.47X_{2,t-6} - 0.09X_{2,t-7}$$

$$\hat{X}_{3,t} = X_{3,t} + 0.39X_{3,t-6} - 0.39X_{3,t-7} - 0.48a_{3,t}$$

where $a_{3,t}$ are the one-step-ahead forecast errors for X_3.

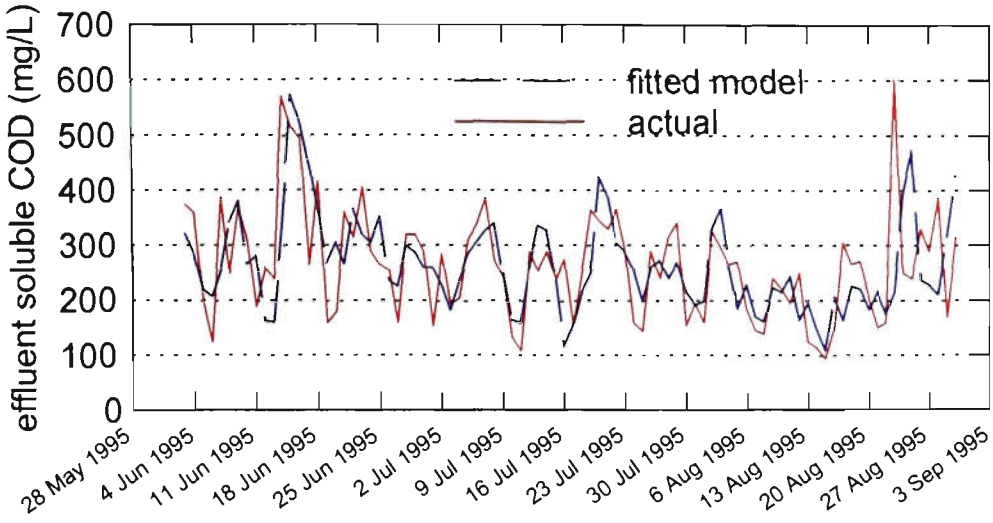

Figure 7-30 Fitted transfer function-noise model.

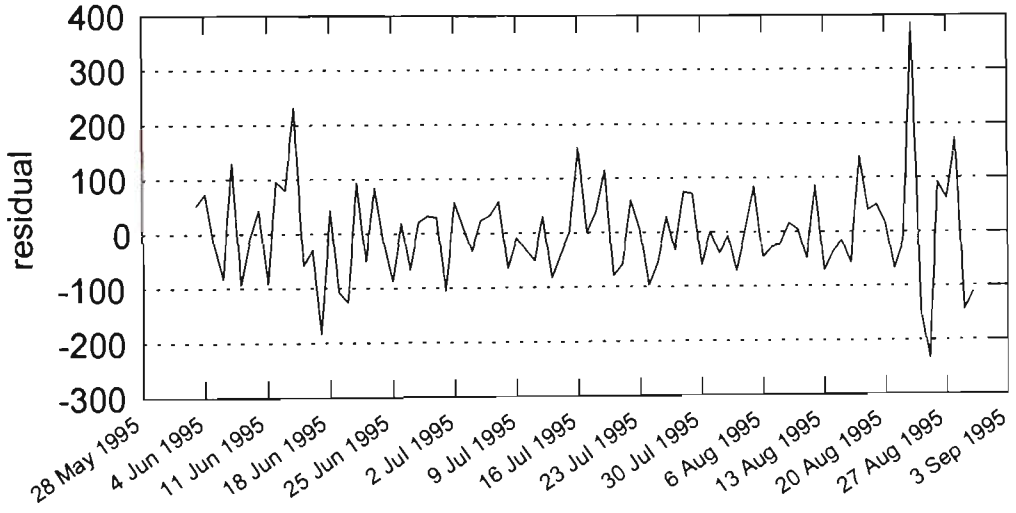

Figure 7-31 Residuals of the transfer function-noise model.

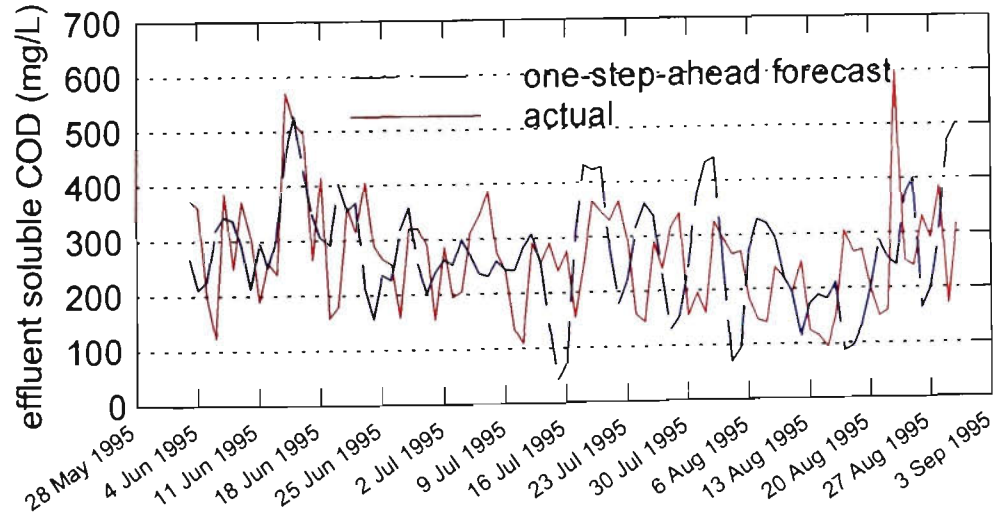

Figure 7-32 One-step-ahead forecasts using **Equation 7-14**.

Plots of the fitted transfer function-noise model, model residuals and one-step-ahead forecasts for ESCOD are given as Figure 7-30 to Figure 7-32. Note that, generally, there is no advantage in forecasting using leading indicators, as was done here, or in feedforward control, if the lag between the response and the indicator (or disturbance) is zero. This was true in this case, where the univariate model of the effluent SCOD produced better forecasts than the multivariate transfer-function noise model. The effluent SCOD was well represented by an ARIMA$(1,0,0)(1,0,0)_7$ model.

In addition to forecasting, the transfer function-noise model can be used to calculate the optimal flow control action that will minimise the error at the output, that is, the deviation of the effluent SCOD from a prescribed target value. In using the model this way, a critical assumption made is that the flow control actions were independent of the noise at the output. In this particular case, the experiment was not 'designed', by generating the raw sewage flowrates according to some external random process. As a consequence, it is not known whether this assumption has been satisfied and the parameter estimates may have been affected. For exploratory purposes, however, the feedforward-feedback control equation has been formulated below.

The model given by Equation 7-13 can be rewritten, using the notation of Box and Jenkins[45], as follows:

$$\nabla \varepsilon_t = L_1^{-1}(B)L_2(B)\nabla X_{1,t-1+} + \delta_2^{-1}(B)\omega_2(B)\nabla X_{2,t} + \delta_3^{-1}(B)\omega_3(B)\nabla X_{3,t} + \nabla N_t$$

or as

$$\varepsilon_t = Y_t - T = L_1^{-1}(B)L_2(B)X_{1,t-1+} + \delta_2^{-1}(B)\omega_2(B)X_{2,t} + \delta_3^{-1}(B)\omega_3(B)X_{3,t} + N_t$$

where $L_1(B)$ and $L_2(B)$ are the same as δ_1 and δ_2 given earlier.

Now, firstly addressing the feedback part of the control equation, if ε_t=0 (i.e. Y_t maintained at the target T), then:

$$X_{t+} = -L_1(B)L_2^{-1}(B)N_{t+1}$$

However, N_{t+1} is not known at time t and is, therefore, replaced by its one-step-ahead forecast $\hat{N}_t(1)$:

$$X_{t+} = -L_1(B)L_2^{-1}(B)\hat{N}_t(1)$$

$\hat{N}_t(1)$ can then be expressed in terms of ε_t using the fitted noise model $(1+0.56B)\nabla N_t = a_t$ as follows:

$$\hat{N}_t(1) = \frac{(0.44+0.56B)}{(1-0.44B-0.56B^2)}\varepsilon_t$$

and the feedback part of the control equation can be written:

$$X_{t+} = -\frac{(1-0.16B)(0.44+0.56B)}{1.12(1-0.44B-0.56B^2)}\varepsilon_t$$

The feedforward component of the control equation is:

$$X_{1,t+} = -\frac{L_1(B)}{L_2(B)}\left\{\delta_2^{-1}(B)\omega_2(B)X_{2,t+1} + \delta_3^{-1}(B)\omega_3(B)X_{3,t+1}\right\}$$

but, because $X_{2,t+1}$ and $X_{3,t+1}$ are not known at time t, they are also replaced by their one-step-ahead forecasts, and the feedforward part of the control equation is:

$$X_{1,t+} = -\frac{(1-0.02B)}{1.12}\left\{\frac{0.18}{(1-0.30B)}\hat{X}_{2,t}(1) + \frac{(2.22-21.60B)}{(1-1.03B+0.78B^2)}\hat{X}_{3,t}(1)\right\}$$

Hence, the feedforward-feedback control equation is:

$$X_{1,t+} = -\frac{(1-0.02B)}{1.12}\left\{\frac{0.18}{(1-0.30B)}\hat{X}_{2,t}(1) + \frac{(2.22-21.60B)}{(1-1.03B+0.78B^2)}\hat{X}_{3,t}(1) + \frac{(0.44+0.56B)}{(1-0.44B-0.56B^2)}\varepsilon_t\right\}$$

which can be rewritten as follows:

$$\begin{aligned} X_{1,t+} &= 1.77X_{1,t-1+} - 1.11X_{1,t-2+} - 0.04X_{1,t-3+} + 0.51X_{1,t-4+} - 0.13X_{1,t-5} \\ &\quad - 0.16\hat{X}_{2,t}(1) + 0.24\hat{X}_{2,t-1}(1) - 0.11\hat{X}_{2,t-2}(1) - 0.04\hat{X}_{2,t-3}(1) + 0.07\hat{X}_{2,t-4}(1) - 0.001\hat{X}_{2,t-5}(1) \\ &\quad - 1.98\hat{X}_{3,t}(1) + 20.81\hat{X}_{3,t-1}(1) - 13.78\hat{X}_{3,t-2}(1) - 8.45\hat{X}_{3,t-3}(1) + 3.46\hat{X}_{3,t-4}(1) - 0.05\hat{X}_{3,t-5}(1) \\ &\quad - 0.39\varepsilon_t + 0.02\varepsilon_{t-1} + 0.25\varepsilon_{t-2} - 0.46\varepsilon_{t-3} + 0.13\varepsilon_{t-4} - 0.002\varepsilon_{t-5} \end{aligned}$$

Equation 7-15

Now, the disturbance record can be reconstructed as if the flowrate was held constant at its initial value of 54 ML/d and then reproduced as if the new flow control actions were made according to Equation 7-15. The effluent SCOD record is reconstructed as if the flow was held constant from:

$$\nabla Y_t' = \nabla Y_t - \delta_1^{-1}(B)\omega_1(B)\nabla X_{1,t}$$

which can also be written as:

$$Y_t' = 1.02Y_{t-1}' - 0.02Y_{t-2}' + Y_t - 1.02Y_{t-1} + 0.02Y_{t-2} - 1.12X_{1,t} + 1.12X_{1,t-1} \qquad \textbf{Equation 7-16}$$

where Y_t' is the approximate disturbance that would have resulted if the flow was maintained at 54 ML/d. In a similar fashion, the effluent SCOD record can be reproduced according to the new flow control actions:

$$Y_t'' = 1.02Y_{t-1}'' - 0.02Y_{t-2}'' + Y_t' - 1.02Y_{t-1}' + 0.02Y_{t-2}' - 1.12X_{1,t+} + 1.12X_{1,t-1+} \qquad \textbf{Equation 7-17}$$

where Y_t'' is the approximate effluent SCOD that would have resulted with the new flow control actions.

Using Equation 7-16, the disturbance record was reconstructed as if the flow was held at 54 ML/d and is given as Figure 7-33. The flow control action

required to maintain the effluent SCOD at a mean level of 270 mg/L was calculated from Equation 7-15 and is given as Figure 7-34. The new effluent SCOD that could be expected from the new control actions was generated from Equation 7-17 and is shown in Figure 7-35.

It appears from Figure 7-34 and Figure 7-35 that while the effluent SCOD was maintained at the target in the long term, the control equation overcompensated for the feedforward and feedback disturbances resulting in cyclical control actions and effluent SCOD concentration. This suggests that the control equation is not properly tuned. This may be the result of not having collected the data according to a designed experiment. It may also be that the coefficients in the model were affected by the unusually high SCOD that occurred on 23rd August. Replacing the high SCOD with the mean SCOD had considerable impact on the coefficients for the flowrate. If the model was correctly tuned, then it may be possible to maintain the effluent SCOD about a particular target value without the control equation calling for negative flowrates. The target value need not be a fixed mean level, as in this example, but could follow a deterministic annual cycle. Assuming that the model has been correctly identified, two options are available for improving the parameter estimates: 1). repeating the analysis using flows that were generated randomly, or; 2). using the control equation in a pilot control scheme and refitting the model when sufficient data were gathered.

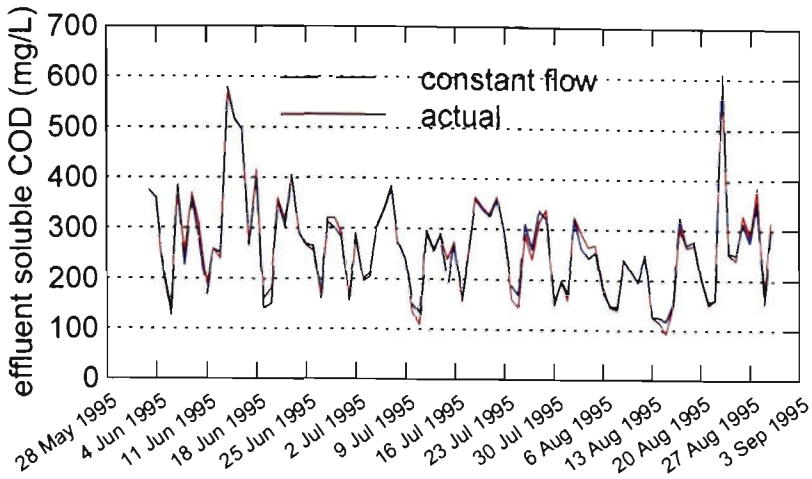

Figure 7-33 Effluent disturbance reconstructed as if the flow was maintained at 54 ML/d.

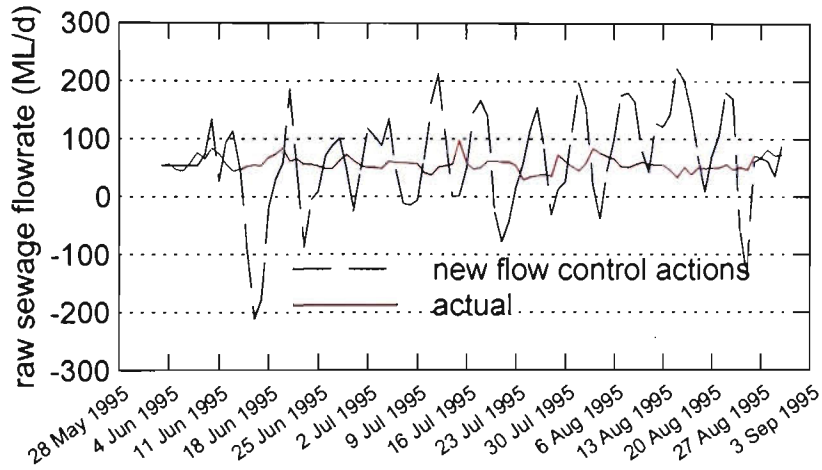

Figure 7-34 New flow control actions made according to the feedforward-feedback control equation, with a target of 270 mg/L for the effluent SCOD.

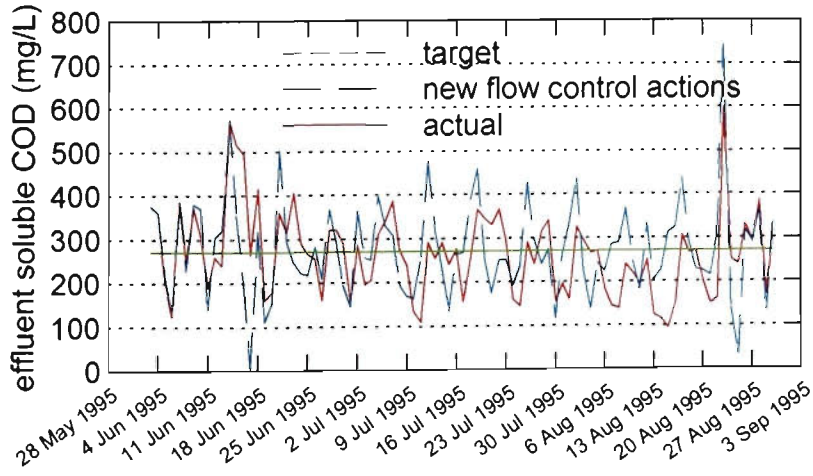

Figure 7-35 The effluent SCOD that could be expected to result from the new flow control actions.

7.3.1.4 Conclusion

The above analysis has provided useful information on the control of anaerobic ponds and may provide some leads as to the physical mechanisms occurring within these ponds. The dynamics of the process have been identified and it seems possible to maintain the effluent SCOD at some desired target value through manipulation of the flow, according to a feedforward-feedback or feedback only control equation. However, it is likely that rather large flow control actions would be required and the Plant may simply not have the capacity or flexibility to divert flows to other systems. This will particularly be true in the future as it has recently been decided to phase out the application of raw sewage to land at WTP. Nonetheless, the advantages of such a control scheme would need to be assessed in terms of the value of the methane produced, savings in aeration and the effect on final effluent quality. It may be more practical to devise a control equation for the aerated ponds (following the anaerobic ponds) to minimise fluctuations in loading on downstream ponds and optimise aeration. Control of anaerobic ponds would then be achieved by defining normal process variability with a time series model that incorporates weekly and annual seasonality and then using this model to identify and eliminate assignable causes of variation. SPC methods applicable to anaerobic ponds will be explored in more detail in Section 7.3.2.

7.3.2 Statistical Process Control

Most workers in the field of anaerobic digestion control agree that no one variable (or process indicator) contains the information needed for the control of the anaerobic digestion process[7,34,105] and it is generally recommended that a combination of variables be measured. Switzenbaum[7] has stated that the ideal process indicator would be easy to measure (preferably on-line) and directly related to the metabolic status of the digester. More to the point, however, there is only value in measuring such process indicators, as opposed to simply measuring the outputs like methane flowrate and effluent COD, if: 1), they provide an early warning of process failure, and/or; 2) they are useful in identifying the cause of the upset and the remedial action to be taken. This section examines the value of process indicators, choice of process indicators and the application of SPC methods to the control of anaerobic ponds.

7.3.2.1 The value of process indicators for the early warning of upsets

The term "early warning" indicator implies that changes at the output of the digester can be anticipated by changes in the indicator. This is due to differences in the dynamics of the indicator and output variables. An indicator that has fast dynamics (or small time constant) compared to the output variable will achieve its steady state level more quickly and therefore provide an indication of where the process outputs will be at some point in the future (in the absence of corrective action). Time constants have been reported for the various

Table 7-2 Time constants for various process indicators.

Variable	Time constant	Reference
H_2	15 s	7
Glucose	3 min	7
CO_2	1 h	7
Acetate	2 h	7
Propionate	4 h	7
Methane	2 d	7
Acidogens	30 min	7
Propionate degraders	5 d	7
Acetoclastic methanogens	10 d	7
Hydrogenotrophic methanogens	25 d	7
Gas production	< 1 d	33
COD	3 h	33
pH	1 d	33

process variables used in anaerobic digestion control (Table 7-2). Time constants, however, are influenced by the digester temperature and hydraulic residence time and the values given in Table 7-2 apply to heated digesters with short HRT's.

To estimate the time constants for the 115E Anaerobic Reactor, a frequency response analysis was carried out to determine the effect of a step response in raw sewage COD on the concentration of hydrogen. The analysis

was done in a similar fashion to that carried out in Section 7.3.1, though the calculations were much simpler for the single input case. The RCOD and H_2 series were filtered into the frequency bands 0.12-0.17 and 0.25-0.33 cpd to avoid problems due to leakage from the spectral window. The frequency response function was estimated for each frequency band and the gain and phase estimates were then combined. The impulse and step response functions were obtained from the inverse Fourier transform of the final gain and phase spectra. For comparison, the step response function for RCOD and ESCOD was estimated in the same way. The transfer function for RCOD and ESCOD was previously estimated in the multivariate spectral analysis in Section 7.3.1.3, though the gain and phase estimates were believed to have been affected by leakage. The step response functions are given as Figure 7-36 and Figure 7-37. The time constant for the hydrogen response was estimated to be 2.5 d, by graphically fitting a first order model to the gain and phase spectra. The ESCOD response appears to be a quadratic lag (second order) with a resonance frequency of 0.25 cpd and damping factor of 0.7. The sum of the two time constants for the ESCOD response is approximately 0.9 d.

In this study, sampling was conducted at intervals of one day, largely for practical reasons, although it appears from the step response functions for hydrogen and effluent SCOD that this is appropriate for anaerobic ponds. There does not appear to be a significant "early warning" benefit, however, in

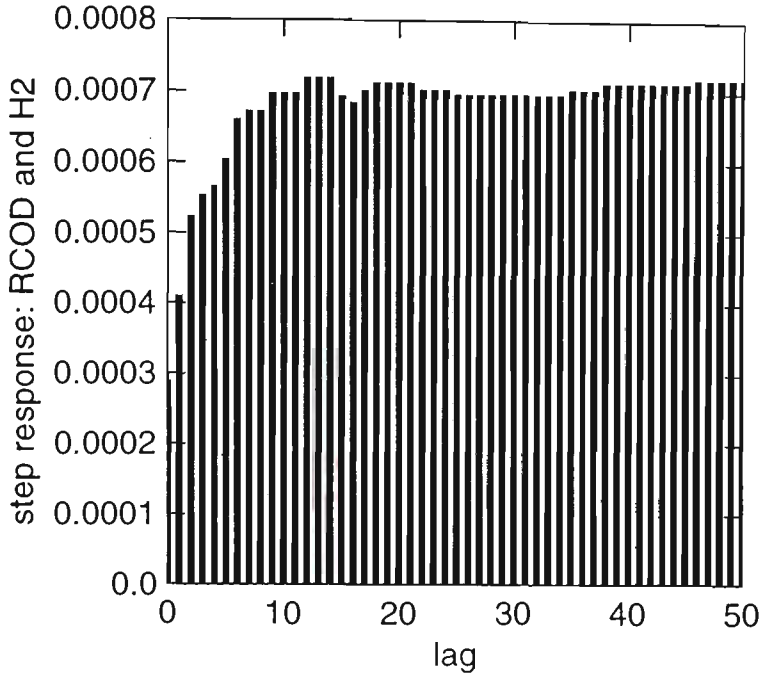

Figure 7-36 Step response function for RCOD and Hydrogen.

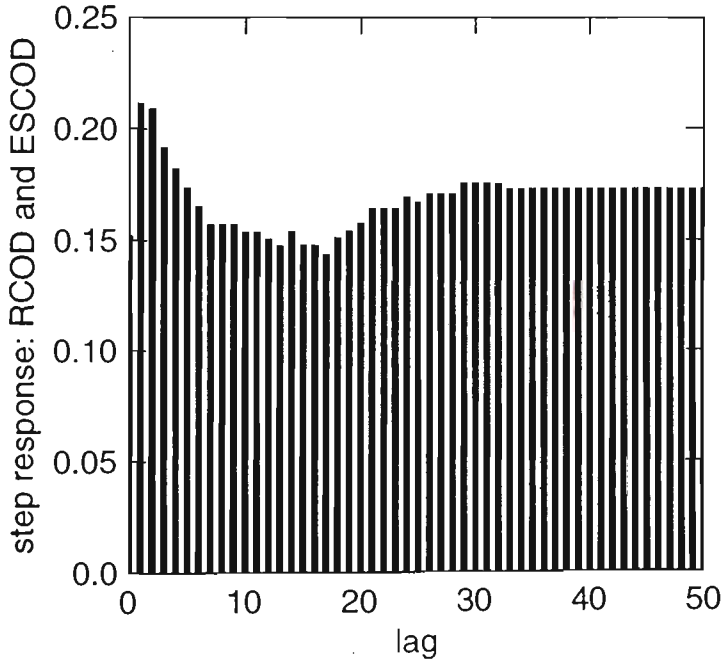

Figure 7-37 Step response function for RCOD and ESCOD.

monitoring (say) hydrogen in place of the actual outputs, effluent COD or methane flowrate. Furthermore, the most economic sampling interval would depend on the frequency and duration of upsets, the cost of upsets (in terms of reduced methane production, increased aeration on downstream ponds and EPA penalties) and the cost of sampling and testing. A discussion of the economic selection of sampling interval (and control chart parameters) for process monitoring is given by Berthouex[40], which was reviewed in Section 2.4. The cost model developed by Berthouex takes into consideration the cost of sampling and testing, the cost of investigating false alarms, and the cost of producing poor quality effluent. However, the model assumes that the assignable cause continues to affect the process until it is identified and removed, which is not the case for shock loads. The model would need to be modified for impulse rather than step changes in the quality characteristic of interest.

7.3.2.2 The value of process indicators as diagnostic tools

The process indicators commonly used in anaerobic digestion control include pH, individual and total VFA concentration, alkalinity, electrode potential, volatile solids concentration, and methane, carbon dioxide and hydrogen concentrations. It is thought that some of these indicators may be helpful in identifying the cause of an imbalance. For example, Mathiot and Escoffier et. al.[34] investigated the effects of organic (quantitative and qualitative), hydraulic and temperature shock loads on the concentrations of VFA's, H_2, CH_4

and CO_2, and found that the multivariate pattern in these variables was different in most cases (see Section 2.3). Hickey[110,111,112] studied the effects of toxic and organic shock loads on the hydrogen concentration in the gas phase of sewage digesters, and observed that the hydrogen concentration gave a different response for the different perturbations. Switzenbaum and Giraldo-Gomez et. al.[7] provide an excellent account of the studies that have been performed on process indicators for anaerobic digestion control, although it is apparent from their review that it is not yet possible to easily or confidently distinguish the type of shock load from patterns in the response variables.

7.3.2.3 Preliminary data assessment

All control charting methods assume that successive observations behave as independent and identically distributed variables. Most environmental data, however, exhibit serial correlation and nonuniform variance. The nonuniform variance property can usually be overcome by transforming the data (usually a log transformation) and is not a serious problem. Serial correlation, on the other hand, can have a profound effect on the performance of a control chart, usually resulting in a higher frequency of false alarms, and is not as easily dealt with. The usual approach to handling serial correlation is to fit an appropriate time series model to the data and then apply the control chart to the model's residuals. The residuals would satisfy the assumption of independence. The process would be deemed in control as long as it conformed to the model. Large residuals or

systematic patterns in the residuals would indicate that the process had changed. The characteristics of data from the 115E Anaerobic reactor were initially investigated using time series plots which are given as Figure 7-38 to Figure 7-48.

The time series plots, supplemented with plots of autocorrelation functions and autospectra (not shown), indicate that all variables exhibit serial correlation and weekly seasonality. The apparent nonstationarity (trending) in some variables is probably the result of an annual seasonal pattern, which could not be estimated given the data were only collected over a three month period. The interesting pattern in methane and carbon dioxide concentrations appears to be related to the pH of the reactor. The Pearson correlation coefficeint for carbon dioxide concentration and reactor pH was -0.3 (n=92, p=.003). In turn, the correlation coefficient for reactor pH and raw sewage pH was estimated to be 0.3 (n=92, p=.008). The apparent dependence of reactor pH on raw sewage pH is probably attributable to the relatively low alkalinity of 1000 mg/L $CaCO_3$, compared to digesters fed with primary and waste activated sludge (with a total solids concentration of about 5% w/w) which have an alkalinity of about 3000 mg/L $CaCO_3$.

The presence of serial correlation in all process indicators and output variables meant that time series modelling was required before statistically valid control charts could be constructed.

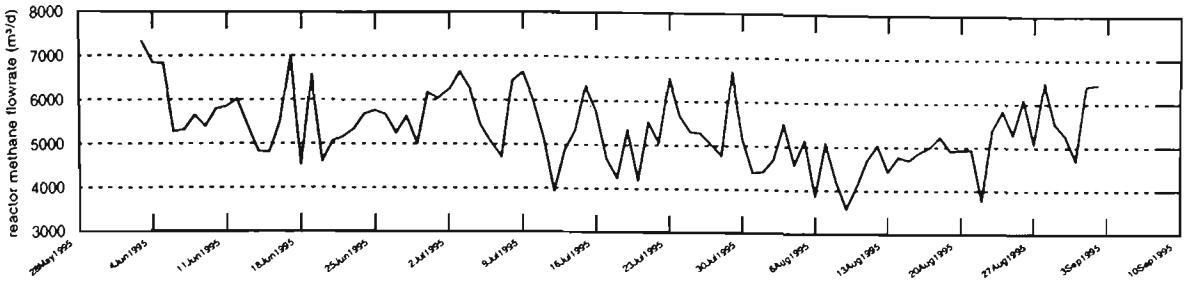

Figure 7-38 Methane flowrate (m^3/d).

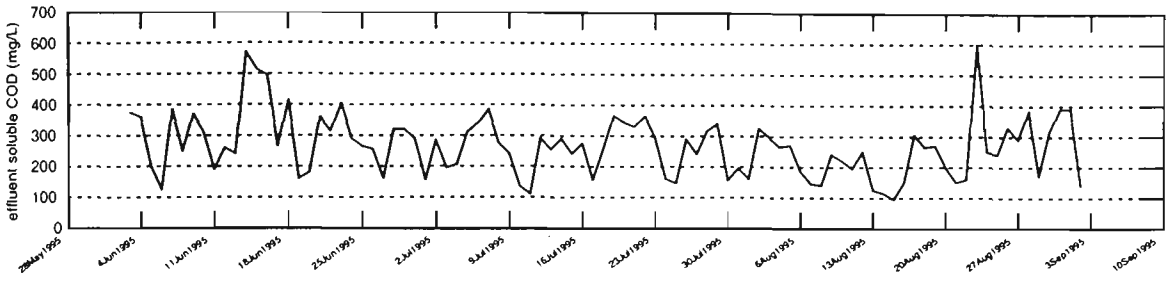

Figure 7-39 Effluent SCOD (mg/L).

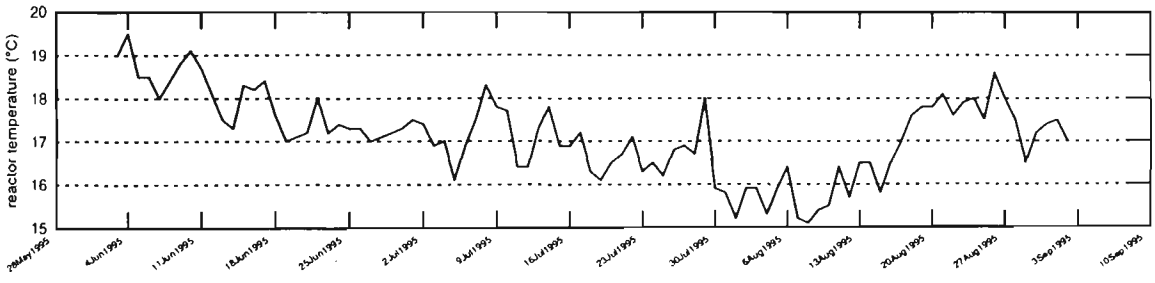

Figure 7-40 Reactor temperature (°C).

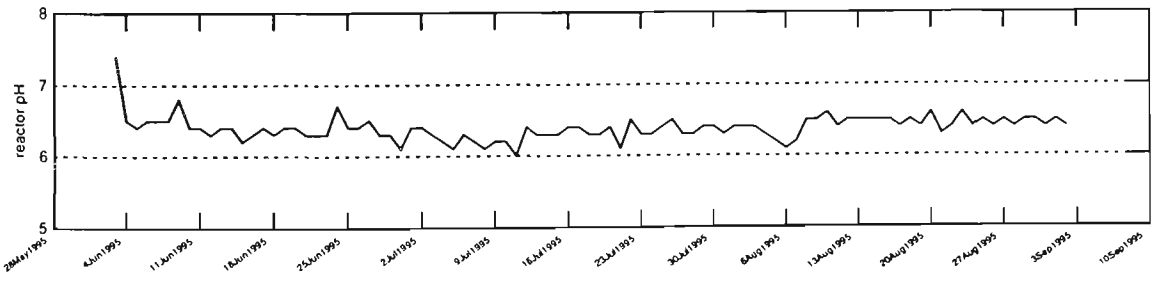

Figure 7-41 pH.

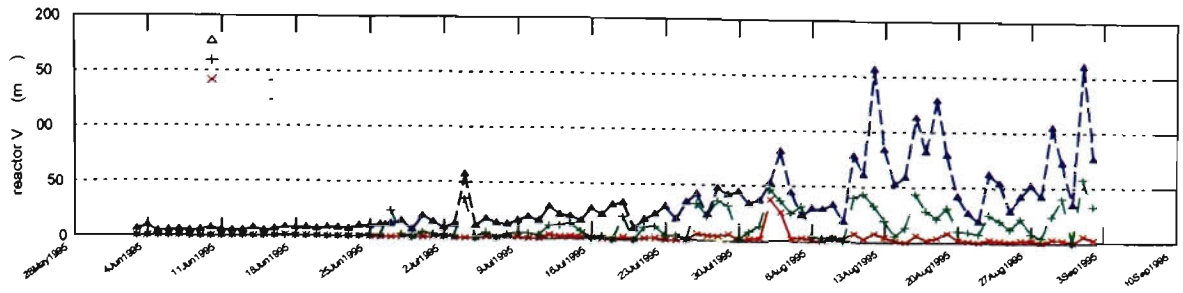

Figure 7-42 C_2-C_4 volatile fatty acids determined by chromatography (mg/L).

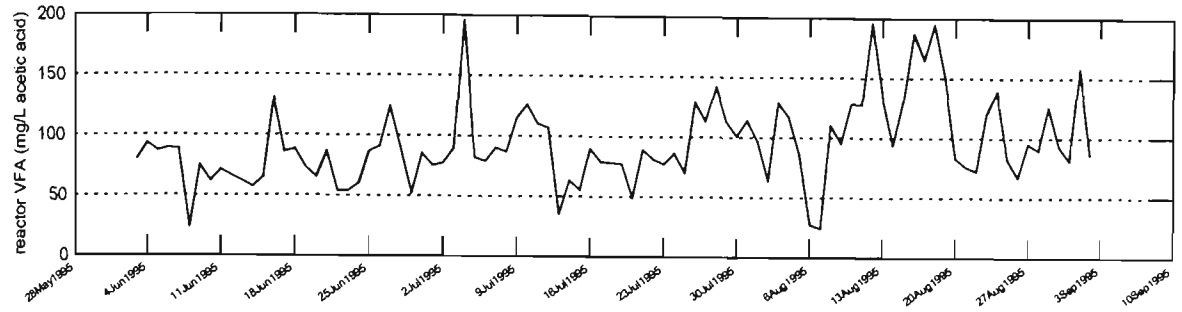

Figure 7-43 Total volatile fatty acids determined by colorimetry (mg/L acetic acid).

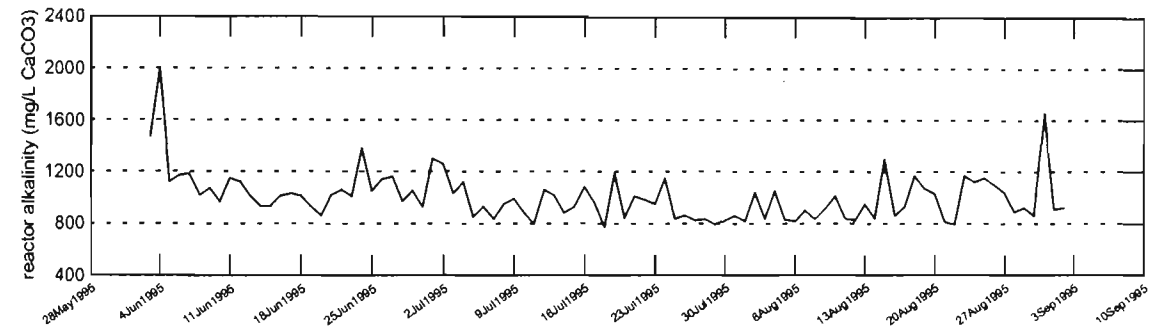

Figure 7-44 Alkalinity (mg/L $CaCO_3$).

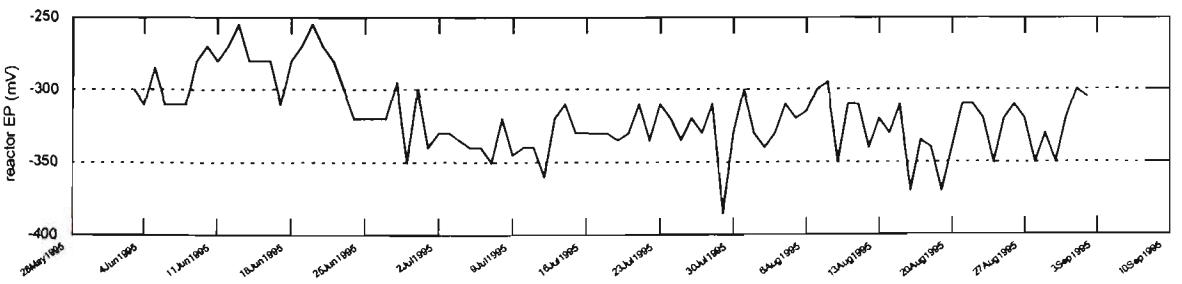

Figure 7-45 Electrode potential (mV).

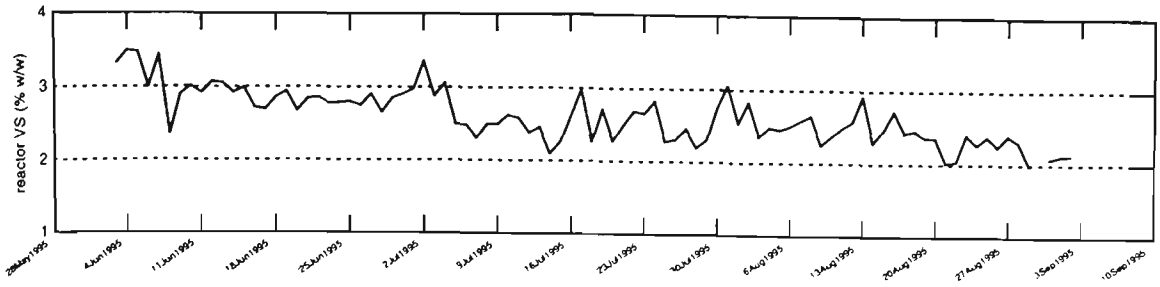

Figure 7-46 Volatile solids (% w/w).

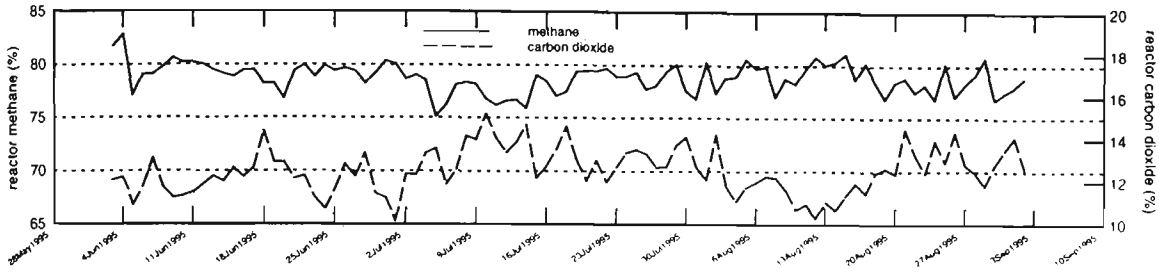

Figure 7-47 Methane and carbon dioxide (%).

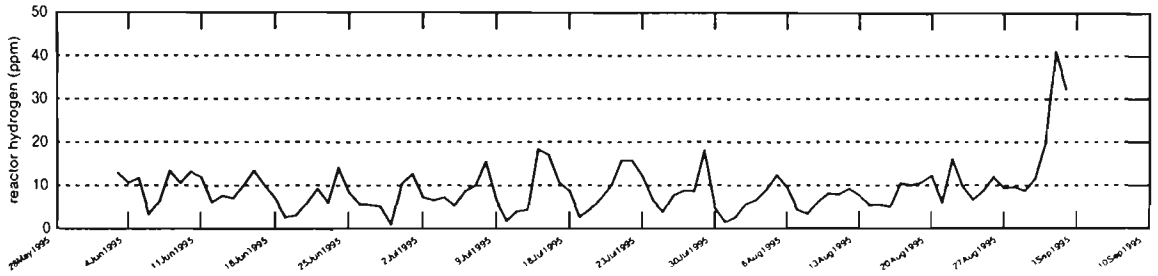

Figure 7-48 Hydrogen (ppm).

7.3.2.4 Time series modelling of process indicators and output variables

Autospectra of all variables exhibited a low frequency component, due to short and long term trends, and seasonality with period 7 days. This suggested that the data could be represented by a combination of an AR(1) or IMA(1,1) model and perhaps a seasonal AR(1) model. Given that the objective of the modelling was not to produce optimal forecasts, but to transform the variables into new independent and normally distributed variables, the control charting process would be greatly simplified if the same model could be applied to all variables.

Through a process of model fitting and checking, it was found that an ARIMA(1,0,0)(1,0,0)$_7$ model adequately represented all variables, although, for certain variables the low frequency component overshadowed the weekly seasonality and these variables were therefore modelled as AR(1) processes. In all cases, the error sequences were approximately random and normally distributed. The ARIMA(1,0,0)(1,0,0)$_7$ model can be written as follows:

$$(1-\phi_1 B)(x_t - \hat{\mu}) = (1-\phi_7 B^7)a_t$$

where x_t= value of the variable x at time t

$\hat{\mu}$ = estimated mean of x

ϕ_1 , ϕ_7= autoregressive and seasonal autoregressive parameters

B= backward shift operator

a_t= model residuals~N(0, $\hat{\sigma}_a^2$)

The parameters for the various models are given in Table 7-3.

Table 7-3 Time series model parameters for the variables used in anaerobic digestion control.

X	transformation	ϕ_1	ϕ_7	$\hat{\mu}$	$\hat{\sigma}_a$
CH_4 (%v/v)		.38	0	78.8	1.3
CH_4 flow (m^3/d)		.29	.26	5390	720
CO_2 (%v/v)		.56	0	12.5	.9
Effluent SCOD (mg/L)		.24	.39	270	92
H_2 (ppm)		.61	.32	10.1	4.6
Acetate (mg/L)	log(x+1)	.84	0	3.1	.51
Propionate (mg/L)	log(x+1)	.31	.50	1.6	1.1
i-Butyrate (mg/L)	log(x+1)	.58	.33	.74	.56
n-Butyrate (mg/L)	log(x+1)	.39	.5	.67	.62
EP (mV)		.47	.32	-317	20
pH		.44	0	6.4	.16
Reactor temperature (°C)		.75	.36	17.2	.55
Total VFA (mg/L)		.44	.18	94	32
Volatile solids (mg/L)		.57	.30	2.6	.3
Alkalinity (mg/L)		.28	0	1010	180

7.3.2.5 Process monitoring of anaerobic ponds

As mentioned earlier, the objective of process monitoring is to maintain a process in a state of statistical control through the detection of process upsets and subsequent identification and elimination of the cause(s). In this section, the control state of the 115E Anaerobic Reactor was investigated using control charts applied to the methane flowrate and effluent SCOD. While it appears from the foregoing that process indicators such as volatile fatty acid concentration and hydrogen concentration offer little benefit as "early warning" or diagnostic tools for anaerobic ponds, control charts were also applied to these variables for comparison.

In this study, eleven process indicators were measured (not including the methane flowrate and effluent SCOD) and, given that these variables were likely correlated, it was reasonable to employ a multivariate control chart based on Hotelling's T^2 statistic. The T^2 statistic provides a single measure of the conformance of an observation vector to its mean or target, with a prescribed Type I error size. As was discussed in Section 2.4, a T^2 chart can overcome problems with Type I and Type II errors that arise when separate charts are used. That is, when several related variables are charted separately the process may appear in statistical control when it is not, or vice versa.

The ARIMA model residuals were used in place of the original variables and the T^2 values were calculated from the standardised principal components. As it was not obvious which variables to include on the T^2 chart, all of the eleven process indicators were employed including pH, C_2-C_4 VFA concentrations,

alkalinity, electrode potential, volatile solids concentration, and methane, carbon dioxide and hydrogen concentrations.

In the first principal component analysis it was found that the individual C_2-C_4 volatile fatty acids all loaded highly on the first component and their coefficients were approximately equal. This suggested that the total VFA concentration could be used in place of the individual acids and the analysis was therefore repeated. Based on the component loadings from this second analysis it appeared that the first three or four components had physical meaning to the process. A chi-square test[38] was used to test the hypothesis that that the remaining components were equal to zero, given that the first three or four components were different. For the three component model χ^2=24.2, which is only just significant at the 5% level ($\chi^2_{14,.05} = 23.7$). For the four component model χ^2=14.4, which was not significant at the 5% level ($\chi^2_{9,.05} = 16.9$). An analysis of the residuals from the three and four component models indicated few large residuals. For each model, 5 out 92 residuals were significant at the 5% level. This evidence indicated that either a three or four component model would suffice, and for the sake of parsimony, the three component model was selected. The Systat output for the three component model is given in the following:

```
>MODEL EP VS PH ALK VFA CH4 H2 CO2
>ESTIMATE / METHOD=PCA LISTWISE CORR SORT NUMBER=3 ROTATE= VARIMAX
Latent Roots (Eigenvalues)
        1       2       3       4       5       6       7       8
    1.886   1.346   1.151   1.051   0.837   0.782   0.529   0.417
Component loadings
                1       2       3
```

ALK	0.676	0.382	-0.044
CH4	0.674	-0.335	0.155
PH	0.620	-0.170	0.010
CO2	-0.529	0.577	-0.129
VS	0.522	0.610	-0.354
EP	0.122	0.586	0.495
H2	0.057	0.037	0.719
VFA	0.141	-0.094	-0.470

Variance Explained by Components

1	2	3
1.886	1.346	1.151

Percent of Total Variance Explained

1	2	3
23.578	16.822	14.392

Rotated Loading Matrix (VARIMAX, Gamma = 1.0000)

	1	2	3
CO2	-0.780	0.134	0.048
CH4	0.756	0.134	0.043
PH	0.589	0.255	-0.049
VS	-0.019	0.859	-0.176
ALK	0.295	0.717	0.054
H2	0.159	-0.089	0.699
EP	-0.159	0.413	0.638
VFA	0.077	0.116	-0.480

"Variance" Explained by Rotated Components

1	2	3
1.670	1.546	1.167

Percent of Total Variance Explained

1	2	3
20.879	19.325	14.588

Coefficients for Standardized Factor Scores

	1	2	3
CO2	-0.495	0.173	0.019
CH4	0.453	0.006	0.053
PH	0.334	0.107	-0.033
VS	-0.110	0.579	-0.172
ALK	0.105	0.445	0.038
H2	0.125	-0.092	0.606
EP	-0.127	0.278	0.534
VFA	0.023	0.080	-0.413

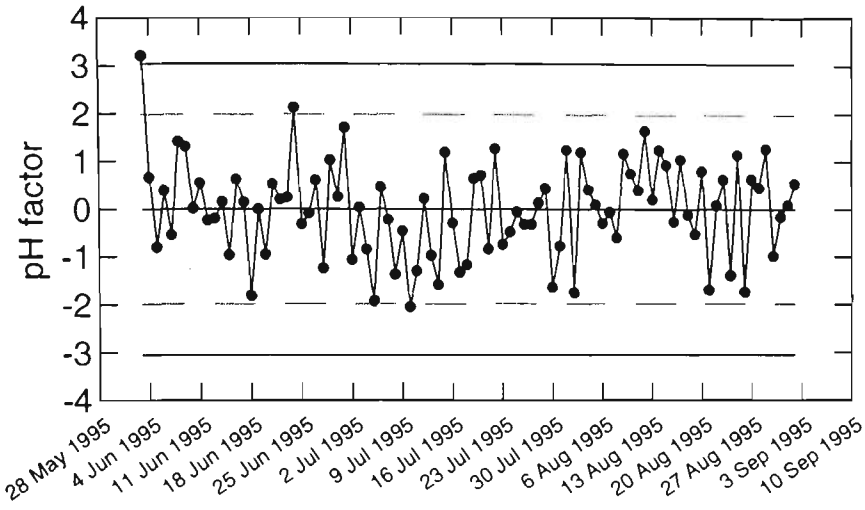

Figure 7-49 Shewhart chart of the pH factor.

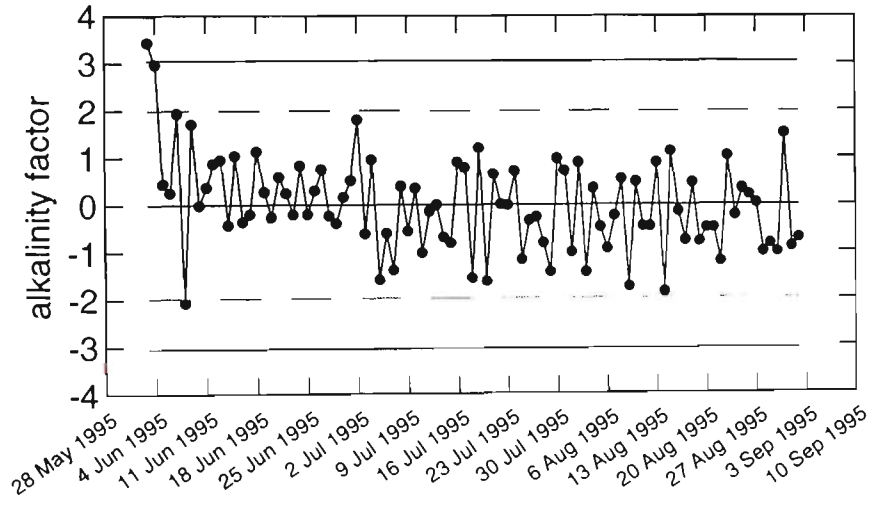

Figure 7-50 Shewhart chart of the alkalinity factor.

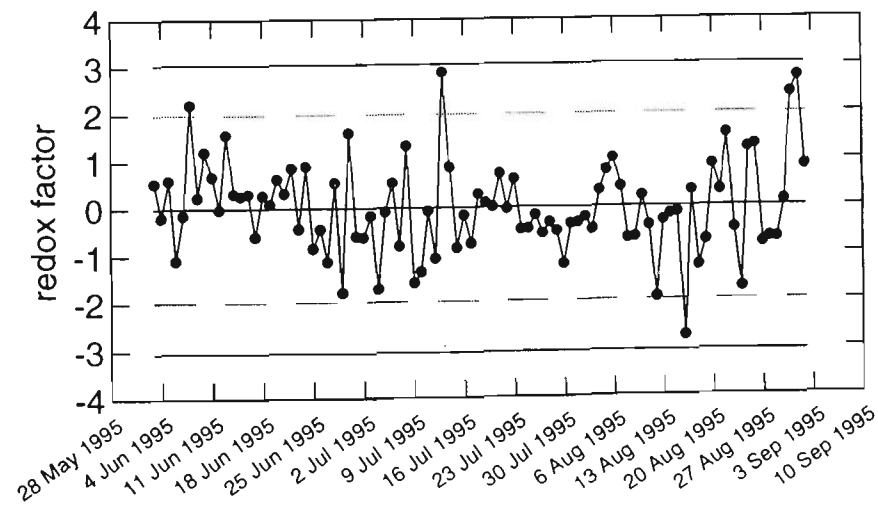

Figure 7-51 Shewhart chart of the redox factor.

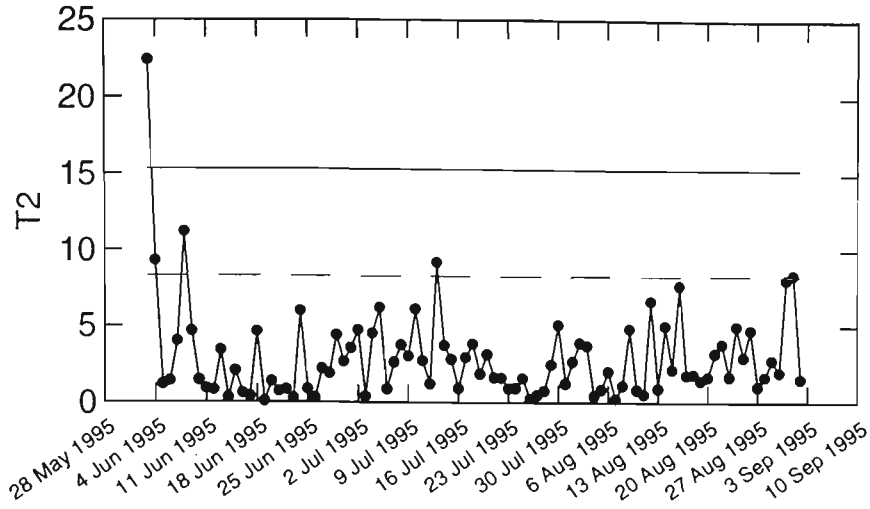

Figure 7-52 T^2 chart for the three component model.

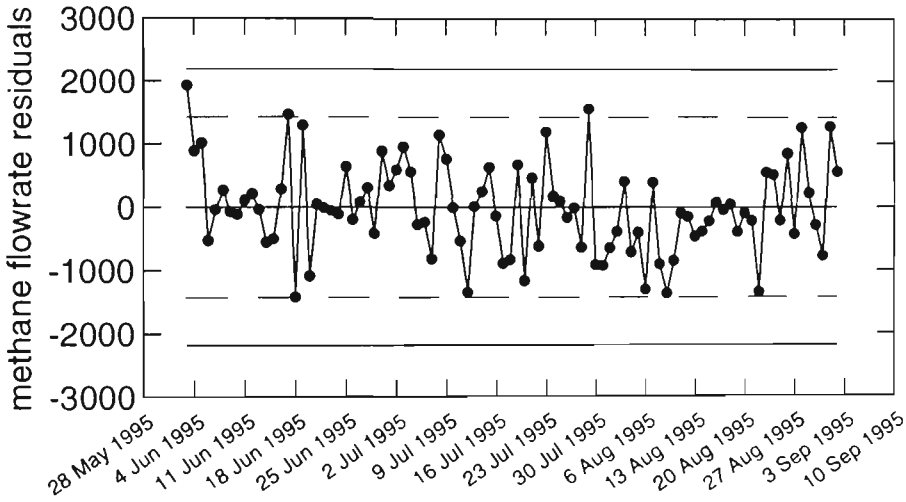

Figure 7-53 Shewhart chart of the methane flowrate residuals.

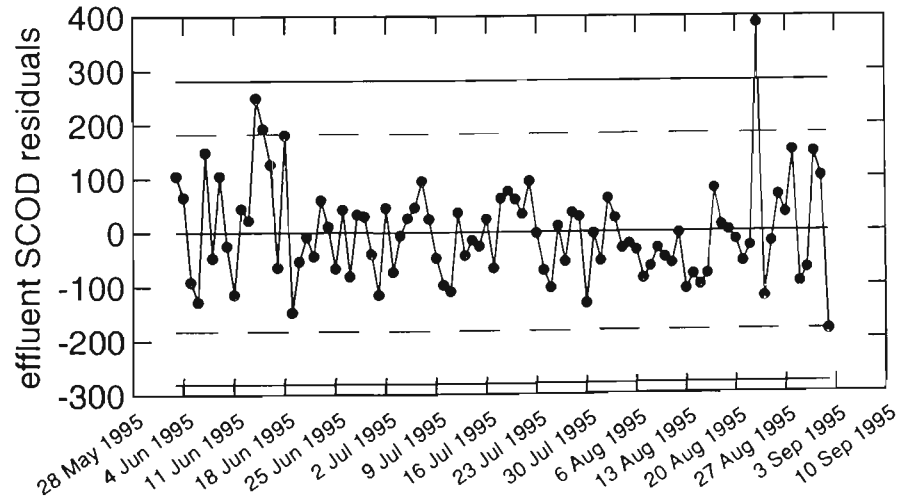

Figure 7-54 Shewhart chart of the effluent SCOD residuals.

It is apparent from the rotated loading matrix in the above output that the first three components are measures or dimensions of the process variability. The first component appears to represent pH variability, the second represents alkalinity and the third represents redox potential. Plots of the autocorrelation functions and χ^2 goodness of fit tests indicate that the three components are approximately random and normally distributed.

Shewhart control charts for each of the components (or factors) and the T^2 chart are given as Figure 7-49 to Figure 7-54. Control lines on these charts were drawn at α=.003 (control limits) and α=.05 (warning limits). The out-of-control signals on the T^2 chart and univariate charts for methane flowrate and effluent SCOD did not generally coincide and, given that only 3-5 observations out of 92 exceeded the warning limits, it would appear that the process was in a state of statistical control throughout the study period.

As there were apparently no identifiable process upsets, it is not possible to compare the performance of the multivariate and univariate charts, or indeed to establish the merit in simple time series plots of the original variables. However, given the relatively slow and comparable dynamics of both the process indicators and the process outputs it is reasonable to suggest that monitoring the process outputs would suffice and, given the weekly and annual seasonality, it may be better to use time series techniques (perhaps with a deterministic weekly and annual component) rather than rely on simple time series plots of the original variables. Furthermore, the apparent stability of the process suggests that routine monitoring could be done at a frequency of less than once per day.

7.3.3 Measurement Control in the Laboratory

Measurement control is essential for effective process control. Control charts, which are popular in many industries, are now widely used in the analytical chemistry laboratory to attain and maintain statistical control of measuring systems. When an out-of-control condition is detected the analyst must search for the cause and rectify the situation before re-doing some of the previous measurements and continuing with other analyses. The analyst decides when the measuring system is out-of-control by reference to control lines on the control chart which are positioned according to "normal" measurement variability and with a pre-specified Type I error probability (or risk of judging the system out of control when it is actually in control). When data are correlated, however, as is typically the case for instrumental analyses, estimating the variance in the usual manner is deficient and may render the control chart a liability rather than an asset. Instrumental methods of analysis are used for many of the common process indicators used in anaerobic digestion control, including methane, carbon dioxide, hydrogen, volatile fatty acids and pH, and indeed the majority of variables studied in this research including metals, sulphate and ammonia. If the measuring system is not in a state of statistical control then measurement accuracy is affected and the capacity to control processes such as anaerobic digestion will be greatly impaired[113].

Instrumental methods of analysis are usually comparative in nature and the analytical instruments used for measurement require periodic recalibration to compensate for the effects of uncontrollable environmental factors and gradual

changes in instrument performance. These effects are a fact of life for all methods of analysis where quantification is based on comparison of a physical property in a standard with the same property in an analyte. With respect to calibration, two questions need to be asked: 1), how does the analyst know the calibration process was free of systematic error and; 2), how does (s)he know that the calibration will be valid for all determinations made within a particular analytical set (i.e. before recalibrating)? Clearly to be confident of the test results the analyst should have systems for monitoring and controlling the accuracy and precision of the test method.

Measurement process control (MPC) can help[114]. The principles of measurement control are the same as those of statistical process control, except that it is the quality of the measurements, not the product, that is being controlled. In the analytical laboratory, control charts are used to control the accuracy and precision of an analytical method; QC samples are regularly measured in the course of an analytical run and the results plotted on an individual-observations chart (ICHART) and a moving-range chart (MRCHART). The ICHART is used to control the accuracy of the analytical method, and the MRCHART is used to control the precision (note that accuracy is taken here to mean the "closeness of agreement between an observed value and an accepted reference value"[115]).

General guidelines for the construction of laboratory control charts are given in the literature[116,117]. The ICHART and MRCHART, the individual-observation counterparts of the Shewhart $\overline{X}$ (sample mean) and R (sample range) charts, are most commonly recommended for use in the laboratory, and these

charts are usually constructed with three-sigma control limits to give a Type I error probability of 0.003.

One problem that has been overlooked when control charting instrumental analyses is data correlation. All of the standard control charting methods, including the ICHART, assume that the a_t are independent and normally distributed random disturbances, with zero mean and constant variance. However, the assumption of independence does not hold for comparative methods of analysis. The reason for this is that control samples analysed within a particular set (as defined above), and hence derived from the same calibration curve, will be positively correlated.

The recommended procedures for constructing laboratory control charts[116,117] do not account for data correlation; although the ASTM does state that "If duplicates are used to monitor precision, they should be analysed in different runs when a between run measure of variability is employed in setting control limits". When sample data are correlated, an estimate of the variance calculated in the usual way and used to construct a control chart will result in the control limits being inappropriately located. This can translate into a higher incidence of incorrect control decisions and may actually increase a laboratory's quality costs. In this section, a way of overcoming this problem and constructing statistically effective control charts for instrumental analyses is presented.

7.3.3.1 Calibration

When calibrating an instrument, the analyst is quantifying the relationship between some physical property (e.g. light absorption or emission, electrical current, potential) and the analyte concentration, for a given set of environmental factors such as pH, temperature, viscosity, etc.. The calibration curve arrived at is, however, only an estimate of the true relationship.

Each time an instrument is calibrated the calibration curve will be slightly different owing to the random effects of noise. The estimated concentration of a control sample will vary both between and within analytical sets (i.e. calibration periods) and replicates stemming from a common calibration curve will usually agree more closely than control samples interpolated from different calibration curves. This behaviour is known as intraclass correlation[118] and it has a pronounced effect on the way the standard deviation should be estimated for a series of replicate control sample measurements.

7.3.3.2 Control charting instrumental analyses

The first steps in constructing an ICHART are the collection of some data (usually 25 or more measurements of a QC sample) and calculation of the mean and standard deviation. Owing to intraclass correlation, however, calculating the standard deviation in the usual manner will give misleading estimates of the variance of instrumental analyses and, hence, the band over which the estimated concentrations of control samples should reasonably vary.

To overcome this problem, the model of the process, which forms the basis of the control charting procedure, should be modified to account for the effect of calibration. It is worth noting that this applies not only to the ICHART, but to all of the standard control charting methods.

Where intraclass correlation is present, an individual observation, X, of the concentration of a control sample is made up of the following components[118]:

$$Xij = \mu + e_i + \varepsilon_{ij} \qquad \textbf{Equation 7-18}$$

where i = set number = 1...m

j = replicate number within a set = 1...n

X_{ij} = individual measurement of a control sample

μ = "true" value of the control sample

$e_i \sim N(0, \sigma_e^2)$

$\varepsilon_{ij} \sim N(0, \sigma^2)$

m = number of sets or calibrations

n = number of replicates within each set.

The symbol e_i represents the calibration effect and ε_{ij} the environmental effect.

The model represented by Equation 7-18 is in fact identical to the model for cyclic data proposed by Johnson and Counts[119]. The "normal" variability in the production data considered by these authors exhibited subgroup averages that rose and fell about a central line rather than in a random manner.

The variance of an individual observation can therefore be shown to be:

$$\mathrm{var}(X_{ij}) = \sigma_x^2 = \sigma_e^2 + \sigma^2 \qquad \textbf{Equation 7-19}$$

where σ_e^2 and σ^2 are known as the components of variance.

The components of variance in Equation 7-19 are estimated from a one-way analysis of variance (ANOVA)[118]. The between-set mean-squares,

$$BMS = \frac{n}{m-1}\sum_{i=1}^{m}(\overline{x_i} - \overline{\overline{x}})^2 \qquad \textbf{Equation 7-20}$$

can be shown to be an unbiased estimate of $(\sigma^2 + n\sigma_e^2)$, and the within-set mean-squares,

$$WMS = \frac{1}{m(n-1)}\sum_{i=1}^{m}\sum_{j=1}^{n}(x_{ij} - \overline{x_i})^2 \qquad \textbf{Equation 7-21}$$

an unbiased estimate of σ^2. The estimated variance of an individual observation is therefore:

$$\hat{\sigma}_x^2 = \frac{(n-1)WMS + BMS}{n} \qquad \textbf{Equation 7-22}$$

This is used to compute the control limits for an individual-observations chart. For simplicity, the control limits for the moving-range chart could also be based on Equation 7-22, although there is a good case for using Equation 7-21 in its place.

The role of the moving-range chart is to detect gross changes or trends in the precision of the measurement. If the control limits are based on Equation 7-22 the chart will be relatively insensitive to changes in precision occurring within a set (because $\hat{\sigma}_x^2$ is greater than WMS). To make the chart responsive to out-of-control conditions occurring within an analytical set, control limits for the

moving-range should be based on Equation 7-21, the within-set variance estimate. Accordingly, between-set differences should be omitted on the moving-range chart, and only within-set moving-ranges need be plotted. Alternatively the moving-range chart could have two sets of control limits: "within-set" control limits based on Equation 7-21 and "overall" limits based on Equation 7-22. To assist interpretation of the chart, within-set moving ranges (i.e. the difference between successive observations belonging to the same set) could be plotted as circles and between-set moving ranges (i.e. the difference between successive observations belonging to different sets) as squares.

Using two sets of control limits could enhance the utility of the control chart for detecting certain out-of-control conditions that, otherwise, would only be clearly detected on more sophisticated charts. For example, the combination of an ICHART with an MRCHART having only "within-set" control limits, is not suitable for detecting small changes in calibration standards - the consequence being that an increase in measurement variability would go undetected. One option in this case is to replace the ICHART with a moving-average chart, EWMA chart or even a combined Shewhart-CUSUM chart[120]. However, this would introduce extra complexity and should not be a decision taken lightly. A moving-range chart with both "within-set" and "overall" control limits, on the otherhand, would as likely detect a small change in a calibration standard (as an increase in the overall variability) without the added complexity.

Control chart lines for the ICHART and MRCHART can be computed from the formulae in Table 7-4. As a rule of thumb, the degrees of freedom for

Table 7-4 Formulae for control lines on the ICHART and MRCHART.

	ICHART	MRCHART
Centre Line	μ	$\overline{MR} = d_2 . \hat{\sigma}$
Upper Control Limit	$\mu + 3\hat{\sigma}_x$	$D_4 . \overline{MR} = D_2 . \hat{\sigma}$
Lower Control Limit	$\mu - 3\hat{\sigma}_x$	$D_3 . \overline{MR} = D_1 . \hat{\sigma}$

note: (1) for n=2, D_2=3.686, D_1=0, d_2=1.128 (see Appendix II, Table A, in ref. 36)

(2) "overall" control limits for the MRCHART can be obtained by substituting $\hat{\sigma}_x$ for $\hat{\sigma}$

(3) μ is the accepted reference value in this case.

$\hat{\sigma}_x$ is taken to be equal to the degrees of freedom of the larger of the within-set mean squares and the between-set mean squares[36]. To ensure that $\hat{\sigma}_x$ has sufficient degrees of freedom to accurately represent the population standard deviation, and without prior knowledge of which mean is the larger, it is necessary to collect the control chart data in such a way that each mean square has at least 25 degrees of freedom. This can be achieved by making two measurements of the control sample with each calibration for a total of 25 calibrations or more.

Provided the standard deviation estimates are based on 25 or more degrees of freedom, it should be unnecessary to frequently update the control lines. The only occasions for re-evaluating control lines are when the analytical method or instrument is changed, or another analyst is able to achieve better accuracy and precision (in which case this analyst would become the benchmark).

Finally, when control charting instrumental analyses, the usual criteria for statistical control will not necessarily apply when intraclass correlation is present. For example, a typical control chart rule is that when two out of three points in a row lie between two and three standard deviations from the target value, the system is judged out of control. However, if two or three of the measurements belong to the same set, it is quite likely that they will lie in the same region on the control chart. This behaviour cannot be taken to mean that the system is out of control. It may simply be a consequence of the positive correlation between members of the same set.

Control chart rules need to account for intraclass correlation. For, instance, some rules could be stated in terms of sets (or set-means) instead of individual values. This could apply only to rules that make no reference to control limits or warning limits, however, because these limits are based on the variance of an individual observation, not the variance of the mean. Obviously this restricts the choice of rules that can be used, but given that most out-of-control conditions in instrumental methods will be manifested in drifting (trending) measurements, the set of rules for ICHARTS and MRCHARTS in Table 7-5 should be adequate in most cases.

Table 7-5 Control chart rules for the ICHART and MRCHART.

ICHART

1. If one point (QC sample measurement) falls outside the control limits, repeat the analysis immediately. If the repeat is within the control limits, continue analyses; if not, stop and correct the problem.

2. If there is a run of nine consecutive *sets* on one side of the mean, stop and correct the problem.

3. If six consecutive measurements, within an analytical set, are in increasing or decreasing order, immediately analyse the control sample again. If the next point changes the order, continue the analyses; otherwise stop and correct the problem.

MRCHART

1. If a within-set difference (i.e. the difference between two control samples from the same set) falls above the upper control limit, repeat the analysis. If the repeat falls within the control limits, continue the analyses; if it falls above the UCL, stop and correct the problem.

As recommended in Standard Methods for the Examination of Water and Wastewater[116], once a problem has been identified and corrected, half of the samples between the last in-control QC sample measurement and the out-of-control one should be re-analysed.

It should be noted that it is not always necessary to recalibrate after a fault has been rectified, or at the beginning of each day for that matter. Perhaps the only time recalibration will be required is when the calibration standards are identified as the source of an out-of-control condition or if the fault occurred during calibration. Otherwise, it is sufficient to check the accuracy of the measuring system by analysing a single control sample before each batch of samples is analysed.

Of course, there will always be exceptions to the aforementioned guidelines. In the case of colorimetry, for example, standards and samples frequently have to be measured within a certain time of initiating the colour-forming reaction. In this situation, it would be more practical to prepare calibration standards with each batch of samples. With automated instruments, it is a relatively simple matter to include calibration standards with each lot of samples and there would be little or no advantage in changing this practice. Also in the case of automated instruments, the measuring system will often be evaluated for statistical control after a run has finished; so the usual practice will be to repeat all samples analysed after an upset is signalled.

7.3.3.3 An example: ammonia by flow injection analysis

Ammonia-nitrogen can be determined by flow injection analysis. An aqueous sample is injected into a carrier stream of distilled water which then mixes with a solution of sodium hydroxide. The joint stream passes along a

PTFE line into a gas diffusion cell. Gaseous ammonia diffuses through the membrane into an indicator stream and the resulting colour change is measured at 590 nm. The relationship between the absorbance and ammonia concentration is not linear over the working range (0-75 mg/L) and the La Grange interpolation method, which fits a polynomial regression model to the data, is used to predict the NH_3-N concentration in the sample.

Data for control charts were collected by analysing a 50 mg/L NH_3-N control sample twice with every calibration for 25 calibrations. In the course of routine analyses, a control sample was inserted after each 10 samples (approximately) according to the recommendations of the ASTM[117].

A scatter plot of each pair of replicates (Figure 7-55) was constructed to see whether intraclass correlation was important in calculating control limits. Because it is unclear which replicate should correspond to the ordinate, and which to the abscissa, it is usual to plot each pair of replicates twice, as (x_{i1}, x_{i2}) and (x_{i2}, x_{i1}). Indeed, it appears from the scatter plot, that the within-set replicates are correlated. In Figure 7-55 the 50% confidence ellipse is shown, which indicates that the data are reasonably bivariate normal because 24 of the 50 data points (approximately 50%) fall within the ellipse.

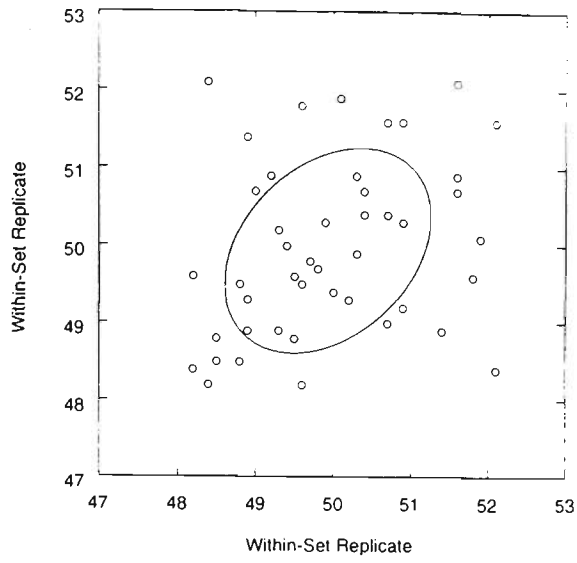

Figure 7-55 Scatter plot with 50% confidence ellipse demonstrating the presence of intraclass correlation.

Formulae for calculating the sample intraclass correlation coefficient (r_I) and the corresponding confidence limits are given by Snedecor and Cochran[118]. In this example, the sample intraclass correlation coefficient is 0.350 ($0.05<p<0.10$). As will be shown later in this section, the 10th set (or 19th and 20th observations) appears to be an outlier: if rejected from the data set, r_I is calculated to be 0.517 ($p<0.05$). This confirms the prior belief that the within-set replicates are correlated.

Testing the hypothesis that ρ_I equals zero is essentially the same as testing the hypothesis that σ_e^2 is zero in a one-way ANOVA[118]. In practice it is easier to use the analysis of variance approach, because ANOVA is a standard tool in most statistical computing packages.

Given that the data are consistent with coming from a normal distribution and that intraclass correlation is in evidence, the next step is to establish whether

or not the measuring system was in retrospective statistical control. From a one-way analysis of variance, initial estimates for control limits were 50.0±3.3 for the ICHART, and 3.3 (based on the within-set standard deviation) for the MRCHART. It is purely co-incidental that both $3\hat{\sigma}_x$ and $D_2\hat{\sigma}$ equal 3.3 in this case.

The moving range for the 10th set exceeded the upper control limit on the moving-range chart. This suggests that this set is an outlier and that the observations belonging to the set should be rejected and the control limits recalculated.

As a general rule, no observation should be rejected unless there is supporting evidence of an out-of-control condition. In this particular instance the problem was self-correcting and an assignable cause was not identified. However, since setting up a control chart for this particular instrument, four of seventy within-set differences have exceeded the UCL on the MRCHART, suggesting that this condition is not part of the normal variability. In fact, it is quite likely that the increased variability is caused by air bubbles which become temporarily lodged in the flow cell. Therefore, rejection of the suspect observations appears to be justified and a further analysis of variance was performed. $\hat{\sigma}^2$ was calculated to be 0.549, $\hat{\sigma}_e^2$ was 0.588 and $\hat{\sigma}_x$ 1.066. The new control lines on the ICHART were 50.0 for the centre line, 53.2 and 46.8 for the upper and lower control limits, respectively. The centre line on the MRCHART was 0.8 and the upper control limit was 2.7 (based on the within-set

standard deviation). Both charts, including all data points (i.e. including set number 10), are shown as Figure 7-56 and Figure 7-57.

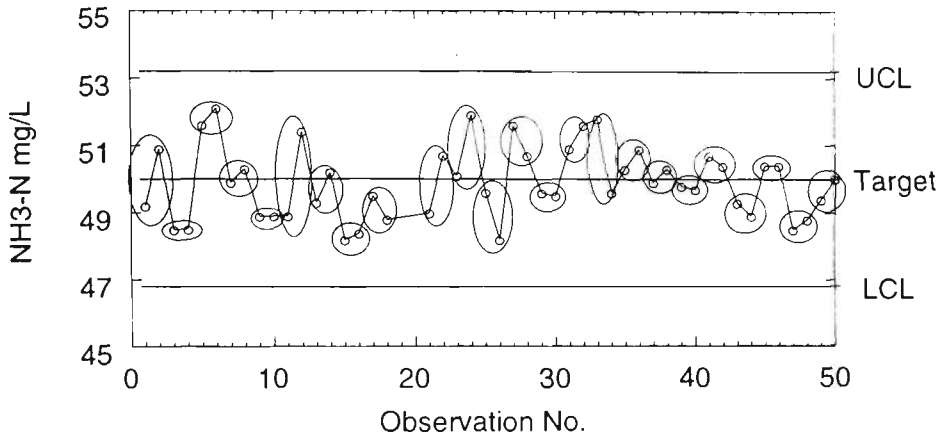

Figure 7-56 ICHART with all data points included and the within-set replicates shown circled.

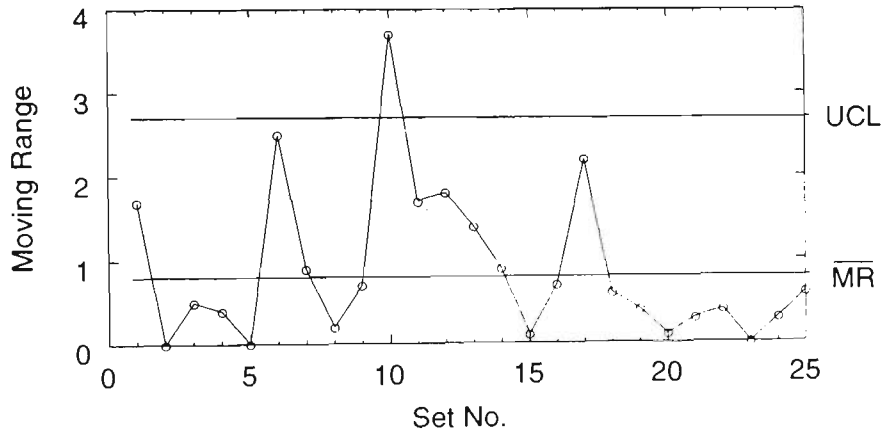

Figure 7-57 MRCHART with all data points shown and only "within-set" control lines.

7.3.3.4 Conclusion

Control charts, like the ones shown here, enable laboratories to control and improve their measurements and measuring equipment, and reduce quality costs. With regard to instrumental analyses, control charts can also lead to a reduced calibration effort, which means savings in time and materials.

Analytical instruments require periodic recalibration to compensate for uncontrollable environmental disturbances and changes that occur in instrument behaviour over time. Replicate QC sample measurements stemming from the same calibration curve tend to be correlated. If intraclass correlation is in evidence, then the model of the measurement process should be modified to include the calibration effect.

Standard control charting methods assume that the QC sample data are independent. Neglecting to account for intraclass correlation, however, will mean either mistakenly accepting "poor quality" test results, or time and money wasted on unnecessarily repeating analyses and searching for assignable causes when none exist.

7.4 CONCLUSION

Process control may be effected by way of *process regulation* or *process monitoring*. The former involves the estimation of disturbances ahead of time and compensation for these disturbances through manipulation of some control variable in order that the process be maintained at a prescribed target level. Process regulation is appropriate when the process suffers from uncontrollable variables that may cause the process to wander off target if continual adjustments are not made. Process monitoring, on the other hand, involves identifying and eliminating assignable causes of variation in order that the process be kept in a state of statistical control. Process monitoring is applicable when the process

tends to remain in a state of statistical control without continual adjustment. Each technique has qualities that make it suitable for the control of anaerobic ponds.

Process regulation was investigated by developing a feedforward-feedback control equation using the raw sewage COD concentration and reactor temperature as feedforward inputs, the effluent SCOD as the output to be controlled, and the raw sewage flowrate as the controllable variable. Both spectral and time domain analyses were used to identify the transfer function-noise model which underpins the control equation. However, the resulting equation tended to over correct for disturbances (i.e. the controller was improperly tuned) and this may be the result of not having randomised the flows during data collection. It was also found that there is little benefit in adding a feedforward component to the control equation because there was no observable delay between the inputs and outputs of the process (i.e. the water column in the pond was virtually completely mixed). Nonetheless, it seems that process regulation is technically possible, although, the size of the flow control actions would likely make it unfeasible due to the lack of capacity to store or divert flows to other treatment systems within the Plant.

Process monitoring, therefore, seemed more appropriate for the control of anaerobic ponds at WTP. While it initially seemed that several variables would need to be monitored, principally because some variables are reported to have value as early warning indicators or as diagnostic tools, it was shown in this study that the time constants for the process outputs (specifically, the effluent SCOD)

are of a similar magnitude to the hydrogen concentration in the gas phase. Furthermore, the diagnostic value of these process indicators has not yet been confirmed. This meant that monitoring the process outputs of effluent SCOD and/or methane flowrate would likely provide as much information as a suite of other variables including hydrogen and volatile fatty acid concentrations. Monitoring one or two variables greatly simplified the development of control charts.

The effluent SCOD concentration exhibited weekly (and probably annual) seasonality and control charts were therefore based on the residuals from an appropriate time series model. The control charts that were constructed in this study suggested that the process was in statistical control throughout the three month study period and, therefore, future monitoring of the anaerobic ponds at WTP could reasonably be done with a sampling interval of greater than one day.

While control charting with respect to a time series model is not particularly complex, the technique may not be practical for most wastewater treatment plant operators. The need for a time series model stems from the presence of serial correlation and seasonality in many environmental data and the main difficulty lies in the identification of an appropriate model. Various methods have been proposed for simplifying the charting procedure in the presence of serial correlation and/or seasonality including limiting model identification to a family of models that have applicability to wastewater treatment plant data or the use of an exponentially weighted moving average (EWMA) statistic to approximate the actual ARIMA model. The simplest

procedure, however, is still time series plots of the original variables, perhaps with some form of smoothing to clarify trends in the data. While this method may not be particularly sensitive to out-of-control conditions, it is still a better means of extracting information from data than tables of numbers. These procedures were discussed in detail in Section 2.4. Further work is required on simple methods for process monitoring of wastewater treatment plants where the data exhibit seasonality and, specifically, when both weekly and annual seasonality are present.

8. Design of Anaerobic Ponds

8.1 INTRODUCTION

In January 1997, the BOD_5 concentration in the effluent from the 115E Anaerobic Reactor increased from about 180 mg/L to 300 mg/L (Figure 8-1), the total VFA level rose from 100 mg/L to 150 mg/L, and the VFA:Alkalinity ratio increased from 0.2 to 0.4. The cause was not immediately clear. The flowrate and BOD_5 concentration of raw sewage had not changed appreciably, though the scum layer within the reactor had continued to increase. In Chapter 4, a study was made of the distribution of methanogens and total anaerobes in the 115E Reactor and the apparent relationship between the scum layer and the "active zone" (i.e. the point at which the densities in methanogens and total anaerobes peak) within the reactor was noted. This chapter investigates this relationship further and discusses the implications for the design and operation of anaerobic ponds.

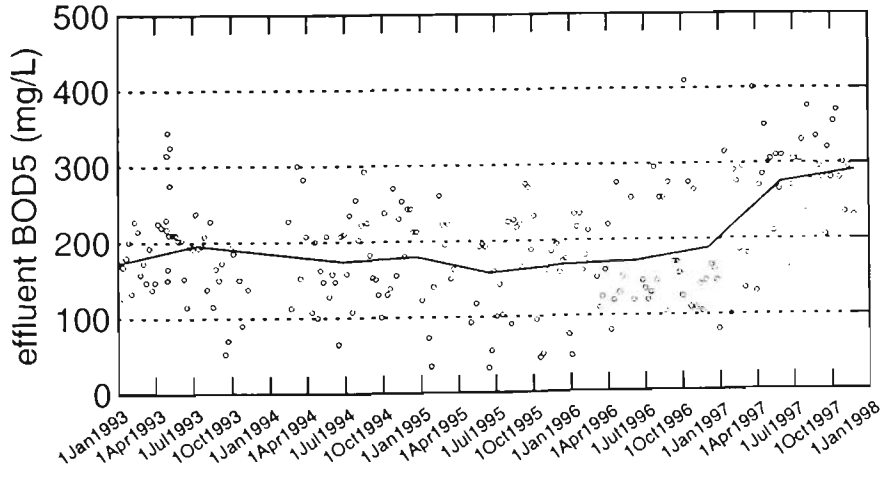

Figure 8-1 Effluent BOD_5 concentration from the 115E Reactor.

8.2 MATERIALS AND METHODS

8.2.1 Description of Sampling Sites and Methods

Sampling sites and methods of sampling anaerobic sludge from the 115E Anaerobic Reactor were detailed in Section 4.2.1. Samples of anaerobic sludge from the 25W Anaerobic Reactor (an uncovered reactor) were taken along a transect from the inlet to outlet of the pond using a Ponar grab dredge (Extech catalogue number E-05471-10).

8.2.2 Anaerobic Methods

The anaerobic methods for culturing methanogens and total anaerobes were described in Section 4.2, though an anaerobic cabinet was used instead of the VPI Anaerobic Culture System.

8.2.3 Measuring the Size of the Scum Layer

The size of the scum layer beneath the cover of the 115E Reactor was measured using ground penetrating radar (GPR). Measurements of the scum and mixed liquor interface were taken at approximately 1 m intervals on 8 longitudinal transects spaced evenly over the 150 m width of the cover The technique was developed by Rock Solid Pty. Ltd.[121].

8.3 RESULTS AND DISCUSSION

8.3.1 Progression of Scum Layer

As mentioned in Chapter 4, a permanent scum layer developed on the 115E Reactor following covering with the HDPE membrane in 1992. Further progression of the scum layer was monitored using ground penetrating radar (GPR). Measurements of the scum thickness for each monitoring occasion, averaged over 10 m intervals along the reactor, are shown in Figure 8-2. The GPR method could not define exactly the interface between scum and liquid, and calibration relied on probing with a stick at some of the sampling ports. It should be noted that, during sampling for the process control study in 1995, the firm scum layer appeared to diminish after the 100 m mark. It may be reasonable therefore to subtract 0.5 m from all depth measurements.

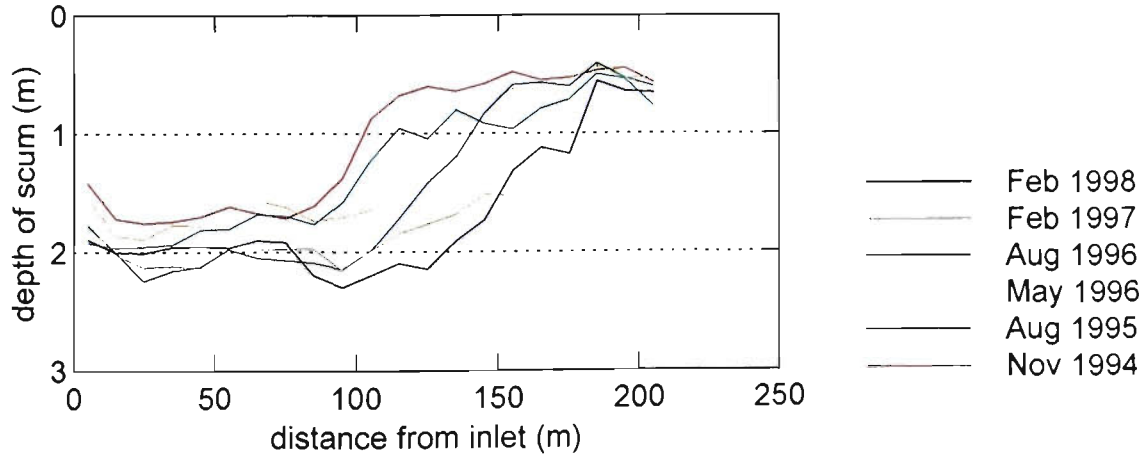

Figure 8-2 Progression of scum layer thickness between 1994 and 1998 (note the reactor is 3 m deep, 150 m wide and 220 m long).

8.3.2 Relationship Between Active Zone and Scum Layer

Following the shift in the effluent BOD_5 in January 1997, the profile of methanogen and total anaerobe densities that was performed in July 1995 was repeated in September 1997. Plots of the cultural counts and the profile of the scum layer at approximately the same time are shown as Figure 8-3 and Figure 8-4.

As pointed out in Section 4.3.5 the peak in methanogen and total anaerobe densities in 1995 seemed to coincide with the end of the scum layer. This was true also for the samples taken in 1997. This is further evidence to support the explanation advanced in Section 4.3.5 that the scum forms as a result of the formation and entrapment of gases within the anaerobic floc and granules resulting in the flotation of the sludge. The scum is essentially "floating" sludge.

It was also hypothesised, in Section 4.4, that the active zone corresponds to the area where most of the influent suspended matter (including colloidal matter flocculated naturally within the reactor) settles in the pond. To test this hypothesis, the flowrate to the 115E Reactor was reduced from about 60 ML/d to 50 ML/d in July 1997. The profile of bacterial densities was measured again in June 1998. It was expected that the active zone should establish again earlier within the reactor, i.e. toward the inlet. Figure 8-5 shows that the active zone did in fact appear to move back from the outlet of the reactor to the 150 m mark.

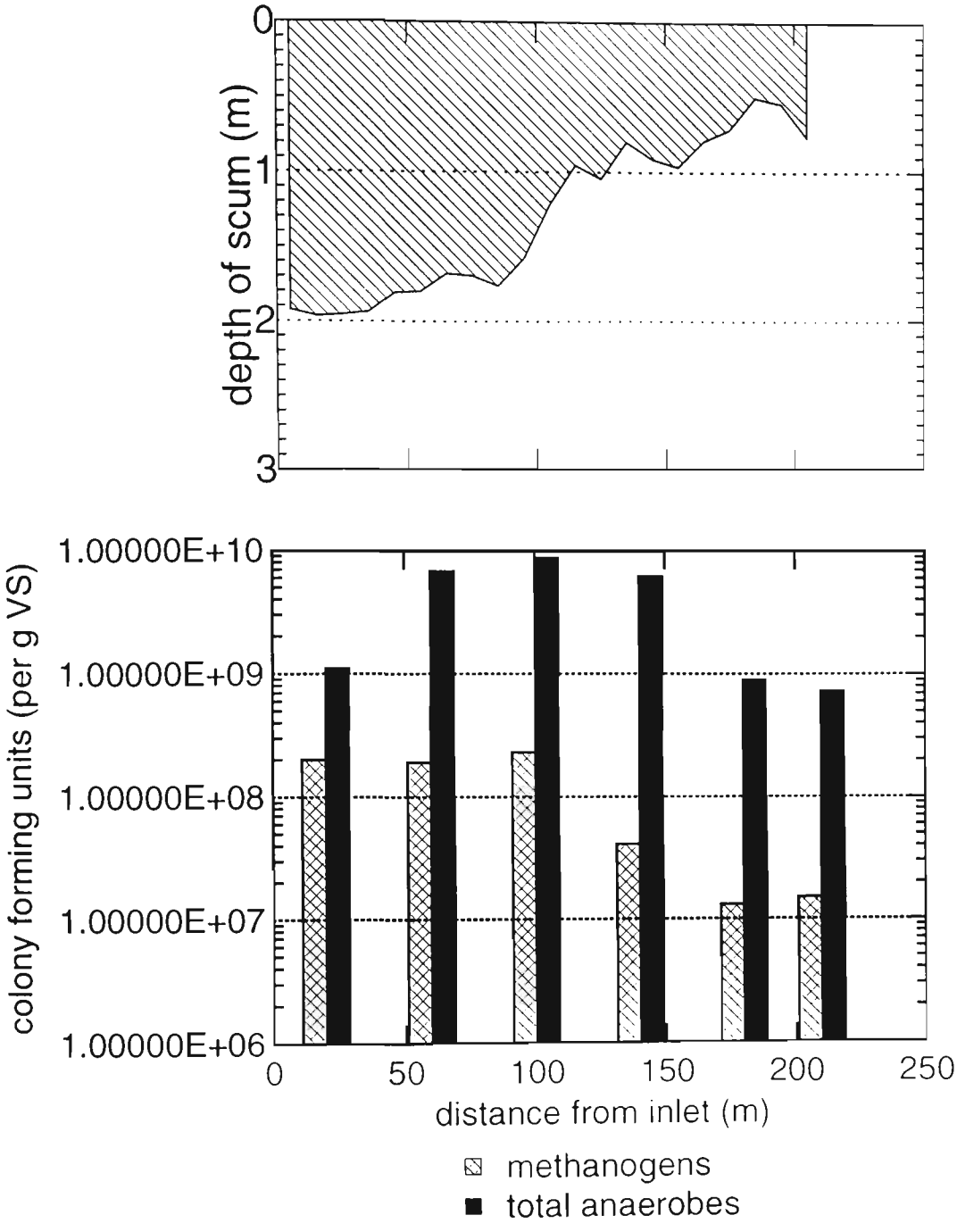

Figure 8-3 Correspondence of the scum layer and active zone in 1995.

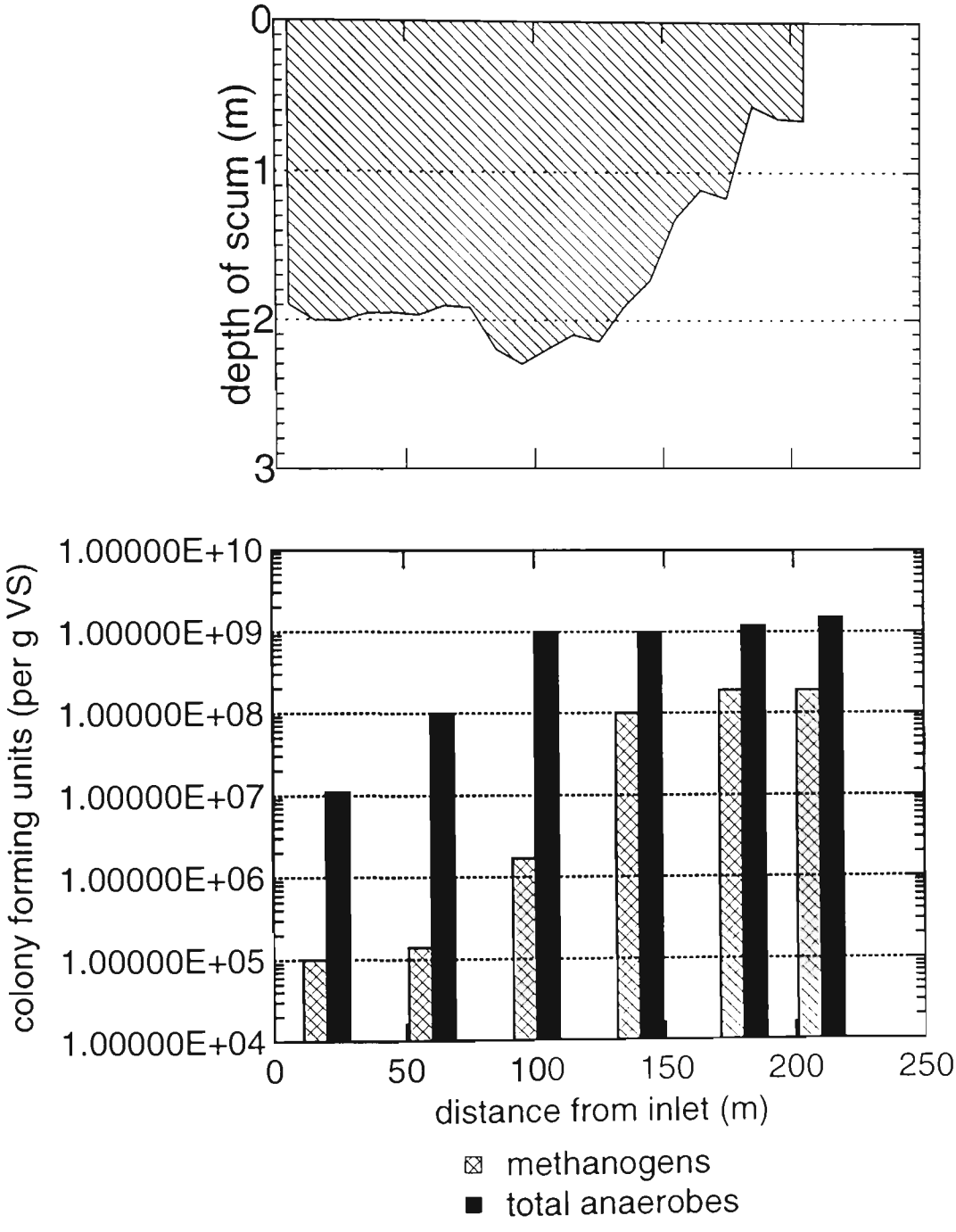

Figure 8-4 Correspondence of the scum layer and active zone in 1997.

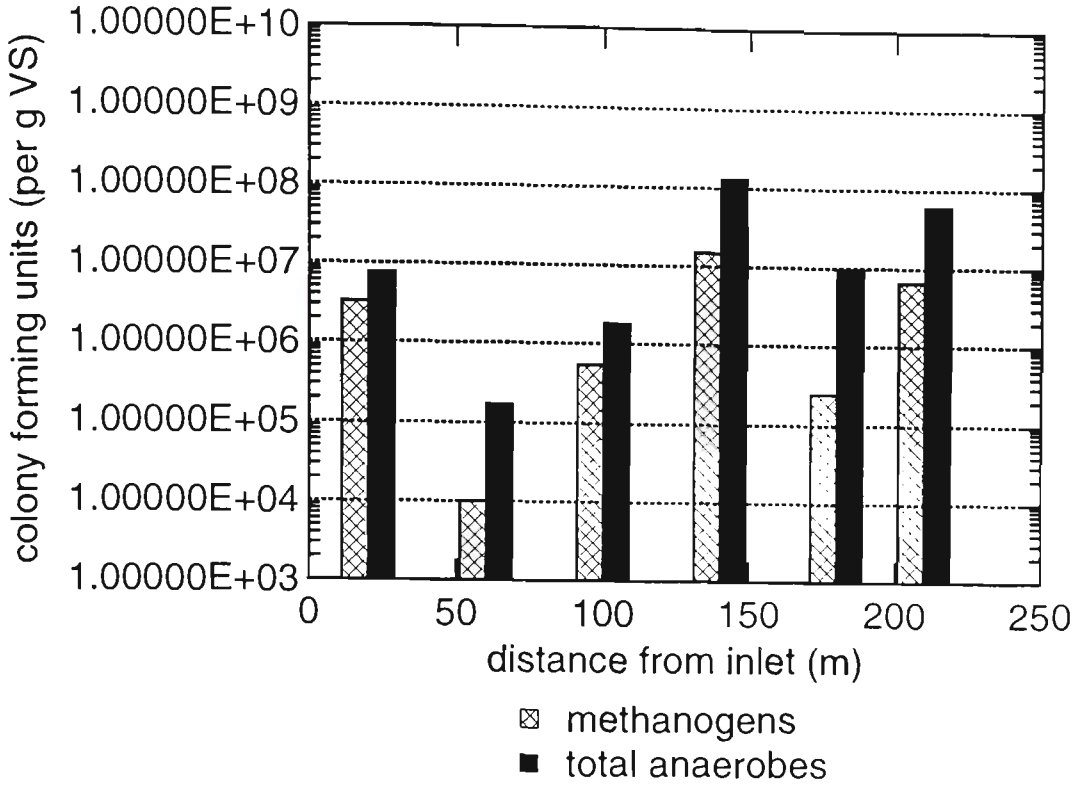

Figure 8-5 Profile of methanogen and total anaerobe densities in the 115E Reactor in June 1998.

8.3.3 Modelling the Location of the Active Zone

A simple mathematical model can be used to describe the effect of scum and sludge accumulation on the position of the active zone. The premise of the model is that the hydraulic velocity in the reactor increases almost exponentially with increasing volume of sludge and scum within the pond, resulting in the settlement of suspended matter further along the reactor and the movement of the active zone toward the outlet of the pond. The hydraulic velocity through the pond is given by:

$$v = \frac{\text{flowrate into pond}}{\text{cross sectional area of pond}} = \frac{Q}{w_p(d_p - h_s)}$$ **Equation 8-1**

where v=hydraulic velocity (m/d)

Q=flowrate into pond (m^3/d)

w_p=width of pond (m)

d_p=depth of pond (m)

h_s=height of sludge (m).

The height of sludge can be determined from the sludge volume (discussed below) and surface area of the pond. Equation 8-1 and the sludge height calculation assumed that the cross section of the pond was rectangular, although, it is actually trapezoidal.

The position of the active zone from the inlet of the pond can then be deduced from the hydraulic velocity and the settling velocity of sludge:

$$Z_a = \frac{v \times d_p}{v_s}$$ **Equation 8-2**

where Z_a=distance of active zone from inlet of pond (m)

v=hydraulic velocity (m/d) from Equation 8-1

d_p=depth of pond (m)

v_s=sludge settling velocity (m/d)

Equation 8-1 and Equation 8-2 can then be combined to give the "active zone" model:

$$Z_a = \frac{Q.d_p}{w_p.(d_p - h_s).v_s} \qquad \textbf{Equation 8-3}$$

where Z_a, the distance of the active zone from the inlet in metres, is equivalent to the required design length of the pond. Interestingly, if $d_p >> h_s$ then d_p cancels out in Equation 8-3 and the position of the active zone depends only on the flowrate, width of the pond and settling velocity of the sludge. Or, alternatively, the required area of the pond is determined by the flowrate divided by the settling velocity of the sludge. That is, deeper ponds will not necessarily mean a smaller pond surface area or plastic cover. The advantage of deeper ponds, therefore, seems to lie only in their greater capacity to store sludge. For open ponds, depth also minimises air entrainment due to wind-induced mixing.

In order to predict the position of the active zone, a model of the sludge accumulation rate is required. Saqqar and Pescod[122] developed a model of sludge accumulation for anaerobic ponds which is given as .

$$V_{AS} = 0.6(1.7F_{XVSS,i} + 4.5F_{XFSS,i} + F_{CBOD,i}) \qquad \textbf{Equation 8-4}$$

where V_{AS} = sludge accumulation rate (m^3/d)

$F_{XVSS,i}$ = mass loading of raw sewage volatile suspended solids (kg/d)

$F_{XFSS,i}$ = mass loading of raw sewage fixed suspended solids (kg.d)

$F_{CBOD,i}$ = mass loading of carbonaceous BOD_5 (kg/d).

The model takes into account fixed and volatile solids loading rates, the BOD_5 removal rate, production of bacterial biomass, and decay of both volatile and fixed suspended solids. It seems incorrect, though, that the model uses both the carbonaceous BOD_5 ($CBOD_5$) and volatile suspended solids (VSS) to calculate

the sludge produced. The model assumes that the influent VSS settles as sludge and that the $CBOD_5$ is converted to biomass which then settles as sludge. However, the VSS is a component of the $CBOD_5$ and will potentially be metabolised to form biomass, thus resulting in a "double counting" of the VSS contribution to sludge. It is fair to say, though, that toilet tissue fibres make up a large part of the VSS and toilet tissue, which is composed of cellulose, is not readily biodegraded.

Using Equation 8-3 and Equation 8-4 the location of the active zone was plotted as a function of time in Figure 8-6. Note that the rate of sludge accumulation in the 115E Reactor was calculated to be 20 m^3/d and a sludge settling velocity of 10 m/h was assumed (which is typical for primary sludges). The calculation must initially assume a pond area (and therefore length) to calculate the height of the sludge. This has little effect, however, on the initial shape of the curve.

The 115E Lagoon was commissioned in March 1986 with a flowrate of 30 ML/d. The flowrate was increased gradually to its normal operating level of 60 ML/d by early 1989. Making the approximation that this is equivalent to about 10 years of operation at full flow by September 1997, Equation 8-4 predicts that the 115E Reactor would have had an accumulated sludge volume of about 70 ML. While the sludge volume is difficult to measure, it is estimated from GPR

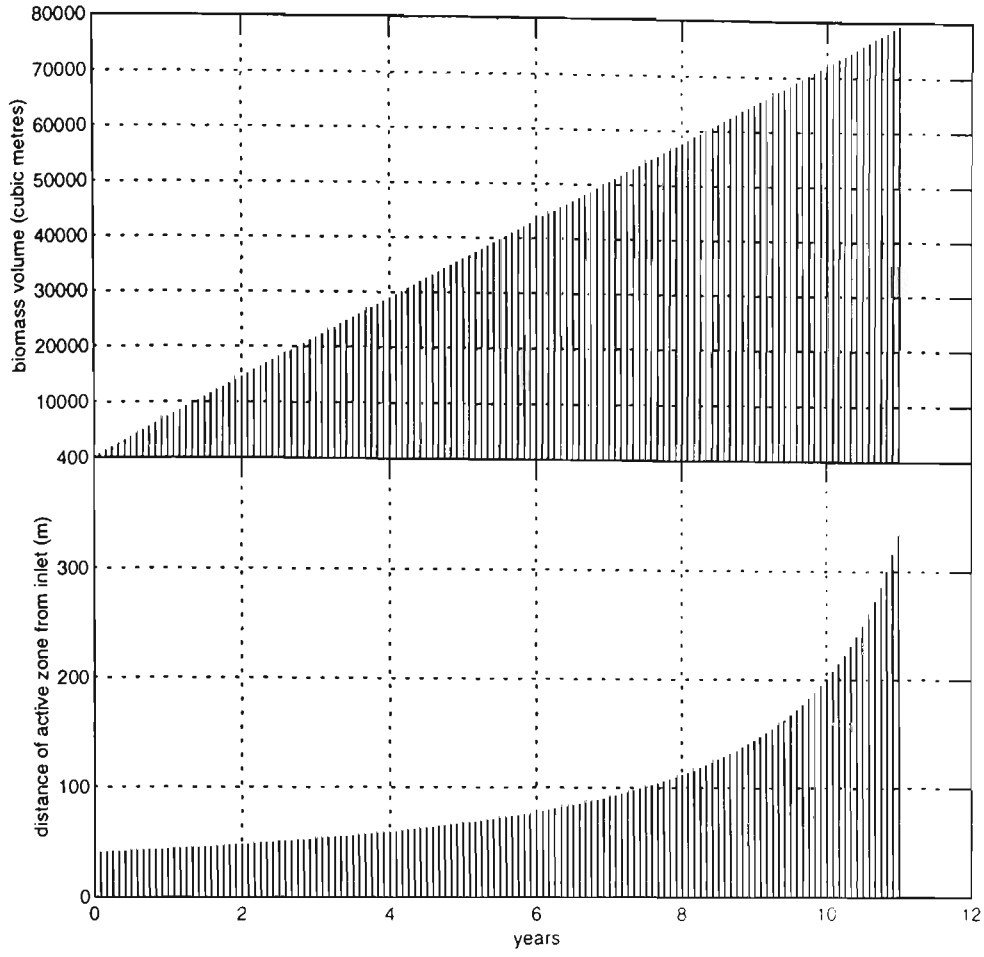

Figure 8-6 Predicted sludge volume and position of active zone in the 115E Reactor.

and probing surveys that the total volume of sludge and scum at this time was approximately equal to this value. Equation 8-3 predicts that the active zone would be at the end of the reactor, with this volume of sludge and scum, which agrees with the observation given in Figure 8-4. Now, the effect of reducing the flowrate to 50 ML/d can also be predicted and is given in Figure 8-7. The model predicts that the active zone would re-establish at 150-160 m from the inlet of the reactor and this corresponds with the profile of methanogens and total anaerobes measured in June 1998 (Figure 8-5).

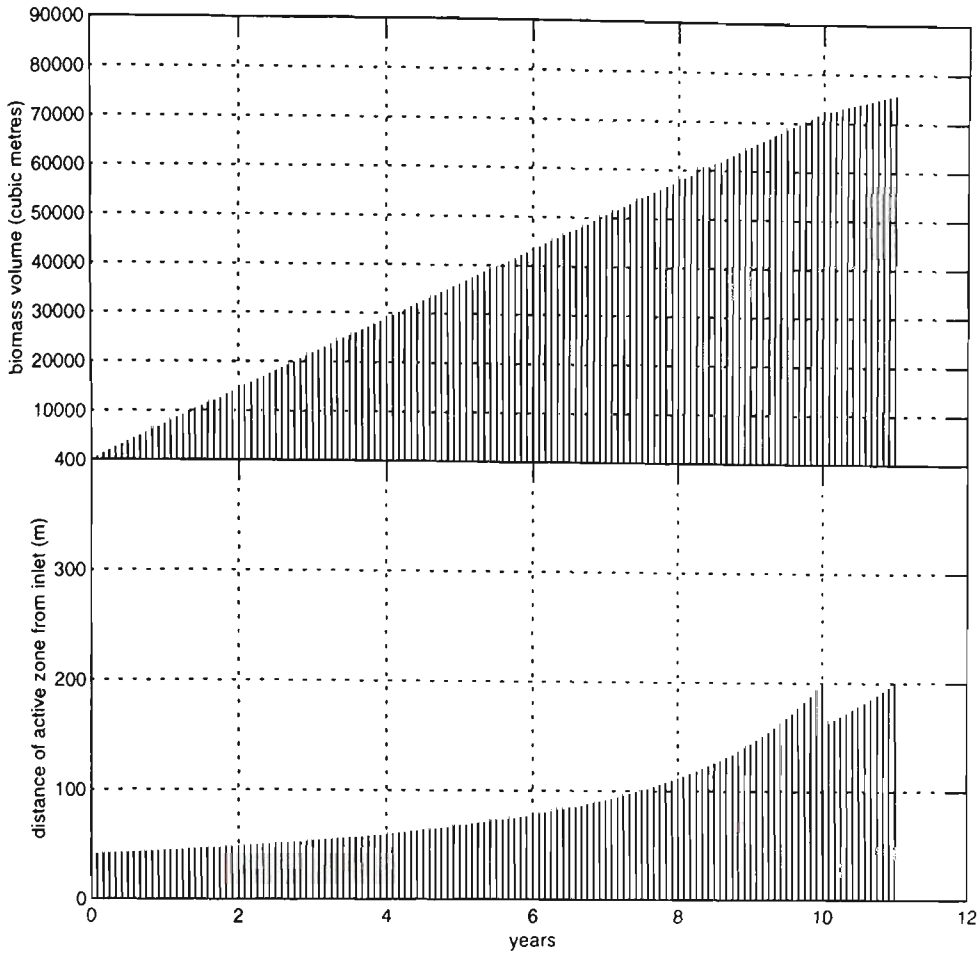

Figure 8-7 Effect of reducing the flowrate from 60 ML/d to 50 ML/d, after 10 years, on the position of the active zone in the 115E Reactor.

The model was also tested on the 25W Reactor, which has been in operation since 1993 (approximately 5 years). The 25W Reactor has a volume of about 250 ML, a depth of 8 m, and width of 190 m. At the time of this study the reactor was uncovered and had no observable scum layer. The 25W Reactor receives approximately 100 ML/d of raw sewage and recent sludge surveys indicated the volume of sludge to be about 80 ML. The models predicted that there would be an accumulated sludge volume of about 75 ML after 5 years of operation, and the active zone would be 75 m from the inlet (Figure 8-8). The

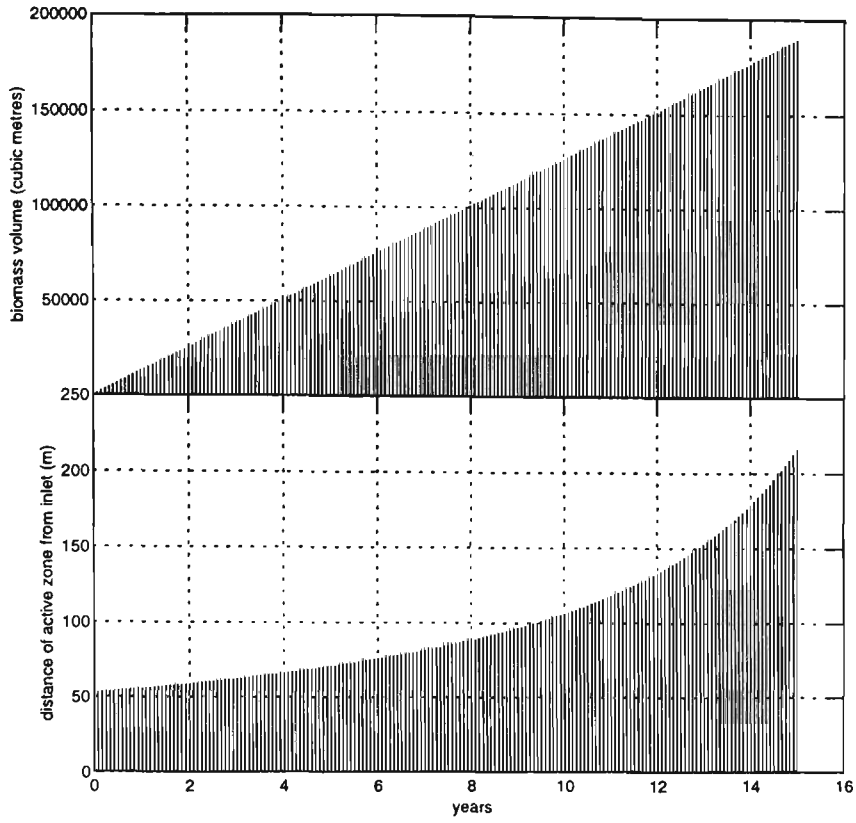

Figure 8-8 Predicted sludge volume and position of active zone in the 25W Reactor.

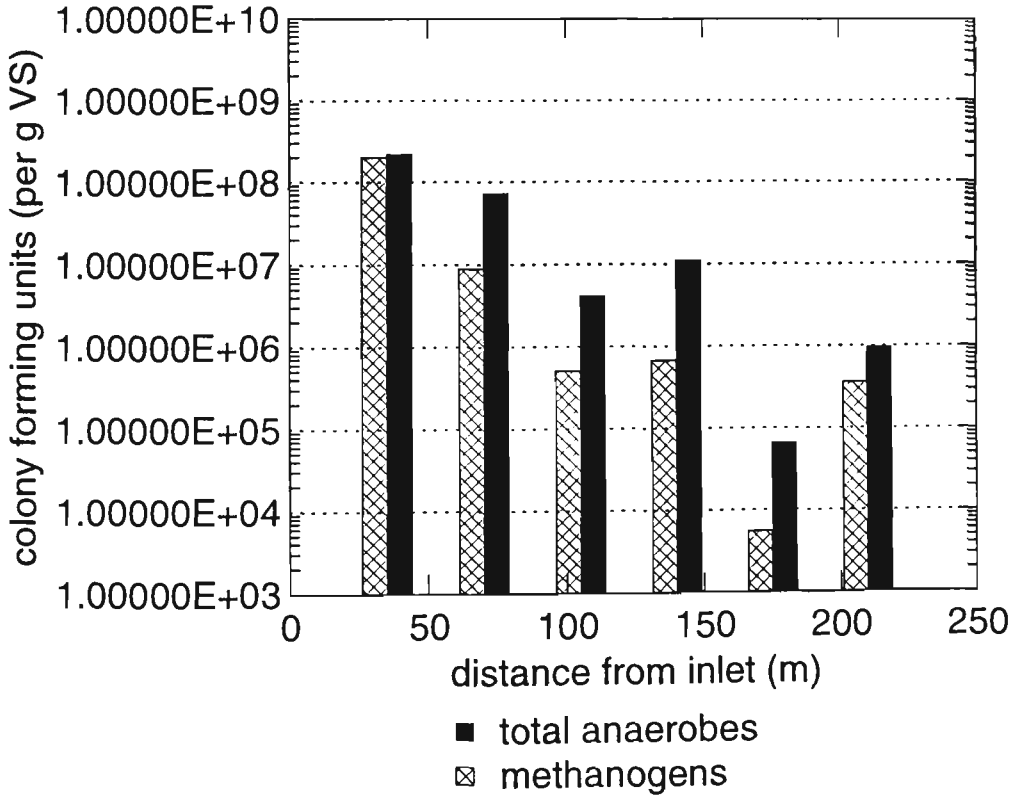

Figure 8-9 Profile of methanogen and total anaerobe densities in the 25W Reactor.

profile of methanogens and total anaerobes was measured in June 1998 and is shown in Figure 8-9. The observed and predicted position of the active zone agree reasonably well.

8.3.4 Optimal Sludge Level for Operation of Anaerobic Ponds

It is apparent from the preceding that if desludging does not happen, then the accumulated sludge volume could reach a critical level where the active zone is washed out of the pond. The optimal sludge volume can be determined from the time taken for a newly commissioned pond to reach steady state in terms of the effluent BOD_5 concentration. Previous work at WTP[123] indicated that anaerobic ponds reach steady state 80-120 days after commissioning. For the 115E Reactor, using an accumulation rate of 20 m^3/d calculated from Equation 8-4, this is equivalent to sludge volume of about 2.5 ML, or a sludge height of 8 cm which is about 3% of the pond depth. Sludge levels beyond this optimal value represent wasted treatment capacity and/or reactor over-design.

8.3.5 Design of Anaerobic Ponds

As scum and sludge have accumulated in the 115E Reactor, the effective hydraulic residence time (HRT) has decreased from about 1.5 d to 0.3 d. There was, however, no discernible increase in the effluent BOD_5 concentration (see Figure 8-1), until January 1997, and no decrease in gas and power production.

This suggests that HRT does not significantly affect BOD_5 removal, which agrees with the findings of Section 7.3.1.

Given that approximately 60% BOD_5 removal is achieved by anaerobic ponds, which is significantly greater than the 20% BOD_5 removal expected from primary sedimentation alone, and that most bacterial activity occurs within the sludge layer, the removal of BOD_5 likely includes the destabilisation and settlement of colloidal organic matter through the action of natural polyelectrolytes produced by anaerobic bacteria. The gross solids, coalesced suspended matter and flocculated colloids then settle on the invert of reactor where they are degraded. As long as the solids residence time (SRT) is sufficient to allow a methanogenic population to establish, the reactor should function effectively. Soluble organic matter, however, may largely pass through the pond untreated unless some form of mechanical mixing or sludge recirculation was introduced.

The optimal size of an anaerobic pond, therefore, seems to be determined by the required sludge age and corresponding location of the active zone. The location of the active zone will, in turn, be determined by the volumetric flowrate, the lateral cross sectional area of the pond and the settling velocity of the sludge. For the 115E Reactor, with a sludge age of 120 d, the minimum length of the reactor would be about 40 m (from Figure 8-6) or 0.3 d HRT. Given the effect of variability in hydraulic and settling velocities, which is evidenced in the broadness of the peaks in the profiles of methanogen and total anaerobe densities (Figure 8-3), the maximum length of the reactor would need to be about 100 m or

0.75 d HRT. A pond of this size (0.75 d HRT), equates to an organic loading rate of 600 g $BOD_5/m^3.d$.

These findings suggest that the area of the 115E Reactor could have been halved and the capital savings, for the cover alone, may have been in excess of $1M. However, this would necessitate reasonably frequent desludging (once or twice per year) and at present there is no means of desludging beneath the fixed cover. Covered anaerobic ponds, or Bulk Volume Fermenters, designed and constructed by ADI Pty. Ltd[124], usually have a system of sludge withdrawal pipes that are used also for sludge recirculation. For WTP, the only drawback to such a system is that pre-screening of the influent may be required

8.4 CONCLUSION

While it was not the original intention of this thesis to address the design of anaerobic ponds, certain findings have been made which may provide an alternative design approach. Specifically, it appears that BOD_5 removal is achieved firstly through a physical process of flocculation and settlement of suspended and colloidal matter, followed by anaerobic degradation in the sediment or sludge layer. Not surprisingly, this mechanism is similar to that described for stormwater pollution control ponds[125]. The design factors that need to be considered are the flowrate, lateral cross sectional area of the pond and settling velocity of the sludge. Armed with these three factors, the length of the pond can be determined. The depth of the pond has little effect on the required

length or surface area of the pond and the advantage of depth seems to lie in a greater capacity to store sludge (and therefore increase the desludging interval) and reduced air entrainment from wind-induced mixing. It should be noted that the settling velocity of the sludge would need to be determined after mixing a sample of raw sewage with digester liquor containing the exoploysaccharides that act as flocculants.

Previously, anaerobic ponds had been designed on the basis of organic loading and/or hydraulic residence time, with reported loadings varying between 30 and 600 g BOD_5/m^3.d and HRT's from 0.5 to 50 d for ponds treating domestic wastewater[74]. More recently, the consideration of the settleable solids fraction in the sewage has been recommended for design of anaerobic ponds[74,126], which is along similar lines to the design concept presented here.

The description of the BOD_5 removal process given in this chapter needs to be reconciled with the dynamics of the process reported in Section 7.3.1. In particular, the considerable effect of temperature is difficult to explain (a conundrum recognised by Pinto and Needer et. al[126]). Saqqar and Pescod have suggested that increasing temperature improves the settleability of suspended matter according to Stokes Law. It may also be that the increased bacterial activity and gas production leads to better contact between bacteria and soluble substrate. Further work to clarify the mechanisms involved may lead to more definitive design models.

The significance of temperature highlights the value in insulating covers for anaerobic ponds. The raw sewage at WTP has an August (Winter)

temperature of about 19°C, whereas the water in the 115E Reactor (even with a HDPE cover) has a temperature of around 15.5°C. Given that heating the influent is uneconomical, and most of the heat loss probably occurs at the pond's surface, a well insulated cover could reduce the effluent COD by an average of 90 mg/L or 30% (based on the relationship between effluent SCOD and temperature given in Section 7.3.1). A similar percentage increase in gas production might also be expected.

9. Conclusion

This research has demonstrated the benefits of an empirical study of the dynamics of anaerobic ponds, and biological wastewater treatment processes in general, to developing an appropriate process control scheme. This study showed quantitatively the relationship between effluent COD concentration and flowrate (the only controllable variable), raw sewage COD concentration and pond temperature. The transfer function-noise model that was derived made the choice between process regulation and process monitoring much clearer.

Both process regulation and process monitoring have qualities that make them suitable for the control of anaerobic ponds. Process regulation, however, requires that there be sufficient capacity to store or divert flows to other treatment systems to be effective. This research demonstrated that there was probably insufficient capacity at WTP to practice process regulation and, therefore, process monitoring using control charts is likely more appropriate to the control of anaerobic ponds and natural treatment systems in general. However, to ensure the acceptance and routine use of control charting techniques by wastewater treatment plant operators, more work is required to simplify the construction of statistically effective charts where serial correlation is in evidence.

The transfer function can also suggest ways of improving the process. For example, temperature was found to be the main cause of variation in methane yield (and effluent COD) and, while it is not economic to heat the anaerobic pond, better cover designs may reduce the loss of heat at the pond's surface and

improve performance by as much as 20-30 %. This is certainly one area for further research.

Furthermore, studying the dynamics of the process indicators and examining the reasons for their measurement helps to clarify exactly what is needed in the eventual process control scheme. In this study it was found that measurement of the effluent COD or methane flowrate would provide as much information as the eleven variables typically recommended for anaerobic digestion control.

Moreover, this research has shown clearly the need to go beyond input-output analyses to improve understanding of the treatment mechanisms occurring within anaerobic ponds. Measurement of viable methanogens and total anaerobes within the sludge (and scum) layer of anaerobic ponds has provided considerable insight into the workings of the process. This information can be used to optimise the design of anaerobic ponds and avoid unnecessary failure of these systems. While this work has provided some insight into the dynamics and mechanisms of BOD_5 removal in anaerobic ponds, further research is needed to bring these two together in the form a dynamic-mechanistic model. Such a model would be an invaluable tool in making further advancements in the design and operation of anaerobic ponds. The model could, for example, be expanded to include the effects of mixing or recirculation of biomass to improve the removal of soluble organic matter.

Finally, it was shown that there can be a cost benefit in identifying and managing the risks posed by trade wastes. This research indicated that sulphate

ion is inhibitory to anaerobic digestion at WTP, where it is present in raw sewage at approximately 30 mg/L SO_4^{2-}-S, while calcium ion appears deficient. Minimising the concentrations of inhibitory chemicals, and encouraging stimulatory ones, is just one way to improve the performance and sustainability of biological wastewater treatment plants.

A limitation on reducing the sulphate ion concentration in trade wastes is the theoretical solubility of calcium sulphate. Slaked lime, or calcium hydroxide, is typically used to treat sulphate bearing wastes by precipitating the sulphate ion as calcium sulphate. The solubility product for calcium sulphate is 2.5×10^{-5} at 25°C, which equates to an equilibrium sulphate concentration of about 150 mg/L SO_4^{2-}-S. Further research into alternative methods for treating sulphate bearing wastes, or replacing sulphur compounds in industrial processes, is required.

This research has provided a number of options for improving the design and performance of anaerobic ponds and this chapter has outlined the direction for further research which should see continued improvement.

Appendix A . Data for Spatial and Temporal Variability of Process Control Variables

Table Appendix A -1 Spatial and temporal variability of some common process control variables in the 115E reactor* over a single loading period.

3/3/92 6:00 PM

Site No.	Influent
pH	6.8
Temp	23.8
EP	-340
TS	1410
VS	560
VFA	190
Alk	395
VFA/Alk	0.48
BOD_5	420

Site No. (coordinates)	1 (25m, 20m)		2 (75m, 20m)		3 (125m, 20m)	
Depth	0.75m	**2.25m**	0.75m	**2.25m**	0.75m	**2.25m**
pH	6.6	**6.7**	6.7	**6.6**	6.6	**6.5**
Temp	23.7	**23.8**	23.8	**23.7**	23.7	**23.7**
EP	-370	**-360**	-360	**-370**	-350	**-370**
TS	1700	**3070**	1840	**5700**	2280	**52860**
VS	500	**1490**	630	**3160**	1030	**32770**
VFA	115	**90**	105	**30**	155	**230**
Alk	465	**530**	465	**835**	525	**1740**
VFA/Alk	0.25	**0.17**	0.23	**0.04**	0.30	**0.13**
Site No. (coordinates)	4 (25m, 60m)		5 (75m, 60m)		6 (125m, 60m)	
Depth	0.75m	**2.25m**	0.75m	**2.25m**	0.75m	**2.25m**
pH	-	-	-	-	-	-
Temp	-	-	-	-	-	-
EP	-	-	-	-	-	-
TS	-	-	-	-	-	-
VS	-	-	-	-	-	-
VFA	-	-	-	-	-	-
Alk	-	-	-	-	-	-
VFA/Alk	-	-	-	-	-	-
Site No. (coordinates)	7 (25m, 100m)		8 (75m, 100m)		9 (125m, 100m)	
Depth	0.75m	**2.25m**	0.75m	**2.25m**	0.75m	**2.25m**
pH	6.7	**6.6**	6.6	**6.6**	6.6	**6.6**
Temp	23.3	**23.6**	23.5	**23.6**	23.7	**23.8**
EP	-350	**-380**	-350	**-350**	-330	**-360**
TS	2560	**46290**	1950	**48130**	2190	**42170**
VS	1130	**28050**	700	**29500**	880	**25980**
VFA	70	**55**	60	**75**	80	**125**
Alk	495	**1425**	480	**1475**	475	**1595**
VFA/Alk	0.14	**0.04**	0.12	**0.05**	0.17	**0.08**

* Refer to the plan of the sampling sites given as Figure 3-1, p.3-2. Note that the coordinates of the sampling sites, relative to the north corner of the reactor, are given in brackets adjacent to the site number.

Table Appendix A -1 continued

3/3/92 6:00 PM

Site No. (coordinates)	10 (25m, 140m)		11 (75m, 140m)		12 (125m, 140m)	
Depth	0.75 m	**2.25 m**	0.75 m	**2.25 m**	0.75 m	**2.25 m**
pH	-	-	-	-	-	-
Temp	-	-	-	-	-	-
EP	-	-	-	-	-	-
TS	-	-	-	-	-	-
VS	-	-	-	-	-	-
VFA	-	-	-	-	-	-
Alk	-	-	-	-	-	-
VFA/Alk	-	-	-	-	-	-
Site No. (coordinates)	13 (25m, 180m)		14 (75m, 180m)		15 (125m, 180m)	
Depth	0.75 m	**2.25 m**	0.75 m	**2.25 m**	0.75 m	**2.25 m**
pH	6.7	**6.6**	6.7	**6.6**	6.7	**6.6**
Temp	23.3	**23.1**	23.6	**23.6**	23.5	**23.5**
EP	-340	**-350**	-340	**-370**	-330	**-360**
TS	1340	**62850**	1280	**56680**	1200	**48650**
VS	350	**37020**	220	**34400**	280	**29190**
VFA	85	**50**	70	**155**	65	55
Alk	460	**1825**	455	**1590**	465	1545
VFA/Alk	0.18	**0.03**	0.15	**0.10**	0.14	0.04
Site No. (coordinates)	16 (25m, 220m)		17 (75m, 220m)		18 (125m, 220m)	
Depth	0.75 m	**2.25 m**	0.75 m	**2.25 m**	0.75 m	2.25 m
pH	-	-	-	-	-	-
Temp	-	-	-	-	-	-
EP	-	-	-	-	-	-
TS	-	-	-	-	-	-
VS	-	-	-	-	-	-
VFA	-	-	-	-	-	-
Alk	-	-	-	-	-	-
VFA/Alk	-	-	-	-	-	-
Site No. (coordinates)	19 (25m, 240m)		20 (75m, 240m)		21 (125m, 240m)	
Depth	0.75 m	**2.25 m**	0.75 m	2.25 m	0.75 m	2.25 m
pH	6.7	**6.6**	6.7	**6.6**	6.7	6.7
Temp	23.7	**23.3**	23.5	**23.1**	23.5	**23.4**
EP	-330	**-350**	-330	**-360**	-340	**-380**
TS	1380	**59700**	1270	**85000**	1200	**44930**
VS	450	**35220**	230	**32900**	100	**26460**
VFA	80	**120**	100	**105**	70	**110**
Alk	465	**1855**	465	**1720**	460	**1630**
VFA/Alk	0.17	**0.06**	0.22	**0.06**	0.15	**0.07**
BOD_5	210	**750**	190	**290**	180	730

Table Appendix A -1 continued

4/3/92 3:00 AM

Site No.	Influent
pH	6.8
Temp	23.6
EP	-220
TS	1430
VS	400
VFA	235
Alk	395
VFA/Alk	0.59
BOD_5	470

Site No. (coordinates)	1 (25m, 20m)		2 (75m, 20m)		3 (125m, 20m)	
Depth	0.75m	**2.25m**	0.75m	**2.25m**	0.75m	**2.25m**
pH	6.7	**6.6**	6.8	**6.7**	6.7	**6.6**
Temp	23.5	**23.5**	23.5	**23.6**	23.5	**23.5**
EP	-280	**-300**	-300	**-330**	-320	**-330**
TS	1260	**3680**	1460	**9520**	2190	**37460**
VS	310	**1920**	440	**5490**	940	**21910**
VFA	100	**100**	95	**60**	105	**125**
Alk	460	**525**	465	**645**	495	**1495**
VFA/Alk	0.22	**0.19**	0.20	**0.09**	0.21	**0.08**

Site No. (coordinates)	4 (25m, 60m)		5 (75m, 60m)		6 (125m, 60m)	
Depth	0.75m	**2.25m**	0.75m	**2.25m**	0.75m	**2.25m**
pH	-	**-**	-	**-**	-	**-**
Temp	-	**-**	-	**-**	-	**-**
EP	-	**-**	-	**-**	-	**-**
TS	-	**-**	-	**-**	-	**-**
VS	-	**-**	-	**-**	-	**-**
VFA	-	**-**	-	**-**	-	**-**
Alk	-	**-**	-	**-**	-	**-**
VFA/Alk	-	**-**	-	**-**	-	**-**

Site No. (coordinates)	7 (25m, 100m)		8 (75m, 100m)		9 (125m, 100m)	
Depth	0.75m	**2.25m**	0.75m	**2.25m**	0.75m	**2.25m**
pH	6.7	**6.6**	6.7	**6.6**	6.7	**6.6**
Temp	23.4	**23.6**	23.5	**23.6**	23.5	**23.5**
EP	-310	**-320**	-310	**-320**	-330	**-320**
TS	1840	**58810**	1450	**45030**	1920	**35930**
VS	710	**33870**	490	**27560**	760	**22460**
VFA	80	**245**	85	**205**	105	**145**
Alk	480	**1745**	485	**1655**	475	**1460**
VFA/Alk	0.17	**0.14**	0.18	**0.12**	0.22	**0.10**

Table Appendix A -1 continued

4/3/92 3:00 AM

Site No. (coordinates)	10 (25m, 140m)		11 (75m, 140m)		12 (125m, 140m)	
Depth	0.75 m	**2.25 m**	0.75 m	**2.25 m**	0.75 m	**2.25 m**
pH	-	-	-	-	-	-
Temp	-	-	-	-	-	-
EP	-	-	-	-	-	-
TS	-	-	-	-	-	-
VS	-	-	-	-	-	-
VFA	-	-	-	-	-	-
Alk	-	-	-	-	-	-
VFA/Alk	-	-	-	-	-	-
Site No. (coordinates)	13 (25m, 180m)		14 (75m, 180m)		15 (125m, 180m)	
Depth	0.75 m	**2.25 m**	0.75 m	**2.25 m**	0.75 m	**2.25 m**
pH	6.7	**6.6**	6.7	**6.6**	6.7	**6.6**
Temp	23.4	**23.6**	23.6	**23.7**	23.3	**23.5**
EP	-320	**-310**	-315	**-330**	-320	**-320**
TS	1370	**73570**	1330	**50000**	1480	**63000**
VS	220	**44880**	370	**30400**	450	**41640**
VFA	70	**305**	85	**45**	110	**435**
Alk	465	**2075**	465	**1520**	480	**1715**
VFA/Alk	0.15	**0.15**	0.18	**0.03**	0.23	**0.25**
Site No. (coordinates)	16 (25m, 220m)		17 (75m, 220m)		18 (125m, 220m)	
Depth	0.75 m	**2.25 m**	0.75 m	**2.25 m**	0.75 m	**2.25 m**
pH	-	-	-	-	-	-
Temp	-	-	-	-	-	-
EP	-	-	-	-	-	-
TS	-	-	-	-	-	-
VS	-	-	-	-	-	-
VFA	-	-	-	-	-	-
Alk	-	-	-	-	-	-
VFA/Alk	-	-	-	-	-	-
Site No. (coordinates)	19 (25m, 240m)		20 (75m, 240m)		21 (125m, 240m)	
Depth	0.75 m	**2.25 m**	0.75 m	**2.25 m**	0.75 m	**2.25 m**
pH	6.7	**6.6**	6.7	**6.6**	6.7	**6.7**
Temp	23.1	**23.3**	23.3	**23.3**	23.3	**23.2**
EP	-320	**-330**	-310	**-320**	-310	**-320**
TS	1900	**56200**	1730	**71090**	1230	**42820**
VS	690	**34110**	580	**43860**	260	**25730**
VFA	85	**55**	90	**65**	80	**60**
Alk	500	**1775**	475	**2305**	485	**1360**
VFA/Alk	0.17	**0.03**	0.19	**0.03**	0.16	**0.04**
BOD_5	230	**190**	200	**720**	170	**710**

Table Appendix A -1 continued

4/3/92 10:00 AM

Site No.	Influent
pH	-
Temp	-
EP	-
TS	-
VS	-
VFA	-
Alk	-
VFA/Alk	-
BOD_5	-

Site No. (coordinates)	1 (25m, 20m)		2 (75m, 20m)		3 (125m, 20m)	
Depth	0.75m	**2.25m**	0.75m	**2.25m**	0.75m	**2.25m**
pH	6.8	**6.7**	6.7	**6.7**	6.7	**6.6**
Temp	24.0	**23.8**	23.8	**23.7**	23.8	**23.8**
EP	-230	**-280**	-290	**-310**	-320	**-320**
TS	1460	**22710**	1490	**26440**	1490	**50100**
VS	440	**13670**	230	**18110**	360	**30760**
VFA	75	**45**	90	**100**	75	**190**
Alk	475	**725**	495	**930**	490	**1320**
VFA/Alk	0.16	**0.06**	0.18	**0.11**	0.15	**0.14**
Site No. (coordinates)	4 (25m, 60m)		5 (75m, 60m)		6 (125m, 60m)	
Depth	0.75m	**2.25m**	0.75m	**2.25m**	0.75m	2.25m
pH	6.7	**6.7**	6.7	**6.6**	6.7	6.6
Temp	23.6	**23.6**	23.6	**23.3**	23.7	23.5
EP	-320	**-320**	-340	**-340**	-340	-330
TS	1590	**7380**	1190	**62980**	1540	**28880**
VS	480	**4390**	300	**36840**	350	**14120**
VFA	85	**60**	75	**220**	70	**130**
Alk	480	**575**	480	**1450**	510	**980**
VFA/Alk	0.18	**0.10**	0.16	**0.15**	0.14	**0.13**
Site No. (coordinates)	7 (25m, 100m)		8 (75m, 100m)		9 (125m, 100m)	
Depth	0.75m	**2.25m**	0.75m	**2.25m**	0.75m	**2.25m**
pH	6.7	**6.6**	6.7	**6.6**	6.7	6.7
Temp	23.6	**23.4**	23.7	**23.2**	23.6	23.5
EP	-320	**-340**	-330	**-330**	-330	-350
TS	1260	**32010**	2580	**42000**	1350	**11140**
VS	250	**15430**	630	**22930**	380	**5640**
VFA	70	**-**	-	**140**	90	**165**
Alk	480	**905**	485	**1455**	485	**755**
VFA/Alk	0.15	**-**	-	**0.10**	0.19	**0.22**

Table Appendix A -1 continued

4/3/92 10:00 AM

Site No. (coordinates)	10 (25m, 140m)		11 (75m, 140m)		12 (125m, 140m)	
Depth	0.75 m	**2.25 m**	0.75 m	**2.25 m**	0.75 m	**2.25 m**
pH	6.7	**6.6**	6.7	**6.6**	6.7	**6.6**
Temp	23.6	**23.2**	23.8	**23.3**	23.8	**23.4**
EP	-320	**-340**	-310	**-330**	-340	**-340**
TS	1030	**52340**	1200	**41800**	1060	**45890**
VS	220	**26480**	240	**22910**	20	**25470**
VFA	130	**55**	80	**150**	95	**100**
Alk	495	**1830**	480	**1615**	465	**1680**
VFA/Alk	0.26	**0.03**	0.17	**0.09**	0.20	**0.06**
Site No. (coordinates)	13 (25m, 180m)		14 (75m, 180m)		15 (125m, 180m)	
Depth	0.75 m	**2.25 m**	0.75 m	**2.25 m**	0.75 m	**2.25 m**
pH	6.7	**6.6**	6.7	**6.6**	6.7	**6.6**
Temp	23.6	**23.3**	23.8	**23.3**	23.7	**23.5**
EP	-310	**-330**	-320	**-320**	-300	**-320**
TS	1220	**55920**	1050	**62430**	1230	**37520**
VS	150	**33500**	20	**33590**	150	**20190**
VFA	135	**210**	100	**160**	85	**280**
Alk	495	**1485**	475	**1885**	465	**1345**
VFA/Alk	0.27	**0.14**	0.21	**0.08**	0.18	**0.21**
Site No. (coordinates)	16 (25m, 220m)		17 (75m, 220m)		18 (125m, 220m)	
Depth	0.75 m	**2.25 m**	0.75 m	**2.25 m**	0.75 m	**2.25 m**
pH	6.7	**6.6**	6.7	**6.6**	6.7	**6.6**
Temp	23.7	**23.1**	23.8	**23.3**	23.9	**23.2**
EP	-280	**-310**	-310	**-320**	-310	**-320**
TS	1150	**72720**	1080	**43170**	1150	**55860**
VS	80	**43560**	80	**20810**	50	**32060**
VFA	95	**125**	75	**210**	80	**145**
Alk	480	**1805**	480	**1645**	475	**1665**
VFA/Alk	0.20	**0.07**	0.16	**0.13**	0.17	**0.09**
Site No. (coordinates)	19 (25m, 240m)		20 (75m, 240m)		21 (125m, 240m)	
Depth	0.75 m	**2.25 m**	0.75 m	**2.25 m**	0.75 m	2.25 m
pH	6.7	**6.6**	6.7	**6.6**	6.7	**6.6**
Temp	23.7	**23.1**	23.9	**23.1**	23.8	**23.0**
EP	-310	**-300**	-290	**-320**	-300	**-310**
TS	1250	**64100**	1060	**79630**	1340	**56210**
VS	160	**36860**	90	**46270**	200	**31590**
VFA	105	**140**	90	**185**	95	**445**
Alk	470	**1760**	470	**2135**	470	**1775**
VFA/Alk	0.22	**0.08**	0.19	**0.08**	0.20	**0.25**
BOD_5	160	**760**	180	**730**	130	**730**

Appendix B . Data for Regression and Process Control Studies

		RAW SEWAGE											REACTOR										DIGESTER GAS				EFFLUENT
DATE	TIME	FLOW ML/d	PH	COD mg/L	SCOD mg/L	SO4-S mg/L	NH3-N mg/L	TKN mg/L	O&G mg/L	CARB mg/L	Ca mg/L	K mg/L	TEMP deg C	EP mV	VS % w/w	PH	ALK mg/L CaCO3	ACET mg/L	PROP mg/L	NBUT mg/L	IBUT mg/L	VFA mg/L	CH4 % v/v	H2 ppm	CO2 % v/v	CH4FLOW m3/d	ESCOD mg/L
2-Jun-95	10:30	53.9	6.8	1180	550								19	-300	3.32	7.4	1470	6.1	0	0	0	80	81.7	12.8	12.1	7321	375
3-Jun-95	10:00	56.2	6.8	935	490								19.5	-310	3.49	6.5	2000	9.3	0	0	0	93	82.8	10.6	12.2	6839	360
4-Jun-95	10:00	46.5	6.7	685	295								18.5	-285	3.47	6.4	1120	4.1	0	0	0	87	77.1	11.7	10.9	6829	200
5-Jun-95	9:30	44.8	6.8	715	280								18.5	-310	3	6.5	1170	5.2	0	0	0	89	79.1	3.3	11.77	5281	125
6-Jun-95	10:00	59.5	6.7	1000	415								18	-310	3.43	6.5	1180	5.7	0	0	0	88	79.1	6.3	13.1	5320	385
7-Jun-95	9:30	76.3	6.7	805	295								18.4	-310	2.36	6.5	1020	4.8	0	0	0	24	79.8	13.3	11.74	5640	250
8-Jun-95	9:00	65.6	6.8	950	500								18.8	-280	2.89	6.8	1070	6	0	0	0	75	80.6	10.5	11.24	5395	370
9-Jun-95	10:00	83.4	6.6	685	225								19.1	-270	3.01	6.4	970	7.5	0	0	0	62	80.2	13.1	11.32	5785	310
10-Jun-95	10:00	74.9	6.7	900	410								18.7	-280	2.92	6.4	1150	5.4	0	0	0	71	80.2	11.9	11.49	5849	190
11-Jun-95	9:45	56.4	6.8	680	305								18.1	-270	3.07	6.3	1120	5.2	0	0	0	66	80.0	6.1	11.88	6003	260
12-Jun-95	10:00	45	6.9	555	285								17.5	-255	3.05	6.4	1010	5	0	0	0	62	79.5	7.6	12.26	5396	240
13-Jun-95	9:00	47.6	6.8	805	380								17.3	-280	2.92	6.4	935	7.3	0	0	0	57	79.1	7	12	4825	570
14-Jun-95	10:00	53.2	6.7	1200	340								18.3	-280	2.99	6.2	935	4.8	0	0	0	65	78.9	10	12.65	4796	515
15-Jun-95	9:15	55.6	6.7	620	250								18.2	-280	2.72	6.3	1010	6.2	0	0	0	131	79.5	13.4	12.22	5485	495
16-Jun-95	10:30	53.9	6.7	1050	560								18.4	-310	2.7	6.4	1030	8.1	0	1	0	86	79.5	10	12.66	6988	265
17-Jun-95	10:00	68.7	6.7	1000	575								17.6	-280	2.86	6.3	1010	7.2	0	0	0	88	78.2	7	14.36	4525	415
18-Jun-95	9:30	73.8	6.9	615	225								17	-270	2.94	6.4	930	7.7	0	0	0	73	78.2	2.6	12.92	6559	160
19-Jun-95	9:00	83.4	6.9	505	200								17.1	-255	2.68	6.4	860	6.7	0	0	0	65	76.8	3	12.9	4595	180
20-Jun-95	9:30	62.1	7	870	350								17.2	-270	2.84	6.3	1020	8.3	0	0	0.9	87	79.4	5.8	12.12	5059	360
21-Jun-95	8:30	65.4	6.6	1070	460								18	-280	2.86	6.3	1060	7.9	0	0	0	54	80.0	9.1	12.27	5172	315
22-Jun-95	9:00	56	7	1030	370								17.2	-300	2.78	6.3	1010	6.9	0	0	0	54	78.8	6	11.24	5344	405
23-Jun-95	9:30	55.8	6.8	1150	475								17.4	-320	2.79	6.7	1380	9.7	0	0	1	60	79.9	14	10.7	5682	290
24-Jun-95	10:15	53	6.5	1200	615								17.3	-320	2.8	6.4	1050	9.5	1.7	0	0	87	79.4	8.3	11.65	5762	265
25-Jun-95	10:15	48.3	6.7	785	460								17.3	-320	2.75	6.4	1140	10.9	1.9	0	0	91	79.7	5.7	12.82	5675	255
26-Jun-95	8:45	47.8	6.8	685	330								17	-320	2.9	6.5	1160	11.8	23.9	0	0	124	79.4	5.5	12.25	5254	160
27-Jun-95	8:45	63	6.5	1050	535	28	30	63	145	109	23	40	17.1	-295	2.66	6.3	970	14	2.7	0	1.7	89	78.2	5.1	13.32	5625	320
28-Jun-95	9:30	72.6	6.6	985	440	17	28	54	95	97	27	33	17.2	-350	2.85	6.3	1050	6.6	0	0	0	52	79.2	1	11.45	5010	320
29-Jun-95	8:45	62.5	6.6	820	395	32	31	56	40	100	34	29	17.3	-300	2.9	6.1	925	19.1	4.7	0	0	85	80.4	10.4	11.24	6172	290
30-Jun-95	10:15	53.9	6.8	980	410	29	31	58	70	107	42	33	17.5	-340	2.97	6.4	1300	13.4	2.8	0	1	75	80.1	12.6	10.15	6038	155
1-Jul-95	10:00	50.7	6.8	1020	350	41	31	54	50	127	48	34	17.4	-330	3.35	6.4	1260	8.1	0	0	0	77	78.6	7.2	12.36	6245	285
2-Jul-95	9:45	50.9	6.7	780	340	25	24	48	45	102	33	44	16.9	-330	2.88	6.3	1030	11.3	1.7	0	0	89	79.0	6.5	12.32	6637	195
3-Jul-95	8:30	49.5	6.8	745	230	20	26	49	45	98	23	20	17	-335	3.05	6.2	1120	57.3	35.3	0	1.3	196	78.5	7.1	13.34	6252	205
4-Jul-95	8:45	61.6	6.3	1070	445	29	25	57	85	124	30	36	16.1	-340	2.5	6.1	850	10.5	0	0	0	82	75.1	5.3	13.55	5437	310
5-Jul-95	9:30	59.2	6.7	960	380	20	29	54	100	95	30	69	16.9	-340	2.49	6.3	930	17.1	5.4	1	0	79	76.2	8.7	11.85	5048	310

		RAW SEWAGE											REACTOR										DIGESTER GAS				EFFLUENT
DATE	TIME	FLOW ML/d	PH	COD mg/L	SCOD mg/L	SO4-S mg/L	NH3-N mg/L	TKN mg/L	O&G mg/L	CARB mg/L	Ca mg/L	K mg/L	TEMP deg C	EP mV	VS % w/w	PH	ALK mg/L CaCO3	ACET mg/L	PROP mg/L	NBUT mg/L	IBUT mg/L	VFA mg/L	CH4 % v/v	H2 ppm	CO2 % v/v	CH4FLOW m3/d	ESCOD mg/L
6-Jul-95	8:45	58.9	6.5	1020	375	16	29	51	50	112	31	30	17.5	-350	2.31	6.2	835	13.1	0	0	0	90	78.1	10	12.57	4708	385
7-Jul-95	8:30	58.4	6.6	1100	480	16	29	56	95	122	51	33	18.3	-320	2.5	6.1	950	12.1	3.1	1.1	1.3	87	78.4	15.5	14.17	6447	275
8-Jul-95	9:45	57.6	6.5	900	375	21	29	55	140	137	35	40	17.8	-345	2.5	6.2	990	15.6	5.1	0.9	0	115	78.2	6.6	13.98	6634	240
9-Jul-95	9:45	41.6	6.7	820	295	9	25	45	95	76	23	39	17.7	-340	2.62	6.2	885	19.2	4.6	0	0	126	76.8	1.8	15.18	6013	135
10-Jul-95	8:45	37	6.7	720	255	15	29	52	90	100	30	22	16.4	-340	2.58	6	795	15.6	3.5	0	0	110	76.2	4	14.05	5167	110
11-Jul-95	8:30	50.9	6.9	1100	465	16	38	65	60	144	31	40	16.4	-360	2.38	6.4	1060	28.5	11.7	3.6	2.5	107	76.6	4.3	13.37	3924	290
12-Jul-95	9:30	53.4	6.8	1120	400	18	35	59	90	133	36	27	17.3	-320	2.46	6.3	1015	21.6	11.8	2	1.1	35	76.7	18.3	13.85	4883	255
13-Jul-95	8:30	55.6	6.8	1250	315	28	33	61	140	137	33	38	17.8	-310	2.1	6.3	880	20.3	13.7	2.7	1.6	63	75.9	17	14.67	5335	290
14-Jul-95	8:45	97.3	6.4	1100	410	21	30	61	80	139	36	54	16.9	-330	2.26	6.3	925	15.8	7.2	1.6	1.7	55	79.0	10.6	12.18	6332	240
15-Jul-95	9:45	59.5	6.7	845	375	19	25	47	100	102	29	26	16.9	-330	2.62	6.4	1080	27.6	0	1	1.2	90	78.5	8.6	12.73	5775	275
16-Jul-95	10:00	47.9	6.8	755	300	19	24	45	75	94	34	30	17.2	-330	2.98	6.4	960	22	3.1	0	1.1	79	77.1	2.6	13.5	4680	155
17-Jul-95	8:45	51	6.8	650	210	13	26	47	55	232	27	48	16.3	-330	2.27	6.3	770	31.3	0	0	0.9	78	77.5	4.4	14.57	4245	255
18-Jul-95	9:00	61.2	6.4	645	300	19	23	47	65	106	24	33	16.1	-335	2.71	6.3	1190	33.1	20.2	2.3	3.4	77	79.3	7	13.05	5355	365
19-Jul-95	9:45	61.3	6.5	1070	435	27	24	53	75	181	30	34	16.5	-330	2.28	6.4	845	9.8	0	0	0	49	79.4	9.9	12.03	4192	345
20-Jul-95	8:45	60.5	6.5	935	355	19	22	41	110	85	38	44	16.7	-310	2.5	6.1	1010	18.1	11.2	1.6	0	89	79.5	15.7	13.02	5525	330
21-Jul-95	9:30	60.5	6.5	1050	460	23	26	60	95	102	31	41	17.1	-335	2.69	6.5	980	22.8	11.8	1.8	0	81	79.7	15.7	11.99	5065	365
22-Jul-95	9:45	55	6.7	1010	460	25	30	58	75	156	25	24	16.3	-310	2.66	6.3	950	30.2	4.2	0	1	77	78.9	12.2	12.68	6515	295
23-Jul-95	10:00	29.9	6.7	810	280	19	30	54	70	119	23	25	16.5	-320	2.83	6.3	1150	18.9	4.6	0	0	86	78.9	6.6	13.36	5672	160
24-Jul-95	8:35	34.7	6.8	610	205	20	28	48	50	94	26	25	16.2	-335	2.28	6.4	835	34.4	0	0	0	70	79.3	3.8	13.52	5318	145
25-Jul-95	8:30	37.6	7	1090	370	24	28	55	125	94	29	38	16.8	-320	2.31	6.5	860	42	33.5	5.7	5.5	129	77.8	7.6	13.32	5285	290
26-Jul-95	8:45	37.8	6.7	995	425	25	30	60	80	138	56	27	16.9	-330	2.46	6.3	825	22.8	22.1	4.5	1.9	113	78.1	8.7	12.69	5036	240
27-Jul-95	8:45	36.8	6.5	1020	425	23	30	60	30	140	26	52	16.7	-310	2.2	6.3	830	47	35.8	4.2	0	142	79.4	8.6	12.7	4777	315
28-Jul-95	9:00	72.9	6.5	990	520	23	30	52	90	160	30	19	18	-385	2.31	6.4	790	41.6	31.9	6.2	2.1	113	80.0	18	13.7	6673	340
29-Jul-95	9:45	61.5	6.5	590	190	15	18	38	160	102	31	19	15.9	-330	2.75	6.4	825	44.3	2	1.6	1.2	101	77.6	4.84	14.09	5170	155
30-Jul-95	9:45	53.2	6.6	590	245	22	19	36	50	98	27	45	15.8	-300	3.05	6.3	860	33.7	8.5	1.8	1.7	114	76.8	1.4	12.71	4390	195
31-Jul-95	10:15	45.6	6.7	500	160	22	26	44	104	109	26	26	15.2	-330	2.54	6.4	820	36.8	14	2.6	2.4	97	80.3	2.5	12.09	4411	160
1-Aug-95	8:45	59	6.6	940	400	24	25	52	35	122	45	19	15.9	-340	2.83	6.4	1040	52.9	47	37.8	24.5	64	77.3	5.6	14.19	4697	325
2-Aug-95	9:15	84.1	6.6	1030	730	26	29	57	40	149	36	27	15.9	-330	2.36	6.4	835	81.2	37	26.3	6	129	78.8	6.6	11.79	5506	295
3-Aug-95	8:30	75.3	6.6	835	350	20	23	48	90	97	42	22	15.3	-310	2.49	6.3	1050	44.4	25.6	2.6	1.9	117	78.9	9	11.08	4578	265
4-Aug-95	8:45	69.8	6.3	795	335	27	23	43	10	110	48	13	15.9	-320	2.46	6.2	830	23.3	32	3.7	1	86	80.6	12.3	11.75	5138	270
5-Aug-95	9:45	65.5	6.5	820	310	19	21	49	60	109	40	20	16.4	-315	2.51	6.1	815	30.1	5	1.4	1	27	79.7	9.4	11.98	3856	185
6-Aug-95	10:00	53.2	6.6	550	190	13	19	36	55	103	34	20	15.2	-300	2.58	6.2	900	29.5	2.9	0	1.2	24	79.9	4.3	12.26	5087	145
7-Aug-95	8:45	51	6.7	605	200	16	24	40	60	95	28	24	15.1	-295	2.65	6.5	830	33.6	3.6	2.8	1.1	110	77.0	3.3	12.19	4217	110
8-Aug-95	8:45	55.5	6.9	760	330	28	28	49	55	102	34	59	15.4	-350	2.25	6.5	910	18.4	0	1.6	0	95	78.8	6.2	11.6	3575	240
9-Aug-95	8:45	59.7	6.9	645	265	31	22	40	110	83	35	20	15.5	-310	2.37	6.6	1010	77.6	40.2	7.6	7.3	128	78.3	8	10.68	4095	220
10-Aug-95	9:00	56	6.7	915	435	25	23	47	30	137	33	23	16.4	-310	2.49	6.4	835	61.4	44	2.8	5.6	128	79.7	7.8	10.95	4694	195
11-Aug-95	9:00	55.8	6.6	805	380	28	25	45	40	109	33	20	15.7	-340	2.57	6.5	825	156.6	33.4	8.1	6.8	196	80.8	9.1	10.3	5032	250
12-Aug-95	9:45	55.2	6.8	935	345	19	28	51	90	122	34	18	16.5	-320	2.92	6.5	950	84	20	4.4	3.1	134	80.1	7.5	11.04	4432	125

		RAW SEWAGE											REACTOR										DIGESTER GAS				EFFLUENT
DATE	TIME	FLOW ML/d	PH	COD mg/L	SCOD mg/L	SO4-S mg/L	NH3-N mg/L	TKN mg/L	O&G mg/L	CARB mg/L	Ca mg/L	K mg/L	TEMP deg C	EP mV	VS % w/w	PH	ALK mg/L CaCO3	ACET mg/L	PROP mg/L	NBUT mg/L	IBUT mg/L	VFA mg/L	CH4 % v/v	H2 ppm	CO2 % v/v	CH4FLOW m3/d	ESCOD mg/L
13-Aug-95	9:45	46.9	6.8	640	250	21	23	43	60	94	26	15	16.5	-330	2.29	6.5	840	52.9	5.5	1.2	1.5	94	80.3	5.4	10.66	4765	115
14-Aug-95	8:45	34.7	6.7	810	210	19	24	43	55	107	25	14	15.8	-310	2.47	6.5	1300	59.2	13.3	0	1.6	131	81.1	5.5	11.34	4696	95
15-Aug-95	9:00	51.7	6.6	1030	385	20	28	54	175	141	31	22	16.5	-370	2.72	6.5	860	113.1	44.1	6.3	6.3	187	78.7	5	11.91	4872	150
16-Aug-95	8:45	39.2	6.7	985	430	32	28	52	20	120	42	26	17	-335	2.43	6.4	930	82.2	28.7	2	4.8	165	80.3	10.5	11.46	4992	305
17-Aug-95	9:00	51.2	6.8	1120	350	28	31	64	10	152	37	36	17.6	-340	2.46	6.5	1170	128.6	21.6	4	6.6	195	78.5	10	12.43	5236	265
18-Aug-95	9:00	49.3	6.5	920	415	41	30	60	40	127	30	23	17.8	-370	2.37	6.4	1070	79.3	31.7	8.4	7.7	150	76.8	10.6	12.64	4913	270
19-Aug-95	10:00	50	6.3	880	410	28	26	68	65	144	30	22	17.8	-340	2.36	6.6	1030	41.9	10.5	2.1	2.8	83	78.4	12.2	12.37	4930	200
20-Aug-95	10:00	50.9	6.2	875	380	17	28	55	85	199	31	22	18.1	-310	2.02	6.3	810	26.8	9.7	1.1	1.6	76	78.8	5.8	14.48	4948	150
21-Aug-95	8:30	56.2	6.6	725	235	19	30	44	50	111	24	32	17.6	-310	2.04	6.4	790	18.9	7.8	0	1.5	72	77.5	16	13.25	3781	160
22-Aug-95	8:45	47.7	6.6	1020	430	32	31	60	70	127	39	42	17.9	-320	2.41	6.6	1170	62.3	24.9	2.8	3	120	78.2	9.6	12.4	5384	600
23-Aug-95	9:00	52.3	6.4	920	395	29	29	55	40	124	43	18	18	-350	2.27	6.4	1120	54.2	20.2	1.9	2.5	139	76.8	6.6	13.94	5833	250
24-Aug-95	9:00	47.4	6.7	1180	435	20	31	42	35	283	43	24	17.5	-320	2.38	6.5	1150	29	12.7	1.1	2.3	82	80.1	8.6	12.9	5294	240
25-Aug-95	9:00	70.9	6.5	900	450	25	30	53	85	112	30	18	18.6	-310	2.25	6.4	1100	42.3	22.2	2.4	2.9	67	77.0	11.8	14.33	6096	330
26-Aug-95	10:00	68.5	6.7	875	455	40	32	35	35	118	40	36	18	-320	2.4	6.5	1040	52.6	8.8	2.2	2.6	95	78.2	9.32	12.8	5083	290
27-Aug-95	9:45	81.7	6.6	395	245	35	26	43	35	249	34	43	17.5	-350	2.31	6.4	890	42.3	4.5	0	1.3	90	79.1	9.6	12.45	6481	385
28-Aug-95	8:45	70.8	6.7	645	230	25	28	31	45	89	32	20	16.5	-330	1.99	6.5	920	105	24.2	3.5	4.1	126	80.7	8.6	11.79	5538	170
29-Aug-95	9:00	73	6.6	995	440	22	32	31	50	125	38	28	17.2	-350		6.5	860	72.9	40.5	2.6	5.8	93	76.8	11.5	12.8	5271	315
30-Aug-95	9:00	72.4	6.6	1130	475	32	30	37	85	131	42	37	17.4	-320	2.08	6.4	1660	34.9	0	0	8.6	81	77.4	19.7	13.5	4696	390
31-Aug-95	8:45	73.2	6.9	935	445	30	32	75	55	142	46	85	17.5	-300	2.12	6.5	910	160.5	58.2	6.4	6.8	158	78.0	41.1	14.1	6407	390
1-Sep-95	9:00	71.8	6.4	700	640	32	31	45	145	167	42	42	17	-305	2.13	6.4	920	76.7	33.6	2.9	5.5	86	78.8	32.3	12.6	6436	140

Appendix C . Derivation of Discrete Estimation Formulae for the Cross Spectral Analysis

GAIN AND PHASE ESTIMATES

The discrete system equation is

$$x_{4,t} = v_{41}(B)x_{1,t} + v_{42}(B)x_{2,t} + v_{43}(B)x_{3,t} + n_t \quad \textbf{Equation C-1}$$

where X_4=effluent soluble COD (mg/L)

X_1=raw sewage flowrate (ML/d)

X_2=raw sewage COD (mg/L)

X_3=reactor water temperature (°C)

N=noise

$x_4=\nabla X_4$

$x_1=\nabla X_1$

$x_2=\nabla X_2$

$x_3=\nabla X_3$

$n=\nabla N$

$v(B)$=impulse response function

t=time

The dependent variable was given the symbol x_4 instead of y to simplify the notation in the following equations.

Multiplying Equation C-1 throughout by $x_{1,t-k}$, $x_{2,t-k}$ and $x_{3,t-k}$ in turn and taking expectations gives the cross covariance functions

$$\begin{aligned}
\gamma_{14}(B) &= v_{41}(B)\gamma_{11}(B) + v_{42}(B)\gamma_{12}(B) + v_{43}(B)\gamma_{13}(B) \\
\gamma_{24}(B) &= v_{41}(B)\gamma_{21}(B) + v_{42}(B)\gamma_{22}(B) + v_{43}(B)\gamma_{23}(B) \quad \textbf{Equation C-2} \\
\gamma_{34}(B) &= v_{41}(B)\gamma_{31}(B) + v_{42}(B)\gamma_{32}(B) + v_{43}(B)\gamma_{33}(B)
\end{aligned}$$

Taking Fourier transforms of Equation C-2, by substituting $B=e^{-i2\pi f}$, gives the cross spectral equations

$$\begin{aligned}\Gamma_{14}(f) &= H_{41}(f)\Gamma_{11}(f)+H_{42}(f)\Gamma_{12}(f)+H_{43}(f)\Gamma_{13}(f)\\ \Gamma_{24}(f) &= H_{41}(f)\Gamma_{21}(f)+H_{42}(f)\Gamma_{22}(f)+H_{43}(f)\Gamma_{23}(f)\\ \Gamma_{34}(f) &= H_{41}(f)\Gamma_{31}(f)+H_{42}(f)\Gamma_{32}(f)+H_{43}(f)\Gamma_{33}(f)\end{aligned}$$

Equation C-3

Dropping the dependence on f and solving the simultaneous equations, given as Equation C-3, gives the frequency response functions

Equation C-4

$$H_{41}=\frac{\Gamma_{12}\Gamma_{23}\Gamma_{34}-\Gamma_{12}\Gamma_{24}\Gamma_{33}+\Gamma_{13}\Gamma_{24}\Gamma_{32}-\Gamma_{13}\Gamma_{22}\Gamma_{34}+\Gamma_{14}\Gamma_{22}\Gamma_{33}-\Gamma_{14}|\Gamma_{23}|^2}{\Gamma_{11}\Gamma_{22}\Gamma_{33}+\Gamma_{12}\Gamma_{23}\Gamma_{31}+\Gamma_{13}\Gamma_{21}\Gamma_{32}-\Gamma_{11}|\Gamma_{23}|^2-\Gamma_{22}|\Gamma_{13}|^2-\Gamma_{33}|\Gamma_{12}|^2}$$

Equation C-5

$$H_{42}=\frac{\Gamma_{11}\Gamma_{24}\Gamma_{33}-\Gamma_{11}\Gamma_{23}\Gamma_{34}+\Gamma_{13}\Gamma_{21}\Gamma_{34}-\Gamma_{14}\Gamma_{21}\Gamma_{33}+\Gamma_{14}\Gamma_{23}\Gamma_{31}-\Gamma_{24}|\Gamma_{13}|^2}{\Gamma_{11}\Gamma_{22}\Gamma_{33}+\Gamma_{12}\Gamma_{23}\Gamma_{31}+\Gamma_{13}\Gamma_{21}\Gamma_{32}-\Gamma_{11}|\Gamma_{23}|^2-\Gamma_{22}|\Gamma_{13}|^2-\Gamma_{33}|\Gamma_{12}|^2}$$

Equation C-6

$$H_{43}=\frac{\Gamma_{11}\Gamma_{22}\Gamma_{34}-\Gamma_{12}\Gamma_{24}\Gamma_{32}+\Gamma_{12}\Gamma_{24}\Gamma_{31}-\Gamma_{14}\Gamma_{22}\Gamma_{31}+\Gamma_{14}\Gamma_{21}\Gamma_{32}-\Gamma_{34}|\Gamma_{12}|^2}{\Gamma_{11}\Gamma_{22}\Gamma_{33}+\Gamma_{12}\Gamma_{23}\Gamma_{31}+\Gamma_{13}\Gamma_{21}\Gamma_{32}-\Gamma_{11}|\Gamma_{23}|^2-\Gamma_{22}|\Gamma_{13}|^2-\Gamma_{33}|\Gamma_{12}|^2}$$

The cross spectra in Equation C-4, Equation C-5, and Equation C-6 are complex quantities. Each frequency response function is therefore represented by two parts, the gain function and the phase spectrum.

$$H(f)=G(f)e^{j\phi(f)}=A+jB \qquad \textbf{Equation C-7}$$

where $H(f)$=frequency response function

$G(f)=\sqrt{A^2+B^2}$ =gain function

$\phi(f)=\arctan\left(-\frac{B}{A}\right)$=phase spectrum

To obtain expressions for the gains and phases it is necessary to take the modulus and argument of Equation C-4, Equation C-5, and Equation C-6. This is done by first decomposing these equations into their real (A) and imaginary (B) components using the relationship $\Gamma_{ab}(f) = \Lambda_{ab}(f) - j\Psi_{ab}(f)$ where $\Lambda_{ab}(f)$ and $\Psi_{ab}(f)$ are the co-spectrum and quadrature spectrum, respectively.

Equation C-8

$$A_{41} = \frac{\begin{array}{l}\{\Lambda_{12}\Lambda_{23}\Lambda_{34} - \Lambda_{12}\Psi_{23}\Psi_{34} - \Lambda_{23}\Psi_{12}\Psi_{34} - \Lambda_{34}\Psi_{12}\Psi_{23} + \Gamma_{33}\Psi_{12}\Psi_{24} - \Gamma_{33}\Lambda_{12}\Lambda_{24} \\ +\Lambda_{13}\Lambda_{24}\Lambda_{32} - \Lambda_{13}\Psi_{24}\Psi_{32} - \Lambda_{24}\Psi_{13}\Psi_{32} - \Lambda_{32}\Psi_{13}\Psi_{24} + \Gamma_{22}\Psi_{13}\Psi_{34} - \Gamma_{22}\Lambda_{13}\Lambda_{34} \\ +\Gamma_{22}\Gamma_{33}\Lambda_{14} - \Lambda_{14}|\Gamma_{23}|^2\}\end{array}}{\begin{array}{l}\{\Gamma_{11}\Gamma_{22}\Gamma_{33} + 2(\Lambda_{12}\Lambda_{23}\Lambda_{31} - \Lambda_{12}\Psi_{23}\Psi_{31} - \Lambda_{23}\Psi_{12}\Psi_{31} - \Lambda_{31}\Psi_{12}\Psi_{23}) - \Gamma_{11}|\Gamma_{23}|^2 \\ -\Gamma_{22}|\Gamma_{13}|^2 - \Gamma_{33}|\Gamma_{12}|^2\}\end{array}}$$

$$B_{41} = \frac{\begin{array}{l}\{\Lambda_{12}\Lambda_{23}\Psi_{34} + \Lambda_{12}\Lambda_{34}\Psi_{23} + \Lambda_{23}\Lambda_{34}\Psi_{12} - \Psi_{12}\Psi_{23}\Psi_{34} - \Gamma_{33}\Lambda_{12}\Psi_{24} - \Gamma_{33}\Lambda_{24}\Psi_{12} \\ +\Lambda_{13}\Lambda_{24}\Psi_{32} + \Lambda_{13}\Lambda_{32}\Psi_{24} + \Lambda_{24}\Lambda_{32}\Psi_{13} - \Psi_{13}\Psi_{24}\Psi_{32} - \Gamma_{22}\Lambda_{13}\Psi_{34} - \Gamma_{22}\Lambda_{34}\Psi_{13} \\ +\Gamma_{22}\Gamma_{33}\Psi_{14} - \Psi_{14}|\Gamma_{23}|^2\}\end{array}}{\begin{array}{l}\{\Gamma_{11}\Gamma_{22}\Gamma_{33} + 2(\Lambda_{12}\Lambda_{23}\Lambda_{31} - \Lambda_{12}\Psi_{23}\Psi_{31} - \Lambda_{23}\Psi_{12}\Psi_{31} - \Lambda_{31}\Psi_{12}\Psi_{23}) - \Gamma_{11}|\Gamma_{23}|^2 \\ -\Gamma_{22}|\Gamma_{13}|^2 - \Gamma_{33}|\Gamma_{12}|^2\}\end{array}}$$

Equation C-9

$$A_{42} = \frac{\begin{array}{l}\{\Lambda_{13}\Lambda_{21}\Lambda_{34} - \Lambda_{13}\Psi_{21}\Psi_{34} - \Lambda_{21}\Psi_{13}\Psi_{34} - \Lambda_{34}\Psi_{13}\Psi_{21} + \Gamma_{33}\Psi_{14}\Psi_{21} - \Gamma_{33}\Lambda_{14}\Lambda_{21} \\ +\Lambda_{14}\Lambda_{23}\Lambda_{31} - \Lambda_{14}\Psi_{23}\Psi_{31} - \Lambda_{23}\Psi_{14}\Psi_{31} - \Lambda_{31}\Psi_{14}\Psi_{23} + \Gamma_{11}\Psi_{23}\Psi_{34} - \Gamma_{11}\Lambda_{23}\Lambda_{34} \\ +\Gamma_{11}\Gamma_{33}\Lambda_{24} - \Lambda_{24}|\Gamma_{13}|^2\}\end{array}}{\begin{array}{l}\{\Gamma_{11}\Gamma_{22}\Gamma_{33} + 2(\Lambda_{12}\Lambda_{23}\Lambda_{31} - \Lambda_{12}\Psi_{23}\Psi_{31} - \Lambda_{23}\Psi_{12}\Psi_{31} - \Lambda_{31}\Psi_{12}\Psi_{23}) - \Gamma_{11}|\Gamma_{23}|^2 \\ -\Gamma_{22}|\Gamma_{13}|^2 - \Gamma_{33}|\Gamma_{12}|^2\}\end{array}}$$

$$B_{42} = \frac{\begin{array}{l}\{\Lambda_{13}\Lambda_{21}\Psi_{34} + \Lambda_{13}\Lambda_{34}\Psi_{21} + \Lambda_{21}\Lambda_{34}\Psi_{13} - \Psi_{13}\Psi_{21}\Psi_{34} - \Gamma_{33}\Lambda_{14}\Psi_{21} - \Gamma_{33}\Lambda_{21}\Psi_{14} \\ +\Lambda_{14}\Lambda_{23}\Psi_{31} + \Lambda_{14}\Lambda_{31}\Psi_{23} + \Lambda_{23}\Lambda_{31}\Psi_{14} - \Psi_{14}\Psi_{23}\Psi_{31} - \Gamma_{11}\Lambda_{23}\Psi_{34} - \Gamma_{11}\Lambda_{34}\Psi_{23} \\ +\Gamma_{11}\Gamma_{33}\Psi_{24} - \Psi_{24}|\Gamma_{13}|^2\}\end{array}}{\begin{array}{l}\{\Gamma_{11}\Gamma_{22}\Gamma_{33} + 2(\Lambda_{12}\Lambda_{23}\Lambda_{31} - \Lambda_{12}\Psi_{23}\Psi_{31} - \Lambda_{23}\Psi_{12}\Psi_{31} - \Lambda_{31}\Psi_{12}\Psi_{23}) - \Gamma_{11}|\Gamma_{23}|^2 \\ -\Gamma_{22}|\Gamma_{13}|^2 - \Gamma_{33}|\Gamma_{12}|^2\}\end{array}}$$

Equation C-10

$$A_{43} = \frac{\begin{array}{l}\{\Lambda_{12}\Lambda_{24}\Lambda_{31} - \Lambda_{12}\Psi_{24}\Psi_{31} - \Lambda_{24}\Psi_{12}\Psi_{31} - \Lambda_{31}\Psi_{12}\Psi_{24} + \Gamma_{22}\Psi_{14}\Psi_{31} - \Gamma_{22}\Lambda_{14}\Lambda_{31} \\ +\Lambda_{14}\Lambda_{21}\Lambda_{32} - \Lambda_{14}\Psi_{21}\Psi_{32} - \Lambda_{21}\Psi_{14}\Psi_{32} - \Lambda_{32}\Psi_{14}\Psi_{21} + \Gamma_{11}\Psi_{24}\Psi_{32} - \Gamma_{11}\Lambda_{24}\Lambda_{32} \\ +\Gamma_{11}\Gamma_{22}\Lambda_{34} - \Lambda_{34}|\Gamma_{12}|^2\}\end{array}}{\begin{array}{l}\{\Gamma_{11}\Gamma_{22}\Gamma_{33} + 2(\Lambda_{12}\Lambda_{23}\Lambda_{31} - \Lambda_{12}\Psi_{23}\Psi_{31} - \Lambda_{23}\Psi_{12}\Psi_{31} - \Lambda_{31}\Psi_{12}\Psi_{23}) - \Gamma_{11}|\Gamma_{23}|^2 \\ -\Gamma_{22}|\Gamma_{13}|^2 - \Gamma_{33}|\Gamma_{12}|^2\}\end{array}}$$

$$B_{43} = \frac{\begin{array}{l}\{\Lambda_{12}\Lambda_{24}\Psi_{31} + \Lambda_{12}\Lambda_{31}\Psi_{24} + \Lambda_{24}\Lambda_{31}\Psi_{12} - \Psi_{12}\Psi_{24}\Psi_{31} - \Gamma_{22}\Lambda_{14}\Psi_{31} - \Gamma_{22}\Lambda_{31}\Psi_{14} \\ +\Lambda_{14}\Lambda_{21}\Psi_{32} + \Lambda_{14}\Lambda_{32}\Psi_{21} + \Lambda_{21}\Lambda_{32}\Psi_{14} - \Psi_{14}\Psi_{21}\Psi_{32} - \Gamma_{11}\Lambda_{24}\Psi_{32} - \Gamma_{11}\Lambda_{32}\Psi_{24} \\ +\Gamma_{11}\Gamma_{22}\Psi_{34} - \Psi_{34}|\Gamma_{12}|^2\}\end{array}}{\begin{array}{l}\{\Gamma_{11}\Gamma_{22}\Gamma_{33} + 2(\Lambda_{12}\Lambda_{23}\Lambda_{31} - \Lambda_{12}\Psi_{23}\Psi_{31} - \Lambda_{23}\Psi_{12}\Psi_{31} - \Lambda_{31}\Psi_{12}\Psi_{23}) - \Gamma_{11}|\Gamma_{23}|^2 \\ -\Gamma_{22}|\Gamma_{13}|^2 - \Gamma_{33}|\Gamma_{12}|^2\}\end{array}}$$

Estimates for the gains and phases are then obtained by replacing the theoretical values in Equation C-8, Equation C-9, and Equation C-10 with the corresponding sample values. The notation for the sample values is given in Table Appendix C -1.

SQUARED COHERENCY ESTIMATES

Squared Coherency Spectra

The squared coherency is analogous to the correlation coefficient in the time domain. Given the model

$$x_{2,t} = v(B)x_{1,t} + n_t \qquad \textbf{Equation C-11}$$

the covariance function can be obtained by squaring both sides and taking expectations

$$\gamma_{22}(B) = v^2(B)\gamma_{11}(B) + \gamma_{nn}(B) \qquad \textbf{Equation C-12}$$

Transforming Equation C-12 (by substituting $B = e^{-j2\pi}$) gives

$$\Gamma_{22}(f) = |H(f)|^2 \Gamma_{11}(f) + \Gamma_{nn}(f) \qquad \textbf{Equation C-13}$$

Given that $|H(f)|^2 = \dfrac{\alpha_{12}^2(f)}{\Gamma_{11}^2(f)}$ Equation C-13 can be written

$$\Gamma_{nn}(f) = \Gamma_{22}(f)\left[1 - \kappa_{12}^2(f)\right] \qquad \textbf{Equation C-14}$$

where

$$\kappa_{12}^2(f) = \frac{\alpha_{12}^2(f)}{\Gamma_{11}(f)\Gamma_{22}(f)} \qquad \textbf{Equation C-15}$$

is called the *squared coherency* between the input and output at frequency f.

Squared Multiple Coherency Spectrum

Like the squared coherency, the squared multiple coherency spectrum is a generalisation to the frequency domain of the multiple correlation coefficient and it too is derived from the spectrum of the residual process.

Extending Equation C-13 to q inputs and noting that $\Gamma_{11}(f) = \dfrac{\Gamma_{12}(f)}{H(f)}$,

the *residual or noise spectrum* can be written

Equation C-16

$$\Gamma_{nn}(f) = \Gamma_{(q+1)(q+1)}(f) - H_{(q+1)1}(f)\Gamma_{(q+1)1}(f) - \ldots - H_{(q+1)q}(f)\Gamma_{(q+1)q}(f)$$

or

$$\Gamma_{nn}(f) = \Gamma_{(q+1)(q+1)}(f)[1 - \kappa^2_{(q+1)12\ldots q}(f)]$$

where

$$\kappa^2_{(q+1)12\ldots q}(f) = \frac{H_{(q+1)1}(f)\Gamma_{(q+1)1}(f) + \ldots + H_{(q+1)q}(f)\Gamma_{(q+1)q}(f)}{\Gamma_{(q+1)(q+1)}(f)}$$

An alternative expression for the *squared multiple coherency spectrum* is obtained by substituting $\Gamma_{(q+1)}(f) = \Gamma_{qq}(f)\mathrm{H}_{(q+1)}(f)$ for the frequency response function in Equation C-16

$$\kappa^2_{(q+1)12\ldots q}(f) = 1 - \frac{\left|\Gamma_{(q+1)(q+1)}(f)\right|}{\Gamma_{(q+1)(q+1)}(f)\left|\Gamma_{qq}(f)\right|} \qquad \textbf{Equation C-17}$$

For the case of 1 output and 3 inputs the squared multiple coherency spectrum is

$$\kappa^2_{4123} = 1 - \frac{\begin{vmatrix} \Gamma_{11} & \Gamma_{12} & \Gamma_{13} & \Gamma_{14} \\ \Gamma_{21} & \Gamma_{22} & \Gamma_{23} & \Gamma_{24} \\ \Gamma_{31} & \Gamma_{32} & \Gamma_{33} & \Gamma_{34} \\ \Gamma_{41} & \Gamma_{42} & \Gamma_{43} & \Gamma_{44} \end{vmatrix}}{\Gamma_{44}\begin{vmatrix} \Gamma_{11} & \Gamma_{12} & \Gamma_{13} \\ \Gamma_{21} & \Gamma_{22} & \Gamma_{23} \\ \Gamma_{31} & \Gamma_{32} & \Gamma_{33} \end{vmatrix}}$$

therefore

$$\kappa^2_{4123} = \frac{\begin{array}{l}[\Gamma_{11}\Gamma_{22}|\Gamma_{34}|^2 + \Gamma_{11}\Gamma_{33}|\Gamma_{24}|^2 + \Gamma_{22}\Gamma_{33}|\Gamma_{14}|^2 - |\Gamma_{12}|^2|\Gamma_{34}|^2 - |\Gamma_{13}|^2|\Gamma_{24}|^2 - |\Gamma_{14}|^2|\Gamma_{23}|^2 \\ -2(\Gamma_{11}\Lambda_{23}\Lambda_{34}\Lambda_{42} - \Gamma_{11}\Lambda_{23}\Psi_{34}\Psi_{42} - \Gamma_{11}\Lambda_{34}\Psi_{23}\Psi_{42} - \Gamma_{11}\Lambda_{42}\Psi_{23}\Psi_{34} - \Lambda_{12}\Lambda_{23}\Lambda_{34}\Lambda_{4} \\ +\Lambda_{12}\Lambda_{23}\Psi_{34}\Psi_{41} + \Lambda_{12}\Lambda_{34}\Psi_{23}\Psi_{41} + \Lambda_{12}\Lambda_{41}\Psi_{23}\Psi_{34} + \Lambda_{23}\Lambda_{34}\Psi_{12}\Psi_{41} + \Lambda_{23}\Lambda_{41}\Psi_{12}\Psi_{34} \\ +\Lambda_{34}\Lambda_{41}\Psi_{12}\Psi_{23} - \Psi_{12}\Psi_{23}\Psi_{34}\Psi_{41} - \Lambda_{12}\Lambda_{24}\Lambda_{31}\Lambda_{43} + \Lambda_{12}\Lambda_{24}\Psi_{31}\Psi_{43} + \Lambda_{12}\Lambda_{31}\Psi_{24}\Psi_{43} \\ +\Lambda_{12}\Lambda_{43}\Psi_{24}\Psi_{31} + \Lambda_{24}\Lambda_{31}\Psi_{12}\Psi_{43} + \Lambda_{24}\Lambda_{43}\Psi_{12}\Psi_{31} + \Lambda_{31}\Lambda_{43}\Psi_{12}\Psi_{24} - \Psi_{12}\Psi_{24}\Psi_{31}\Psi_{43} \\ +\Gamma_{33}\Lambda_{12}\Lambda_{24}\Lambda_{41} - \Gamma_{33}\Lambda_{12}\Psi_{24}\Psi_{41} - \Gamma_{33}\Lambda_{24}\Psi_{12}\Psi_{41} - \Gamma_{33}\Lambda_{41}\Psi_{12}\Psi_{24} + \Gamma_{22}\Lambda_{13}\Lambda_{34}\Lambda_{41} \\ -\Gamma_{22}\Lambda_{13}\Psi_{34}\Psi_{41} - \Gamma_{22}\Lambda_{34}\Psi_{13}\Psi_{41} - \Gamma_{22}\Lambda_{41}\Psi_{13}\Psi_{34} - \Lambda_{13}\Lambda_{24}\Lambda_{32}\Lambda_{41} + \Lambda_{13}\Lambda_{24}\Psi_{32}\Psi_{41} \\ +\Lambda_{13}\Lambda_{32}\Psi_{24}\Psi_{41} + \Lambda_{13}\Lambda_{41}\Psi_{24}\Psi_{32} + \Lambda_{24}\Lambda_{32}\Psi_{13}\Psi_{41} + \Lambda_{24}\Lambda_{41}\Psi_{13}\Psi_{32} + \Lambda_{32}\Lambda_{41}\Psi_{13}\Psi_{24} \\ -\Psi_{13}\Psi_{24}\Psi_{32}\Psi_{41}]\end{array}}{\begin{array}{l}[\Gamma_{44}(\Gamma_{11}\Gamma_{22}\Gamma_{33} + 2\{\Lambda_{12}\Lambda_{23}\Lambda_{31} - \Lambda_{12}\Psi_{23}\Psi_{31} - \Lambda_{23}\Psi_{12}\Psi_{31} - \Lambda_{31}\Psi_{12}\Psi_{23}\} \\ -\Gamma_{11}|\Gamma_{23}|^2 - \Gamma_{22}|\Gamma_{13}|^2 - \Gamma_{33}|\Gamma_{12}|^2]\end{array}}$$

Partial Squared Coherency Spectra

The partial squared coherency is the spectral analogue of the partial correlation coefficient. For the case of one output and three inputs the *partial squared coherency spectra* are

$$\kappa^2_{41/23} = 1 - \frac{(1-\kappa^2_{4123})}{(1-\kappa^2_{423})}$$

$$\kappa^2_{42/13} = 1 - \frac{(1-\kappa^2_{4123})}{(1-\kappa^2_{413})}$$

$$\kappa^2_{43/12} = 1 - \frac{(1-\kappa^2_{4123})}{(1-\kappa^2_{412})}$$

where

$$\kappa^2_{423} = \frac{\begin{array}{l}[\Gamma_{33}(\Lambda^2_{24} + \Psi^2_{24}) + \Gamma_{22}(\Lambda^2_{34} + \Psi^2_{34}) - 2(\Lambda_{23}\Lambda_{34}\Lambda_{24} + \Lambda_{23}\Psi_{34}\Psi_{24} \\ -\Psi_{23}\Psi_{34}\Lambda_{24} + \Psi_{23}\Lambda_{34}\Psi_{24})]\end{array}}{\Gamma_{44}(\Gamma_{22}\Gamma_{33} - |\Gamma_{23}|^2)}$$

$$\kappa^2_{413} = \frac{[\Gamma_{33}(\Lambda^2_{14} + \Psi^2_{14}) + \Gamma_{11}(\Lambda^2_{34} + \Psi^2_{34}) - 2(\Lambda_{13}\Lambda_{34}\Lambda_{14} + \Lambda_{13}\Psi_{34}\Psi_{14} - \Psi_{13}\Psi_{34}\Lambda_{14} + \Psi_{13}\Lambda_{34}\Psi_{14})]}{\Gamma_{44}(\Gamma_{11}\Gamma_{33} - |\Gamma_{13}|^2)}$$

$$\kappa^2_{412} = \frac{[\Gamma_{22}(\Lambda^2_{14} + \Psi^2_{14}) + \Gamma_{11}(\Lambda^2_{24} + \Psi^2_{24}) - 2(\Lambda_{12}\Lambda_{24}\Lambda_{14} + \Lambda_{12}\Psi_{24}\Psi_{14} - \Psi_{12}\Psi_{24}\Lambda_{14} + \Psi_{12}\Lambda_{24}\Psi_{14})]}{\Gamma_{44}(\Gamma_{11}\Gamma_{22} - |\Gamma_{12}|^2)}$$

Estimation of Multivariate Spectra

Estimating the gain and phase spectra, squared coherency spectra and residual spectrum is achieved by substituting the theoretical spectra with their smoothed estimators. Smoothed spectral estimators were discussed on page 7-17. The notation for the smoothed estimators is given in Table Appendix C -1.

Table Appendix C -1 Notation used in frequency domain analyses

Function	Theoretical values	Sample values
auto spectrum	$\Gamma_{aa}(f)$	$C_{aa}(f)$
cross spectrum	$\Gamma_{ab}(f)$	$C_{ab}(f)$
co-spectrum	$\Lambda_{ab}(f)$	$L_{ab}(f)$
quadrature spectrum	$\Psi_{ab}(f)$	$Q_{ab}(f)$
real component of $H_{ab}(f)$	$A_{ab}(f)$	$\overline{A}_{ab}(f)$
imaginary component of $H_{ab}(f)$	$B_{ab}(f)$	$\overline{B}_{ab}(f)$
gain spectrum	$G_{ab}(f)$	$\overline{G}_{ab}(f)$
phase spectrum	$\phi_{ab}(f)$	$\overline{\phi}_{ab}(f)$
Squared coherency spectrum	κ^2_{ab}	$\overline{K}^2_{ab}$
Residual spectrum	Γ_{nn}	$\overline{R}_{nn}$

References

1. Gulovsen, T., Hansen, P., Hutchison, D., Russel, J. and Scott, P.: "Odour Minimisation at Werribee", WATER, June 1992, p. 16-23.

2. Andrews, J. F. and Graef, S. P.: "Dynamic Modelling and Simulation of the Anaerobic Digestion Process". In R. F. Gould (Ed.): Anaerobic Biological Treatment Processes, (American Chemical Society: USA, 1971).

3. Mosey, F. E.: "Mathematical Modelling of the Anaerobic Digestion Process: Regulatory Mechanisms for the Formation of Short-Chain Volatile Acids from Glucose" Wat. Sci. Tech., Vol. 15, 1983, p209-232.

4. Hickey, R. F., Wu, W.-M., Veiga, M. C. and Jones, R.: "Start-Up, Operation, Monitoring and Control of High-Rate Anaerobic Treatment Systems", Wat. Sci. Tech., Vol. 24, No. 8, 1991, p. 207-255.

5. Iza, J., Colleran, E., Paris, J. M. and Wu, W. M.: "International Workshop on Anaerobic Treatment Technology for Municipal and Industrial Wastewaters: Summary Paper", Wat. Sci. Tech., Vol. 24, No. 8, 1991, p. 1-16.

6. Duncan, A.: "Anaerobic Digestion in Australia", WATER, June 1993, p. 34-35.

7. Switzenbaum, M. S., Giraldo-Gomez, E. and Hickey, R. F.: "Monitoring of the anaerobic methane fermentation process", Enzyme Microb. Technol., Vol. 12, 1990, p. 722-729.

8. Balch, W. E., Fox, G. E., Magrum, L. J., Woese, C. R. and Wolfe, R. S.: "Methanogens: Reevaluation of a Unique Biological Group", Microbiological Reviews, Vol. 43, No. 2, 1972, p260-296.

9. Levett, P. M.: Anaerobic Bacteria, (Open University Press: USA, 1990).

10. Hobson, P. N.: "The Bacteriology of Anaerobic Sewage Digestion", Process Biochemistry, Vol. 8, 1973, p. 19-25.

11. Mah, R. A. and Susman, C., Appl. Microbiol., 1968, 16, 358 (cited in ref. 10).

12. Bryant, M. P., Wolin, E. A., Wolin, M. J. and Wolfe, R. S. (1967). "*Methanobacillus omelianski*, a symbiotic association of two species of bacteria", Arch. Mikrobiol., 59, 20 (cited in ref. 13)

13. Wolfe, R. S.: "Microbial Formation of Methane". In A. H. Rose and J. F. Wilkinson (Eds): Advances in Microbiological Physiology Vol. 6 (Academic Press Inc.: New York, 1971), p. 107-146.

14. Reddy, C. A., Bryant, M. P. and Wolin, M. J.: "Characteristics of S organism isolated from *Methanobacillus omelianski*", Journal of Bacteriology, Vol. 109, p. 539-545.

15. Winfrey, M. R. and Zeikus, J. G.: "Effect of Sulphate on Carbon and Electron Flow During Microbial Methanogenesis in Freshwater Sediments", Applied and Environmental Microbiology, Vol. 33, No. 2, 1977, p. 275-281.

16. Zeikus, J. G.: "Microbial Populations in Digesters". In D. A. Stafford,B. I. Wheatly and D. E. Hughes (Eds): Anaerobic Digestion (Applied Science Publishers Ltd.: London, 1980) p. 61-89.

17. Archer, D. B. and Kirsop, B. H.: "The microbiology and control of anaerobic digestion". In A. Wheatly (Ed): Anaerobic Digestion: A Waste Treatment Technology (Elsevier Science Publishers Ltd.: London, 1990) p. 44-91.

18. Miller, T. L. And Wolin, M. J.: "A Serum Bottle Modification of the Hungate Technique for Cultivating Obligate Anaerobes", Applied Microbiology, Vol. 27, No. 5, 1974, p. 985-987.

19. Gerhardt, P., Murray, R., Costilar, R., Nester, E., Wood, W., Krieg, N. and Phillips, G. (Eds): Manual of Methods for General Bacteriology (American Society for Microbiology: Washington DC, 1981), p. 75-77.

20. Holdeman, L. V., Cato, E. P. And Moore, W. E. C.: Anaerobe Laboratory Manual (Virginia Polytechnic Institute: Blacksburg, 4th ed., 1977).

21. Hobson, P. N. And Summers, R.: "Anaerobic Bacteria in Mixed Cultures; Ecology of the Rumen and Sewage Digesters". In R. Davies and D. W. Lovelock (Eds): Techniques for the Study of Mixed Populations (Academic Press: New York, 1978), p. 126-141.

22. Dolfing, J. And Bloemen, W. G. B. M.: "Activity measurements as a tool to characterize the microbial composition of methanogenic environments", Journal of Microbiological Methods, Vol. 4, 1985, p. 1-12.

23. Smith, P. H.: "The Microbial Ecology of Sludge Methanogenesis", Developments in Industrial Microbiology, Vol. 7, 1966, p. 156-161.

24. Jeris, J. S. and McCarty, P. L.: "The biochemistry of methane fermentation using C^{14} tracers", J. Water Pollution Control Federation, Vol. 37, p. 178-192 (cited in ref. 23).

25. Smith, P. H. and Mah, R. A.: "Kinetics of acetate metabolism during sludge digestion", Appl. Microbiol., in press, 1965 (cited in ref. 23).

26. Hanaki, K., Noike, T. and Matsumoto, J.: "Mathematical Modelling of the Anaerobic Digestion Process". In M. J. Gromeic and S. E. Jørgensen (Eds): Mathematical Models in Biological Waste Water Treatment (Elsevier Science Publishers: Amsterdam, 1985), p. 583-635.

27. Graef, S. P. and Andrews, J. F.: "Stability and control of anaerobic digestion", J. Water Poll. Control Fed., Vol. 46, 1974, p.666-683 (cited in ref. 26)

28. Graef, S. P. and Andrews, J. F.: "Mathematical modeling and control of anaerobic digestion", AIChE Symposium Series, 70, No. 136, p. 101-131 (cited in ref. 26)

29. Collins, A. S. and Gilliland, B. E.: "Control of anaerobic digestion process", Proc. Amer. Soc. Civil Eng., Env. Eng. Div., 100, EE2, p. 487-505 (cited in ref. 26).

30. Smith, D. P. and McCarty, P. L.: "Factors governing methane fluctuations following shock loading of digesters", J. Water Pollut. Control Fed., Vol. 62, No. 1, 1990, p. 58-64.

31. Jones, R. M., MacGregor, J. F and Murphy, K. L.: "State Estimation in Wastewater Engineering: Application to an Anaerobic Process", Environmental Monitoring and Assessment, Vol. 12, 1989, p. 271-282.

32. Jones, R. M., MacGregor, J. F., Murphy, K. L. and Hall, E. R.: "Towards a useful dynamic model of the anaerobic wastewater treatment process. A practical illustration of process identification." Wat. Sci. Tech., Vol. 25, No. 7, 1992. p. 61-71.

33. Fitzgerald, P. A.: "Rapid Monitoring and Control of Anaerobic Digestion", AWWA 15th Federal Convention Technical Papers, Vol. 2, 1993, p. 441-448.

34. Mathiot, S., Escoffier, Y., Ehlinger, F., Couderc, J. P., Leyris, J. P. and Moletta, R.: "Control parameter variations in an anaerobic fluidised bed reactor subjected to organic shockloads", Wat. Sci. Tech., Vol. 25, No. 7. 1992, p.93-101.

35. Cayless, S. M., Damotta Marques, D. M. L. and Lester, J. N.: "The effect of transient loading, pH, and temperature shocks on anaerobic filters and fluidised beds", Env. Technol. Letters, 10, p.951-968 (cited in ref. 34).

36. Juran, J. M. and Gryna, F. M. (Eds): Juran's Quality Control Handbook (McGraw-Hill Book Co.: USA, 1988).

37. Berthouex, P. M.: "Constructing control charts for wastewater treatment plant operation", Journal WPCF, Vol. 61, No.9, 1989, p. 1534-1551.

38. Jackson, J. E.: "Principal Components and Factor Analysis: Part I - Principal Components", Journal of Quality Technology, Vol. 12, No. 4, 1980, p. 201-213.

39. Tang, P. F.: "Mean control for multivariate processes with specific reference to short runs". Unpublished manuscript, Victoria University of Technology, 1995.

40. Berthouex, P. M. and Hunter, W. G.: "Treatment plant monitoring programs: A preliminary analysis", Journal WPCF, Vol. 47, No. 8, 1975, p. 2143-2156.

41. Fairall, J. M.: "Statistical Quality Control charts For Wastewater Evaluation", Proc. Ind. Waste Conf. (Purdue University, W. Lafayette, Ind.) 1973, p. 340-348.

42. Adams, B. J. and Gemmell, R. S.: "Performance of regionally related wastewater treatment plants", Journal WPCF, Vol. 45, No. 10, 1973, p. 2088-2103.

43. Vasilopoulos, A. V. and Stamboulis, A. P.: "Modification of Control Chart Limits in the Presence of Data Correlation", Journal of Quality Technology, Vol. 10, No. 1, 1978, p. 20-30.

44. Berthouex, P. M., Hunter, W. G. and Pallesen, L.: "Monitoring Sewage Treatment Plants: Some Quality Control Aspects", Journal of Quality Technology, Vol. 10, No. 4, 1978, p. 139-149.

45. Box, G. E. P. and Jenkins, G. M.: TME SERIES ANALYSIS forecasting and control (Prentice Hall: New Jersey, 2nd ed., 1976).

46. Paul, W. L.: "Risk of digesters causing an odour event at the Eastern Treatment Plant", Melbourne Water internal report, 1994.

47. Montgomery, D. C. and Mastrangelo, C. M.: "Some Statistical Process Control Methods for Autocorrelated Data", Journal of Quality Technology, Vol. 23, No. 3, 1991, p. 179-193.

48. Bagshaw, M. and Johnson, R. A.: "Sequential Procedures for Detecting Parameter Changes in a Time-Series Model", Journal of the American Statistical Association, Vol. 72, No. 359, 1977, p. 593-597.

49. Box, G. and Kramer, T.: "Statistical Process Monitoring and Feedback Adjustment - A Discussion", Technometrics, Vol. 34, No. 3, 1992, p. 251-267.

50. Berthouex, P. M., Hunter, W. G., Pallesen, L. and Shih, C. Y.: "The use of stochastic models in the interpretation of historical data from sewage treatment plants", Water Research, Vol. 10, 1976, p. 689-698.

51. Berthouex, P. M., Lai, W. and Darjatmoko, A.: "Statistics-Based Approach to Wastewater Treatment Plant Operations", Journal of Environmental Engineering, Vol. 115, No. 3, 1989, p. 650-671.

52. Berthouex, P. M. and Fan, R.: "Evaluation of treatment plant performance: causes, frequency, and duration of upsets", Journal WPCF, Vol. 58, No. 5, 1986, p. 368-375.

53. Berthouex, P. M. and Hunter, W. G.: "Simple statistics for interpreting environmental data", Journal WPCF, Vol. 53, No. 2, 1981, p. 167-175.

54. Berthouex, P. M. and Hunter, W. G.: "How to construct reference distributions to evaluate treatment plant effluent quality", Journal WPCF, Vol. 55, No. 12, 1983, p. 1417-1424.

55. Ward, R. C., Loftis, J. C. and McBride, G. B.: "The 'Data-rich but Information-poor' Syndrome in Water Quality Monitoring", Environmental Management, Vol. 10, No. 3, 1986, p. 291-297.

56. Ferrara, R. A.: "Hydraulic Modelling for Waste Stabilization Ponds", ASCE Journal of Environmental Engineering Division, Vol. 107, No. EE4, 1981, p. 817-829.

57. Chapman, M.: "Hydraulic Studies in the 115 East Lagoon, Interim Reports 1-4", Melbourne Water Technical Report, File 850/201/0099, 1988.

58. Safley, L. M. and Westerman, P. W.: "Biogas Production from Anaerobic Lagoons", Biological Wastes, Vol. 23, 1988, p. 181-193.

59. Hungate, R. E.: "A roll tube method for cultivation of strict anaerobes". In J. R. Norris and D. W. Ribbons (Eds): Methods in microbiology, Vol. 3B (Academic Press Inc.: New York, 1969).

60. Latham, M. J. and Wolin, M. J.: "Use of a serum bottle technique to study interactions between strict anaerobes in mixed culture". In R. Davies and D. W. Lovelock (Eds): Techniques for the Study of Mixed Populations, (Academic Press: New York, 1978).

61. Speece, R. E.: "A survey of municipal anaerobic sludge digesters and diagnostic activity assays", Wat. Res., Vol. 22, No. 3, 1988, p. 365-372.

62. Soto, M., Méndez, R. and Lema, J. M.: "Methanogenic and non-methanogenic activity tests. Theoretical basis and experimental set up.", Wat. Res., Vol. 27, No. 8, 1993, p. 1361-1376.

63. Sørensen, A. H. and Ahring, B. K.: "Measurements of specific methanogenic activity of anaerobic digester biomass", App. Microbiol.Biotech., Vol. 40,1993, p. 427-431.

64. Owen, W. F., Stuckey, J. B., Healy Jr., J. B., Young, L. Y. and McCarty, P. L.: "Bioassay for monitoring biochemical methane potential and anaerobic toxicity", Water Research, Vol. 13, 1979, p. 485-492.

65. Miller, T. L. and Wolin, M. J.: "Enumeration of *Methanobrevibacter smithii* in Human Feces", Arch. Microbiol, Vol. 131, 1982, p. 14-18.

66. Kaspar, H. F. and Wuhrmann, K.: "Kinetic parameters and relative turnovers of some important catabolic reactions in digesting sludge", App. Environ. Microbiol., Vol. 36, 1978, p. 1-7 (cited in ref. 63).

67. Ahring, B. K. and Westermann, P.: "Methanogenesis from acetate: physiology of a thermophilic, acetate-utilizing methanogenic bacterium", FEMS Microbiol. Lett., Vol. 28, 1985, p. 15-19. (cited in ref. 63).

68. Andrews, J. F.: "Dynamic model of the anaerobic digestion process", Proc. Amer. Soc. Civil Eng., San. Eng. Div., Vol. 95, No. SA1, 1969, p. 95-116 (cited in ref. 26).

69. Pearson, F., Chang, S.-C. and Gautier, M.: "Toxic inhibition of anaerobic biodegradation", Wat. Res., Vol. 13, 1979, p. 485-492.

70. Zeikus, J. G. and Winfrey, M. R.: "Temperature Limitation of Methanogenesis in Aquatic Sediments", Appl. and Environ. Microbiol., Vol. 31, No. 1, 1976, p. 99-107.

71. Paul, W. L.: An investigation of scum formation in the 115E covered anaerobic reactor at Werribee, Melbourne Water technical report, 1993.

72. Paspaliaris, P.: 115E lagoon scum blanket formation/characterisation, Melbourne Water technical report, 1993.

73. Mara, D. D. and Silva, S. A.: "Waste Stabilisation Pond Research at Extrabes in Northeast Brazil", Regional Research Seminar on Waste Stabilisation Ponds, C.E.P.I.S., Lima, 1986.

74. Saqqar, M. M. and Pescod, M. B.: "Modelling the performance of anaerobic wastewater stabilisation ponds", 2nd IAWQ International Specialist Conference on Waste Stabilisation Ponds and the Reuse of Pond Effluents, USA, 1993.

75. van Haandel, A. C. and Catunda, P. F. C.: "Improved performance and increased applicability of waste stabilisation ponds by pre-treatment in a UASB reactor", 3rd IAWQ International Specialist Conference on Waste Stabilisation Ponds Technology and Application, Brazil, 1995.

76. Gloyna, E. F.: Waste Stabilization Ponds, (World Health Organization: Geneva, 1971).

77. Noone, G. P.: "The treatment of domestic wastes". In A. Wheatly (Ed.): Anaerobic Digestion: A Waste Treatment Technology, (Elsevier Science Publishers Ltd.: London, 1990), p. 139-170.

78. Osborn, F. D.: "Anaerobic Digestion: What's Going on Here?", Operation Forum, Vol. 9, No. 8, 1992, p. 28-30.

79. Wheatly, A. D.: "Anaerobic digestion: industrial waste treatment". In A. Wheatly (Ed.): Anaerobic Digestion: A Waste Treatment Technology, (Elsevier Science Publishers Ltd.: London, 1990), p. 171-223.

80. Dinges, R.: Natural Systems for Water Pollution Control, (Van Nostrand Reinhold Co.: New York, 1982).

81. Zickefoose, C. and Hayes, R.: Operations Manual: Anaerobic Sludge Digestion, (USEPA: Washington, 1976).

82. Thiele, J. H., Wu, W.-M., Jain, M. K. and Zeikus, J. G.: "Ecoengineering high rate biomethanation systems: design of improved syntrophic biomethanation catalysts", Biotechnol. and Bioeng., Vol. 35, 1990, p.990-999 (cited in ref. 4).

83. Selinger, B.: Chemistry in the Marketplace, (Harcourt Brace Jovanovich, Publishers: Sydney, 1986, 3rd edition).

84. Bhattacharya, S. K., Madura, R. L., Uberoi, V. and Haghighi-Podeh, M. R.: "Toxic effects of cadmium on methanogenic systems", Wat. Res, Vol. 29, No. 10, 1995, p. 339-2345.

85. Gould, M. S. and Genetelli, E. J.: "Heavy metal complexation behaviour in anaerobically digested sludges", Wat. Res, Vol. 12, 1978, p. 505 (cited in ref. 84).

86. Mueller, R. F. and Steiner, A.: "Inhibition of anaerobic digestion caused by heavy metals", Wat. Sci Tech., Vol. 26, No. 3-4, 1992, p. 835-846.

87. Fletcher, P. and Beckett, P. H. T.: "The chemistry of heavy metals in digested sewage sludge - I. Copper (II) complexation with soluble organic matter", Wat Res., Vol. 21, No. 10, 1987, p. 1153-1161 (cited in ref. 86).

88. Volesky, B.: "Removal and recovery of metals by biosorbent materials", Biotec., Vol. 2, 1988, p. 135-149 (cited in ref. 86).

89. Churchill, S. A., Walters, J. V. and Churchill, P. F.: "Sorption of heavy metals by prepared bacterial cell surfaces", J. Env. Eng., Oct 1995, p. 706-711.

90. Lange, C. R. and Weber, A. S.: "Cadmium inhibition of a defined mixed population under continuous culture", Proc. Wat. Envir. Fed. 66th Ann. Conf. and Expo., Anaheim, Calif., 1993, p. 11 (cited in ref. 84).

91. Shen, C. F., Kosaric, N. and Blaszczyk, R.: "The effect of selected heavy metals (Ni, Co, Fe) on anaerobic granules and their extracellular polymeric substances (EPS)", Wat. Res., Vol. 27, 1993, p. 25 (cited in ref. 84).

92. Nielson, J. S., Hurdey, S. E. and Cantwell, F. F.: "Role of the free metal ion species in soluble nickel removal by activated sludge", Environ. Sci. Technol., Vol. 18, 1984, p. 883 (cited in ref. 84).

93. Kuo, W.-C., Sneve, M. A. and Parkin, G. F.: "Production of soluble microbial products during anaerobic treatment", Proc. Wat. Envir. Fed. 66th Ann. Conf. and Expo., Anaheim, Calif., 1993, 1993, p.169.

94. Callendar, I. J. and Barford, J. P.: "Precipitation, chelation, and the availability of metals as nutrients in anaerobic digestion - I. Methodology", Biotech. Bioeng., Vol. 25, 1983a, p.1947 (cited in ref. 84).

95. Brown, M. J. and Lester, J. N.: "Role of bacterial extracellular polymers in metal uptake in pure bacterial culture and activated sludge - 1. Effects of metal concentration", Wat. Res., Vol. 16, 1982, p. 1539 (cited in ref. 84).

96. Jones, R. P. and Greenfield, P. F.: "A review of yeast ionic nutrition - I. Growth and fermentation requirements", Process Biochemistry, April 1984, p. 48-60.

97. Schönheit, P., Moll, J. and Thauer, R. K.: "Growth parameters (K_s, μ_{max}, Y_s) of *Methanobacterium thermoautotrophicum*", Archives of Microbiology, Vol. 127, 1980, p. 77-80 (cited in ref. 17).

98. Wilkie, P. J., Hatzimihalis, G., Koutoufides, P and Conner, M. A.: "Background levels of key organic and inorganic pollutants in domestic sewage", Chemistry in Australia, June 1996, p. 272-273.

99. SYSTAT for DOS: Using SYSTAT, Version 6 Edition (SYSTAT, Inc.: Evanston, IL, 1994).

100. Kuznetsov, S. E. and Khalileev, A. A.: MESOSAUR: A Companion to SYSTAT, (SYSTAT, Inc: Evanston, IL, 1991).

101. Gaudy, A. S. and Gaudy, E. T.: Microbiology for Environmental Scientists and Engineers, (McGraw-Hill: New York, USA, 1980).

102. Myers, R. H.: Classical and Modern Regression With Applications, (PWS-Kent: Boston, USA, 1986).

103. O'Halloran, R. J., Sexton, B. A. and Pilkington, N. H.: "Continuous monitoring of sewage and industrial effluents: The Sewer Sentinel". In L. O. Kolarik and A. J. Priestly (Eds): Modern Techniques in Water and Wastewater Treatment, (CSIRO: Melbourne, 1995), p. 183-189.

104. Box, G.: "GEORGE'S COLUMN Feedback Control by Manual Adjustment", Quality Engineering, Vol. 4, No. 1, 1991-92, p. 143-151.

105. Weiland, P. and Rozzi, A.: "The start-up, operation and monitoring of high-rate anaerobic treatment systems: Discusser's report", Wat. Sci Tech., Vol. 24, No. 8, 1991, p. 257-277.

106. Berthouex, P. M., Hunter, W. G., Pallesen, L. C. and Shih, C.-Y.: "Modelling Sewage Treatment Plant Input BOD Data", J. Env. Eng. Div., Feb 1975, p.127-138.

107. Microsoft EXCEL: User's Guide, Version 5.0, (Microsoft Corporation: USA, 1993).

108. Jenkins, G. M. and Watts, D. G.: Spectral Analysis and its applications, (Holden-Day: San Francisco, USA, 1968).

109. Scharzenbach, J. and Gill, K. F.: System Modelling and Control, (Edward Arnold Pty. Ltd.: Australia, 2nd ed, 1984).

110. Hickey, R. F., Vanderwielen, J. and Switzenbaum, M. S., Wat. Res., Vol. 21, 1987, p. 1417-1427 (cited in ref. 7).

111. Hickey, R. F., Vanderwielen, J. and Switzenbaum, M. S., Wat. Res., Vol. 23, 1989, p. 207-218 (cited in ref. 7).

112. Hickey, R. F. PhD dissertation, University of Massachusetts, Amherst, 1987 (cited in ref. 7).

113. Barnett, N. S.: "Measurement error and implications to SPC", Quality Australia, Vol. 9, No. 3, 1992, p. 70-72.

114. Coleman, D. E. and Stein, P. G.: "Improving Measurements", Quality Progress, Vol. 23, No. 11, 1990, p. 35-39.

115. ASQC Statistics Division: Glossary and Tables for Statistical Quality Control, (ASQC Quality Press: Milwaukee, WI, 2nd ed., 1983).

116. Standard Methods for the Examination of Water and Wastewater (APHA: USA, 18th ed., 1992).

117. Annual Book of ASTM Standards, (ASTM: Philadelphia, 1988), D4210-83.

118. Snedecor, G. W. and Cochran, W. G.: Statistical Methods, (The Iowa State University Press: USA, 6th ed., 1971).

119. Johnson, E. J. and Counts, R. W., J. Qual. Tech., Vol. 11, No. 1, 1979, p. 28-35.

120. Lucas, J. M.: "Combined Shewhart-CUSUM Quality Control Schemes", J. Qual. Tech., Vol. 14, No. 2, 1983, p. 51-59.

121. Survey to determine scum accumulation under floating sewerage (sic) lagoon cover, Anaerobic section 115 East Lagoon Western Treatment Plant, WBCM group, 1995.

122. Saqqar, M. M. and Pescod, M. B.: "Modelling sludge accumulation in anaerobic wastewater stabilisation ponds", 2nd IAWQ International Specialist Conference on Waste Stabilisation Ponds and the Reuse of Pond Effluents, USA, 1993.

123. Hudson, L: "Commissioning of Anaerobic Reactors at WTP", Melbourne Water technical report, 1996.

124. Cocci, A. A., Landine, R. C., Wilson, D. R and Grant, S. R.: "Low-rate anaerobic pretreatment effective, forgiving and simple: ADI-BVF Digester case histories", 2nd Annual Niagara Mohawk Gas Wastewater Treatment Conference, New York, 1993.

125. Breen, P. and Lawrence, I.: "Guidelines for designing pollution control ponds", WATER, Vol. 25, No. 3, 1998, p.25-26.

126. Pinto, M. A., Neder, K. D. and Luduvice, M. L.: "Assessing oxidation ponds design criteria in a tropical town with low water availability", 3rd IAWQ International Specialist Conference and Workshop on Waste Stabilisation Ponds Technology and Applications, Brazil, 1995.